University of Calabria

Faculty of Pharmacy and Nutritional Health Science
Department Pharmaco-Biology

Ph.D program in
"Cellular Biochemistry and Drug Activity in Oncology"
(XIII ciclo)
SSD BIO/10

Dynamic effects of Retinoic Acid and its isomers on cancer and physiology

Ph.D Director

Prof. Diego Sisci

Tutor

Prof. Daniela Bonofiglio

Graduate Student

Dr. Mariarita Perri

Academic Year 2009-2010

INDEX

ABSTRACT

In the search for new cancer chemo-preventive compounds, hundreds of naturally occurring molecules have been evaluated. Among these, antioxidants appear to be very promising. In this contest, over the last decade retinoids, natural and synthetic substances structurally related to vitamin A, are often used as part of a combined therapy and have been object of intense investigation. However, clinical trials have shown that retinoids can also be deleterious and are associated with the activation of proto-oncogenes, leading to an increased incidence of neoplasias. In fact, retinoic acid (RA) partition is regulated by cognate intracellular lipid binding proteins (iLBPs): cellular retinoic acid binding protein II (CRABP-II) delivers RA to RARs, while fatty acid binding protein 5 (FABP5) shuttles the RA to PPARβ/δ. In cells with high CRABP-II/FABP5 ratio, RA functions through RAR acting as a pro-apoptotic agent, while signaling through PPARβ/δ promotes survival in those cells highly expressing FABP5. So that, in some tissues RA promotes cell survival and hyperplasia. The apparently conflicting data regarding the pro-oxidant/ anti-oxidant and proliferative/anti-proliferative potential of different retinoids molecules, stimulated us to investigate the effect of RA on cell proliferation and its mechanisms in two different tumor Leydig cell lines (MLTC-1 and R2C) using as normal phenotype counterpart the Leydig TM-3 cell line. Our previous data demonstrated how pharmacological doses of RA induce cell death via the apoptotic pathway in Leydic TM-3 cell line. Recently dose-response treatment of TM-3, MLTC-1 and R2C with RA at nutraceutic/physiological doses, promotes cell proliferation accompanied by stimulation of antioxidant enzymes activity (CAT, GST), decreases p21 levels and fosters cell cycle progression via activation of the IP3K/Akt pathway in the cancer cell line, while administration of pharmacological doses of RA still results in apoptosis. Interestingly treatment with 500 nM of RA resulted in cytosolic vacuolization, hallmark of the autophagic process. Autophagy is a major cellular pathway for the degradation of long-lived proteins and organelles in eukaryotic cells. A large number of intracellular/extracellular stimuli, including amino acid starvation, testosterone production and invasion of microorganisms are able to induce autophagic response. In addition, retinoic acid is also implicated in a post-translation modification called retinoylation that modify, *in vitro*, the activity of the mitochondrial carrier oxo-chetoglutarate (OCG).

Moreover, retinoids are often used as part of a combined therapy, their action is prevalently mediated by two types of receptor RAR and RXR. This latter, is also called master coordinator due to its versatility to heterodimering with several nuclear receptor. Thus, we have elucidated the molecular mechanism by which combined

treatment with rosiglitazone (BRL) and 9 cis retinoic acid (9cRA) at nanomolar doses triggers apoptotic events in breast cancer cells, suggesting potential therapeutic uses for these compounds, demonstrating an up-regulation of tumor suppressor gene p53 and its activity is due to the NFkB site, giving emphasis to the potential use of the combined therapy with low doses of both BRL and 9cRA as novel therapeutic tool particularly for breast cancer patients who develop resistance to anti-estrogen therapy. Recently, 9cRA was found as endogenous in pancreas highlighted its rule in both glucose stimulated insulin secretion (GSIS) mechanism and glucose homeostasis, establishing it as autocoid hormone with a unique physiological function among retinoids, and broaden insight into mechanisms of GSIS.

INTRODUCTION

1. atRA: multiple effects in different biological systems

Current approaches to cancer treatment are mostly based on cytotoxic and cytostatic mechanisms to eliminate malignant cells. These pharmacological strategies, although efficacious toward the malignant cells, show a number of toxic side effects which frequently hamper or drastically reduce their use. A newer dimension in cancer management is the increasing awareness that chemoprevention, namely the administration of chemical agents (both natural and synthetic) to prevent the early events of carcinogenesis, could be the most direct way to counteract malignancy development and progression (Della Ragione et al. 2000). In the search for new cancer chemopreventive compounds, hundreds of naturally occurring molecules have been evaluated over the past few years. Among the agents able to lower the rate of malignant transformation, antioxidants appear to be very promising. Indeed, diets rich in antioxidant molecules are clearly associated with a diminished risk of cancer at various anatomical sites (Della Ragione et al. 2000). The oncoprotective properties of exogenous antioxidants have been documented in a number of epidemiological, intervention and *in vitro* studies. However, the mechanisms implicated are far from being clarified. Antioxidant effects, steroid receptor binding, direct interaction with intracellular elements and signaling systems and, recently, aryl hydrocarbon receptor (AhR) binding and modification of subsequent signaling pathways (Ciolino et al. 1999; Jellinck et al. 1993; Le Ferrec et al. 2002; Lee & Safe 2001; Liu et al. 1994; McDougal et al. 2001) have been proposed as possible mechanisms for the mediation of the oncoprotective effect of these agents. Exogenous antioxidants are exclusively produced by plants; they are divided into water-soluble antioxidants (e.g. vitamin C) and lipid-soluble antioxidants (e.g. vitamin A, vitamin E, β-carotene). Some intervention studies have questioned the effectiveness of specific antioxidants in tumor prevention. This suggests that the use of these compounds as chemopreventive

agents must await more detailed knowledge of their mechanism of action and their interactions with genetic phenotypes and environment (Della Ragione et al. 2000).

In this contest, over the last decade retinoids have been the object of intense investigation. Retinoids are natural and synthetic substances structurally related to retinol, the vitamin A (ROL). Major sources of natural retinoids are animal fats, fish liver oil (retinylesters), and yellow and green vegetables (carotenoids). Ingested retinylesters (RE) are hydrolyzed to ROL by enteral hydrolases in the intestine. ROL and carotenoids are absorbed by intestinal mucosa cells. Of the carotenoids, b-carotene is the most potent ROL precursor, yet it is six-fold less effective than preformed ROL, which results from incomplete resorption and conversion (One ROL equivalent is equal to 1 mg of ROL, 6 mg of b-carotene, or 12 mg of mixed carotenoids) (Blomhoff et al. 1991). After intestinal absorption, retinoid production from carotenoids can occur by two pathways: first, retinal (RAL) can be synthesized by oxidative cleavage of the central double bond followed by reduction to ROL by a microsomal retinal reductase (Kakkad & Ong 1988). Here, the cellular retinol binding protein-II (CRBP-II) protects RAL from oxidation into retinoic acid (RA). Second, apo-carotenoids are formed through excentric cleavage followed by transformation of the apo-carotenoid acids into RAs (Wang et al. 1991). In the intestinal cell, ROL also forms complexes with CRBP-II. This ROL-CRBP-II complex serves as substrate for the esterification of ROL to RE by a lecithin:retinol acyltransferase (LRAT) (MacDonald & Ong 1988) with long-chain fatty acids, which are incorporated by chylomicrons (Blomhoff et al. 1990). The fatty acids reach the general circulation where they undergo several biochemical changes via the lymph RE-chylomicron complexes. This leads to the formation of several chylomicron remnants, which in turn are cleared primarily by the liver, although extrahepatic chylomicron uptake has been shown also in bone marrow and spleen, and to a lesser degree in testes, lungs, kidneys, fat, and skeletal muscle (Blomhoff 1994; Blomhoff et al. 1991). In the parenchymal hepatocytes, chylomicron-RE complexes are hydrolyzed and free ROL binds to retinol binding protein (RBP), its serum transport protein. Excess ROL

undergoes a paracrinic transfer from the hepatocytes to the perisinusoidal stellate cells, called *vitamin A storage* or *Ito cells*, for storage (Hirosawa & Yamada 1973). Approximately 50 to 80% of the total body vitamin A in humans is stored in the stellate cells in the liver in the form of REs. Depending on their lipophilic character, exogenous and endogenous RA derivatives accumulate in the human body with highly variable elimination half-lives. This has to be considered especially for the use of synthetic RA derivatives in clinical therapy (Chien et al. 1992). To maintain constant physiological ROL concentrations in the plasma of approximately 2 mmol/L, ROL can be released from the stellate cells. The RA concentration in the plasma and other body fluids is approximately 100-fold lower (7 to 14 nmol/L) (Napoli et al. 1985; De Leenheer et al. 1982; Tang & Russel 1990; Eckhoff & Nau 1990). ROL-RBP complexes released from the liver bind to transthyretin, a serum protein named for its ability to bind and transport simultaneously but independently from both the thyroid hormone and the ROL-RBP complex (Blomhoff et al. 1991).The transfer of retinol to target cells involves a specific membrane-bound receptors (Sivaprasadarao et al. 1998**)**. It has been recently demonstrated that cellular retinol penetration is based on the interaction between the RBP-retinol complex and a membrane receptor STRA6. STRA6 is a multitransmembrane domain protein not homologous to any other proteins with known function. It functions as the high-affinity receptor for plasma retinol binding protein (RBP) and mediates cellular uptake of vitamin A from the vitamin A-RBP complex. The complexity of the metabolic pathways for retinoids and the likelihood that these are altered by diseases suggest that such novel strategies will be forthcoming. Multiple studies are underway to define the steps of retinoid metabolism where the use of modulating drugs might influence the results of therapy thereby leading to the most profound effects with regard to the clinical outcome.

Retinoids are promising agents in the chemoprevention and treatment of the neoplastic disease. They exert antiproliferative and differentiation-inducing effects on cancer cells and are used in the prevention and treatment of certain types of human

cancer and precancerous lesions (Gudas et al. 1994; Lotan 1996). Their action is mediated by two types of receptors, the retinoic acid receptors (RARs) and retinoid X receptors (RXRs) (Chambon 1996) belonging to the steroid/thyroid hormone receptors superfamily. There is substantial evidence in vitro that retinoids exert their effect through the induction of apoptosis in tumor cells including hepatoma, leukemia, breast cancer and embryonal carcinoma cell lines (Nagy et al. 1995; Nakamura et al. 1995; Horn et al. 1996; Kim et al. 1996; Li et al. 1999). The action of retinoids in promoting apoptosis may explain the anticarcinogenic properties of these compounds. Apoptosis, an active and programmed form of cell death, is a multistep process (Hengartner 2000) that plays an important role in the regulation of development morphogenesis (Vaux & Korsmeyer 1999), cell homeostasis, and diseases such as cancer, stroke, and ischemic heart disease (Thompson 1995). Apoptosis is characterized by morphological changes including progressive cell shrinkage with condensation, fragmentation of nuclear chromatin and membrane blebbing (Kerr et al. 1980). Two apoptotic pathways by which cells can initiate and execute the cell death process, the extrinsic and the intrinsic, have been identified (Green 2000; Johnstone et al. 2002). The extrinsic pathway is initiated by ligation of transmembrane death receptors (CD95, TNF receptor, and TRAIL receptor) to activate membrane proximal caspases (caspase-8 and -10). The mammalian caspase family comprises at least 13 known members, most of which have been definitively implicated in apoptosis. In vitro experiments suggest that several caspases could activate by themselves, while others require activation by other caspases, acting as a proteolytic cascade (Nicholson & Thornberry 1997). Caspase-3, -6, and -7 are terminal members of caspase cascade and recognize critical cellular substrates, whose cleavage contributes to the morphological and functional changes associated with apoptosis (Thornberry & Lazebnik 1998). Caspase-3 activation also results in DNA cleavage via inactivation of an inhibitor of the DNA fragmentation factor, the endonuclease responsible for internucleosomal cleavage of chromatin (Wickremasinghe & Hoffbrand 1999). Recent findings showed that caspase-3 has a

mitochondrial and cytosolic distribution in non-apoptotic cells (Mancini et al. 1998). The mitochondrial caspase-3, which is located in the intermembrane space, was shown to be activated by numerous pro-apoptotic stimuli and this activation could be blocked by bcl-2 (Mancini et al. 1998). Once the caspases are activated, the cell is irreversibly committed to cell death (Reed et al. 1996). The intrinsic pathway is initiated in the cells by the loss of integrity of the outer mitochondrial membrane and the release of cytochrome c into the cytosol (Hirsch et al. 1997; Green & Reed 1998; Joza et al. 2001; Zamzami & Kroemer 2001). Then cytochrome c, an essential constituent of the respiratory chain, is released from mitochondria into the cytosol and induces a conformational change in Apaf-1 (apoptotic protease activating factor-1) that results in the activation of a cascade of caspase proteases with consequent cell death (Yang & Cortopassi 1998; Susin et al. 1999). The release of cytochrome c is associated with the mitochondrial permeability transition (MPT). Indeed, it is associated with depolarization of the mitochondrial inner membrane potential, loss of the H+ gradient, uncoupling of oxidative phosphorylation, ATP depletion, mitochondrial swelling and disruption of the outer mitochondrial membrane (Wudarczyk et al. 1996; Bindoli et al. 1997; Kowaltowski et al. 1997; Bossy-Wetzel et al. 1998; Vieira et al. 2000). Among the non proteic effectors, calcium ion is the most important inducer of MPT (Petronilli et al. 1993; Schild et al. 2001). Mitochondria are vulnerable targets to toxic injury by a variety of compounds because of their crucial role in maintaining cellular structure and function via oxidative phosphorylation and ATP production. The translocation of cytochrome c into the cytosol represents a central point in many forms of apoptosis, since cytochrome c is a fundamental component of the apoptosome, responsible for caspase activation.

There are a growing number of in vitro experiments demonstrating that active retinoids, as well as RA, antagonize cell growth in a variety of non-tumoral and tumoral cells, characterizing them as potential chemotherapeutic agents (Okuno et al. 2004; Kuratomi et al. 1999; Dragnev et al 2003). Indeed, this class of agents finds

clinical application or is proposed also in the treatment of various neoplastic diseases, among which, acute promyelocytic leukemia (APL) is the most prominent example. The observation that atRA induces remission in APL through a mechanism of action that is dinstinct from cytotoxicity, is regarded as a milestone in the history of medicine (Huang et al. 1988). The retinoid is the first and only example of clinically succesfull cytodifferentiating agent. Fenretinide, a synthetic retinoid, has shown efficacy in the secondary chemoprevention of breast cancer (Veronesi et al. 1999). Cytodifferentiation is a particularly attractive modality of treatment and differentiating agents promise to be less toxic and more specific than conventional chemotherapy. Currently, the promise of differentiation therapy is only partially met and a more general use of atRA and other retinoids as differentiating agents in oncology is hampered by a number of problems including natural and acquired resistance as well as local and systemic toxicity. Therefore, retinoids are often used as part of a combined therapy. atRA and derivatives modulate the activity of numerous genes and intracellular pathways. On the other hand, the activity of nuclear RARs is controlled by various signals, including different types of kinase cascades. Often the cross talk between atRA-dependent and other intracellular pathways modulates the cytodifferentiating activity of the retinoid. The knowledge on the molecular mechanism underlying this cross talk has increased tremendously over the course of the last few years. In cell cultures, the cytodifferentiating activity of retinoids is almost invariably accompanied by growth inhibition and the two processes are difficult to dissociate (Gianni et al. 2000). On the other hand, retinoid-dependent cytodifferentiation is not necessarily associated with cell death or apoptosis. Indeed, classical retinoids are relatively weak apoptotic agents and, in some cases, they even exert a prosurvival action (Lomo et al. 1998). These aspects of retinoids pharmacology need to be considered when discussing the use of such agents in oncology. An antiproliferative effect superimposed to cytodifferentiation is highly desirable, whereas an antiapoptotic action should be avoided.
A generalized use of retinoids in oncology is hampered by a number of unresolved

problems including natural and induced resistance as well as toxicity issues are of particular evidence, given the fact that differentiation therapy with retinoids requires prolonged administration of the agents. Chronic exposure to retinoids is accompanied by serious effects at the level of central nervous and hepatic systems, as well as the well-know teratogenic problems associated with the administration of these compounds. Clearly these problems call for strategies aimed at increasing the efficacy and the therapeutic index of retinoids developing novel, more powerful and less toxic syntethic retinoids and identifing non-retinoid agents capable of potentiating the pharmacological activity of retinoids without affecting their toxicity.

It has been suggested that retinoids act as antioxidants in biological systems, assuming a role in antioxidant therapies for treatment and prevention of malignant and neurodegenerative diseases (Okuno et al. 2004). However, clinical trials have shown that retinoids can also be deleterious and are associated with the activation of proto-oncogenes, leading to an increased incidence of neoplasias (Omenn 2007). Transcriptional activation of the nuclear receptor RAR by RA often leads to inhibition of cell growth. However, in some tissues RA promotes cell survival and hyperplasia: these activities are unlikely to be mediated by RAR (Henion & Weston 1994; Rodriguez-Tebar & Rohrer 1991). In addition to activate RARs, RA can also stimulate the nuclear receptor PPARβ/δ (peroxisome proliferator-activated receptor β/δ), and therefore the list of genes and cellular responses controlled by this hormone include both RAR and PPARβ/δ-targets. The partition of RA between its two receptors is regulated by cognate intracellular lipid binding proteins (iLBPs); moreover, cellular retinoic acid binding protein II (CRABP-II) delivers RA to RARs, while fatty acid binding protein 5 (FABP5) shuttles the RA to PPARβ/δ (Shug et al. 2007). In cells with high CRABP-II/FABP5 ratio, RA functions through RAR acting as a pro-apoptotic agent, while signaling through PPARβ/δ promotes survival in those cells highly expressing FABP5. The opposing effects of RA on cell growth thus emanate from alternate activation of two different nuclear receptors (Shug et al. 2007). The apparently conflicting data regarding the pro-oxidant/ anti-oxidant and

proliferative/anti-proliferative potential of different retinoids molecules, stimulated us to investigate the effect of RA on cell proliferation and its mechanisms in two different tumor Leydig cell lines (MLTC-1 and R2C) using as normal phenotype counterpart the Leydig TM-3 cell line. Previous datas demonstrated how pharmacological doses of RA induce cell death via the apoptotic pathway in Leydic TM-3 cell line (Tucci et al. 2008). Here we report that dose–response treatment of TM-3, MLTC-1 and R2C with RA at nutraceutic/physiological doses, promotes cell proliferation accompanied by stimulation of antioxidant enzymes activity (CAT, GST), decreases p21 levels and fosters cell cycle progression via activation of the IP3K/Akt pathway in the cancer cell line while administration of pharmacological doses of RA results in apoptosis either in TM-3 in agreement with the literature (Tucci et al. 2008) and R2C and MLTC-1 tumoral cell line. Interestingly treatment with 0.5 μM RA resulted in cytosolic vacuolization, hallmark of the autophagic process. Autophagy is a major cellular pathway for the degradation of long-lived proteins and organelles in eukaryotic cells(Yoshimori 2004). A large number of intracellular/extracellular stimuli, including amino acid starvation and invasion of microorganisms, are able to induce the autophagic response in cells. Autophagic cell death is morphologically characterized by an accumulation of autophagic vacuoles. Macroautophagy (which we will refer to as 'autophagy') involves the sequestration of cytosol or cytoplasmic organelles within double membranes, thus creating autophagosomes (also called autophagic vacuoles). Autophagosomes subsequently fuse with endosomes and eventually with lysosomes, thereby creating autophagolysosomes or autolysosomes. In the lumen of these latter structures, lysosomal enzymes operating at low pH then catabolize the autophagic material (Levine & Klionsky 2004; Shintani & Klionsky 2004). In addition to the degradation of cellular proteins and organelles, autophagy can serve as a temporary survival strategy to defend against damage caused by environmental changes through the sequestration of noxious substance (such as certain aggregation-prone proteins or the expression of aggregating mutant variants of specific proteins) and injured organelles.

Furthermore, autophagy may also be a strategy for self-destruction through the induction of programmed cell death (PCD), which is different from apoptosis (Bursch et al. 2004). Both apoptosis and autophagy can occur concomitantly in the same cells, suggesting the involvement of common regulatory mechanisms (Kondo et al. 2005). Moreover the redox environment of the cell is currently thought to be extremely important to control either apoptosis or autophagy (Jaattela 2004; Gurusamy & Das 2009).

It has generally been believed that most of the functions of vitamin A are mediated by the nuclear retinoic acid receptors, RAR and RXR (Kastner et al. 1994; Mangelsdorf et al. 1994; Wolf 2000). The activation of retinoic acid (RA) in development and cell differentiation is mediated by these receptors, which interact directly by binding to specific DNA sequences. In addition to binding nuclear retinoid receptors, RA acts elsewhere in the cells (Bolmer & Wolf, 1982; Smith et al. 1989; Varani et al. 1996). Retinoylation (acylation by RA of protein), a post-translational non-genomic modification, is another mechanism by which RA may act on cells. RA is incorporated into proteins of cells in culture (Breitman and Takahashi, 1996; Takahashi and Breitman, 1989, 1990, 1994; Tournier et al. 1996) and into proteins of rat tissues, both in vivo (Myhre et al. 1996) and in vitro (Genchi & Olson, 2001; Myhre et al. 1998; Renstrom & DeLuca, 1989). The covalent linkage between RA and proteins is probably a thioester or labile O-ester bond in most cases. Retinoylated proteins that have been identified so far include cAMP binding proteins, vimentin, the cytokeratins, and some nuclear proteins (Takahashi & Breitman 1989, 1990, 1994; Tournier et al. 1996; Myhre et al. 1996, 1998; Renstrom & DeLuca 1996). In our current investigation, we have studied OGC carrier activity both from mitochondria extracted from whole rat testes and TM-3 cells. Previously we have demonstrated that mitochondria from rat testes (Genchi &Olson 2001; Cione & Genchi 2004) and TM-3 cells (Cione et al. 2005) were extremely active in incorporating retinoic acid. Moreover, it was highlighted how the retinoylation reaction and testosterone biosynthesis are positively correlated when Leydig cell

cultures are incubated with atRA at 100 nM (Tucci et al. 2008). It is well known that many biosynthetic pathways of testosterone are NAPDH or NADH dependent; therefore OGC was chosen as the experimental target for its involvement in the malate–aspartate shuttle and oxoglutarate–isocitrate shuttle to provide the necessary reducing equivalents between cytosol and mitochondria and viceversa. This study indicates the evidence of a specific interaction between atRA and OGC and establishes a novel mechanism for atRA action, which could influence the physiological biosynthesis of testosterone in situations such as retinoic acid treatment.

2. 9cRA: antitumoral effects in breast cancer and therapeutic potential for the treatment of the metabolic syndrome

At nuclear level it is well known that RA functions by binding to ligand-inducible transcription factors (nuclear receptor proteins belonging to the steroid/thyroid hormone receptor superfamily) that activate or repress the transcription of downstream target genes (Chambon, 1996; Soprano & Soprano, 2003). Six nuclear receptors, termed RARα, RARβ, RARγ, RXRα, RXRβ and RXRγ, encoded by different genes, have been demonstrated to mediate the actions of RA. The natural metabolite all-*trans* RA (atRA) and 9-*cis* RA are high affinity ligands for RARs, whereas 9-*cis* RA, phytanic acid, docosahexanoic acid, and unsaturated fatty acids, have been suggested to bind RXRs. These proteins, as heterodimers (RAR/RXR) or homodimers (RXR/RXR), function to regulate transcription by binding to DNA sequences located within the promoter of target genes called retinoic acid response elements (RARE) or retinoid X response elements (RXRE), respectively. RAREs consist of direct repeats of the consensus half-site sequence AGGTCA separated most commonly by five nucleotides (DR-5) while RXREs are typically direct repeats of AGGTCA with one nucleotide spacing (DR-1). The RAR/RXR heterodimer binds to the RARE with RXR occupying the 5’ upstream half-site and RAR occupying the 3’

downstream half-site. atRA and 13-*cis* RA bind to and transactivate only RXR/RAR complexes, while 9-*cis* RA interacts with both RXR/RAR heterodimers and RXR/RXR homodimers. RXR/RAR dimers are believed to be nonpermissive complexes, in which RXRs act as silent partner. In other words, when the cognate ligand is bound to the RAR moiety, the RXR counterparts loses the ability to bind its corresponding ligand (Mangelsdorf et al. 1993; Mangelsdorf & Evans 1995). In basal conditions, the RXR/RAR heterodimer is bound to the cognate DNA sequence (RARE) and interacts with a multiprotein complex known as the corepressor (Weston et al. 2003; Wei 2004). The corepressor (RIP140 receptor interacting protein 140) contains protein endowed with the histone deacetylase (HDAC) and DNA-methylating activity that concur to keep the surrounding chromatin structure in a "closed" state, effectively suppressing the transcriptional activity of RNA polymerase II. On ligand binding the corepressor is released from the RXR/RAR dimer and substituted by the "coactivator", which consists of a multiprotein complex with histone acetylase and demethylase activity (Xu et al. 1999; Westin et al. 2000) opening the chromatine structure and favouring transcription. The activity of the RXR/RAR dimer is also controlled by a number of accessory signals in which phosphorylation events stand out (Gianni et al. 2002, 2006). A further layer of control is represented by the rate of proteolitic degradation of the RXR/RAR dimer and the various components of the corepressor and coactivator complexes (Gianni et al. 2006). Little is known about the RXR/RXR pathway which is far less studied than the RXR/RAR counterpart.

This second part of the thesis is based on the experimental evidence that the nuclear receptor pathway interacts with numerous other intracellular pathways, some of which are of obvious significance from a therapeutic point of view. Retinoids have been proposed in the adjuvant treatment of breast carcinoma for their ability to inhibit growth and induce morphological or phenotypic differentiation of breast carcinoma cell lines (Paik et al. 2003; Yang et al. 2002) and most of the studies have focused on the antiproliferative activity of retinoids (Del Rincon et al. 2003). It is generally

accepted that breast cancer cells express RARα, RARγ and RXRα but also Peroxisome Proliferator-Activated Receptor gamma (PPARγ) that can regulate cell proliferation, differentiation and survival (Lemberger et. al. 1996; Lefebvre et al. 2006). PPARγ functions as a transcription factor by heterodimerizing with RXR, after which this complex binds to specific DNA sequence elements called Peroxisome Proliferator Response Elements (PPREs). PPREs are direct repeats of the consensus sequence with a spacing of one nucleotide (AGGTCA-N-AGGTCA) (Palmer et al. 1995). The heterodimer PPAR/RXR activated with their ligands, can bind to PPREs in promoter regions of target genes recruiting coactivator or corepressor to this complex to modulate gene expression (DiRenzo et al. 1997; McIerney et al. 1998; Yuan et al. 1998). Previous data show that PPARγ, poorly expressed in normal breast epithelial cells (Elstenr et al. 1998), is present at higher levels in breast cancer cells (Tontonoz et al. 1994) and its synthetic ligands, such as thiazolidinediones (TZDs), induce growth arrest and differentiation in breast carcinoma cells in vitro and in animal models (Mueller et al. 1998; Suh et al. 1999). Previous data show that the combination of PPARg ligand with either all-*trans* retinoic acid or 9-*cis*-retinoic acid (9RA) can induce apoptosis in some breast cancer cells (Elstenr et al. 2002). Furthermore, Elstner et al demonstrated that the combination of these drugs at micromolar concentrations reduced tumor mass without any toxic effects in mice (Elstenr et al. 1998). Thus, in the present study we have elucidated the molecular mechanism by which combined treatment with BRL and 9RA at nanomolar doses triggers apoptotic events in breast cancer cells, suggesting potential therapeutic uses for these compounds. We demonstrated the molecular mechanism underlying antitumoral effects induced by combined low doses of both ligands in MCF-7 cells, when an up-regulation of tumor suppressor gene p53 was concomitantly observed. Functional assays with delection constructs of the p53 promoter showed that the NFkB site is required for the transcriptional response to BRL plus 9RA treatment. NFkB was shown to physically interact with PPARg which in some circumstances binds to DNA cooperatively with NFkB. Only BRL and 9RA in combination

increased the binding and the recruitment of either PPARg or RXRa on the NFkB site located in the p53 promoter sequence. The crucial role of p53 gene in mediating apoptosis is raised by the evidence that the effects on the apoptotic cascade were abrogated in the presence of AS/p53 in all breast cancer cell lines tested, including tamoxifen resistant breast cancer cells. These results give emphasis to the potential use of the combined therapy with low doses of both BRL and 9RA as novel therapeutic tool particularly for breast cancer patients who develop resistance to anti-estrogen therapy. However, high doses of both ligands have remarkable side effects including weight gain due to increased adiposity, edema, hemodilution, and plasma-volume expansion, which preclude their clinical application in patients with heart failure (Arakawa et al. 2004; Rangwala & Lazar 2004; Staels 2005). The undesirable effects of RXR-specific ligands on hypertriglyceridemia and suppression of the thyroid hormone axis have been also reported (Pinaire & Reifel-Miller 2007).

Chronic over-nutrition and genetic factors can impair GSIS, leading to glucose intolerance and hyperglycemia, and ultimately to Type 2 diabetes (Muoio & Newgard 2008). Impaired GSIS develops through multiple mechanisms, including actions of metabolic hormones and inflammatory cytokines, products of metabolic overload, and endoplasmic reticulum stress (Henquin et al. 2003). Glucose sensing and uptake by the pancreas transporter Glut2 and glucose phosphorylation catalyzed by GK constitute the first and rate-limiting steps, respectively, that couple blood glucose levels to insulin release. Metabolism of glucose-6-phosphate increases mitochondrial metabolites, including ATP. A rise in ATP closes the β-cell K^{+}_{ATP} channel, which allows Ca^{2+} influx to trigger the first phase of GSIS (Jensen et al. 2008). Despite these insights, mechanisms of GSIS and impaired glucose tolerance remain incompletely understood. Also uncertain is the contribution of impaired glucose tolerance to diminished pancreatic β-cell function and mass associated with type 2 diabetes (Lowell & Shulman 2005). Vitamin A has been identified as a factor important to pancreas development, islet formation and pancreatic function (Chertow & Baker 1978; Matthews et al. 2004; McCarroll et al. 2006).Vitamin A-restriction

during development impairs islet development and promotes glucose intolerance in adult rodents. atRA regulates pancreas development (Noy 2007; Germain et al. 2006; Kadison et al. 2001). On the other hand, restricting vitamin A in mature diabetes-prone rats reduces diabetes and insulitis, possibly though enhanced glucose sensing and metabolism (Kobayashi et al. 2002). Interestingly, the vitamin A-derived hormone atRA does not reproduce the effects of vitamin A on the incidence of diabetes in diabetes prone rats. Although the contribution of vitamin A to pancreas development through atRA seems clear, mechanisms whereby vitamin A affects mature pancreas function have not been determined in depth, nor have the specific vitamin A-metabolites been identified that contribute to physiological control of GSIS.

A class of compounds that selectively bind and activate RXR, are being studied as a potential option for the treatment of metabolic syndrome. These compounds have glucose-lowering, insulin-sensitizing, and antiobesity effects in animal models of insulin resistance and type 2 diabetes (Pinaire & Reifel-Miller 2007). These recent findings suggest that, with continued research efforts, RXR-specific ligands with improved pharmacological profiles may eventually be available as additional treatment options for the current epidemic of obesity, insulin resistance, type 2 diabetes, and all of the associated metabolic sequelae. Specific retinoid X receptor (RXR) agonists, such as LG100268 (LG268), and the thiazolidinedione (TZD) PPARg agonists, such as rosiglitazone, produce insulin sensitization in rodent models of insulin resistance and type 2 diabetes. In sharp contrast to the TZDs that produce significant increases in body weight gain, RXR agonists reduce body weight gain and food consumption. Unfortunately RXRagonists also suppress the thyroid hormone axis and generally produce hypertriglyceridemia. Heterodimer-selective RXR modulators have been identified that, in rodents, retain the metabolic benefits of RXR agonists with reduced side effects. These modulators bind specifically to RXR with high affinity and are RXR homodimer partial agonists. Although RXR agonists activate many heterodimer partners, these modulators selectively activate

RXR:PPARa and RXR:PPARg, but not RXR:RARa, RXR: LXRa, RXR:LXRb, or RXR:FXRa. Therefore, selective RXR modulators are a promising approach for developing improved therapies for type 2 diabetes, although additional studies are needed to understand the strain-specific effects on triglycerides (Leibowitz et al. 2006).

9cRA activation of RXRs has prompted evaluation of synthetic analogs (rexinoids) to treat metabolic disease (McCarroll et al. 2006; Noy 2007). 9cRA and rexinoids have diverse pharmacological actions that regulate biological endpoints independent of atRA (Germain et al.2006). For example, treating embryo day 11 pancreas organ cultures with 9cRA inhibits stellate cell activation more potently and quickly than atRA, and inhibits acini differentiation, but prompts ductal differentiation and endocrine maturation (Kadison et al. 2001; Kobayashi et al. 2002). atRA, in contrast, induces acini rather than ductal differentiation, and has no apparent endocrine effects. Longer-term systemic treatment with rexinoids promotes insulin sensitization, presumably through cumulative effects on multiple receptor distributed throughout multiple tissues (Cheng et al. 2008). Regardless of the pharmacological utility of 9cRA, sensitive analytically validated assays have not detected endogenous 9cRA in serum and many tissues that contribute to glucose homeostasis, including brain, liver, kidney, adipose and muscle (Ahuja et al. 2003). This leaves unsettled whether 9cRA *in vivo*, and if so, whether it has discrete physiological functions. In this study, we used a sensitive and specific LC/MS/MS assay developed to distinguish and quantify RA isomers in tissue samples, and found that 9cRA occurs endogenously in pancreas. Pancreas 9cRA reacts within minutes to blood glucose fluctuations, modifies the impact of glucose in GSIS, and occurs in abnormally high concentrations in models of impaired glucose tolerance. These data establish the presence of 9cRA as an endogenous retinoid, show that it has a physiological function unique among retinoids, and broaden insight into mechanisms of GSIS.

RESULTS AND DISCUSSION

1. AtRA induces apoptosis in Leydig TM-3 cells via activation of the mitochondrial death pathway and antioxidant enzyme regulation

In order to examine the cytotoxic effect of RA on TM-3 cells, they were cultured with RA in a concentration range from 0.1 to 20μM for 24h and MTT assay was carried out with cells cultured in RA-free media as control. No significant change in viability was observed in TM-3 treated in 0–0.5μM RA concentration range (Fig. 1A). Upon incubation with RA concentration of 1–20μM a significant reduction of vitality, however, observed. As shown in Fig. 1A, the cell viability was less than 20% after exposure to 20μM RA for 24h. The effect of RA at μM doses on cell viability was also time-dependent, since the cell survival declined drastically following an increase in the treatment time from 3 to 24h in cells incubated with 10 and 20μM RA (Fig. 1B). The present results show that RA exerts a cytotoxic effect on TM-3 cells in a concentration and time dependent manner (Fig. 1A,B).

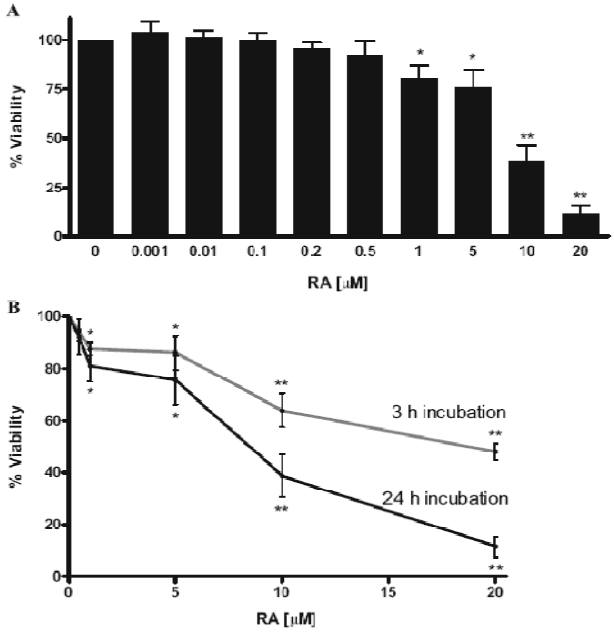

Fig.1 The effect of RA on TM-3 cell survival. A Cells were incubated with indicated concentrations of RA and then the cell viability was determined by MTT assay as described in "Materials and methods". B The cell viability was evaluated at 3 and 24 h post-exposure with RA (at μM doses). The data represent means±SD of four independent experiments with triplicate well and are presented as the percentage of the control cell number. *P<0.05 compared to the control. **P<0.01 compared to the control

In order to examine whether apoptosis was the cause of the loss of cell viability, the cells were treated with μM doses of RA and subjected to various biochemical analyses to detect biomarkers of apoptosis. Mitochondria are vulnerable targets for toxic injury and act as crucial executors of apoptosis by releasing cytochrome c into the cytoplasm (Cai et al. 1998). 24h post-exposure TM-3 cells were collected and the cytosolic protein fraction was assayed for cytochrome c release. As shown in Fig. 2A,B, cytochrome c was detectable in cytoplasm following exposure to 0.5μM RA and the protein increased significantly at higher RA exposure (10–20μM) when compared to time matched controls. The time-course of cytochrome c release from the mitochondria into the cytosol was also determined after 3, 6, 18 and 24h of incubation in the presence of 20μM RA. As shown in Fig. 2C,D, detectable release of cytochrome c was, only apparent, after 18h of treatment. The activation of the caspase family members is a hallmark of apoptosis. After treatment for 24h with RA, western blot analysis, using a caspase-3 antibody that recognizes the caspase-3 holoenzyme as well as the p17 cleavage product of caspase-3, was performed to investigate whether enzymatic processes had been activated. Procaspase-3 is synthesized as a precursor of 32kDa which is then proteolitically cleaved. Immunoblotting analysis revealed that procaspase-3 levels decreased in cells treated with 5, 10 and 20μM RA for 24h in a dose-dependent manner; while a band, corresponding to the activated form of caspase-3 (17kDa), was increased over the same dose response curve (Fig. 2E). In order to evaluate the induction of apoptosis by RA we measured DNA fragmentation using DNA electrophoresis and fluorescent staining. The genomic DNA extracted from cells, treated with 5, 10 and 20μM RA for 24h, was subjected to 1.2% agarose gel electrophoresis. DNA ladders, which are typical of apoptosis, were detected only in the cells treated with 10 and 20μM RA (Fig. 2F). LDH activity in the culture media was measured spectrophotometrically as an index of plasma membrane damage and loss of membrane integrity and therefore a parameter of cytotoxicity. RA treatment for 24h resulted in a dose-dependent induction of LDH release (Fig. 3A). To summarize, we have demonstrated that RA-

induced cell death occurred by classical apoptosis, whilst at higher concentrations there is also evidence of necrotic death.

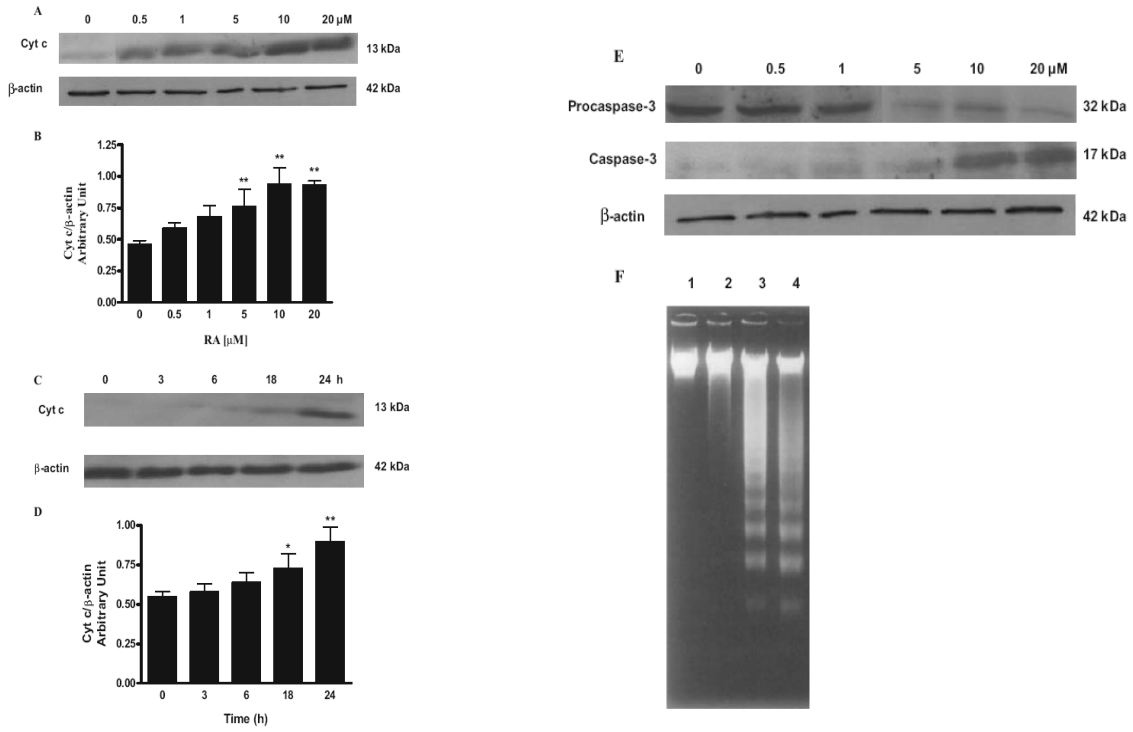

Fig.2 Biochemical markers of apoptosis. A TM-3 cells were incubated both in the absence and in the presence of 0.5, 1, 5, 10 and 20 μM RA for 24 h. After incubation, cells were washed with PBS; equal amounts of cytosolic proteins (2–5 μg) were separated by 15% SDS-PAGE, transferred to a nitrocellulose membrane, and probed as described in "Materials and methods". Cytochrome c was detected by chemiluminescence. β-actin, used as internal control, was detected at the position corresponding to a molecular weight of 42 kDa. B The cytochrome c protein content was determined densitometrically. Results are presented as the mean±SD of three independent experiments. *P<0.05 compared to the control; **P<0.01 compared to the control. C TM-3 cells were incubated with 20 μM RA and release of cytochrome was evaluated at 0, 3, 6, 18 and 24 h post-exposure. D The cytochrome c protein content was determined densitometrically. Results are presented as the mean±SD of three independent experiments. *P<0.05 compared to the control; **P<0.01 compared to the control. E Cells were incubated with 0, 0.5, 1, 5, 10 and 20 μM RA. At 24 h post-exposure, cells were washed with PBS. Equal amounts of cytosolic proteins (20 μg) were separated by 15% SDS-PAGE, transferred to a nitrocellulose membrane, and probed as described in "Materials and methods". Procaspase-3 and p17 fragment were detected by chemiluminescence. β-actin, used as internal control, was detected at the position corresponding to a molecular weight of 42 kDa. F The cells were treated with various concentrations of RA for 24 h; then the DNA was extracted, separated by electrophoresis on 1.2% agarose gel and visualized by staining with ethidium bromide. Lane 1, control; lane 2, 5 μM RA; lane 3, 10 μM RA; lane 4, 20 μM RA

Ceramide, as a second messenger, is generated by the hydrolysis of the cell membrane sphingomyelin or is derived from de novo synthesis in response to inducers of apoptosis (Bose et al. 1995). Previous studies have shown that ceramide

induces cell apoptosis by the mechanisms of activation of a ceramide-activated protein phosphatase (CAPP); moreover, ceramide up-regulates the apoptosis effector, Bax, or down-regulates the apoptosis inhibitor, Bcl-2, leading to caspase activation (Pinton et al. 2001; Kolesnick 2002; Von Haefen et al. 2002). To identify the possible mechanisms mediating RA-induced Leydig cell apoptosis we measured the cytotoxicity of RA in cell cultures in the presence or absence of the ceramide synthase inhibitor, fumonisin B1. As shown in Fig. 3B, fumonisin B1 treatment alone had no effect on cell survival. The apoptotic effect of RA was not mediated by ceramide because 50μM of this compound could not prevent the apoptotic effect of various concentrations of RA (5–10μM range). At 20μM RA there was an increase in ceramide generation providing evidence of necrotic death.

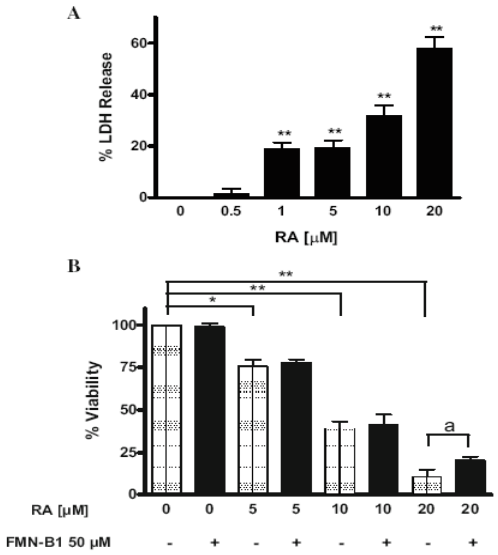

Fig.3 The effect of RA on LDH release and the effect of ceramide synthase inhibitor on TM-3 cell survival. A The TM-3 cells were treated with various concentrations of RA as indicated for 24 h, and the amount of LDH released was determined as described in "Materials and methods". B The cells were treated with various concentrations of RA (0, 5, 10 and 20 μM) with and without 50 μM fumonisin B1 (FMN-B1), a ceramide synthase inhibitor, for 24 h, and the cell viability was determined by MTT assay as described in "Materials and methods". The data represent means±SD of four independent experiments with triplicate well and are presented as a percentage of viable cells in the control sample. *P<0.05 compared to the control. **P<0.01 compared to the control. a P<0.05 compared to identical RA group

TM-3 cells were treated with RA and the lipid peroxidation was estimated by TBARS formation as described in "Materials and methods". RA treatment (0–1μM concentration range, for 24h treatment) did not considerably increase TBARS content

in cultured TM-3 cells, while RA doses higher than 1μM increased lipid peroxidation levels (Fig. 4A). In agreement with this, RA at higher doses (at μM doses) induced a decrease in cell viability (Fig. 1A). As higher RA doses induced lipid peroxidation and apoptosis, we decided to investigate only the effects of RA treatment at nM physiological concentrations in TM-3 cells. In order to investigate changes in antioxidant defences we measured the GST, SOD and CAT activities in RA treated and non treated TM-3 cells. GST activity increased with 10, 100 and 200nM RA (Fig. 4B), while SOD and CAT activities increased only with 100 and 200nM RA (Fig. 4C,D).

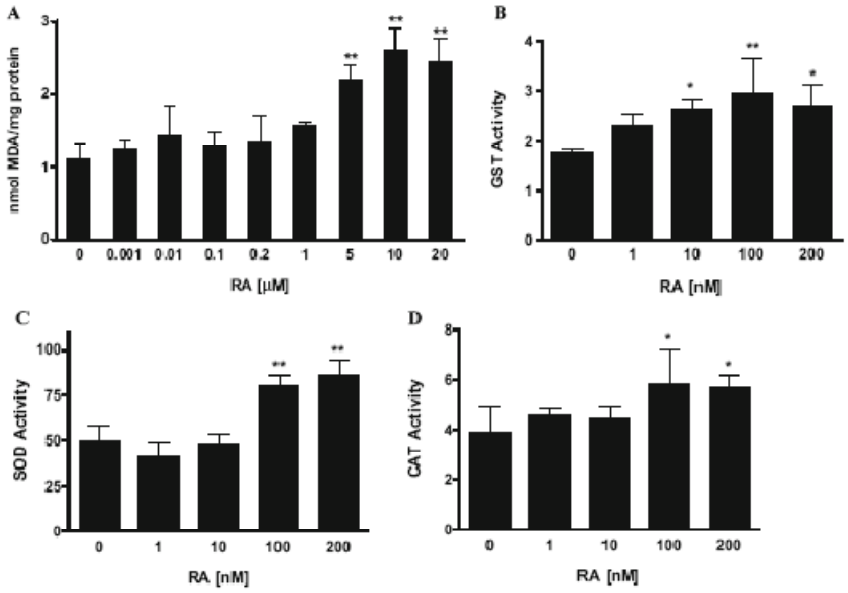

Fig.4 Determination of TBARS and antioxidant enzymes activities in TM-3 treated with RA for 24 h. A Cells were incubated with increasing concentrations of RA as indicated and lipid peroxidation was evaluated by TBARS assay as described in "Materials and methods". Cells were treated with the indicated concentrations of RA for 24 h and GST (B), SOD (C) e CAT (D) activities were measured as described in "Materials and methods". Enzymes activities are expressed as μmol substrate/min/mg protein. Results are presented as the mean±SD of three individual experiments. *P<0.05 compared to the control. **P<0.01 compared to the control.

Our data strongly suggest that RA induces apoptosis as determined by cytochrome c release from the mitochondria to bind to Apaf-1, which in turn initiates a caspase cascade, the executionary machinery of apoptotic cell death. Our results showed there was a measurable release of cytochrome c into the cytoplasm following exposure to RA. This release of cytochrome c may result in the activation of members of the

caspase family of proteases, another hallmark of apoptosis. Caspases, and in particular caspase-3, play a central role in the terminal biochemical events that ultimately lead to apoptotic cell death. We observed a dosedependent increase in caspase-3 activity after incubation for 24h with RA. As a consequence, DNA was cleaved by endonucleases, as observed by condensation and fragmentation of chromatin. Taken together, these observations suggest that RA activates the classic mitochondrial dependent apoptotic process. Since higher doses of RA (μM) induced lipid peroxidation and cell death, we decided to investigate only the effects of RA treatment at physiological doses in TM-3 cells. In order to investigate changes in antioxidant defences we measured the SOD, CAT and GST activities in TM-3 cells treated with RA. The SOD, CAT and GST activities increased with 100 and 200nM RA treatment. Interestingly, at these same doses RA did not increase lipid peroxidation and no effect on cell viability was observed. These findings suggest that RA increased the activity of antioxidant enzymes at physiological doses, thereby preventing oxidative cell damage which is manifest at higher doses of RA as may be evidenced by TBARS content and cell viability. In accordance with earlier studies (Livera et al. 2000) we observed no significant effect of 1μM RA on DNA fragmentation (date not shown). This concentration of RA was able, however, to decrease cell viability by 15–18% and trigger a low level of cytochrome c release indicating that 1μM RA could represent a threshold limit for non apoptosis inducing RA treatments. RA can also directly increase free radical generations which could result in increased lipid peroxidation (Davis et al. 1990). It is noteworthy that every antioxidant is in fact a redox agent, protecting against free radicals in some circumstances and promoting free radicals generation in others (Herbert 1996). Our results suggest the importance of keeping vitamin status within the normal range, as a deficit or administration of greater than the upper physiological limits could explain in part the adverse effects found in the literature. The concentrations of RA used in this study range from physiological to pharmacological plasma concentrations. RA is present constitutively in the plasma at a concentration of 4–14nM (De Leen Heer et

al. 1982; Kane et al. 2005). Pharmacological RA doses result in transient plasma concentration in the same μM range at which we observed TBARS formation and decreased cell viability.

2. Proliferative and anti-proliferative effects of atRA in Leydig MLTC-1/R2C/TM-3 cells

The pro-oxidant retinoid molecules, the mechanisms underlying their pro-oxidant effects, and their consequences on cell proliferation or death remain to be better elucidated. Indeed, despite the important physiological functions of retinoids, the effects of supra-physiological doses of retinoids as well as their physiological action are not well defined. In an interesting work, Hurnanen et al. (1997) showed that low RA concentrations stimulated growth proliferation, but high concentrations inhibited proliferation in human breast cancer cells. In the present work we show that RA, at endogenous concentrations (0–250 nM), increases cell viability in tumor Leydig cell lines but not in the normal TM-3 counterpart. This suggests that slight variations in the concentrations of RA may trigger changes in the cellular redox state. The ability to survive the threat posed by endogenous levels of retinoids represents a biological adaptation, in many cases, to survival (Hayes & McLellan 1999). Strategies such as sequestration, scavenging and binding, and catalytic biotransformation have evolved as important biochemical protection mechanisms against toxic chemical species. Cells possess an impressive array of enzymes capable of bio-transforming a wide range of different chemical structures and functionalities. Since higher doses of RA induced apoptosis, we decided to investigate only the effects of low doses of RA treatment in TM-3, MLTC-1 and R2C cells showing that physiological levels of RA trigger proliferation and growth of the testicular tumoral mass.

As shown in Fig. 1, treatment of MLTC-1 (A) and R2C (B) with RA resulted in a significant cell proliferation in a concentration range of 10–250 nM with a slight but not significant decrement at 500 nM RA (≈10%) compared to the control. Although

the data show dose dependence, no time dependence could be addresses as there is no difference in proliferation between 72 and 48 h. No change in cell viability was observed in RA treated TM-3 (C). In order to investigate a potential modulation of the antioxidant defenses, cell lines were treated with RA (0–200 nM) for 6 h and the activities of CAT and GST were assayed comparing RA treated TM-3, MLTC-1 and R2C versus untreated ones (control). No modulation of these activities was reported in TM-3 at any RA concentration while CAT and cytosolic GST activities increased significantly both in MLTC-1 and R2C in a dose dependent manner (Fig. 2A and B). The mitochondrial GST (mGST) activity increased in both MLTC-1 and R2C, in particular at 100 nM (Fig. 2C).

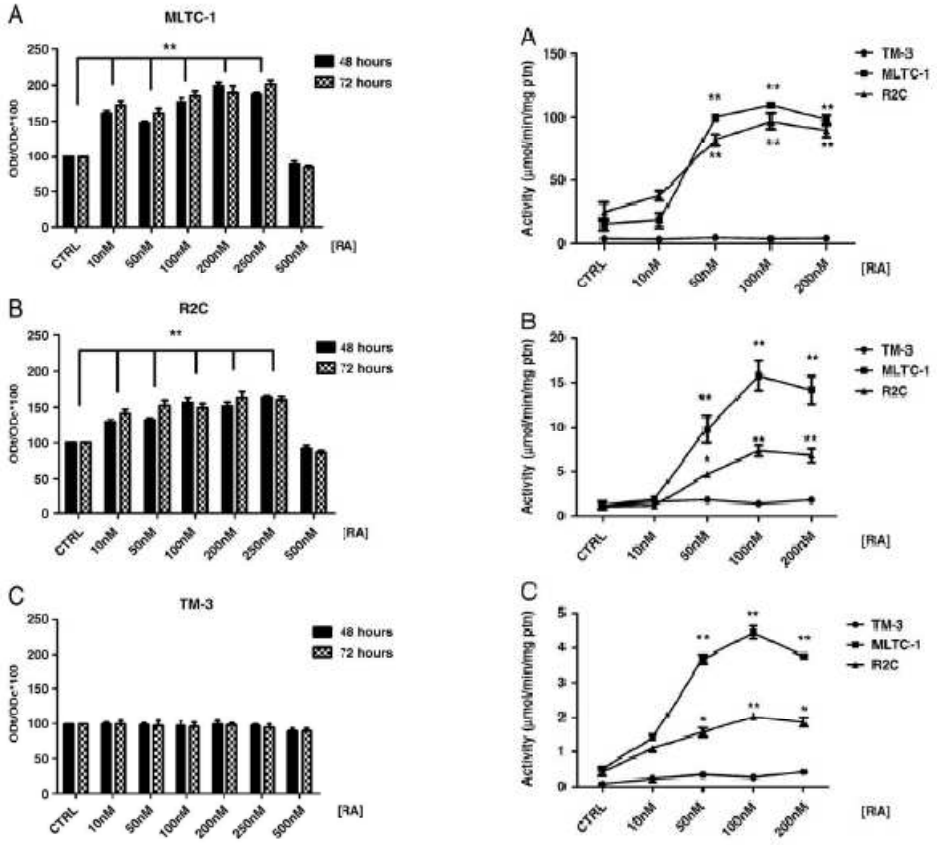

Fig.1 Cell viability by MTT assayMLTC-1 (A),R2C (B) and TM-3 (C) cellswere incubated at the indicated concentrations of RA. Cell viability was determined by MTT assay as described inMaterials and methods at 48 and 72 h post-exposure. **Fig.2** Antioxidant enzyme activity Cells were treated at the indicated concentrations of RA for 6 h and CAT (A), GST (B) and mitochondrial GST (C) activities were measured as described in Materials and methods. Enzyme activity is expressed as μmol substrate/min/mg protein. Results are presented as the mean±SD of three individual experiments. *P<0.05, **P<0.01 compared to the control.

Moreover, activation of the anti-apoptotic factor Akt was assayed by WB using an antibody raised against its phosphorylated form(p-Akt). As shown in Fig. 3A, 10 nM RA induced a rapid activation of p-Akt after 15 min of incubation. A strong signal of p-Akt was reported in MLTC-1 and R2C with no activation of ERK (Fig. 3B). Furthermore, RA supplementation increased cyclin D1 protein levels both in MLTC 1 and R2C cell lines (Fig. 3C) with a concomitant decrement of p21 expression already at 10 nM RA and in both MLTC-1 and R2C after 48 h treatment (Fig. 3D). Neither Akt was activated nor p21 levels modified in the TM-3.

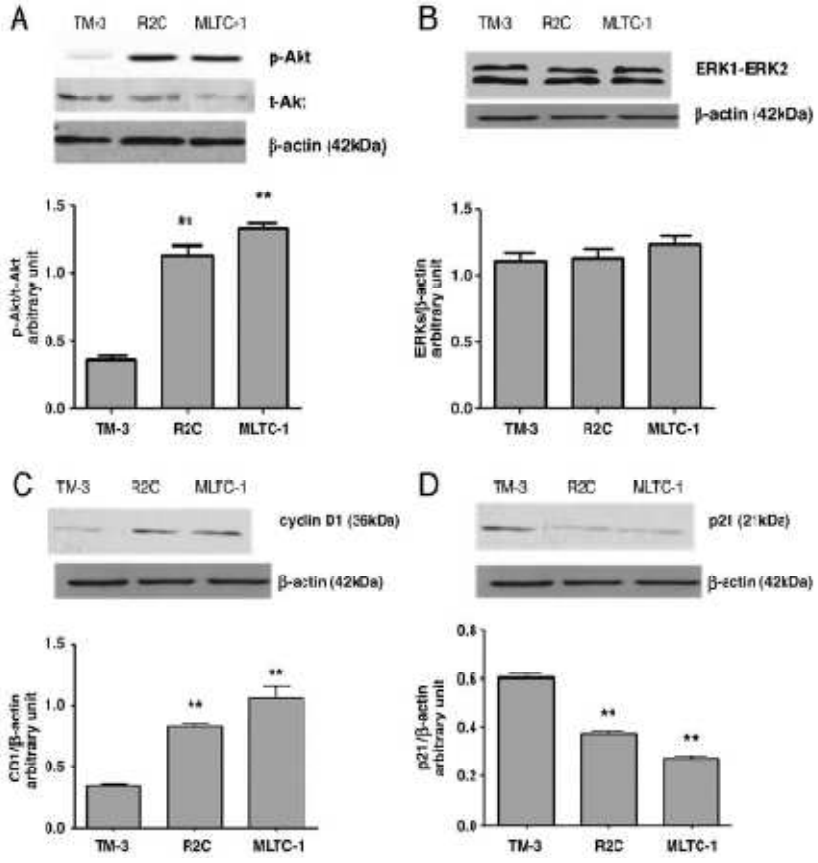

Fig.3 Effect of RA on IP3K/Akt signaling pathways and cell cycle progression TM-3, R2C, MLTC-1 cells were incubated in the presence of 10 nM RA for 48 h. After incubation, cells were washed with PBS; 50 μg of protein was separated by 15% SDS-PAGE, transferred to a nitrocellulose membrane, and blotted as described in Materials and methods. β-Actin was used as internal control. Activation of p-Akt after 15 min (A). No activation of ERK1/2 pathway (B). Up-regulation of cyclin D1 (C). Down-regulation of p21 (D). Protein content was determined densitometrically. Results are presented as the mean±SD of three independent experiments. **Pb0.01 compared to the normal TM-3 cell line (as control).

As to pharmacological treatment with RA of MLTC-1/R2C, 1 μMRA for 24 h resulted in disruption of mitochondrial membrane potential evidenced with a change in the emission of the lipophilic dye JC-1 (Fig. 4A and B) turning more towards green than red. At the same time, cytochrome c release occurred already at 0.5 μM RA (Fig. 4C) followed by no activation of caspases 3 and 9 (data not shown) while the amount of mitochondrial ATP decreased after 24 h treatment with RA 0.5 and 1 μM in dose-dependent manner (Table 1).

	ATP concentration (nM)
MLTC-1 DMSO	10.20± 0.32
MLTC-1 0.5 μM RA	4.12± 0.11
MLTC-1 1 μM RA	2.23± 0.13
R2C DMSO	10.84± 0.42
R2C 0.5 μM RA	5.41± 0.26
R2C 1 μM RA	3.78± 0.19

Table 1 Mitochondrial ATP determination. Cells were treated with 0.5–1 μM RA for 24 h and mitochondrial ATP amount was determined as described in Materials and methods. Data are presented as mean±SD of triplicate experiments.

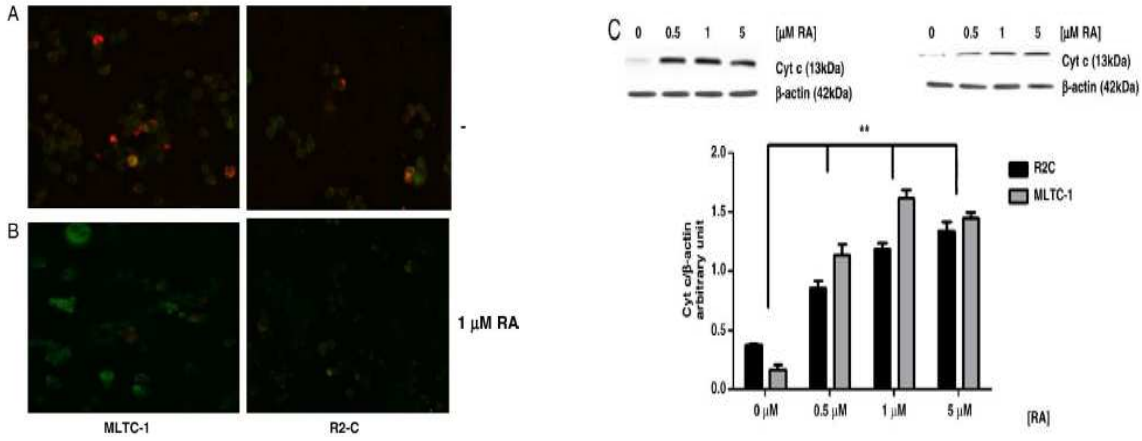

Fig.4 Mitochondria involvement MLTC-1 and R2C cells were treated with 1 μMRA for 24 h and, after washing in ice-cold PBS, incubated with 10 mMJC-1 at 37 °C for 20 min in a 5% CO_2 incubator. The cells were washed twice with PBS and analyzed by fluorescent microscopy. In control non-apoptotic cells, the dye stains the mitochondria in red (A). In treated apoptotic cells, JC-1 remains in the cytoplasm fluorescing green (B). MLTC-1 and R2C were treated for 24 h with 0.5–1–5 μMRA and cytochrome c was detected (C). β-Actin was used as loading control. Figure is representative of three independent experiments.

To identify the potential direct induction of autophagy at 0.5 μM RA, after 24 h treatment, TM-3 cells were labeled with MDC, the selective stain for

autophagosomes (Fig. 5A and B). Moreover it is worthy to note that a specific concentration range of RA (10–200 nM) induces cell proliferation and that a clear threshold value discriminating the proliferative from the anti-proliferative effect of RA does exist in our experimental system. In fact, at 0.5 μM RA we observed the activation of the autophagy process (Fig. 5) which in turns plays a critical role in removing damaged or surplus organelles in order to maintain cellular homeostasis. Autophagy sometimes occurs with apoptosis: the relationship between autophagy and cell death is complex, since autophagy can be involved either in cell death or in survival depending on the cellular context (Alva et al. 2004). Both apoptosis and autophagy can occur concomitantly in the same cells, suggesting the involvement of common regulatory mechanisms (Kondo et al 2005).

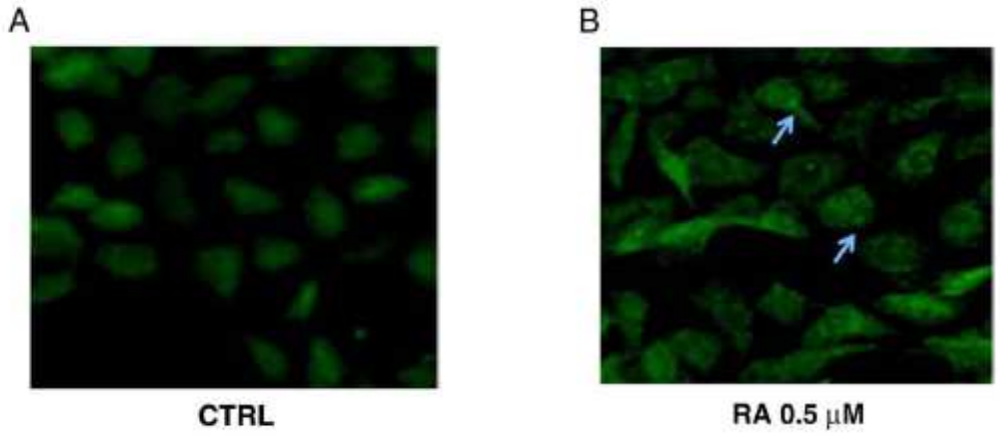

Fig. 5 Autophagy in TM-3 Leydig cells by MDC labeling TM-3 cells were treated with 0.5 μM RA and were incubated for 24 h. Cells were stained with MDC as detailed under Materials and methods. Figure is representative of three independent experiments.

It is documented that when the change in mitochondrial membranes permeability entails less than 66% of the mitochondria, the autophagic pathway is activated, while the apoptotic death is triggered when the percentage raises toward higher values involving most of the mitochondrial population (Alva et al. 2004). Besides that, in both cases, a change of permeability causes swelling and depolarization of the mitochondrial membranes, impairing the oxidative phosphorylation capability. The latter leads to reduced ATP production and a consequent depletion of ATP levels. It

is hypothesized that amino-acidic and insulin regulation (Scorrano 2009) can act in a synergistic manner in the control of autophagy. In our experimental system, treatment for 24 h with 0.5 μM RA triggers disruption of mitochondrial membrane potential (Fig. 4A and B) with release of cytochrome c followed by no activation of caspase 3 and 9 (data not shown) with a notable decrease in endogenous mitochondrial ATP, as shown in Table 1, and cytosolic vacuolization, hallmark of autophagy.

A model outlining the dual proliferative/anti-proliferative effects of RA is described by Schug et al. (2007). CRABP-II and FABP5 target RA to RAR and PPARβ/δ, respectively. In cells that express a high CRABP-II/ FABP5 ratio, RA is 'channeled' to RAR, often resulting in growth inhibition. Conversely, in the presence of a low CRABP-II/FABP5 expression ratio, RA is targeted to PPARβ/δ, thereby up-regulating survival pathways. On these bases the ability of nanomolar doses of RA to modulate FABP5 and CRABPII were investigated in MLTC-1. A 10 nM RA induced a significant up-regulation of FABP-5 mRNA levels after 12 h while the same treatment does no elicit any effect after 24 h. No changes in the CRABPII mRNA were observed in presence of 10 nM RA after 12 and 24 h (Fig. 6). These results provide further strength to the hypothesis of altered retinoid homeostasis/metabolism in neoplastic diseases.

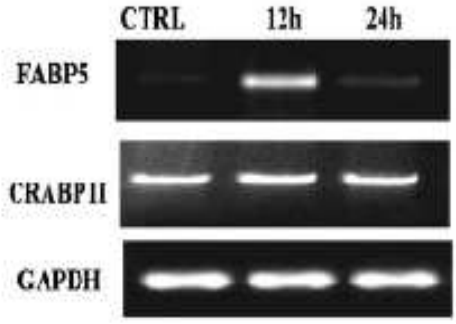

Fig.6 Influence of RA on FABP5 and CRABP II mRNA expressions FABP5 and CRABP II mRNA expression in MLTC-1 cells treated with 10 nM RA for 12/24 h.

Upon treatment with 1 μMRA, we observed a significant induction of cell death by apoptosis. Changes in mitochondrial membrane permeability are concomitant with

collapse of the electrochemical gradient across the mitochondrial membrane through the formation of pores leading to the release of cytochrome c, followed by cleavage of procaspase-9 and DNA fragmentation highlighted by TUNEL assay. This cascade of events was caused by pharmacological doses of RA in both MLTC-1/R2C cells, as already documented in TM-3 (Tucci et al. 2008). As shown in Fig. 7A, tumoral cell lines suffered cell death induction after treatment with 1 and 5 μMRA for 24 h; treatment with 10 μMRA for 24 h resulted in almost 80% reduction of cell viability with a massive decrement of cell growth both in MLTC-1 and R2C, supported by activation of caspase 9 already at RA 1 μM (Table 2).

Treatment	Cell line	% of Caspase-9 activation	SD
CTRL	MLTC-1	12.34	±2.76
RA 1 μM	MLTC-1	25.87	±0.56
RA 5 μM	MLTC-1	28.75	±1.86
RA 10 μM	MLTC-1	37.13	±2.12
CTRL	R2C	15.45	±1.85
RA 1 μM	R2C	27.82	±1.12
RA 5 μM	R2C	24.65	±0.92
RA 10 μM	R2C	32.64	±3.17

Table 2 Caspase 9 activation. MLTC-1 and R2C cells were stimulated for 24 h by the presence of 1–5–10 μM RA. The activation of caspase-9 was analyzed by flow cytometry. Data are presented as mean±SD of triplicate experiments.

To further verify the activation of the programmed cell death, apoptosis in MLTC-1 and R2C was determined by enzymatic labeling of DNA strand breaks via TUNEL assay (Fig. 7B) supporting the already known RA mediated apoptosis induction (Tucci et al. 2008).

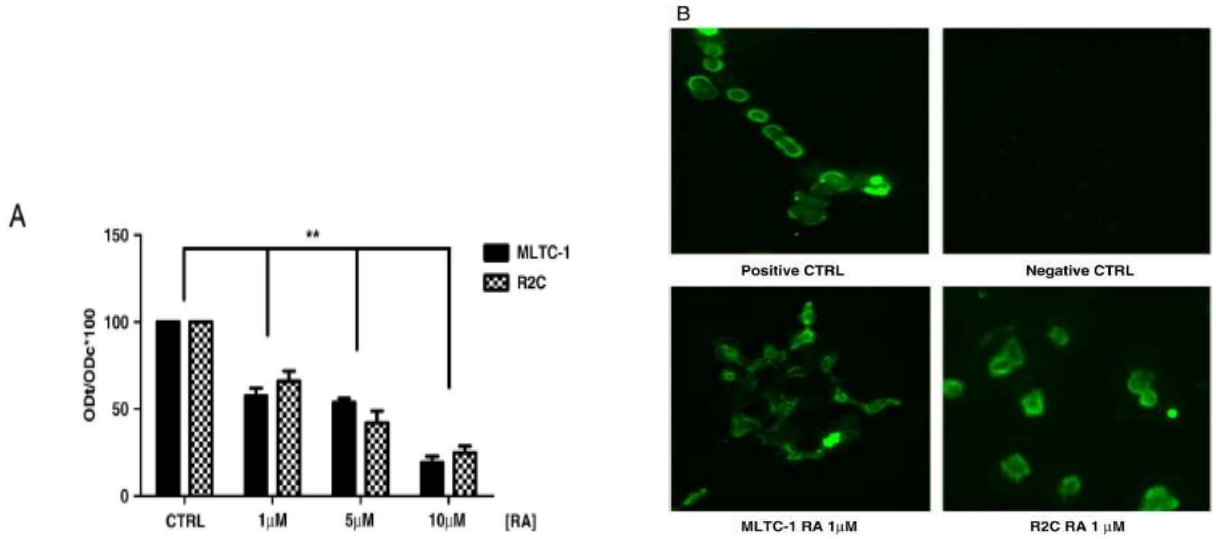

Fig.7 Apoptosis in MLTC-1/R2C cell lines induced with 1–10 μMRA after 24 h incubation MLTC-1 and R2C cells were stimulated for 24 h by the presence of 1, 5 or 10 μMRA. Viability was analyzed by MTT assay (A). Data are presented as mean±SD of triplicate experiments. **Pb0.01 compared to the control. Apoptosis in MLTC-1 and R2C cells was determined by TUNEL assay after treatment with 1 μM RA (B). Figure is representative of three independent experiments.

3. AtRA binds and inhibits 2-oxoglutarate carrier

Previously it has been demonstrated that mitochondria from rat testes (Genchi & Olson 2001; Cione & Genchi 2004) and TM-3 cells (Cione et al. 2005) were extremely active in incorporating retinoic acid. Moreover, it was highlighted how the retinoylation reaction and testosterone biosynthesis are positively correlated when Leydig cell cultures are incubated with 100nM atRA (Tucci et al. 2008). As the biosynthetic steps that lead to testosterone production are mainly NADH/NADPH dependent, the 2-Oxoglutarate carrier (OGC) activity from mitochondria extracted both from whole rat testes and Leydig TM-3 cells, was chosen as the experimental target for its involvement in the malate-aspartate and oxoglutarate–isocitrate shuttle to provide for the necessary exchange of reducing equivalents between the mitochondria and the cytosol. The efforts were focused on the OGC from rat testes as the retinoylation process is more efficient in this tissue and testosterone production in TM-3 positively correlates to atRA supplementation. In addition, the inhibitory effect given by 2-Cyano-4-hydroxycinnamate (an inhibitor of OGC) but not by 1,2,3-benzentricarboxylate (an inhibitor of citrate carrier) on the retinoylation processes

(as highlighted in Table 1) was the start point for further investigation in this work. Indeed, 2-Cyano-4-hydroxycinnamate shows 45% inhibition when used at a concentration of 5mM, while, at the same concentration 1,2,3-benzentricarboxylate has a very weak effect (12% inhibition). In proteoliposomes OGC has been shown to exist as a homodimer and to function according to a sequential antiport mechanism, catalyzing the transport of 2-oxoglutarate in electroneutral exchange for some other dicarboxylates to which malate is bound with the highest affinity. These results have been interpreted by assuming two separate and coordinated substrate translocation pathways, one in each monomer.

Carrier Inhibitors on Retinoylation Reaction	pmol/mg ptn x 90 minutes	SEM	*n*	% Inhibition
Control	21,47	2,44	23	
Mersalyl 1 mM	1,84	0,09	5	91,43
NEM 5 mM	2,47	0,28	5	88,49
2-Cyano-4-hydroxycinnamate 5mM	11,90	1,23	3	44,58
1,2,3-Benzenetricarboxylate 5mM	18,93	1,99	3	11,83

Table 1. Effect of Mitochondrial Carrier Inhibitors on Retinoylation Reaction.
Mitochondria from testes were incubated for 90 minutes in a buffer as decribed in Methods with ^{3}HatRA, 100nM final concentration, at 37 °C. Then the reaction was stopped with TCA and the radioactivity detected in a liquid scintillation counter. Results are presented as Mean ± SEM of three indipendent experiments. **P< 0.01 compared to the control. 1,2,3-Benzenetricarboxylate P >0.05

Our results showed that transport activity of OGC from rat testes mitochondria was strongly influenced by the sulphydryl group reagent N-ethyl-maleimmide (NEM) and atRA. NEM, at 5mM, markedly reduced the OGC activity by 47%. A similar inhibition of 51% was highlighted at 100nM atRA, and when the two compounds are co-incubated the activity was reduced to 49%, equal to RA alone as shown in Fig. 1A. In humans, cows and rats there is only one gene encoding OCG; according to the amino acid sequence the bovine OGC protein contains three cysteines: Cys184 located in TMS IV and Cys221 and Cys224 in TMS V. Mercurials and maleimides interact only with Cys184 of the purified and reconstituted OGC, as Cys221 and Cys224 are linked by a disulphide bridge (Palmieri, 2004). Therefore we propose that

atRA, via retinoylation reaction, could bind the OGC on the same residue (Cys184), as the inhibitory effect of atRA is still the same when NEM is present concomitantly as shown in Fig. 1A, leading us to hypothesize the existence of a putative amino acid sequence related to the atRA binding site in OGC. For what concerns OGC and its involvement in testosterone biosynthesis, the first enzymatic step is to convert cholesterol in pregnenolone: the reaction occurs in the mitochondrial matrix and requires reducing equivalents mainly as NADPH. Conversely the role of the OGC is to carry out reducing equivalents from the mitochondria to the cytoplasm. Previously it was demonstrated that there is a positive correlation between retinoylation reaction and testosterone biosynthesis (Tucci et al. 2008): the action of RA to slow down the OGC transport activity is in agreement with the testosterone synthetic process as reducing equivalents are more necessary to convert cholesterol in the matrix rather than in the cytoplasm (Stocco 2001). At the same time the retinoylation reaction is tightly dependent on the pH: in fact the inhibitory effect of atRA on OGC is lost when the pH is higher than 7.5 (Fig. 1B) as predicted by the general condition of retinoylation described by Cione and Genchi (2004). To gain insight into the interaction of atRA and OGC two separate assays could have been performed: the first through photolabeled testes mitochondrial protein with ^{3}HatRA, because atRA binds covalently to proteins under UV light exposure (Bernstein et al. 1995), and the second via retinoylation reaction with ^{3}HatRA (Takahashi and Breitman, 1990). Performing the latter we observed how the ^{3}HatRA binding to a 31.5 KDa protein was prevented by 2-oxoglutarate, the specific OGC substrate (Fig. 1C). Fluorography of the electrophoresed proteins revealed the labeling of very few mitochondrial proteins. Indeed it was observed that the labeling of the 31.5-kDa protein was prevented when 2-oxoglutarate was added demonstrating that OGC was labeled by ^{3}HatRA. It is presumed that the binding is covalent on the basis of the work of Takahashi & Breitman (1989). Under normal conditions, atRA is present in the testes at nanomolar concentrations (Kane et al. 2008). Our results show that, only in mitochondria derived from the Leydig TM-3 cell line, does atRA have effects on

OGC at concentration of 10nM and in a stronger manner inhibit the OGC activity at a concentration of 100nM: OGC activity decreased to 54% of control values with 10nM atRA and 38% of control values when atRA was used at a concentration of 100nM (Fig. 1D). Interestingly, the concentrations of atRA required for producing this effect in steroidogenic cells are lower than those required with mitochondria isolated from the whole organ, supporting the above-mentioned view that steroidogenic cells can be more sensitive to atRA than isolated mitochondria as no effect was highlighted at 10nM of atRA on OGC extracted from whole tissue (Fig. 1E). In addition 13-*cis* RA has been shown as a competitive inhibitor of atRA in the retinoylation process (Ki =13.50 nM) (Cione & Genchi, 2004). In this case 13-*cis* RA exerts its effects of reducing OGC transport activity on mitochondria from whole tissue at a lower concentration than atRA (Fig. 1F): 10nM 13-*cis* RA was more active in inhibiting OGC activity than atRA, most likely thanks to the altered conformation of this isomer that may allow it to better interact with OGC both in mitochondria from cultured cells or whole tissue (Fig. 1G). Our study, along with others (Rial et al. 1999; Radominska-Pandya et al. 2000), suggests that specific interactions among retinoids and non-nuclear receptor proteins, such as PKC, ANT and OGC, which are different from nuclear receptors, take place. Thus, the extra-nuclear action of retinoids seems to be a more general and important phenomena leading to both physiological and also pharmacological relevance.

It is known that retinoids play an essential role in spermatogenesis in rodents. In fact, a vitamin A-deficient diet causes the cessation of spermatogenesis, loss of mature germ cells and a reduction in testosterone level in mice and rat testes (Wolbach & Howe, 1925; Appling & Chytil, 1981). There is argument in favour of biological action of atRA through OGC binding and inhibition. AtRA does not exist in the cell in free form but is bound to proteins such as cellular retinoic acid binding protein (CRABP). The unexpected discovery of the existence of a CRABP associated with mitochondria that binds and keeps retinoic acid in the organelle has been described (Ruff & Ong 2000). CRABP had been studied for 25 years and has always been

presented as a soluble, presumably cytosolic, protein and mitochondria had not previously been considered to have any role in RA function or metabolism. The only demonstrated function for CRABP is to bind RA. Since this protein is associated with mitochondria, this implies that mitochondria participate in RA management. This mitochondrial CRABP could explain how retinoic acids could concentrate and regulate OGC in the mitochondrial compartment in vivo. The influence of atRA on OGC via retinoylation might therefore be another level of control in steroidogenesis.

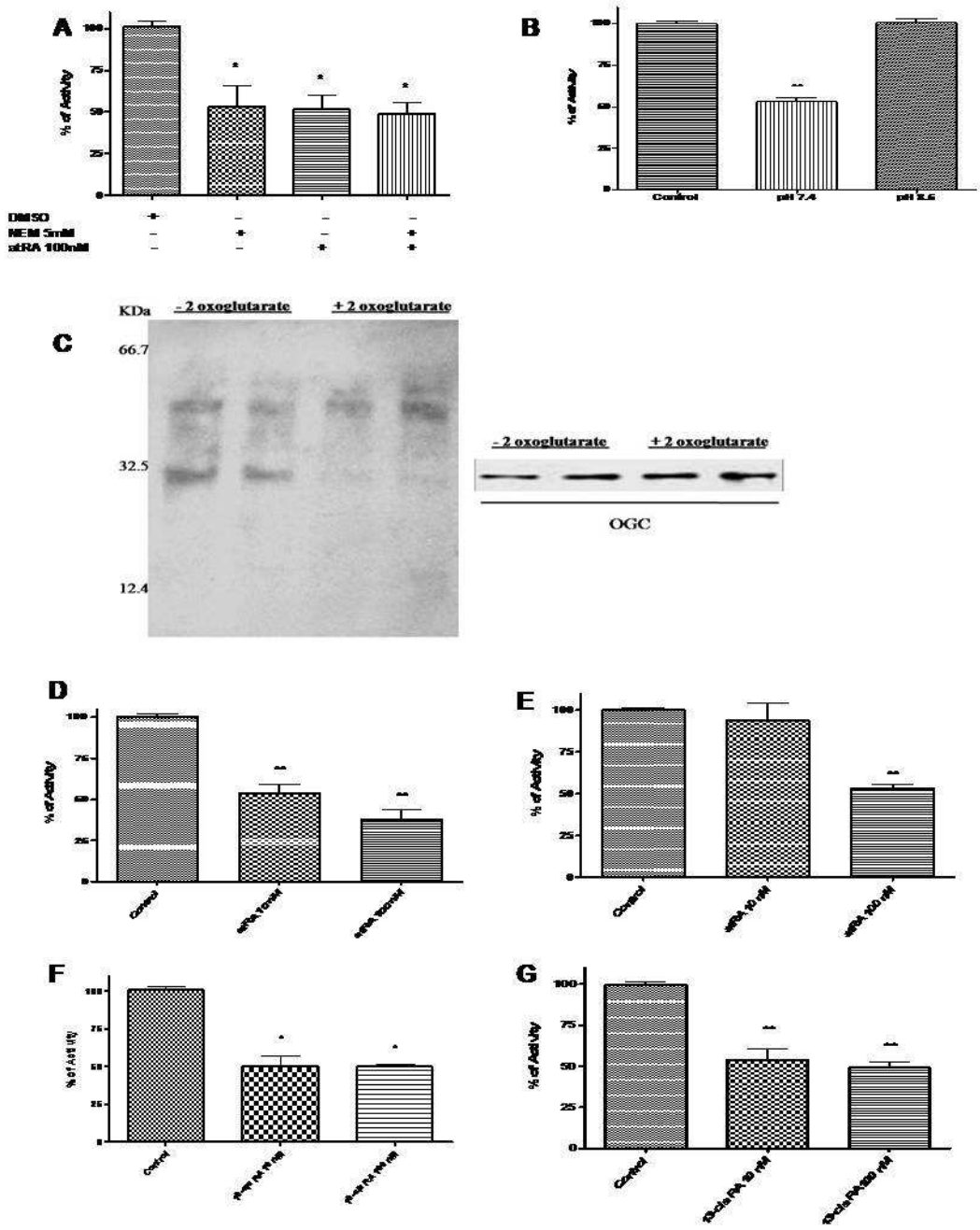

Figure 1. Mitochondria from rat testes were incubated for 90 minutes , at 37 °C , in a buffer with: **(A)** ATP, CoA (control) supplemented with atRA, 100nM final concentration and atRA + NEM 5mM and **(B)** ATP, CoA and atRA 100nM at different pH values. (C) Testes mitochondrial protein labeled with ^{3}HatRA by retinoylation process as described in Materials and Methods. In fluorography, the lanes 1 and 2 correspond to 20 µg of mitochondrial testes protein labeled with ^{3}HatRA. In lanes 3 and 4, 10mM of 2-oxoglutarate was added to 20 µg of mitochondrial testes protein together with ^{3}HatRA. OGC presence was verified by immunoblotting. **(D)**OGC activity from TM-3 cell line after atRA supplementation **(E)** Effect on OGC activity of different concentrations of atRA in mitochondria from testes incubated at 37 °C for 90 min. Effect on OGC after treatment of mitochondria from TM-3 **(F)** and testes **(G)** with 13-*cis* RA. OGC was extracted as decribed in Materials. After extraction and reconstitution into liposomes the exchange activity was assayed by adding ^{14}C 2-oxo-glutarate 0.1mM. Results are presented as Mean ± SEM of three independent experiments. * P< 0.05 .**P<0.01

4. Combined low doses of PPARγ and RXR ligands trigger an intrinsic apoptotic pathway in human breast cancer cells

Recently, studies in human cultured breast cancer cells have shown how thiazolidinediones (TZD), Rosiglitazone (BRL), promotes antiproliferative effects and activates different molecular pathways leading to distinct apoptotic processes (Bonofiglio et al. 2005, 2006, 2009). Previous data show that the combination of PPARγ ligand with either ATRA or 9-*cis*-retinoic acid (9RA) can induce apoptosis in some breast cancer cells (Elstner et al. 2002). Furthermore, Elstner *et al*. demonstrated that the combination of these drugs at micromolar concentrations reduced tumor mass without any toxic effects in mice (Elnster et al. 1998). The ability of PPARγ ligands to induce differentiation and apoptosis in a variety of cancer cell types, as in human lung (Tsubouchi et al. 2000), colon (Kitamura et al. 1999) and breast (Mueller et al. 1998) has been exploited in experimental cancer therapies (Roberts-Thomson 2000). PPARγ agonist administration in liposarcoma patients resulted in histologic and biochemical differentiation markers *in vivo* (Demetri et al. 1999). However, a pilot study of short-term therapy with PPARγ ligand Rosiglitazone in early-stage breast cancer patients does not elicit significant effects on tumor cell proliferation, although the changes observed in PPARγ expression may be relevant to breast cancer progression (Yee et al. 2007). However, in humans PPARγ agonists at high doses exert many side effects including weight gain due to increased adiposity, edema, hemodilution, and plasma-volume expansion, which preclude their clinical application in patients with heart failure (Arakawa et al. 2004; Rangwala & Lazar 2004; Staels 2005). On the other hand, the natural ligand for RXR, 9cRA (Leblanc & Stunnenberg, 1995) has been effective *in vitro* against many types of cancer, including breast tumor (Crouch et al. 1991; Rubin et al. 1994; Sun et al.1997; Wu et al. 1997). Recently, RXR-selective ligands were discovered to inhibit proliferation of ATRA-resistant breast cancer cells *in vitro* and caused regression of the disease in animal models (Bishoff et al. 1998). The undesirable effects of RXR-specific ligands on hypertriglyceridemia and suppression of the thyroid hormone axis have been also

reported (Pinaire & Reifel-Miller 2007). The additive antitumoral effects of PPARγ and RXR agonists, both at elevated doses, have been shown in human breast cancer cells (Elstner et al. 2002; Grommes et al. 2004). However, high doses of both ligands have remarkable side effects in humans such as, weight gain and plasma volume expansion for PPARγ ligands (Arakawa et al. 2004; Rangwala & Lazar 2004; Staels 2005) and hypertriglyceridemia and suppression of the thyroid hormone axis for RXR ligands (Pinaire & Reifel-Miller 2007). Thus, in the present study it has been demonstrated that nanomolar concentrations of BRL and 9RA in combination do not induce noticeable influences in cell vitality on normal breast epithelial cells, whereas they exert significant antiproliferative effects on breast cancer cells. The molecular mechanism by which combined treatment with BRL and 9RA at nanomolar doses triggers apoptotic events in breast cancer cells, have been elucidated, suggesting potential therapeutical uses for these compounds.

To investigate whether low doses of combined agents are able to inhibit cell growth, the capability of 100nM BRL and 50nM 9cRA to affect normal and malignant breast cell lines was first assessed. We observed that treatment with BRL alone does not elicit any significant effect on cell viability in all breast cell lines tested, while 9RA alone reduces cell vitality only in T-47D cells (Fig. 4A). In the presence of both ligands cell viability is strongly reduced in all breast cancer cells: MCF-7, its variant MCF-7TR1, SKBR-3 and T-47D, while MCF-10 normal breast epithelial cells are completely unaffected (Fig. 4A). To evaluate the effectiveness of both ligands in the presence of serum, we performed MTT ([3-(4,5-dimethylthiazol-2-yl)-2,5-diphenyl tetrazolium bromide]) assay in MCF7 cells treated with low doses of BRL and 9RA in SFM (serum free media) as well as in 5% CT-FBS (Fig. 4B). The molecular mechanism underlying these effects has been elucidated in MCF-7 cells in which an upregulation of tumor suppressor gene p53 has been observed. A significant increase in p53 and $p21^{WAF1/Cip1}$ content was observed by Western Blot only upon combined treatment after 24 and 36 h (Fig. 4C). Furthermore, we showed an upregulation of p53 and $p21^{WAF1/Cip1}$ mRNA levels induced by BRL plus 9RA after 12 and 24 h (Fig.

4D). To investigate whether low doses of BRL and 9RA are able to transactivate the p53 promoter gene, we transiently transfected MCF-7 cells with a luciferase reporter construct (named p53-1) containing the upstream region of the p53 gene spanning from -1800 to +12 (Fig. 4E). Treatment for 24 h with 100nM BRL or 50nM 9RA did not induce luciferase expression, whereas the presence of both ligands increased in the transactivation of p53-1 promoter (Fig. 4F). To identify the region within the p53 promoter responsible for its transactivation, we used constructs with deletions to different binding sites such as CTF-1, nuclear factor-Y (NF-Y), NF*k*B and GC sites (Fig. 4E). In transfection experiments performed using the mutants p53-6 and p53-13 encoding the regions from -106 to +12 and from -106 to -40, respectively, the responsiveness to BRL plus 9RA was still observed (Fig. 4F). In contrast, a construct with a deletion in the NF*k*B domain (p53-14) encoding the sequence from -106 to -49, the transactivation of p53 by both ligands was absent (Fig. 4F), suggesting that NF*k*B site is required for p53 transcriptional activity. To gain further insight into the involvement of NF*k*B site in the p53 transcriptional response to BRL plus 9RA, we performed electrophoretic mobility shift assay experiments using syntethic oligodeoxyribonucleotides corresponding to the NF*k*B sequence within p53 promoter. We observed the formation of a specific DNA binding complex in nuclear extracts from MCF-7 cells (Fig. 5A, lane 1), where specificity is supported by the abrogation of the complex by 100-fold molar excess of unlabeled probe (Fig. 5A, lane 2). BRL treatment induced a slightly increase in the specific band (Fig. 5A, lane 3), while no changes were observed on 9cRA exposure (Fig. 5A, lane 4). The combined treatment increased the DNA binding complex (Fig. 5A, lane 5), which was immunodepleted and supershifted using anti-PPARγ (Fig. 5A, lane 6) or anti-RXRα (Fig. 5A, lane 7) antibodies. These data indicate that heterodimer PPARγ/RXRα binds to NF*k*B site located in the promoter of p53 *in vitro*. The interaction of both nuclear receptors with the p53 promoter was further elucidated by chromatin immunoprecipitation assays. Using anti-PPARγ and anti-RXRα antibodies, protein-chromatin complexes were immunoprecipitated from MCF-7 cells treated with 100nM BRL and 50nM 9cRA.

PCR was used to determine the recruitment of PPARγ and RXRα to the p53 region containing the NF*k*B sequence. The results indicated that either PPARγ or RXRα was constitutively bound to the p53 promoter in untreated cells and this recruitment was increased on BRL plus 9cRA exposure (Fig. 5B). Similarly an augmented RNA-Pol II recruitment was obtained by immunoprecipitating cells with an ANTI-RNA-Pol II antibody indicating that a positive regulation of p53 transcription activity was induced by combined treatment (Fig. 5B). The role of p53 signaling in the intrinsic apoptotic cascades involves a mitochondria-dependent process, which results in cytochrome *C* release and activation of caspase-9. Because disruption of mitochondrial integrity is one of the early events leading to apoptosis, we assessed whether BRL plus 9RA could affect the function of mitochondria by analyzing membrane potential with a mitochondria fluorescent dye JC-1 (Cossarizza et al. 1997). In non-apoptotic cells (control) the intact mitochondrial membrane potential allows the accumulation of lipophilic dye in aggregated form in mitochondria which display red fluorescence. MCF-7 cells treated with 100nM BRL or 50nM 9cRA exhibit red fluorescence indicating intact mitochondrial membrane potential (data not shown). Cells treated with both ligands exhibit green fluorescence indicating disrupted mitochondrial membrane potential where JC-1 cannot accumulate within the mitochondria, but instead remains as a monomer in the cytoplasm (Fig. 5C). Changes in mitochondrial membrane permeability, an important step in the induction of cellular apoptosis, is concomitant with the collapse of the electrochemical gradient across the mitochondrial membrane through the formation of pores in the mitochondria leading to the release of cytochrome *C* into the cytoplasm, and subsequently with cleavage of procaspase-9. This cascade of events, featuring the mitochondria-mediated death pathway, were detected in BRL plus 9RA-treated MCF-7 cells. Concomitantly, cytochrome *C* release from mitochondria into the cytosol, a critical step in the apoptotic cascade, was demonstrated after combined treatment (Fig. 5D). BRL and 9RA at nanomolar concentration did not induce any effects on caspase-9 separately, but activation was observed in the presence of both

compounds (Table 7A). No effects were elicited by either the combined or the separate treatment on caspase-8 activation, a marker of extrinsic apoptotic pathway (Table 7B). The activation of caspase 9, in the presence of no changes in the biological activity of caspase 8, support that in our experimental model only the intrinsic apoptotic pathway is the effector of the combined treatment with the two ligands. Since inter-nucleosomal DNA degradation is considered a diagnostic hallmark of cells undergoing apoptosis, we studied DNA fragmentation under BRL plus 9cRA treatment in MCF-7 cells, observing that the induced apoptosis was prevented by either the specific antagonist of PPARγ GW9662 (GW) or by AS/p53, which is able to abolish p53 expression (Fig. 5E). Finally, we examined in three additional human breast malignant cell lines: MCF-7 TR1, SKBR-3 and T-47D the capability of low doses of a PPARγ and an RXR ligand to trigger apoptosis. DNA fragmentation assay showed that only in the presence of combined treatment did cells undergo apoptosis in a p53-mediated manner (Fig. 5F), implicating a general mechanism in breast carcinoma. The crucial role of p53 gene in mediating apoptosis supported by the evidence that the effects on the apoptotic cascade were abrogated in the presence of AS/p53 in all breast cancer cell lines tested, including tamoxifen resistant breast cancer cells. In tamoxifen resistant breast cancer cells, other authors have observed that EGFR, IGF-1R and c-Src signaling are constitutively activated and responsible for a more aggressive phenotype consistent with an increased motility and invasiveness (Knowlden et al. 2003; Hiscox et al., 2005). This gives emphasis to the potential use of the combined therapy with low doses of both BRL and 9cRA as novel therapeutic tool particularly for breast cancer patients who develop resistance to antiestrogen therapy.

Table 7. Activation of caspases in MCF-7 cells. Cells were stimulated for 48 h in presence of BRL 100nM, 9RA 50nM alone or in combination. The activation of caspase-9 (A) and caspase-8 (B) was analysed by Flow Cytometry Assay. Data were presented as mean ± S.D. of triplicate experiments. *p<0.05 combined-treated *vs* untreated cells.

A

Caspase 9	% of Activation	SD
control	14,16	±2,565
BRL100nM	17,23	±1,678
9RA50nM	18,14	±0,986
BRL+9RA	33,88 *	±5,216

B

Caspase 8	% of Activation	SD
control	9,20	±1,430
BRL100nM	8,12	±1,583
9RA50nM	7,90	±0,886
BRL+9RA	10,56	±2,160

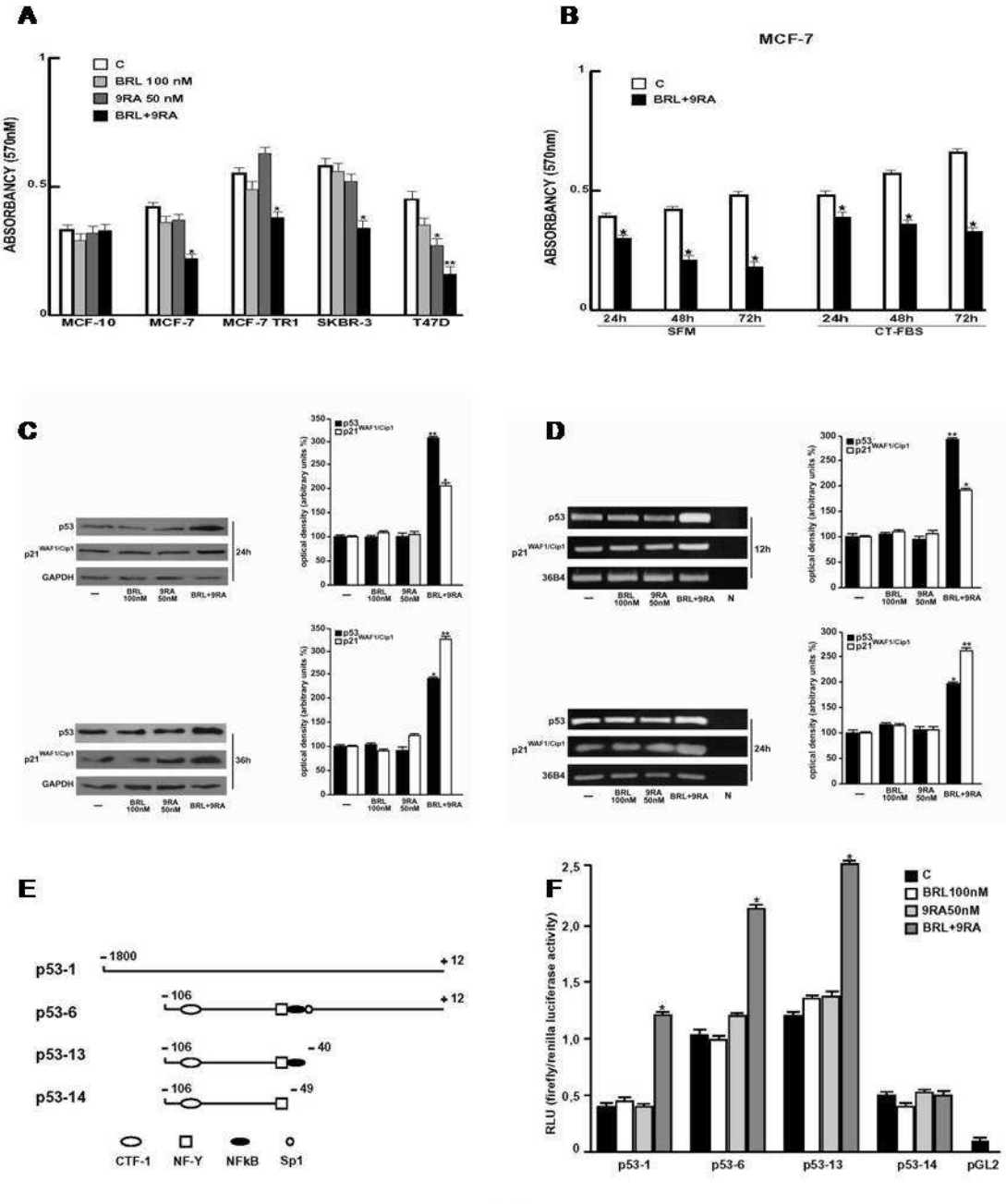

Figure 4.(A) Breast cells were treated for 48 h in SFM in the presence of BRL 100nM or/and 9RA 50nM. Cell vitality was measured by MTT assay. Data were presented as mean ± S.D. of three independent experiments done in triplicate. **(B)** MCF7 cells were treated for 24, 48 and 72 h with BRL 100nM and 9RA 50nM in the presence of SFM and 5% CT-FBS. *p<0.05 and **p<0.01 treated vs untreated cells. **(C)** Immunoblots of p53 and $p21^{WAF1/Cip1}$ from extracts of MCF-7 cell treated with BRL 100nM and 9RA 50nM alone or in combination for 24 and 36 h. GAPDH was used as loading control. The side panels show the quantitative representation of data (mean ± S.D.) of three independent experiments after densitometry. **(D)** p53 and $p21^{WAF1/Cip1}$ mRNA expression in MCF-7 cells treated as in A for 12 and 24 h. The side panels show the quantitative representation of data (mean ± S.D.) of three independent experiments after densitometry and correction for 36B4 expression. *p<0.05 and **p<0.01 combined-treated *vs* untreated cells. N: RNA sample without the addition of reverse transcriptase (negative control). **(E)** Schematic map of the p53 promoter fragments used in this study. **(F)** MCF-7 cells were transiently transfected with p53 gene promoter-luc reporter constructs (p53-1, p53-6, p53-13, p53-14) and treated for 24 h with BRL 100nM and 9RA 50nM alone or in combination. The luciferase activities were normalized to the Renilla luciferase as internal transfection control and data were reported as RLU values. Columns are mean ± S.D. of three independent experiments performed in triplicate. *p<0.05 combined-treated vs untreated cells. pGL2: basal activity measured in cells transfected with pGL2 basal vector; RLU, Relative Light Units. CTF-1, CCAAT-binding transcription factor-1; NF-Y, nuclear factor-Y; NF*k*B, nuclear factor kB.

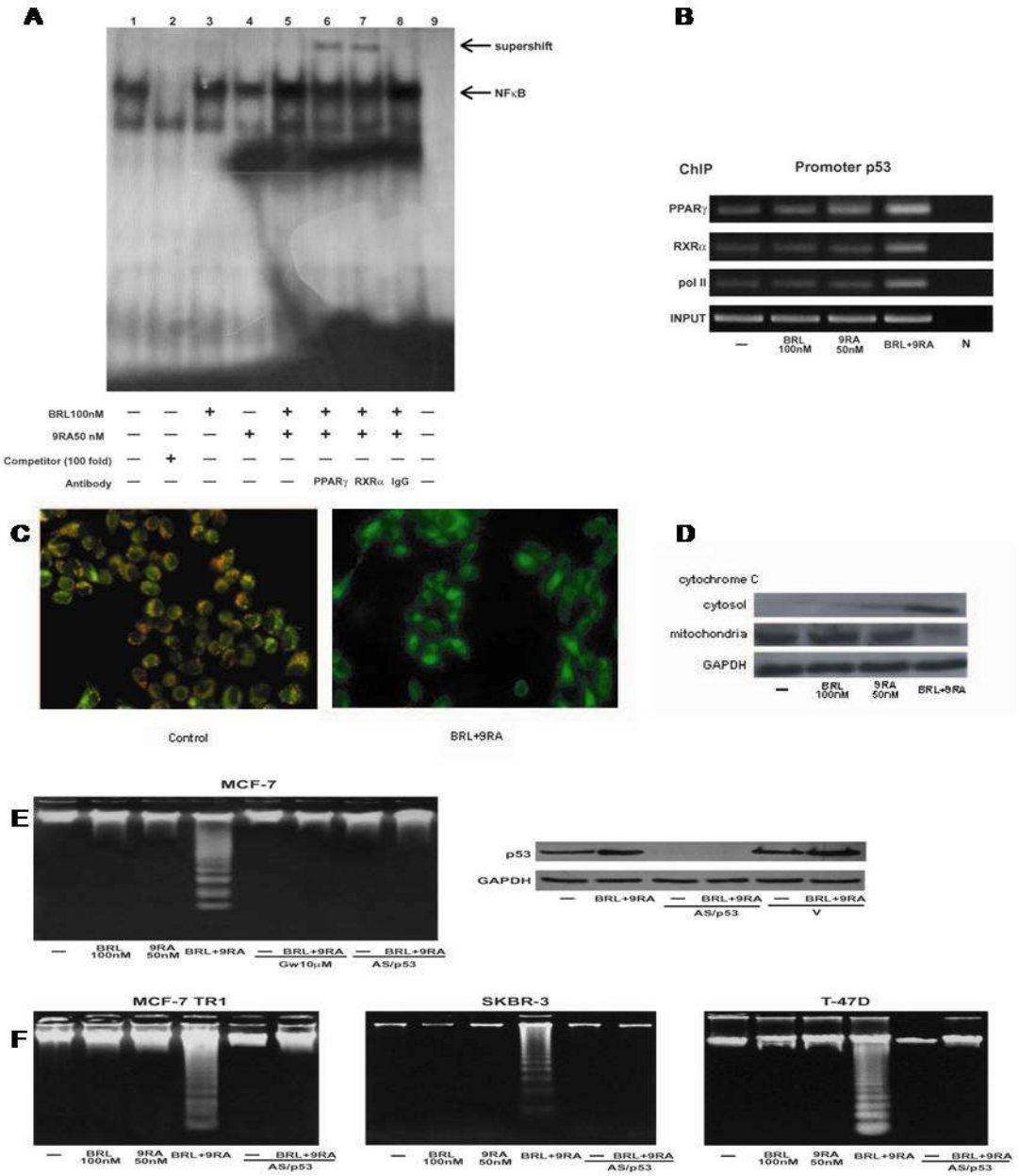

Figure 5. (A) Nuclear extracts from MCF-7 cells (lane 1) were incubated with a double-stranded NF*k*B consensus sequence probe labeled with [^{32}P] and subjected to electrophoresis in a 6% polyacrylamide gel. Competition experiments were done, adding as competitor a 100-fold molar excess of unlabeled probe (lane 2). Nuclear extracts from MCF-7 were treated with 100nM BRL (lane 3), 50nM 9RA (lane 4) and in combination (lane5). Anti-PPARγ (lane 6), anti-RXRα (lane 7) and IgG (lane 8) antibodies were incubated. Lane 9 contains probe alone. **(B)** MCF-7 cells were treated for 1 h with 100nM BRL and/or 50nM 9RA as indicated, and then cross-linked with formaldehyde and lysed. The soluble chromatin was immunoprecipitated with anti-PPARγ, anti-RXRα and anti-RNA Pol II antibodies. The immunocomplexes were reverse cross-linked, and DNA was recovered by phenol/chloroform extraction and ethanol precipitation. The p53 promoter sequence containing NF*k*B was detected by PCR with specific primers. To control input DNA, p53 promoter was amplified from 30 μl of initial preparations of soluble chromatin (before immunoprecipitations). N: negative control provided by PCR amplification without DNA sample. **(C)** MCF-7 cells were treated with 100nM BRL plus 50nM 9RA for 48 h and then used fluorescent microscopy to analyze the results of JC-1 (5,5',6,6'-tetrachloro-1,1',3,3'- tetraethylbenzimidazolylcarbocyanine iodide) kit. In control non-apoptotic cells, the dye stains the mitochondria in red. In treated apoptotic cells, JC-1 remains in the cytoplasm in a green fluorescent form. **(D)** MCF-7 cells were treated for 48 h with BRL 100nM and/or 9RA50nM. GAPDH was used as loading control. **(E)** DNA laddering was performed in MCF-7 cells transfected and treated as indicated for 56 h. One of three similar experiments is presented. The side panel shows the immunoblot of p53 from MCF-7 cells transfected with an expression plasmid encoding for p53 antisense (AS/p53) or empty vector (v) and treated with 100nM BRL plus 50nM 9RA for 56 h. GAPDH was used as loading control. **(F)** DNA laddering was performed in MCF-7 TR1, SKBR-3, T-47D cells transfected with AS/p53 or empty vector (v) and treated as indicated. One of three similar experiments is presented.

5. 9cRA as a pancreas autacoid that attenuates glucose-stimulated insulin secretion

We applied a sensitive LC/MS/MS assay to compare pancreas RA isomers to those in serum and liver, because the endocrine pancreas expresses nuclear receptors that recognize RA isomers and responds to retinoid-induced signaling, and liver serves as the principal storage site of retinoids and contributes to retinoid homeostasis (Napoli 1999; Chuang et al. 2008). Consistent with previous work, prominent physiological RA isomers in serum and liver included atRA and 9,13-di-*cis*-RA (9,13dcRA), an RA isomer without known biological activity, but 9cRA was not detected (Kane et al. 2005, 2008). In contrast, we identified 9cRA in pancreas, along with atRA and 9,13dcRA (Figure 1A). We confirmed that analysis did not generate 9cRA by adding retinoids to pancreata before homogenization, extraction, and assay (Figure 1B). Only 9cRA increased the 9cRA signal, excluding oxidation of the RA precursor retinal and/or isomerization of atRA during analyses as sources of 9cRA. Concentrations of 9cRA in pancreas occur within the range of concentrations of other RA isomers in tissues and serum (Figure 1C). These data provide an analytically rigorous identification of 9cRA as a naturally occurring retinoid. If 9cRA occurs in the tissues assayed other than pancreas, amounts would be <0.05 pmol/g, based on the LC/MS/MS assay's limit of detection in biomatrices.

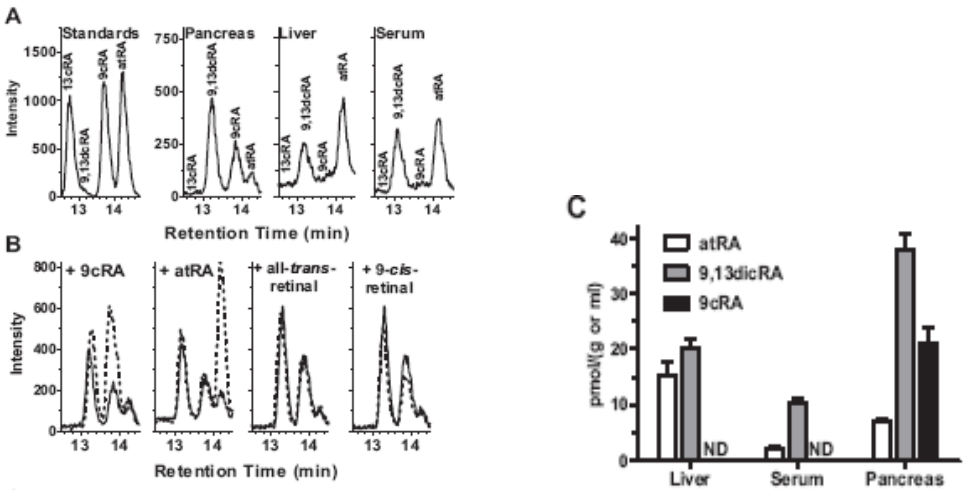

Fig.1 9cRA occurs in pancreas. (A) Representative LC/MS/MS chromatograms of RA isomers from analyses of mouse pancreas, liver and serum. (B) Representative LC/MS/MS chromatograms of pancreatic RA isomers before (solid lines)

and after addition (dashed lines) of retinoids prior to homogenization, extraction and analysis. Each chromatogram shows one of triplicate analyses. (C) Quantification of RA isomers in mouse liver, serum, and pancreas: ND, not detected; 8 mice/group (s.e.m.)

The fasted to fed transition resulted in a 36% decrease in 9cRA, which accompanied the increase in blood glucose and serum insulin, but caused no changes in pancreas atRA, 9,13-dcRA (Figure 2A). Consistent with this observation, challenging fasted 6 mice with a bolus of glucose decreased 9cRA >80% within 15 min, coinciding with the rapid rise in blood glucose (Figure 2B). 9cRA recovered markedly by 30 min and continued to rise thereafter. In contrast, glucose challenge had no impact on pancreas atRA or 9,13dcRA. During glucose challenge, 9cRA correlated inversely with serum insulin, further suggesting a contribution to pancreas function consistent with decreasing GSIS (Figure 2C). In addition, exogenous 9cRA reduced serum insulin during glucose challenge (Figure 2D).

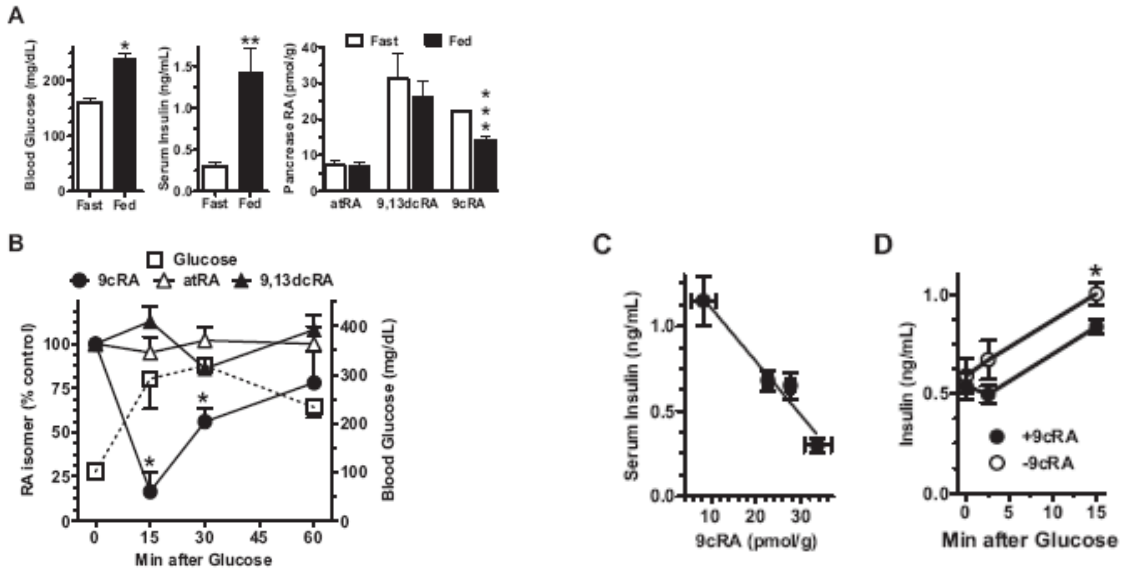

Fig.2 9cRA reflects fasting *vs.* feeding. (A) Blood glucose, serum insulin, and pancreas RA isomers in fed or 12-hr fasted mice. Data are means of 3 experiments with 6-10 mice/group/experiment: **P*≅0.03, ***P*<0.004, ****P*<0.003 *vs.* fed values. (B) 9cRA and atRA responses to a glucose challenge (2 g/kg glucose). Values are means of 2-5 experiments with 5-10 mice/point/experiment, except 9,13dcRA (1 experiment, 10 mice/time): **P*<0.05 from 0 time. The three glucose values after 0 min differ from control: **P*<0.05. (C) Inverse relationship between pancreas 9cRA and serum insulin after a glucose challenge: the slope differs significantly from 0, *P*=0.02; 10 mice/point. (D) 9cRA hinders insulin secretion: 9cRA (0.5 mg/kg in 60 µl DMSO) or vehicle alone were injected i.p. in mice 15 min before an i.p dose of glucose (0.5 g/kg). Data are means of 6-7 mice: **P*<0.05. All data s.e.m.

The inverse relationship between serum insulin and pancreas 9cRA during the GTT, and ability of 9cRA to reduce serum insulin, prompted testing whether 9cRA decreases glucose disposal. Mice were injected with 9-*cis*-retinol, a potential precursor of 9cRA, or 9cRA, prior to a GTT. Mice injected with 9- *cis*-retinol responded with a 2 to 2.7-fold increase in pancreas 9cRA, sustained at least 120 min (Figure 3A). Mice injected with 9cRA responded with a ~30-fold increase in pancreas 9cRA, which declined by 120 min to ~4-fold above control. Note that the decrease in endogenous 9cRA in the control (dosed only with glucose) at 30 min reflected the same degree of decrease (~40%) observed at 30 min in the GTT experiment of Figure 2B. Increases in pancreas 9cRA caused by both 9-*cis*-retinoids resulted in glucose intolerance, such that 120 min after the glucose challenge, blood glucose was at least 2-fold higher than in vehicle-dosed mice (Figure 3B). The lowest concentrations of 9cRA (40 nM) achieved after dosing either 9cRA or 9-*cis*-retinol arrested glucose disposal to the same extent as the higher concentrations achieved, indicating a dose-response relationship with a maximum effect near or below 40 nM 9cRA. These data suggest that the physiological decrease in pancreas 9cRA as glucose increases permits optimum insulin secretion, and reveal that 9-*cis*-retinol can serve as a precursor to 9cRA.

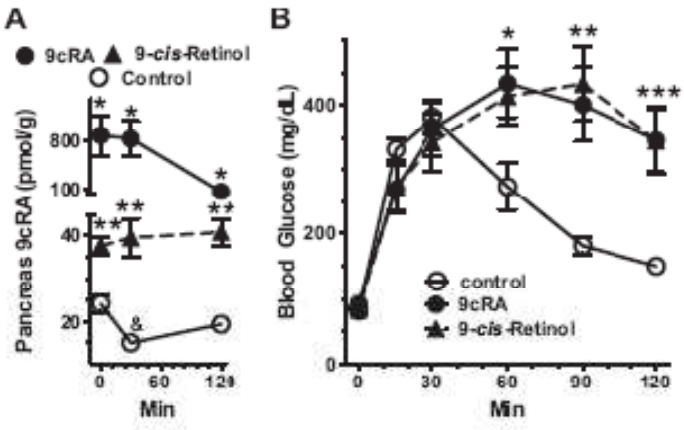

Fig.3 Exogenous 9cRA induces glucose intolerance. (A) Increases in total pancreas 9cRA after dosing with 9-*cis*-retinol or 9cRA (0.5 mg/kg in 100 µl DMSO). 9-*cis*-Retinol and 9cRA were injected 60 and 15 min before glucose, respectively. Glucose (2 g/kg) was injected at 0 min: 5-8 mice/group; **P*≅0.01 and ***P*<0.003 *vs.* vehicle control; &*P*<0.005 *vs.* 0 min. (B) GTT in mice dosed with 9-*cis*-retinol or 9cRA: 5-7 mice/group; **P*<0.04, ***P*<0.002, ****P*<0.005 *vs.* control. Mice were dosed with retinoids as described in A. All data s.e.m.

Glucose uptake by the pancreas rapidly affects both Glut2 and GK activities through post-translational mechanisms (Thorens et al. 1996; Zhang et al. 2006). Although GK activity limits the rate of glucose uptake by the β- cell, Glut2 contributes more than passive glucose transport by signaling glucose concentrations: phosphorylation decreases both the transport and signaling functions of Glut2 (Thorens et al. 1996; Ferber et al. 1994). Forskolin, which stimulates cAMP synthesis and induces protein kinase A-dependent Glut2 phosphorylation in β-cells, decreases Glut2 activity. We repeated the experiment published with forskolin and compared its effect to that of 9cRA in the 832/13 β-cell line, established as a model of GSIS (Hohmeier et al. 2000) (Figure 4A). We duplicated the published results with forskolin, and found that 9cRA decreased glucose-stimulated Glut2 activity ~40% within 15 min, similar to the impact of forskolin. Thirty nM 9cRA was as effective as 100 nM, consistent with the results of Figure 3, which indicated a marked effect of 40 nM 9cRA on glucose disposal. In 15 min, 9cRA inhibited GK activity 70%, which persisted until 60 min in 832/13 β-cells treated with 23 mM glucose (Figure 4B). By 120 min, 9cRA inhibition of GK activity decreased to 34%. Despite the changes in Glut2 and GK activities, 9cRA did not affect Glut2 or GK mRNA by 15 min (data not shown). 9cRA decreased ATP in 832/13 β-cells 30-40% from 15 through 60 min after introduction of 23 mM glucose and ATP recovered by 120 min (Figure 4C). After 60 min of 9cRA exposure in cells treated with 23 mM glucose, 9cRA reduced 832/13 β-cell intracellular Ca2+ 35%; Ca2+ returned to control levels by 2 hr (Figure 4D). Consistent with its impact on glucose sensing, 9cRA reduced GSIS 40% in 832/13 β-cells after 60 min incubation with 23 mM glucose, but did not impair baseline insulin secretion in the presence of 3 mM glucose (Figure 4E). In pancreatic islets, 9cRA reduced GSIS 33-43% induced by 15 to 60 min incubation with 23 mM glucose, with islet sensitivity returning by 120 min (Figure 4F). A rise in ATP closes the β-cell K+ ATP channel, which allows Ca2+ influx. This process serves as a “triggering signal” to initiate the first phase of GSIS (Jensen et al. 2008). KCl induces insulin release in the absence of high glucose by circumventing the ATP effect on the K+ channel.

9cRA had no impact on KCl-stimulated insulin secretion from islets (Figure 4G). After 2 hr, 9cRA decreased expression of *Pdx-1* and *HNF4α* mRNA, 7 and 77- fold, respectively (Figure 4H). Pdx-1 induces glucokinase, Glut2 and insulin gene expression in the mature pancreas (Ashizawa et al. 2004; Babu et al. 2007). HNF4α regulates insulin release through controlling mitochondrial metabolism of glucose and HNF1α, Glut2 and insulin gene expression (Bartoov-Shifman et al. 2002; Wang et al. 2000).

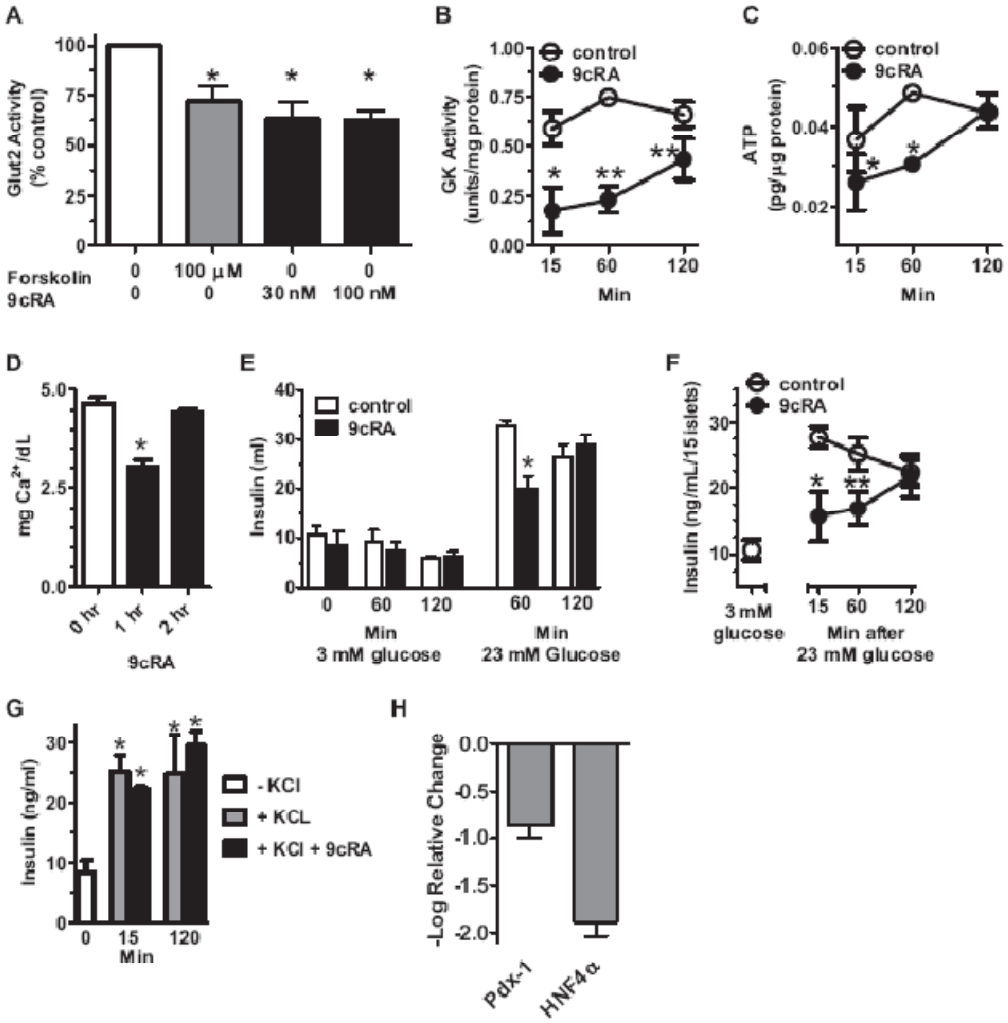

Fig.4 9cRA attenuates pancreas glucose sensing. 832/13 β-cells and islets were pre-incubated 2 hr with 3 mM glucose. At 0 min, the medium was exchanged for medium containing 23 mM and agents indicated for the duration of experiments. (A) 9cRA reduces Glut2 activity in 832/13 cells after 15 min incubation: 4-8 replicates/group; **P*≤0.0003 *vs*. no addition. (B) 9cRA reduces GK activity in 832/13 cells: 3-7 replicates/group, **P*<0.02, ***P*<0.002 *vs.* control. (C) 9cRA reduces ATP content in 832/13 cells: 2-4 replicates/group, **P*<0.008 *vs.* control. (D) 9cRA decreases Ca2+ influx into 832/13 cells: 2 replicates/group; **P*<0.02. (E) 9cRA decreases GSIS by 832/13 cells: 3-11 replicates/group; **P*<0.01 *vs*. control. (F) 9cRA decreases GSIS by pancreatic islets. The graph shows baseline insulin secretion during 3 mM glucose, and the effect of 9cRA on stimulation of insulin secretion by 23 mM glucose: 8-9 replicates/group; **P*<0.02, ***P*<0.002 *vs.* control. (G) 9cRA does not affect KCl stimulated insulin secretion from islets: **P*<0.02 *vs.* 0

time. (H) 9cRA reduces *Pdx-1* and *HNF4α* mRNA after 2 hr in 832/13 cells: 3 replicates/group. One hundred nM 9cRA was used in all experiments, unless noted otherwise. All data s.e.m.

We analyzed pancreata from mice with decreased numbers of β-cells to identify sources of 9cRA. A point mutation in the insulin 2 gene of Ins2Akita mice induces β-cell apoptosis, which reduces the number of β-cells, indicated by a 46% reduction in pancreas insulin (Yoshioka et al. 1997). Pancreata from fed heterozygous Akita mice had 40% lower 9cRA than wild type (WT), consistent with the decrease in β- cells (Figures 5A). In contrast, pancreas atRA increased and retinol did not differ from WT, demonstrating a unique relationship between 9cRA and β-cells. To confirm this insight, we injected mice with Stz, which causes β-cell necrosis (Lenzen 2008). 9cRA in pancreas of Stz-treated mice decreased with time in direct proportion to the decrease in β-cells, assessed by insulin content (Figures 5B and C). Seventy-two hr after Stz dosing, β-cell numbers decreased 67%, accompanied by a 58% decrease in 9cRA, impaired glucose tolerance and elevated non-fasting blood glucose (Figure 5C). By 96 hr, β-cells decreased 95% and 9cRA deceased 70%, consistent with β-cells serving as a major source of pancreas 9cRA. Based on the 9cRA remaining after β-cell destruction, other pancreas cells may contribute ~20-25% to the 9cRA pool. The β-cell line 832/13 generated 9cRA and atRA from their respective 9-*cis*- or all-*trans*- retinol and retinal precursors at similar rates (Figure 5D). Pancreas microsomes contain both 9-*cis*- and all-*trans*-retinol (33 ± 1.4 and 76 ± 2 pmol/g protein, respectively; 3 replicate analyses of a 5 pancreata pool) (Figure 5E). Thus, β-cells have the capacity and a substrate to biosynthesize 9cRA.

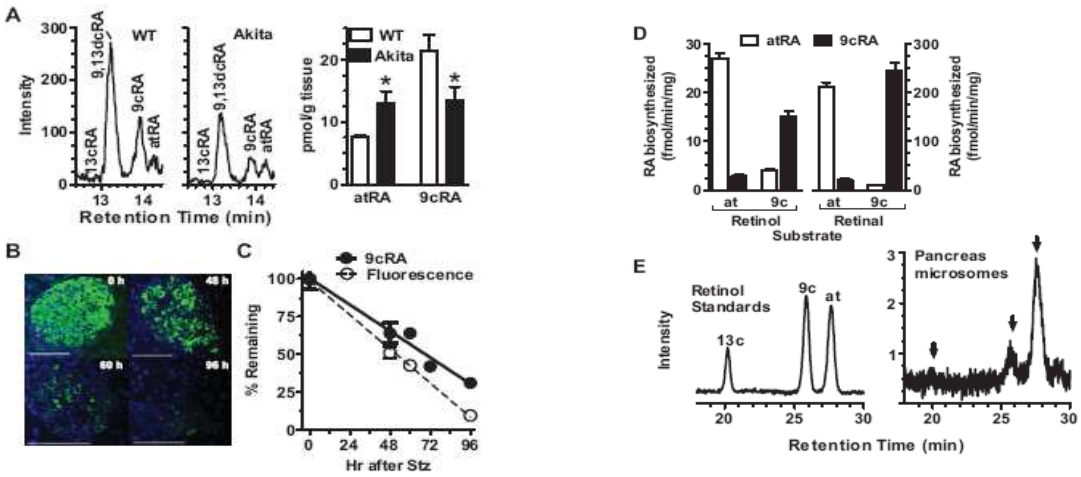

Fig.5 Pancreas β-cells produce 9cRA. (A) Representative LC/MS/MS chromatograms and quantification of RA isomers in pancreas of WT and Akita mice: 8 mice/group; **P*<0.05 *vs.* WT. (B) Immunohistochemistry showing loss of insulin in pancreas with time after a Stz dose: scale bars, 100 μm. (C) Effect of Stz on β-cell numbers (3-6 islets) and pancreas 9cRA (9-18 mice/group). (D) Biosynthesis of RA isomers from retinol and retinal isomers by the pancreas β-cell line 832/13: 3 replicates/substrate. (E) HPLC of retinol standards and representative analyses of pancreas microsomes. Arrows denote elution positions of 13-*cis*-, 9-*cis*- and all-*trans*retinol, respectively. All data s.e.m.

To determine whether mouse models of glucose intolerance are accompanied by 9cRA increases, we assayed pancreata from *ob/ob* and *db/db* mice and mice with diet-induced obesity (DIO) (Leibel et al. 1997). *Ob/ob* mice lack leptin, are obese and have high blood glucose and serum insulin. *Ob/ob* mice had 2.2-fold higher 9cRA than WT controls (Figure 6A). Mice with DIO were glucose intolerant, weighed ~50% more than controls, and had ~2-fold higher 9cRA than controls (Figures 6B). *Db/db* mice, which lack the leptin receptor and have elevated blood glucose and serum insulin, had 34% higher 9cRA than lean controls (Figure 6C). Although atRA also increased in pancreas of *ob/ob* mice, the increase was modest, and atRA did not increase in pancreas of *db/db* mice. In DIO pancreata, the atRA increase exceeded the 9cRA increase. Neither the atRA nor the 9cRA changes in pancreas correlated with changes in retinol. Thus, 9cRA was the only endogenous retinoid assayed (9cRA, atRA and retinol) that changed consistently in pancreas with changes in glucose tolerance, regardless of the underlying cause of impaired glucose tolerance.

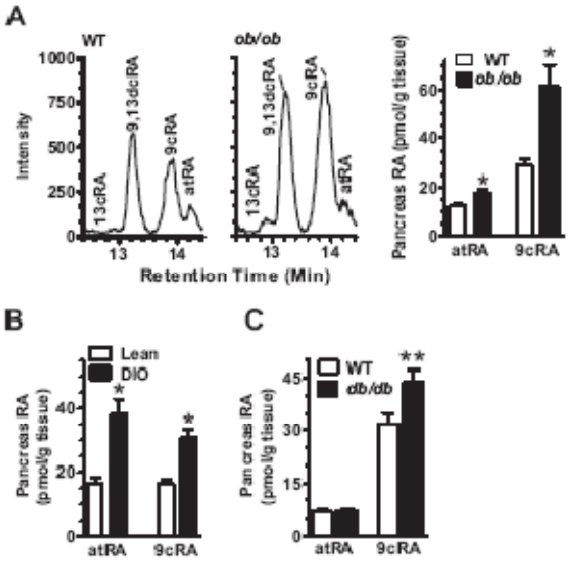

Fig.6 Increased pancreas 9cRA accompanies glucose intolerance. (A) representative LC/MS/MS chromatograms and RA isomers in pancreas of fed WT and *ob/ob* mice: 8 mice/group; **P*<0.008 *vs.* WT. (B) Increased 9cRA in pancreas of mice with DIO: 8-10 mice/group: **P*<0.001 *vs*. lean. (C) RA isomers in pancreas of fed WT and *db/db* mice: 8 mice/group; ***P*=0.033. All data s.e.m.

The novel, rapid physiological effects of 9cRA described here contrast with its effects as a pharmacological agent that regulates transcription and suggest non genomic mechanisms (Noy 2007). This is not unprecedented. Non genomic effects of retinoids have not been investigated as extensively as their transcriptional effects, but 9cRA reportedly stimulates phosphorylation of p38 mitogen-activated protein kinase (De Alvaro et al. 2004). Recent work also has shown that atRA has rapid, non-genomic action (Sidell et al. 2010) indicating that retinoids, like several steroid hormones, do not solely regulate transcription (Stahn et al.2008). Occurrence of 9cRA in pancreas, along with non-detectable concentrations in serum and a host other tissues, support the deduction based on genetic evidence that 9cRA does not serve as a universal retinoid X receptor-activating ligand *in vivo* (Calleja et al. 2006). Validation of 9cRA as an autacoid in pancreas provides framework for evaluating whether it functions *via* RARs and/or RXRs, and for evaluating potential cross-signaling between atRA and 9cRA. The outcome of a potential 9cRA/atRA interaction with pancreas RAR cannot be predicted simply because both retinoids bind the same receptor. Nuclear receptor action depends on the ligand bound and the nucleotide sequence of the gene's

response element both influence receptor conformation, affinity for a particular response element, and function (Meijsing et al. 2009). Pancreas atRA did not change with an increase in blood glucose after the fasted to the fed transition, or after glucose injection, indicating that short-term modulation of GSIS relies only on 9cRA. In summary, this work demonstrates that 9cRA occurs as an endogenous pancreas retinoid, establishes a function for 9cRA in GSIS, and provides novel insight into retinoid function and glucose homeostasis. Of interest are the likely non-genomic effects of 9cRA. These studies provide insight into an essential element of pancreas mediated glucose homeostasis, which should prove useful for understanding mechanisms of GSIS and diabesity.

METHODS

Testicular cell cultures. The Leydig (TM-3) cell line was cultured in DMEM/F12 medium supplemented with 5% horse serum (HS) and 5% fetal calf serum (FCS). Tumoral MLTC-1 cell line was cultured in RPMI-1640 medium supplemented with 10% FCS. The R2C cell line was cultured in F-12 Nutrient Mixture (Ham) supplemented with 2.5% fetal bovin serum (FBS), 15% horse serum (HS). Culture media for all cell lines were supplemented with 2 mM glutamine and 1% of a stock solution containing 10,000 IU/ml penicillin and 10,000 μg/ml streptomycin. Cell cultures were grown on 90 mm plastic tissue culture dishes in a humidified atmosphere of 5% CO_2 in air at 37 °C. Cells from exponentially growing stock cultures were removed from the dishes with trypsin (0.05% w/v) and EDTA (0.02% w/v). The trypsin/EDTA action was inhibited with an equal volume of DMEM/F12, F-12 Nutrient Mixture (Ham) or RPMI-1640 medium. Cell number was estimated with a Burker camera and cell viability by trypan blue dye exclusion. For all cellular lines, the medium was changed twice per week. TM-3 and R2C cells were subcultivated when confluent, while MLTC-1 cells were subcultured when they formed island domes.

Isolation of mitochondria fraction from cells. After trypsinization and centrifugation of cells at 1,800 rpm for 5 min at 4 °C mitochondria were isolated solubilizing the pellet with 200 μl RIPA buffer, supplemented with 0.1% digitonin; the cells were incubated for 15 min at 4 °C and the mitochondria were isolated by differential centrifugations at 4 °C as described by Cione et al. (2004).

Oxidative stress parameters. Following sonication of cells in PBS (phosphate buffered saline, 1.5mM KH_2PO_4, 8.1mM Na_2HPO_4, 136.9mM NaCl, pH7.2) buffer the crude homogenate was divided into two equal parts. One part was processed for assay of lipid peroxidation, while the second part was centrifuged at 10,000rpm for 5min and the supernatant utilized in assays for glutathione S-transferase, superoxide dismutase and catalase activities.

Lipid peroxidation and antioxidant enzymes activity. The level of lipid peroxidation was assayed through the formation of thiobarbituric acid reactive species (TBARS) during an acid-heating reaction as previously described (Esterbauer and Cheeseman 1990). Briefly, the samples were mixed with 1ml of 10% trichloroacetic acid (TCA) and 1ml of 0.67% thiobarbituric acid (TBA), then heated in a boiling water bath for 15min. TBARS were determined by the absorbance at 535nm and were expressed as malondialdehyde equivalents (nmol/mg protein). The enzymatic activities in the cell samples of SOD, CAT and GST were determined by the methods of Das & Chainy (2001), Aebi (1974) and Habig et al. (1974) respectively. Protein concentration in samples was estimated by the Lowry method (Lowry et al. 1951).

MTT assay. Cell viability was determined by MTT assay (Mosmann 1983). Cells ($2x10^5$ cells/ml) were grown in 12 well plates and exposed to different treatments at different time points. Control cells were treated with vehicle alone. One hundred microlitres of MTT (5mg/ml) was added to each well and the plates incubated for 4h at 37°C. Subsequently 1ml 0.04N HCl in isopropanol was added to solubilize the cells. The absorbance was measured with the Ultrospec 2100 pro spectrophotometer (Amersham-Biosciences) at a test wavelength of 570nm with a reference wavelength of 690nm. The optical density (O.D.) was calculated as the difference between the absorbance at the reference wavelength and that at the test wavelength. Percent viability was calculated as (O.D. of drug-treated sample/control O.D.) ×100.

Lactate dehydrogenase assay. The amount of lactate dehydrogenase (LDH) released by the cells was determined as described by Abe & Matsuki (2000) with little modifications. The culture supernatant (250μl) was mixed with 250μl of the LDH substrate mixture (2.5mg/ml L-lactate lithium salt, 2.5mg/ml NAD+, 100μM MPMS, 600μM MTT, and 0.1% Triton X-100 in 0.2M Tris-HCl buffer, pH 8.2). The reaction was carried out for 5min at 37°C and stopped by adding 0.5ml of 0.04N HCl in isopropanol. The absorbance was measured with the spectrophotometer at a test wavelength of 570nm, and a reference wavelength of 655nm. In these assay conditions, MTT was converted into MTT formazan in proportion to LDH activity. LDH release was calculated as (sample LDHblank)/(total LDH-blank) ×100.

Immunoblot analysis of cytochrome c release. Cytochrome c was detected by western blotting in mitochondrial and cytoplasmatic fractions. The cells were harvested by centrifugation at 1,200 × g for 10min at 4°C. The pellets were

suspended in 36µl lysis buffer (250mM sucrose, 1.5mM EGTA, 1.5mM EDTA, 1mM $MgCl_2$, 25mM Tris-HCl, pH6.8, 1mM DTT, 10µg/ml aprotinin, 50mM phenylmethylsulfonylfluoride and 50mM sodium orthovanadate) and then 4µl of 0.1% digitonine was added. The cells were incubated for 15min at 4°C and centrifuged at 12,000rpm for 30min at 4°C. The resulting mitochondrial pellet was resuspended in 3% Triton X-100, 20mM Na_2SO_4, 10mM PIPES and 1mM EDTA, pH7.2, and centrifuged at 12,000rpm for 10min at 4°C. Equal amounts of protein (2–5µg) were resolved by 15% SDS-PAGE and electrotransferred to nitrocellulose membranes. The membranes were incubated in blocking buffer over night at 4°C, followed by incubation with 1:1,000 sheep polyclonal antihuman cytochrome c antibody (2h, room temperature) and then with HRP-conjugated (horse radish peroxidaseconjugated) secondary antibody (1:2,000) for 2h at 4°C. Peroxidase activity was visualized with the Amersham Pharmacia Biotech ECL system according to manufacturer's instructions. The cytochrome c protein content was determined densitometrically. Immunoblotting for β-actin was carried out to confirm equal loading.

Western blot determination of caspase-3. Cells were lysed with ice-cold PBS (pH7.4) containing 1% Triton X-100, 0.5% sodium deoxycholate, 0.1% SDS and protease inhibitors (1mM phenylmethylsulfonylfluoride, 10mg/ml aprotinin and 10mg/ml leupeptin). Lysates were centrifuged (13,000rpm at 4°C for 30min) and supernatant protein content determined. Equal amounts of protein (20µg) were resolved by 15% SDS-PAGE, electrotransferred to nitrocellulose membranes and immunoblotted for caspase-3 as previously described.

Immunoblot analysis of IP_3K/Akt pathways and cell cycle signaling. Cultured cells were lysed with 200 µl ice-cold PBS containing 1% Triton X-100, 0.5% sodium deoxycholate, 0.1% SDS and protease inhibitors (1 mM phenylmethylsulfonylfluoride, 10 mg/ml aprotinin and 10 mg/ml leupeptin). Lysates were centrifuged (13,000×g at 4 °C for 30 min) and the supernatant protein content was determined by the Lowry method (Lowry et al. 1951). Proteins (50 µg) were resolved by 15% SDSPAGE, and transferred to a nitrocellulose membrane (Hybond-C; Amersham Biosciences, Piscataway, NJ). The membrane was blocked with 5% bovine serum albumin and probed with specific primary antibodies such as anti-phospho-Akt1/2/3 (Ser 473)-R (Santa Cruz Biotechnology Inc., Santa Cruz, CA), anti-Akt (Santa Cruz Biotechnology Inc.), anti-cyclin D1 (Santa Cruz Biotechnology Inc.), anti-p21 (Santa Cruz Biotechnology Inc.) and anti-cyt c (Santa Cruz Biotechnology Inc.), respectively. After washing, membranes were incubated with HRP-conjugated secondary antibody. Peroxidase activity was visualized with the Amersham Pharmacia Biotech ECL system according to the manufacturer's instructions. The protein content was determined densitometrically. The loading control was detected by immunoblot of β-actin protein.

DNA extraction and agarose gel electrophoresis. Agarose gel electrophoresis of extracted DNA was performed to detect damage to nuclear chromatin, a characteristic biochemical feature of apoptosis, indicated by laddering of oligonucleosomal fragments (180–200bp) as described by Mu et al. 2001. Briefly, 5×10^6 cells were grown in petri dishes, were trypsinized and washed with PBS. Then the cells were spin down and resuspended in 0.5ml of lysis buffer (50mM Tris-HCl, pH 7.8, 10mM EDTA, and 0.5% SDS). RNase A was added to a concentration of 0.5mg/ml and incubated at 37°C for 60min. The protein content was degraded with proteinase K (0.5mg/ml) at 50°C for 60min. DNA was obtained with two extractions. The first extraction was carried out with an equal volume of phenol–chloroform–isoamylic alcohol (25:24:1) and the second with chloroform–isoamylic alcohol (24:1). DNA was precipitated from the upper aqueous phase with 0.1vol. of 3M sodium acetate, 2.5vol. of ice-cold ethanol and left at −20°C over night. After centrifugation the DNA pellet was solubilized in 25µl sterile water. DNA fragments were separated by electrophoresis in 1.2% agarose gel and visualized by staining with ethidium bromide.

JC-1 mitochondrial membrane potential detection assay. The loss of mitochondrial membrane potential (ΔΨm) was monitored with the 5,5′,6,6′tetra-chloro-1,1′,3,3′-tetraethylbenzimidazolyl- carbocyanine iodide dye (JC-1) (Biotium, Hayward, USA). The negative charge established by the intact ΔΨm, allows the lipophilic dye JC-1 to selectively enter the mitochondrial matrix, where it aggregates and emits a red fluorescence. When the ΔΨm is lost the JC-1 cannot accumulate within these organelles and remains in the cytoplasm in the monomeric form emitting green fluorescence (Cossarizza et al. 1993). Cell lines were grown in 10 cm dishes and treated, then the cells were trypsinized, washed in icecold PBS, and incubated with 10 mM JC-1 at 37 °C in a 5% CO2 incubator for 20 min. Subsequently, cells were washed twice with PBS and analyzed by fluorescence microscopy according to manufacturer's instructions.

Mitochondrial ATP determination. The amount of endogenous ATP in isolated mitochondria and in cytosolic extract from MLTC-1, R2C and 832/13 cell lines was determined using the bioluminescence method described by Drew &

Leeuwenburgh (2003). With a Molecular Probes kit, ATP was assayed in cells lysed with RIPA buffer containing a proteases inhibitors mixture (Sigma) and cleared of cellular debris by centrifugation (10 min, 4 °C). An aliquot of each sample was mixed with 100 µl of reaction cocktail (25 mM Tricine buffer, pH 7.8, 5 mM MgSO4, 100 µM EDTA, 1 mM DTT) containing firefly luciferase and 0.5 mM luciferin. Emitted light was measured in a luminometer (Berthold).

Monodansylcadaverine staining. MDC was used to evaluate autophagic vacuoles in cells as previously reported (Biederbick et al. 1995). A 10 mM stock solution of MDC was prepared in PBS. Following treatments, cells were stained with MDC at a final concentration of 10 µMfor 10 min at 37 °C, and fixed using 3% paraformaldehyde solution in PBS for 30 min. Cells were washed and then examined by fluorescence microscopy (Leica AF2006).

Flow cytometry assay. Cells (1×106 cells/well) were grown in 6 well plates and shifted to serum free medium for 24 h before treatments . Thereafter, cells were trypsinized, centrifuged at 3,000 rpm for 3 min and washed with PBS. A 0.5 µl of fluorescein isothiocyanateconjugated antibodies anti-caspase-9 (Calbiochem, Milan, Italy) was added in all samples and then incubated for 45 min at 37 °C according to manufacturer's instruction. Samples were analyzed with the FACScan (Becton Dickinson and Co., Franklin Lakes, NJ).

TUNEL assay. Apoptosis was determined by enzymatic labeling of DNA strand breaks using terminal deoxynucleotidyl transferase-mediated deoxyuridine triphosphate nick end-labeling (TUNEL). TUNEL labeling was conducted using APO-BrdUTM. TUNEL Assay Kit (Molecular Probes) and performed according to the manufacturer's instructions. Cells were incubated for 30 min at room temperature protected from light and photographed by using a fluorescent microscope (Leica AF2006).

FABP5 and CRABPII mRNA expression. MLTC-1 cells were grown in 10 cm dishes from 70/80% confluence and exposed to RA treatments as indicated in Fig. 4 caption. Total cellular RNAwas extracted using Trizol reagent (Invitrogen) as suggested by the manufacturer. The purity and the integrity of total RNA were checked spectroscopically before carrying out the analytical procedures. RNA was then reverse transcribed with High Capacity cDNA Reverse Transcription Kit (Applied Biosystems). The cDNA obtained was amplified by PCR using the following primers: FABP5 (NM 010634) 5′-ACGGCTTTGAGGAGTACATGA-3′ (forward) and 5′-TCCTACCCTTCTACTAGCAC- 3′ (reverse), CRABP II (NM 007759) 5′-CGATCGGAAAACTTTGAGGA- 3′ (forward) and 5′-CAACACACGTGGTCCCAGAT- 3′ (reverse). The resulting PCR products were separated by electrophoresis in a 2% agarose gel in TBE (Tris-Borate-EDTA) and stained with ethidium bromide.

Isolation of mitochondria from testis. Rats were killed by decapitation, according to good practice procedures approved by the ethics committee, and testes were immediately removed. Rat testes mitochondria were isolated by differential centrifugation as described by Genchi & Olson (2001). Mitochondria were suspended in a medium containing 250 mM sucrose, 10 mM Tris/HCl, pH 7.4, 1 mM EDTA at a concentration of 15–18 mg protein/ml. Protein concentration was determined by the Lowry procedure (Lowry et al. 1951) with BSA as the reference standard. This mitochondrial suspension either was used immediately or was frozen at −70°C.

Incubation of mitochondria and extraction of the 2-oxoglutarate carrier (OGC). AtRA or ^{3}[H]atRA were dissolved in ethanol and 3 µL of the solution was added to the tissue preparation (0.5 mg protein), and incubated in the presence of 10mM ATP,150 µMCoA, 27mM $MgCl_2$, 50mM sucrose, and 100mM Tris, pH 7.4, in a total volume of 0.5 ml at 37 °C for 90 min. The inhibitors were added together with 3HatRA. The mitochondrial suspensions were centrifuged and protein extracted in 3% Triton X-114, 20mM Na_2SO_4, 1mM EDTA, 10mM Pipes, pH 7.0, and after 10 min on ice, the mixture was centrifuged at 13000 rpm for 5 min.

Reconstitution and determination of OGC activity. 20 µg of protein from the Triton X-114 extract of mitochondria were added to 100 µL of sonicated phospholipids (10% w/v), 100 µL of 10% Triton X-114 in Pipes 10 mM, 40 µL of malate 200 mM, 230 µL Pipes 10 mM pH 7.0 in a final volume of 700 µL and were applied to an Amberlite XAD-2 column in agreement with Palmieri & Klingenberg (1979). All the operations were carried out at room temperature. In order to determine the OGC transport activity, the external malate was removed by passing 650 µL of the proteoliposomal suspension through a Sephadex G-75 column pre-equilibrated with 50 mM NaCl and 10 mM Pipes, pH 7.0. The first 600 µL of the slightly turbid eluate, containing the proteoliposomes, were collected, transferred to 1.5 mL microcentrifuge tubes (150 µL each), and used for transport measurements by the inhibitor stop method (Palmieri & Klingenberg 1979). Transport was carried out at 25 °C by adding 0.1 mM [14C] 2-oxoglutarate and stopped after 10

min by the addition of 20mM pyridoxal 5′-phosphate. In control samples, the pyridoxal 5′-phosphate was added together with the labeled substrate at time zero. To remove the external radioactivity, each sample was passed through a Sephadex G-75 column (0.5×8 cm). The liposomes, eluted with 50 mM NaCl, were collected in 4 mL of scintillation cocktail and counted using a Tricarb 2100 TR scintillation counter with a counting efficiency of about 70 – 73%. The exchange activity was evaluated as the difference between the experimental and the control values as previously published by Bisaccia et al. (1988).

Labeling with ^{3}[H]atRA and western blot analysis. Direct labeling with ^{3}[H]atRA was performed according to a method described previously (Takahashi & Breitman 1990). Under yellow safe-light, 5 μCi/ 5 μL of ^{3}[H]atRA (40–60 Ci/mmol) in ethanol (1 μCi/μL) were added to 1.5 mL glass microcentrifuge tubes for each sample tested. After the ethanol was removed under nitrogen, 20 μg of Triton extract of testes mitochondrial protein were added to each tube, and the final volume was adjusted to 10 μL with incubation buffer, pH 7.4, for a final concentration of 10 μM ^{3}[H]atRA, while 2-oxo-glutarate was added at a final concentration of 10 mM. The samples were incubated at 37 °C (Takahashi & Breitman 1990) and shaken for 90 min under yellow light, after which 10 μL of SDS-polyacrylamide gel electrophoresis sample buffer was added, the samples were boiled and then loaded to run with standard SDS-polyacrylamide gel electrophoresis techniques. The gel was stained with Coomassie Brilliant Blue, soaked in Amplify (Amersham Biosciences) and then used for fluorography at −80 °C for 30 days. In order to verify the presence of the OGC protein, western blot analysis was performed using overnight rabbit monoclonal antibody to OGC at 4 °C (1:500 dilution in TBST). On the next day the membrane was incubated for 1 h at room temperature with horseradish peroxidase-conjugate antibodies to rabbit immunoglobulin G (1:2000 dilution) and the immune complex was detected with chemiluminescence reagents (ECL).

Breast cancer cell cultures. Wild-type human breast cancer MCF-7 cells were grown in DMEM-F12 plus glutamax containing 5% new-born calf serum (Invitrogen, Milan, Italy) and 1 mg/ml penicillin-streptomycin. MCF-7 tamoxifen resistant (MCF-7TR1) breast cancer cells were generated in Dr. Fuqua's laboratory maintaining cells in MEM with 10% foetal bovine serum (FBS) (Invitrogen), 6 ng/ml insulin, penicillin (100 units/ml), streptomycin (100 μg/ml) and adding 4-hydroxytamoxifen in 10-fold increasing concentrations every weeks (from 10^{-9} to 10^{-6} final). Cells were thereafter routinely maintained with 1μM 4-hydroxytamoxifen. SKBR-3 breast cancer cells were grown in DMEM without red phenol, plus glutamax containing 10% FBS and 1 mg/ml penicillin-streptomycin. T-47D breast cancer cells were grown in RPMI 1640 with glutamax containing 10% FBS, 1mM sodium pyruvate, 10mM HEPES, 2,5g/L glucose, 0,2 U/ml insulin and 1 mg/ml penicillin-streptomycin. MCF-10 normal breast epithelial cells were grown in DMEM-F12 plus glutamax containing 5% horse serum (Sigma), 1 mg/ml penicillin-streptomycin, 0,5 μg/ml hydrocortisone and 10 μg/ml insulin.

Plasmids. The p53 promoter-luciferase plasmids, kindly provided by Dr. Stephen H. Safe (Texas A&M University, College Station, TX, USA), were generated from the human p53 gene promoter as follows: p53-1 (containing the -1800 to +12 region), p53-6 (containing the -106 to +12 region), p53-13 (containing the -106 to -40 region) and p53-14 (containing the -106 to -49 region). As an internal transfection control, we cotransfected the plasmid pRL-CMV (Promega Corp., Milan, Italy) that expresses Renilla luciferase enzymatically distinguishable from firefly luciferase by the strong cytomegalovirus enhancer promoter. The pGL3 vector containing three copies of a PPRE sequence upstream of the minimal thymidine kinase promoter ligated to a luciferase reporter gene (3XPPRE-TK-pGL3) was a gift from Dr. R. Evans (The Salk Institute, San Diego, CA, USA). The p53 antisense plasmid (AS/p53) was kindly provided from Dr. Moshe Oren (Weizmann Institute of Science, Rehovot, Israel).

Immunoblotting p53 and p21. Cells were grown in 10cm dishes to 70–80% confluence and exposed to treatments in SFM as indicated. Cells were then harvested in cold phosphate-buffered saline (PBS) and resuspended in lysis buffer containing 20mM HEPES (pH 8), 0.1mM EGTA, 5mM $MgCl_2$, 0.5M NaCl, 20% glycerol, 1% Triton, and inhibitors (0.1mM sodium orthovanadate, 1% phenylmethylsulfonylfluoride (PMSF), 20mg/ml aprotinin). Protein concentration was determined by Bio-Rad Protein Assay (Bio-Rad Laboratories, Hercules, CA USA). A 40μg portion of protein lysates was used for Western blotting (WB), resolved on a 10% SDS-polyacrylamide gel, transferred to a nitrocellulose membrane, and probed with an antibody directed against the p53, $p21^{WAF1/Cip1}$ (Santa Cruz Biotechnology, CA USA). As internal control, all membranes were subsequently stripped (0.2 M glycine, pH 2.6, for 30 min at room temperature) of the first antibody and reprobed with anti-GAPDH antibody (Santa Cruz Biotechnology). The antigen-antibody complex was detected by incubation of the membranes for 1 h at room temperature with peroxidase-coupled goat

antimouse or antirabbit IgG and revealed using the enhanced chemiluminescence system (Amersham Pharmacia, Buckinghamshire UK). Blots were then exposed to film (Kodak film, Sigma). The intensity of bands representing relevant proteins was measured by Scion Image laser densitometry scanning program.

RT-PCR Assay p53 and p21. MCF-7 cells were grown in 10cm dishes to 70–80% confluence and exposed to treatments in SFM as indicated. Total cellular RNA was extracted using TRIZOL reagent (Invitrogen) as suggested by the manufacturer. The purity and integrity were checked spectroscopically and by gel electrophoresis before carrying out the analytical procedures. Two micrograms of total RNA were reverse transcribed in a final volume of 20 µl using a RETROscript kit as suggested by the manufacturer (Promega). The cDNAs obtained were amplified by PCR using the following primers: 5'-GTGGAAGGAAATTTGCGTGT-3' (p53 forward) and 5'-CCAGTGTGATGATGGTGAGG-3' (p53 reverse), 5'-GCTTCATGCCAGCTACTTCC-3' (p21 forward) and 5'-CTGTGCTCACTTCAGGGTCA-3' (p21 reverse), 5'-CTCAACATCTCCCCCTTCTC-3' (36B4 forward) and 5'-CAAATCCCATATCCTCGTCC-3' (36B4 reverse) to yield, respectively, products of 190 bp with 18 cycles, 270 bp with 18 cycles, and 408 bp with 12 cycles. To check for the presence of DNA contamination, a reverse transcription PCR was performed on 2 µg of total RNA without Monoley murine leukemia virus reverse transcriptase (the negative control). The results obtained as optical density arbitrary values were transformed to percentage of the control taking the samples from untreated cells as 100%.

Transfection Assay. MCF-7 cells were transferred into 24 well plates with 500µl of regular growth medium/well the day before transfection. The medium was replaced with SFM on the day of transfection, which was performed using Fugene 6 reagent as recommended by the manufacturer (Roche Diagnostics, Mannheim, Germany) with a mixture containing 0.5µg of promoter-luc or reporter-luc plasmid and 5ng of pRL-CMV. After transfection for 24 h, treatments were added in SFM as indicated, and cells were incubated for an additional 24 h. Firefly and Renilla luciferase activities were measured using the Dual Luciferase Kit (Promega). The firefly luciferase values of each sample were normalized by Renilla luciferase activity, and data were reported as Relative Light Units. MCF-7 cells plated into 10cm dishes were transfected with 5µg of AS/p53 using Fugene 6 reagent as recommended by the manufacturer (Roche Diagnostics). The activity of AS/p53 was verified using Western blot to detect changes in p53 protein levels. Empty vector was used to ensure that DNA concentrations were constant in each transfection.

EMSA. Nuclear extracts from MCF-7 cells were prepared as previously described. Briefly, MCF-7 cells plated into 10cm dishes were grown to 70–80% confluence, shifted to SFM for 24 h, and then treated with 100nM BRL, 50nM 9RA alone and in combination for 6 h. Thereafter, cells were scraped into 1.5ml of cold PBS, pelleted for 10 sec and resuspended in 400µl cold buffer A (10mM HEPES-KOH, pH 7.9, at 4 °C, 1.5mM $MgCl_2$, 10mM KCl, 0.5mM dithiothreitol, 0.2mM PMSF, 1mM leupeptin) by flicking the tube. Cells were allowed to swell on ice for 10 min and then vortexed for 10 sec. Samples were then centrifuged for 10 sec and the supernatant fraction was discarded. The pellet was resuspended in 50µl of cold Buffer B (20mM HEPES-KOH, pH 7.9; 25% glycerol; 1.5mM $MgCl_2$; 420mM NaCl; 0.2mM EDTA; 0.5mM dithiothreitol; 0.2mM PMSF; 1mM leupeptin) and incubated in ice for 20 min for high-salt extraction. Cellular debris was removed by centrifugation for 2 min at 4 °C, and the supernatant fraction (containing DNA-binding proteins) was stored at -70 °C. The probe was generated by annealing single-stranded oligonucleotides and labeled with [^{32}P]ATP (Amersham Pharmacia) and T4 polynucleotide kinase (Promega) and then purified using Sephadex G50 spin columns (Amersham Pharmacia). The DNA sequence of the NFκB located within p53 promoter as probe is 5'-AGT TGA GGG GAC TTT CCC AGG C-3' (Sigma Genosys, Cambridge, UK). The protein-binding reactions were carried out in 20µl of buffer [20mM HEPES (pH 8.0), 1mM EDTA, 50mM KCl, 10mM dithiothreitol, 10% glycerol, 1mg/ml BSA, 50µg/ml polydeoxyinosinic deoxycytidylic acid] with 50,000 cpm of labeled probe, 20µg of MCF-7 nuclear protein, and 5µg of polydeoxyinosinic deoxycytidylic acid. The mixtures were incubated at room temperature for 20 min in the presence or absence of unlabeled competitor oligonucleotides. For the experiments involving anti-PPARγ and anti-RXRα antibodies (Santa Cruz Biotechnology), the reaction mixture was incubated with these antibodies at 4 °C for 30 min before addition of labeled probe. The entire reaction mixture was electrophoresed through a 6% polyacrylamide gel in 0.25X Tris borate-EDTA for 3 h at 150 V. Gel was dried and subjected to autoradiography at -70 °C.

ChIP Assay. MCF-7 cells were grown in 10cm dishes to 50–60% confluence, shifted to SFM for 24 h, and then treated for 1 h as indicated. Thereafter, cells were washed twice with PBS and cross-linked with 1% formaldehyde at 37 °C for 10 min. Next, cells were washed twice with PBS at 4 °C, collected and resuspended in 200µl of lysis buffer (1% SDS; 10mM EDTA; 50 mM Tris-HCl, pH 8.1), and left on ice for 10 min. Then, cells were sonicated four times for 10 sec at

30% of maximal power (Vibra Cell 500 W; Sonics and Materials, Inc., Newtown, CT) and collected by centrifugation at 4 °C for 10 min at 14,000 rpm. The supernatants were diluted in 1.3 ml of immunoprecipitation buffer (0.01% SDS; 1.1% Triton X-100; 1.2mM EDTA; 16.7mM Tris-HCl, pH 8.1; 16.7mM NaCl) followed by immunoclearing with 60µl of sonicated salmon sperm DNA/protein A agarose (DBA Srl, Milan, Italy) for 1 h at 4 °C. The precleared chromatin was immunoprecipitated with anti-PPARγ, anti-RXRα or anti-RNA Pol II antibodies (Santa Cruz Biotechnology). At this point, 60µl salmon sperm DNA/protein A agarose was added, and precipitation was further continued for 2 h at 4 °C. After pelleting, precipitates were washed sequentially for 5 min with the following buffers: Wash A [0.1% SDS, 1% Triton X-100, 2mM EDTA, 20mM Tris-HCl (pH 8.1), 150mM NaCl], Wash B [0.1% SDS, 1% Triton X-100, 2mM EDTA, 20mM Tris-HCl (pH 8.1), 500mM NaCl], and Wash C [0.25M LiCl, 1% NP-40, 1% sodium deoxycholate, 1mM EDTA, 10mM Tris-HCl (pH 8.1)], and then twice with TE buffer (10mM Tris, 1mM EDTA). The immunocomplexes were eluted with elution buffer (1% SDS, 0.1 M $NaHCO_3$). The eluates were reverse cross-linked by heating at 65 °C and digested with proteinase K (0.5mg/ml) at 45 °C for 1 h. DNA was obtained by phenol-chloroform-isoamyl alcohol extraction. Two microliters of 10mg/ml yeast tRNA (Sigma) were added to each sample, and DNA was precipitated with 95% ethanol for 24 h at -20 °C and then washed with 70% ethanol and resuspended in 20µl of TE buffer. A 5µl volume of each sample was used for PCR with primers flanking a sequence present in the p53 promoter: 5'-CTGAGAGCAAACGCAAAAG-3' (forward) and 5'-CAGCCCGAACGCAAAGTGTC- 3' (reverse) containing the κB site from -254 to -42 region. The PCR conditions for the p53 promoter fragments were, 45 sec at 94 °C, 40 sec at 57 °C, 90 sec at 72 °C. The amplification products obtained in 30 cycles were analyzed in a 2% agarose gel and visualized by ethidium bromide staining. The negative control was provided by PCR amplification without a DNA sample. The specificity of reactions was ensured using normal mouse and rabbit IgG (Santa Cruz Biotechnology).

Animals. Male C57BL/6 mice were used, unless noted otherwise, in accordance with institutional guidelines. Mice were fed ad libitum or fasted 12-16 hr. Seven to 12-week-old WT, *ob/ob* mice, and mice heterozygous for the Akita spontaneous mutation (Ins2Akita) were purchased from the Jackson Lab. To establish DIO, 1-month-old mice were fed a high-fat diet (50% of calories as fat) for 5 months. To deplete β-cells, Stz (170 mg/kg) was dosed i.p. once in 10 mM sodium citrate, pH 4.5 (45). For glucose-tolerance tests (GTT), glucose (2 g/kg) was dosed i.p. in saline. The *db/db* mice were 5-months-old and fed ad libitum. Insulin levels in this *db/db* colony at this age average 3-fold higher than controls, $P<0.01$ (46).

Retinoids and retinoid quantification. Retinoids were purchased from Sigma, except for 9-cis-retinol, which was synthesized and characterized as described (Kane et al. 2008). Retinoids were used under yellow light as described (16, 17). Samples were harvested under yellow lights, frozen immediately in liquid nitrogen, and kept at -80 ^{o}C until extraction and retinoid quantification within one day by LC/MS/MS using selected reaction monitoring (RA isomers) or HPLC/UV (retinol isomers) as described in detail (Kane et al. 2005, 2008, 2005).

β-cell line function assays. The pancreatic β-cell line 832/13 was cultured in RPMI 1640 with 10% fetal calf serum, 10 mM Hepes, 2 mM L-glutamine, 1 mM sodium pyruvate, and 50 mM β-mercaptoethanol, 100 units/ml penicillin and 100 mg/ml streptomycin at 37 °C and 5% CO_2 in 100 mm Petri dishes as described (Hohmeier et al. 2000). The medium was refreshed every 2-3 days. Cells were subcultured when they approached ≥70% confluence. Endogenous 9cRA in 832/13 cells at the time of experiments was $<0.04 \pm 0.0012$ pmol/10^6 cells (n = 9 plates). To assay Glut2, GK and ATP, cells were transferred to 12-well plates until reaching 85% of confluence. Medium with 5 mM glucose was substituted for growth medium (11 mM glucose) for 16 hr. To initiate assays, this medium was substituted with 2 mL HBSS containing 0.2% fatty-acid free BSA, pH 7.2 (sensing buffer) and 3 mM glucose for 2 hr (except for the glucose uptake assay). Experiments were initiated by changing the sensing buffer to 0.8 ml/well of either fresh secretion buffer with 3 mM glucose or 23 mM glucose and/or 100 nM 9cRA, delivered in 5-10 µL DMSO, or vehicle alone. Incubations were done at 37 °C under yellow light. GK activity was measured by detaching (0.05% trypsin/0.5 mM EDTA) and pelleting cells. Cells were resuspended and sonicated in 500 µl PBS at 4 °C. Sonicates were centrifuged at 4 °C for 15 min at 12,000 rpm. GK activity in the supernatant was determined by a coupled enzyme assay with glucose-6-phosphate dehydrogenase and NAD^+ by monitoring the increase in absorbance at 340 nm at 1 min intervals for 5 min. One unit of activity represents the amount of enzyme that converts 1 µmol substrate into product per min at 30 °C. Data were corrected for blank values, determined in the absence of glucose. To correct for any low K_m hexokinase contribution, activity measured with 0.5 mM glucose was subtracted from activity measured with 100 mM glucose. Glucose uptake (Glut2 activity) was measured after 16 hr incubation with 5 mM glucose. The medium was supplemented with vehicle and isobutylmethylxanthine (1 mM) and/or forskolin (100 µM) and/or 9cRA (30 or 100 nM). After 20 min, the medium

was exchanged for secretion buffer containing 23 mM glucose supplemented with vehicle or 9cRA; incubation was continued 15 min at ambient temperature. (The 2 hr incubation with 3 mM glucose was omitted). Glucose uptake was measured over 1 min at ambient temperature by adding 250 µl of a [^{3}H]glucose solution (23 mM/1.25 µCi). Uptake was ended after 1 min by adding 1 mM $HgCl_2$ in ice-cold PBS. Cells were washed 5 times with the same buffer, lysed with 200 µl 10% SDS, frozen at -80 °C and thawed. [^{3}H]Glucose was recovered with 300 µl water and counted in 4 mL of Ecolite liquid scintillation cocktail. Background was determined in wells treated with [^{3}H]glucose and 1 mM $HgCl_2$ at t_0. Transport activity was calculated subtracting t_0 values from samples. Protein was quantified by Bradford Assay. Ca^{2+} was quantified with a kit according to manufacturer's instructions (Diagnosticum Rt., Budapest, Hungary) in cells that were lysed in culture dishes by adding 0.1 ml of RIPA buffer, scraping several times and centrifuging to remove cellular debris.

9cRA biosynthesis. 832/13 cells were cultured in 12- or 6-well plates. At confluence, the medium was replaced with serum-free medium and retinoids (1 µM) in DMSO (0.1% v/v) or vehicle alone were added and incubated 1 hr. Cells were lysed using Reporter lysis buffer (Promega) and combined with their medium for retinoid analyses.

Insulin secretion studies. Islets were isolated by the UCSF Diabetes & Endocrinology Research Center (San Francisco, CA). Fifteen islets of similar size were incubated at 37 °C in 12-well plates with 5 mM D-glucose in RPMI1640 supplemented with 10% fetal bovine serum, 100 U/ml penicillin, 100 µg/ml streptomycin, 10 mM Hepes, 2 mM L-glutamine, 1 mM sodium pyruvate, 50 µM β-mercaptoethanol and 5% CO_2. After 16 hr, islets were washed and transferred to 1.5 ml tubes in secretion medium (HBSS with 20 mM Hepes and 1% bovine serum albumin, pH 7.2) containing 3 mM glucose. After 2 hr, secretion medium was replaced with fresh secretion medium containing 3 or 23 mM glucose with 100 nM 9cRA or vehicle alone (DMSO). Separate groups of islets were incubated in secretion medium containing 3 mM glucose with 35 mM KCl and 90 mM NaCl. Media were centrifuged for 2 min at 1000 x g to remove non-adherent cells and frozen at -80 ºC. Endogenous 9cRA in islets at the time of the experiment (after isolation and handling of islets) did not exceed 0.12 ± 0.008 pmol/plate (n = 5).

Immunofluorescence. Pancreata from adult mice were dissected and fixed in 10% neutral-buffered formalin (pH 6.8-7.2) for 24 hr and then embedded in paraffin by Histopathology Reference Labs (Hercules, CA). Eight-µm slices were dewaxed with 100% xylene (2 x 3 min) and rehydrated with 100% ethanol (2 x 3 min), 95% ethanol (2 x 3 times) and deionized water. The low-power antigen retrieval technique was done as follows: a maximum of 8 slides were placed in a Pyrex beaker with 250 ml 1:100 Vector unmasking buffer (pH 6.0) according to the manufacturer's instructions (Vector Laboratories, Burlingame, CA). The beaker was heated in a microwave oven with a power setting of 40% for three 5 min cycles, with 1 min breaks. Slides were allowed to cool 30 min at ambient temperature. Unmasking buffer was replaced with Tris-buffered saline containing 0.1% Tween-20 (TBST). Nonspecific binding was blocked with 250 µl 10% normal donkey serum blocking solution (Jackson Immunoresearch) in TBST for at least 30 min before adding primary antibody. Sections were incubated with anti-insulin antibodies (Ab) (1:200, Dako, Carpinteria, CA) overnight at 4 °C, followed by three 5-min washes in PBS. Dylight 488 secondary Ab (Jackson Immunoresearch) incubation was done for 1 hr at ambient temperature. Fluorescence was detected with a Zeiss LSM 510 laser scanning confocal microscope in the College of Natural Resource Imaging Facility at UC-Berkeley.

mRNA expression. Total RNA was isolated with Trizol (Invitrogen, Carlsbad,CA, USA). RNA was reversed transcribed with IScript cDNA Synthesis Kit (Biorad). TaqMan quantitative real-time PCR (qT-PCR) was done using pre-designed and optimized primers (Applied Biosystems, Foster City, CA, USA). Gene expression was measured with ABI-PRISM 7500 Real-Time PCR systems sequence detection (Applied Biosystems, Foster City, CA, USA).

Statistical Analysis. Statistical analysis was performed using one way ANOVA followed by Newman-Keuls testing to determine differences in means or Dunnett's Multiple Comparison test or was assessed by two-tailed, unpaired Student's *t* tests for comparison of two groups, or by two-way ANOVA for comparison of two curves. $P < 0.05$ was considered as statistically significant. Differences were considered significant at values of * $P < 0.05$, ** $P < 0.01$. Data are means ± SE.

REFERENCES

- Abe, K & Matsuki, N. (2000). Measurement of cellular 3-(4,5-dimethylthiazol-2-yl)-2,5-diphenyltetrazolium bromide (MTT) reduction activity and lactate dehydrogenase release using MTT. *Neurosci Res*, 38:325-329.
- Aebi H (1974) Catalase. In: Bergmeyer HU (ed) Methods in enzymatic analysis. Academic Press, New York, pp 631–684.
- Ahuja, HS, Szanto, A, Nagy, L, and Davies, PJ. (2003) The retinoid X receptor and its ligands: versatile regulators of metabolic function, cell differentiation and cell death. *J Biol Regul Homeost Agents*, 17:29-45.
- Alva, AS, Gultekin, SH & Baehrecke, EH. (2004). Autophagy in human tumors: cell survival or death? *Cell Death Differ*, 11:1046-1048.
- Appling, DR & Chytil, F. (1981). Evidence of a role for retinoic acid (vitamin A-acid) in the maintenance of testosterone production in male rats. *Endocrinology*, 108:2120-2124.
- Arakawa, K, Ishihara, T, Aoto, M, Inamasu, M, Kitamura, K & Saito A. (2004) An antidiabetic thiazolidinedione induces eccentric cardiac hypertrophy by cardiac volume overload in rats. *Clin Exp Pharmacol Physiol*, 31:8–13.
- Ashizawa, S, Brunicardi, FC, & Wang, XP. (2004) PDX-1 and the pancreas. *Pancreas*, 28:109-120.
- Babu, DA, Deering, TG & Mirmira, RG. (2007) A feat of metabolic proportions: Pdx1 orchestrates islet development and function in the maintenance of glucose homeostasis. *Mol Genet Metab*, 92:43-55.
- Bartoov-Shifman, R, Hertz, R, Wang, H, Wollheim, CB, Bar-Tana, J & Walker, MD. (2002). Activation of the insulin gene promoter through a direct effect of hepatocyte nuclear factor 4 alpha. *J Biol Chem*, 277:25914-25919.
- Bernstein, PS, Choi, SY, Ho, YC & Rando, RR. (1995). Photoaffinity labeling of retinoic acid-binding proteins. *Proc Natl Acad Sci U S A*, 92, 654-658.
- Biederbick, A, Kern, HF & Elsasser, HP. (1995). Monodansylcadaverine (MDC) is a specific in vivo marker for autophagic vacuoles. *Eur J Cell Biol*, 66:3-14.
- Bindoli, A, Callegaro, MT, Barzon, E, Benetti, M & Rigobello, MP. (1997). Influence of the redox state of pyridine nucleotides on mitochondrial sulfhydryl groups and permeability transition. *Arch Biochem Biophys*, 342, 22-28.
- Bisaccia, F, Indiveri, C & Palmieri, F. (1988). Purification and reconstitution of two anion carriers from rat liver mitochondria: the dicarboxylate and the 2-oxoglutarate carrier. *Biochim Biophys Acta*, 933:229-240.
- Bishoff ED, Gottardis, MM, Moon, TE, Heyman, RA & Lamph, WW. (1998) Beyond tamoxifen: the retinoid X receptor selective ligand LGD1069 (TARGRETIN) causes complete regression of mammary carcinoma. *Cancer Res*, 1998, 58:479-484.
- Blomhoff R (1994) *Vitamin A in Health and Disease*, Marcel Dekker, New York.
- Blomhoff, R, Green, MH, Berg, T & Norum KR. (1990) Transport and storage of vitamin A. *Science (Wash. DC)* 250:399–404.
- Blomhoff, R, Green, MH, Green JB, Berg, T & Norum KR. (1991) Vitamin A metabolism: New perspectives on absorption, transport, and storage. *Physiol Rev*, 71**:**951–990.

- Bolmer, SD & Wolf, G. (1982). Retinoids and phorbol esters alter release of fibronectin from enucleated cells. *Proc Natl Acad Sci U S A*, 79:6541-6545.
- Bonofiglio, D, Aquila, S, Catalano, S, Gabriele, S, Belmonte, M, Middea, E, Qi, H, Morelli, C, Gentile, M, Maggiolini, M & Ando, S. (2006). Peroxisome proliferator-activated receptor-gamma activates p53 gene promoter binding to the nuclear factor-kappaB sequence in human MCF7 breast cancer cells. *Mol Endocrinol*, 20:3083-3092.
- Bonofiglio, D, Gabriele, S, Aquila, S, Catalano, S, Gentile, M, Middea, E, Giordano, F & Ando, S. (2005). Estrogen receptor alpha binds to peroxisome proliferator-activated receptor response element and negatively interferes with peroxisome proliferator-activated receptor gamma signaling in breast cancer cells. *Clin Cancer Res*, 11:6139-6147.
- Bonofiglio, D, Gabriele, S, Aquila, S, Qi, H, Belmonte, M, Catalano, S & Ando, S. (2009). Peroxisome proliferator-activated receptor gamma activates fas ligand gene promoter inducing apoptosis in human breast cancer cells. *Breast Cancer Res Treat*, 113:423-434.
- Bossy-Wetzel, E, Newmeyer, DD & Green, DR. (1998). Mitochondrial cytochrome c release in apoptosis occurs upstream of DEVD-specific caspase activation and independently of mitochondrial transmembrane depolarization. *EMBO J*, 17, 37-49.
- Breitman, TR & Takahashi, N. (1996). Retinoylation of proteins in mammalian cells. *Biochem Soc Trans*, 24: 723-727.
- Bursch, W, Ellinger, A, Gerner, C & Schulte-Hermann, R. (2004) Autophagocytosis and programmed cell death. In: Klionsky DJ, editors. Autophagy. Landes Bioscience, Georgetown, pp 287–303.
- Cai, J, Yang, J & Jones, DP. (1998). Mitochondrial control of apoptosis: the role of cytochrome c. *Biochim Biophys Acta*, 1366:139-149.
- Calleja, C, Messaddeq, N, Chapellier, B, Yang, H, Krezel, W, Li, M, Metzger, D, Mascrez, B, Ohta, K, Kagechika, H, Endo, Y, Mark, M, Ghyselinck, NB & Chambon, P. (2006). Genetic and pharmacological evidence that a retinoic acid cannot be the RXR-activating ligand in mouse epidermis keratinocytes. *Genes Dev*, 20:1525-1538.
- Chambon, P. (1996) A decade of molecular biology of retinoic acid receptors. *FASEB J*, 10, 940-954.
- Chambon, P. (1996) A decade of molecular biology of retinoic acid receptors. *FASEB J*. 10, 940-954.
- Cheng, C, Michaels, J & Scheinfeld, N. (2008) Alitretinoin: a comprehensive review. *Expert Opin Investig Drugs*, 17:437-443.
- Chertow, BS & Baker, GR. (1978) The effects of vitamin A on insulin release and glucose oxidation in isolated rat islets. *Endocrinology*, 103:1562-1572.
- Chien, DS, Sandri, RB & Tang-Liu, DS. (1992) Systemic pharmacokinetics of Acitretin, etretinate, isotretinoin, and acetylenic retinoids in guinea pigs and obese rats. *Drug Metab Dispos Biol Fate Chem*, 20:211–217.
- Chuang, JC, Cha, JY, Garmey, JC, Mirmira, RG & Repa JJ. (2008) Research resource: nuclear hormone receptor expression in the endocrine pancreas. *Mol Endocrinol*, 22:2353-2363.
- Ciolino, HP & Yeh, GC. (1999). The flavonoid galangin is an inhibitor of CYP1A1 activity and an agonist/antagonist of the aryl hydrocarbon receptor. *Br J Cancer*, 79, 1340-1346.
- Cione, E & Genchi, G. (2004) Characterization of rat testes mitochondrial retinoylating system and its partial purification. *J Bioenerg Biomembr*, 36: 211–217.

- Cione, E, Tucci, P, Chimento, A, Pezzi, V & Genchi, G. (2005) Retinoylation reaction of proteins in Leydig (TM-3) cells. *J Bioenerg Biomembr*, 37:43–48.
- Cossarizza, A, Baccarani-Contri, M, Kalashnikova, G & Franceschi, C. (1993). A new method for the cytofluorimetric analysis of mitochondrial membrane potential using the J-aggregate forming lipophilic cation 5,5',6,6'-tetrachloro-1,1',3,3'-tetraethylbenzimidazolcarbocyanine iodide (JC-1). *Biochem Biophys Res Commun*, 197:40-45.
- Crouch, GD & Helman, LJ. (1991) All-trans retinoic acid inhibits the growth of human rhabdomyosarcoma cell lines. *Cancer Res*, 51:4882-4887.
- Das, K & Chainy, GB. (2001). Modulation of rat liver mitochondrial antioxidant defence system by thyroid hormone. *Biochim Biophys Acta*, 1537: 1-13.
- Davis, WL, Crawford, LA, Cooper, OJ, Farmer, GR, Thomas, D & Freeman, BL. (1990). Generation of radical oxygen species by neural crest cells treated in vitro with isotretinoin and 4-oxo-isotretinoin. *J Craniofac Genet Dev Biol*, 10:295-310.
- De Alvaro, C, Teruel, T, Hernandez, R & Lorenzo, M. (2004). Tumor necrosis factor alpha produces insulin resistance in skeletal muscle by activation of inhibitor kappaB kinase in a p38 MAPK-dependent manner. *J Biol Chem*, 279:17070-17078.
- De Leenheer, AP, Lambert, WE & Claeys I. (1982) All-trans retinoic acid: Measurement of reference values in human serum by high performance liquid chromatography. *J Lipid Res*, 23:1362–1367.
- Demetri, GD, Fletcher, CD, Mueller, E, Sarraf, P, Naujoks, R, Campbell, N, Spiegelman, BM & Singer, S. (1999). Induction of solid tumor differentiation by the peroxisome proliferator-activated receptor-gamma ligand troglitazone in patients with liposarcoma. *Proc Natl Acad Sci U S A*, 96:3951-3956
- Del Rincon, SV, Rousseau, C, Samanta, R & Miller, WHJr. (2003) Retinoic acid-induced growth arrest of MCF-7 involves the selective regulation of the IRS-1/PI3-kinase/AKT pathway. *Oncogene*, 22: 3353-3360.
- Della Ragione, F, Cucciolla, V, Borriello, A, Della, P, V, Manna, C, Galletti, P & Zappia, V. (2000). Pyrrolidine dithiocarbamate induces apoptosis by a cytochrome c dependent mechanism. *Biochem Biophys Res Commun*, 268, 942-946.
- Di Renzo, J, Soderstrom, M & Kurokawa, R. (1997) Peroxisome proliferator-activated receptor gamma transcriptionally up-regulates hormone-sensitive lipase via the involvement of specificity protein-1. *Endocrinology*, 147: 875-884.
- Dragnev, KH, Petty, WJ & Dmitrovsky, E. (2003). Retinoid targets in cancer therapy and chemoprevention. *Cancer Biol Ther*, 2, S150-S156.
- Drew, B & Leeuwenburgh, C. (2003). Method for measuring ATP production in isolated mitochondria: ATP production in brain and liver mitochondria of Fischer-344 rats with age and caloric restriction. *Am J Physiol Regul Integr Comp Physiol*, 285:R1259-R1267.
- Eckhoff, C & Nau, H. (1990) Identification and quantitation of all-trans- and 13-cis retinoic acid and 13-cis-4-oxo-retinoic acid in human plasma. *J Lipid Res*, 31:1145 1154.
- Elstner, E, Mu¨ller, C, Koshizuka, K, Williamson, EA, Park, D, Asou, H, Shintaku, P, Said, JW, Heber, D & Koeffler HP. (1998) Ligands for peroxisome proliferator-activated receptor _ and retinoic acid receptor inhibit growth and induce apoptosis of human breast cancer cells *in vitro* and in BNX mice. *Proc Natl Acad Sci*, USA 95:8806–8811.

- Elstner, E, Williamson, EA, Zang C, Fritz, J, Heber, D, Fenner, M, Possinger, K & Koeffler HP. (2002) Novel therapeutic approach: ligands for PPARγ and retinoid receptors induce apoptosis in bcl-2-positive human breast cancer cells. *Breast Cancer Res Treat,* 74:155–165.
- Ferber, S, BeltrandelRio, H, Johnson, JH, Noel, RJ, Cassidy, LE, Clark, S, Becker, TC, Hughes, SD & Newgard, CB. (1994). GLUT-2 gene transfer into insulinoma cells confers both low and high affinity glucose-stimulated insulin release. Relationship to glucokinase activity. *J Biol Chem*, 269:11523-11529.
- Genchi, G & Olson, JA. (2001) Retinoylation of proteins in cell-free fractions of rat tissues in vitro. *Biochim Biophys Acta*, 1530:146–154.
- Germain, P, Chambon, P, Eichele, G, Evans, RM, Lazar, MA., Leid, M, De Lera, AR, Lotan, N, Mangelsdorf, DJ & Gronemeyer, H. (2006) International Union of Pharmacology. LXIII. Retinoid X receptors. *Pharmacol Rev,* 58:760-772.
- Gianni, M, Bauer, A, Garattini, E, Chambon, P & Rochette-Egly, C. (2002) Phosphorylation by p38MAPK and recruitment of SUG-1 are required for RA-induced RAR gamma degradation and transactivation. *EMBO J,* 21:3760-3769.
- Gianni, M, Parrella, E, Raska, I, Jr., Gaillard, E, Nigro, EA, Gaudon, C, Garattini & Rochette-egly, C. (2006) P38MAPK-dependent phosphorylation and degradation of SRC-3/AIB1 and RAR-alpha mediated transcription. *EMBO J*, 25:793-751.
- Gianni,M, Ponzanelli, I, Mologni, L, Reichert, U, Rambaldi, A, Terao, M & Garattini, E. (2000) Retinoid-dependent growth inhibition, differentiation and apoptosis in acute promyelocytic leukemia cells. Expression and activation of caspases. *Cell Death Differ*, 7, 447-460.
- Green, DR & Reed, JC. (1998). Mitochondria and apoptosis. *Science*, 281, 1309-1312.
- Green, DR. (2000). Apoptotic pathways: paper wraps stone blunts scissors. *Cell*, 102, 1-4.
- Grommes, C, Landreth, GE & Heneka MT. (2004) Antineoplastic effects of peroxisome proliferator-activated receptor gamma agonists. *Lancet Oncol,* 5:419-429.
- Gudas, LJ, Sporn, MB, Roberts, AB. (1994) Cellular biology and biochemistry of the retinoids. In: Sporn MB, Roberts AB, Goodman DS (eds) The retinoids: biology, chemistry, and medicine. Raven Press, New York, pp 443–520
- Gurusamy, N & Das, DK. (2009). Is autophagy a double-edged sword for the heart? *Acta Physiol Hung*, 96, 267-276.
- Habig, WH, Pabst, MJ & Jakoby, WB. (1974). Glutathione S-transferases. The first enzymatic step in mercapturic acid formation. *J Biol Chem*, 249:7130-7139.
- Hayes, JD & McLellan, LI. (1999). Glutathione and glutathione-dependent enzymes represent a co-ordinately regulated defence against oxidative stress. *Free Radic Res*, 31:273-300.
- Hengartner, MO. (2000). The biochemistry of apoptosis. *Nature*, 407, 770-776.
- Henion, PD & Weston, JA. (1994). Retinoic acid selectively promotes the survival and proliferation of neurogenic precursors in cultured neural crest cell populations. *Dev Biol*, 161, 243-250.
- Henquin, JC, Ravier, MA, Nenquin, M, Jonas, JC & Gilon, P. (2003) Hierarchy of the beta-cell signals controlling insulin secretion. *Eur J Clin Invest,* 33:742-750.
- Herbert, V. (1996). Prooxidant effects of antioxidant vitamins. Introduction. *J Nutr*, 126:1197S-1200S.
- Hirosawa, K & Yamada, K. (1973) The localization of the vitamin A in the mouse liver as revealed by electron microscope radioautography. *J Electron Microsc (Tokyo),* 22:337–346.

- Hirsch, T, Marzo, I & Kroemer, G. (1997). Role of the mitochondrial permeability transition pore in apoptosis. *Biosci Rep*, 17, 67-76.
- Hiscox, S, Morgan, L, Green, TP, Barrow, D, Gee, J & Nicholson RI. (2005) Elevated Src activity promotes cellular invasion and motility in tamoxifen resistant breast cancer cells. *Breast Cancer Res Treat*, 7:1-12.
- Hohmeier, HE, Mulder, H, Chen, G, Henkel-Rieger, R, Prentki, M & Newgard, CB. (2000) Isolation of INS-1-derived cell lines with robust ATP-sensitive K+ channel-dependent and -independent glucose-stimulated insulin secretion. *Diabetes*, 49:424-430.
- Horn, V, Minucci, S, Ogryzko, VV, Adamson, ED, Howard, BH, Levin, AA, Ozato, K. (1996) RAR and RXR selective ligands cooperatively induce apoptosis and neuronal differentiation in P19 embryonal carcinoma cells. *FASEB J*, 10:1071–1077.
- Huang, ME, Ye, YC, Chen, SR, Chai, JR, Lu, JX, Zhoa, L, Gu, LJ & Wang, ZY. (1988) Use of all-trans retinoic acid in the treatment of acute promyelocytic leukemia. *Blood* 72, 567-572.
- Hurnanen, D, Chan, HM & Kubow, S. (1997). The protective effect of metallothionein against lipid peroxidation caused by retinoic acid in human breast cancer cells. *J Pharmacol Exp Ther*, 283:1520-1528.
- Jaattela, M. (2004). Multiple cell death pathways as regulators of tumour initiation and progression. *Oncogene*, 23, 2746-2756.
- Jellinck, PH, Forkert, PG, Riddick, DS, Okey, AB, Michnovicz, JJ & Bradlow, HL. (1993). Ah receptor binding properties of indole carbinols and induction of hepatic estradiol hydroxylation. *Biochem Pharmacol*, 45, 1129-1136**.**
- Jensen, MV, Joseph, JW, Ronnebaum, SM, Burgess, SC, Sherry, A.D & Newgard, CB. (2008). Metabolic cycling in control of glucose-stimulated insulin secretion. *Am J Physiol Endocrinol Metab*, 295:E1287-1297.
- Johnstone, RW, Ruefli, AA & Lowe, SW. (2002). Apoptosis: a link between cancer genetics and chemotherapy. *Cell*, 108, 153-164.
- Joza, N, Susin, SA, Daugas, E, Stanford, WL, Cho, SK, Li, CY, Sasaki, T, Elia, AJ, Cheng, HY, Ravagnan, L, Ferri, KF, Zamzami, N, Wakeham, A, Hakem, R, Yoshida, H, Kong, YY, Mak, TW, Zuniga-Pflucker, JC, Kroemer, G & Penninger, JM. (2001). Essential role of the mitochondrial apoptosis-inducing factor in programmed cell death. *Nature*, 410, 549-554.
- Kadison, A, Kim, J, Maldonado, T, Crisera, C, Prasadan, K., Manna, P, Preuett, B, Hembree, M, Longaker, M & Gittes, G. (2001) Retinoid signaling directs secondary lineage selection in pancreatic organogenesis. *J Pediatr Surg*, 36:1150-1156.
- Kakkad, B & Ong, DE. (1988) Reduction of retinaldehyde bound to cellular retinolbinding protein (type II) by microsomes from rat small intestine. *J Biol Chem*, 263**:**12916–12919.
- Kane, MA, Chen, N, Sparks, S & Napoli, JL. (2005) Quantification of endogenous retinoic acid in limited biological samples by LC/MS/MS. *Biochem J*, 388:363-369.
- Kane, MA, Folias, AE & Napoli, JL. (2008) HPLC/UV quantitation of retinal, retinol, and retinyl esters in serum and tissues. *Anal Biochem*, 378:71-79.
- Kane, MA, Folias, AE, Wang, C & Napoli, JL. (2008) Quantitative profiling of endogenous retinoic acid in vivo and in vitro by tandem mass spectrometry. *Anal Chem*, 80:1702-1708.
- Kastner, P, Chambon, P & Leid, M. (1994) In Vitamin A in Health and Disease (Blomhoff, R., ed.), Marcel Dekker, New York, pp. 189–238.

- Kim, DG, Jo, BH, You, KR & Ahn, DS. (1996). Apoptosis induced by retinoic acid in Hep 3B cells in vitro. *Cancer Lett*, 107, 149-159.
- Kitamura, S, Miyazaki, Y, Shinomura, Y, Kondo, S, Kanayama, S & Matsuzawa, Y. (1999). Peroxisome proliferator-activated receptor gamma induces growth arrest and differentiation markers of human colon cancer cells. *Jpn J Cancer Res*, 90:75-80.
- Knowlden, JM, Hutcheson, IR, Jones, HE, Madden, T, Gee, JMW, Harper, ME, Barrow, D, Wakeling, AE & Nicholson RI. (2003) Elevated levels of EGFR/c-erbB2 heterodimers mediate an autocrine growth regulatory pathway in Tamoxifen-resistant MCF-7 cells. *Endocrinology*, 144:1032-1044.
- Kobayashi, H, Spilde, TL, Bhatia, A.M., Buckingham, R.B., Hembree, M.J., Prasadan, K., Preuett, B.L., Imamura, M., and Gittes, G.K. (2002) Retinoid signaling controls mouse pancreatic exocrine lineage selection through epithelial-mesenchymal interactions. *Gastroenterology*, 123:1331-1340.
- Kolesnick, R. (2002). The therapeutic potential of modulating the ceramide/sphingomyelin pathway. *J Clin Invest*, 110:3-8.
- Kondo, Y, Kanzawa, T, Sawaya, R & Kondo, S. (2005). The role of autophagy in cancer development and response to therapy. *Nat Rev Cancer*, 5, 726-734.
- Kowaltowski, AJ, Vercesi, AE & Castilho, RF. (1997). Mitochondrial membrane protein thiol reactivity with N-ethylmaleimide or mersalyl is modified by Ca2+: correlation with mitochondrial permeability transition. *Biochim Biophys Acta*, 1318, 395-402.
- Kuratomi, Y, Kumamoto, Y, Yamashita, H, Yamamoto, T, Inokuchi, A, Tomita, K, Masuda, A, Uehara, S, Ohmagari, J, Jingu, K & Komiyama, S. (1999). Comparison of survival rates of patients with nasopharyngeal carcinoma treated with radiotherapy, 5-fluorouracil and vitamin A ("FAR" therapy) vs FAR therapy plus adjunctive cisplatin and peplomycin chemotherapy. *Eur Arch Otorhinolaryngol*, 256 Suppl 1, S60-S63.
- Leblanc, BP & Stunnenberg, HG. (1995). 9-cis retinoic acid signaling: changing partners causes some excitement. *Genes Dev*, 9:1811-1816.
- Le Ferrec, E, Lagadic-Gossmann, D, Rauch, C, Bardiau, C, Maheo, K, Massiere, F, Le, VM, Guillouzo, A & Morel, F. (2002). Transcriptional induction of CYP1A1 by oltipraz in human Caco-2 cells is aryl hydrocarbon receptor- and calcium-dependent. *J Biol Chem*, 277, 24780-24787.
- Lee, JE & Safe, S. (2001). Involvement of a post-transcriptional mechanism in the inhibition of CYP1A1 expression by resveratrol in breast cancer cells. *Biochem Pharmacol*, 62, 1113-1124.
- Lefebvre, P, Chinetti, G, Fruchart, JC & Staels, B. (2006) Sorting out the roles of PPARα in energy metabolism and vascular homeostasis. *Journal of Clinical Investigation*, 116:571-580.
- Leibel, RL, Chung, WK & Chua, SC, Jr. (1997) The molecular genetics of rodent single gene obesities. *J Biol Chem*, 272:31937-31940.
- Leibowitz, MD, Ardecky, RJ, Boehm, MF, Broderick, CL, Carfagna, MA, Crombie, DL, D'Arrigo, J, Etgen, GJ, Faul, MM, Grese, TA, Havel, H, Hein, NI, Heyman, RA, Jolley, D, Klausing, K, Liu, S, Mais, DE, Mapes, CM, Marschke, KB, Michellys, PY, Montrose-Rafizadeh, C, Ogilvie, KM, Pascual, B, Rungta, D, Tyhonas, JS, Urcan, MS, Wardlow, M, Yumibe, N & Reifel-Miller, A. (2006). Biological characterization of a heterodimer-selective retinoid X receptor modulator: potential benefits for the treatment of type 2 diabetes. *Endocrinology*, **147**, 1044-1053.

- Lemberger, T, Desvergne, B & Wahli, W. (1996) Peroxisome proliferator-activated receptors: a nuclear receptor signaling pathway in lipid physiology. *Annual Review of Cell and Developmental Biology,* 12:335-363.
- Lenzen, S. (2008) The mechanisms of alloxan- and streptozotocin-induced diabetes. *Diabetologia,* 51:216-226.
- Levine, B & Klionsky, DJ. (2004) Development by self-digestion: molecular mechanisms and biological functions of autophagy. *Dev Cell*, 6:463-477.
- Li, Y, Hashimoto, Y, Agadir, A, Kagechika, H & Zhang, X. (1999). Identification of a novel class of retinoic acid receptor beta-selective retinoid antagonists and their inhibitory effects on AP-1 activity and retinoic acid-induced apoptosis in human breast cancer cells. *J Biol Chem*, 274, 15360-15366.
- Liu, RM, Vasiliou, V, Zhu, H, Duh, JL, Tabor, MW, Puga, A, Nebert, DW, Sainsbury, M & Shertzer, HG. (1994). Regulation of [Ah] gene battery enzymes and glutathione levels by 5,10-dihydroindeno[1,2-b]indole in mouse hepatoma cell lines. *Carcinogenesis*, 15, 2347-2352.
- Livera, G, Rouiller-Fabre, V, Durand, P & Habert, R. (2000). Multiple effects of retinoids on the development of Sertoli, germ, and Leydig cells of fetal and neonatal rat testis in culture. *Biol Reprod*, 62:1303-1314.
- Lomo, J, Smeland, EB, Ulven, S, Natarajan, V, Blomhoff, R, Ghandi, U, Dawson, MI & Blomhoff, H.K. (1998) RAR-, not RXR, ligands inhibit cell activation and prevent apoptosis in B-limphocytes. . *Cell Physiol*, 175, 67-77.
- Lotan, R. (1996) Retinoids in cancer chemoprevention. *FASEB J*, 10, 1031-1039.
- Lowell, BB & Shulman, GI. (2005) Mitochondrial dysfunction and type 2 diabetes. *Science,* 307:384-387..
- Lowry, OH, Rosebrough, NJ, Farr, AL & Randall, RJ. (1951). Protein measurement with the Folin phenol reagent. *J Biol Chem*, 193: 265-275.
- MacDonald, PN & Ong, DE. (1988) Evidence for a lecithin-retinol acyltransferase activity in the rat small intestine. *J Biol Chem*, 263:12478–12482.
- Mancini, M, Nicholson, DW, Roy, S, Thornberry, NA, Peterson, EP, Casciola-Rosen, LA & Rosen, A. (1998). The caspase-3 precursor has a cytosolic and mitochondrial distribution: implications for apoptotic signaling. *J Cell Biol*, 140, 1485-1495.
- Mangelsdorf, DJ & Evans, RM. (1995) The RXR heterodimers and orphan receptors. *Cell,* 83:841-850.
- Mangelsdorf, DJ, Kliewer, SA, Kakizuca, A, Umesono, K. & Evans, RM. (1993) Retinoid Receptors. *Recent Prog. Horm. Res*, 48:99-121.
- Mangelsdorf, DJ, Umesono, MR, & Evans, RM. (1994) In The Retinoids: Biology, Chemistry and Medicine (Sporn,M.B., Roberts, A. B., and Goodman, D. S., eds.), Raven Press, New York, pp. 319–349.
- Matthews, KA, Rhoten, WB, Driscoll, HK & Chertow, BS. (2004) Vitamin A deficiency impairs fetal islet development and causes subsequent glucose intolerance in adult rats. *J Nut,r* 134:1958-1963.
- Mc Ierney, EM, Rose, DW, and Flynn, SE. (1998) Determinants of coactivator LXXLL motif specififity in nuclear receptor transcriptional activation. *Genes and Development*, 12:3357-3368.
- McCarroll, JA, Phillips, PA, Santucci, N, Pirola, RC, Wilson, JS & Apte, MV. (2006) Vitamin A inhibits pancreatic stellate cell activation: implications for treatment of pancreatic fibrosis. *Gut*, 55:79-89.
- McDougal, A, Wormke, M, Calvin, J & Safe, S. (2001). Tamoxifen-induced antitumorigenic/antiestrogenic action synergized by a selective aryl hydrocarbon receptor modulator. *Cancer Res*, 61, 3902-3907.
- Meijsing, SH, Pufall, MA, So, AY, Bates, DL, Chen, L & Yamamoto, KR. (2009). DNA binding site sequence directs glucocorticoid receptor structure and activity. *Science*, 324:407-410

- Mosmann, T. (1983). Rapid colorimetric assay for cellular growth and survival: application to proliferation and cytotoxicity assays. *J Immunol Methods*, 65:55-63.
- Mu, YM, Yanase, T, Nishi, Y, Tanaka, A, Saito, M, Jin, CH, Mukasa, C, Okabe, T, Nomura, M, Goto, K & Nawata, H. (2001). Saturated FFAs, palmitic acid and stearic acid, induce apoptosis in human granulosa cells. *Endocrinology*, 142:3590-3597.
- Mueller E, Sarraf P, Tontonoz P, Evans RM, Martin KJ, Zhang M, Fletcher C, Singer S, Spiegelman BM. (1998) Terminal differentiation of human breast cancer through PPARγ. *Mol Cell*, 1:465-470.
- Muoio, DM & Newgard, CB. (2008) Mechanisms of disease: molecular and metabolic mechanisms of insulin resistance and beta-cell failure in type 2 diabetes. *Nat Rev Mol Cell Bio,l* 9:193-205.
- Myhre, AM, Hagen, E, Blomhoff, R & Norum, KR. (1998) Retinoylation of proteins in a macrophage tumor cell line J774, following uptake of chylomicron remnant retinyl ester. *J Nutr Biochem*, 9:705–711.
- Myhre, AM, Takahashi, N, Blomhof, R, Breitman, TR & Norum, KR. (1996) Retinoylation of proteins in rat liver, kidney, and lung in vivo. *J Lipid Res*. 37:1971–1977.
- Nagy, L, Thomázy, VA, Shipley, GL, Fésüs, L, Lamph, W, Heyman, RA, Chandraratna, RA & Davies, PJ. (1995) Activation of retinoid X receptors induces apoptosis in HL-60 cell lines. *Mol Cell Bio*, 15(7):3540-51.
- Nakamura, N, Shidoji, Y, Yamada, Y, Hatakeyama, H, Moriwaki, H & Muto, Y. (1995). Induction of apoptosis by acyclic retinoid in the human hepatoma-derived cell line, HuH-7. *Biochem Biophys Res Commun*, 207, 382-388.
- Napoli, JL, Pramanik, BC, Williams, JB, Dawson, MI & Hobbs, PD. (1985) Quantification of retinoic acid by gas-liquid chromatography-mass spectrometry: Total versus all-trans-retinoic acid in human plasma. *J Lipid Res*, 26:387–392.
- Napoli, JL. (1999) Retinoic acid: its biosynthesis and metabolism. *Prog Nucleic Acid Res Mol Biol*, 63:139-188.
- Nicholson, DW & Thornberry, NA. (1997). Caspases: killer proteases. *Trends Biochem Sci*, 22, 299-306.
- Noy, N. (2007) Ligand specificity of nuclear hormone receptors: sifting through promiscuity. *Biochemistry*, 46:13461-13467.
- Okuno, M, Kojima, S, Matsushima-Nishiwaki, R, Tsurumi, H, Muto, Y, Friedman, SL & Moriwaki, H. Retinoids in cancer chemoprevention, *Curr Cancer Drug Targets*, 4 (2004) 285–298.
- Omenn, GS. (2007) Chemoprevention of lung cancers: lessons from CARET, the betacarotene and retinol efficiency trial, and prospects for the future. *Eur J Cancer Prev*, 16 184–191.
- Paik, J, Blaner, WS, Sommer, KM, Moe, R & Swisshlem, K. (2003) Retinoids, retinoic acid receptors, and breast cancer. *Cancer Invest*, 21: 304-312.
- Palmer, CNA, Hsu, MH, Griffin, K.J & Johnson, EF. (1995) Novel sequence determinants in peroxisome proliferator signaling. *Journal of Biological Chemistry*, 270:16114-16121.
- Palmieri, F. (2004). The mitochondrial transporter family (SLC25): physiological and pathological implications. *Pflugers Arch*, 447:689-709.
- Palmieri, F & Klingenberg, M. (1979). Direct methods for measuring metabolite transport and distribution in mitochondria. *Methods Enzymol*, 56:279-301.
- Petronilli, V, Cola, C & Bernardi, P. (1993). Modulation of the mitochondrial cyclosporin A-sensitive permeability transition pore. II. The minimal requirements for pore induction underscore a key role for transmembrane electrical potential, matrix pH, and matrix Ca2+. *J Biol Chem*, 268, 1011-1016.

- Pinaire, JA & Reifel-Miller, A. (2007) Therapeutic potential of retinoid x receptor modulators for the treatment of the metabolic syndrome. *PPAR Res*, 9: 41-56.
- Pinton, P, Ferrari, D, Rapizzi, E, Di, VF, Pozzan, T & Rizzuto, R. (2001). The Ca2+ concentration of the endoplasmic reticulum is a key determinant of ceramide-induced apoptosis: significance for the molecular mechanism of Bcl-2 action. *EMBO J*, 20:2690-2701.
- Radominska-Pandya, A, Chen, G, Czernik, PJ, Little, JM, Samokyszyn, VM, Carter, CA & Nowak, G. (2000). Direct interaction of all-trans-retinoic acid with protein kinase C (PKC). Implications for PKC signaling and cancer therapy. *J Biol Chem*, 275:22324-22330.
- Rangwala, SM & Lazar MA. (2004) Peroxisome proliferator-activated receptor gamma in diabetes and metabolism. *Trends Pharmacol Sci*, 25:331–336.
- Reed, JC, Zha, H, Aime-Sempe, C, Takayama, S & Wang, HG. (1996). Structure-function analysis of Bcl-2 family proteins. Regulators of programmed cell death. *Adv Exp Med Biol*, 406, 99-112.
- Renstrom, B & DeLuca, HF. (1989). Incorporation of retinoic acid into proteins via retinoyl-CoA. *Biochim Biophys Acta*, 998:69-74.
- Rial, E, Gonzalez-Barroso, M, Fleury, C, Iturrizaga, S, Sanchis, D, Jimenez-Jimenez, J, Ricquier, D, Goubern, M & Bouillaud, F. (1999). Retinoids activate proton transport by the uncoupling proteins UCP1 and UCP2. *EMBO J*, 18:5827-5833.
- Roberts-Thomson, SJ. (2000). Peroxisome proliferator-activated receptors in tumorigenesis: targets of tumour promotion and treatment. *Immunol Cell Biol*, 78:436-441.
- Rodriguez-Tebar, A & Rohrer, H. (1991). Retinoic acid induces NGF-dependent survival response and high-affinity NGF receptors in immature chick sympathetic neurons. *Development*, 112, 813-820.
- Ruff, SJ & Ong, DE. (2000). Cellular retinoic acid binding protein is associated with mitochondria. *FEBS Lett*, 487:282-286.
- Rubin, M, Fenig, E, Rosenauer, A, Menendez-Botet, C, Achkar, C, Bentel, J.M, Yahalom, J, Mendelsohn, J & Miller, WH. (1994) 9-cis retinoic acid inhibits growth of breast cancer cells and downregulates estrogen receptor mRNA and protein. *Cancer Res*, 54:6549-6556.
- Schild, L, Keilhoff, G, Augustin, W, Reiser, G & Striggow, F. (2001). Distinct Ca2+ thresholds determine cytochrome c release or permeability transition pore opening in brain mitochondria. *FASEB J*, 15, 565-567.
- Schug, TT, Berry, DC, Shaw, NS, Travis, SN & Noy, N. (2007). Opposing effects of retinoic acid on cell growth result from alternate activation of two different nuclear receptors. *Cell*, 129, 723-733.
- Scorrano, L. (2009). Opening the doors to cytochrome c: changes in mitochondrial shape and apoptosis. *Int J Biochem Cell Biol*, 41:1875-1883.
- Shintani, T & Klionsky, DJ. (2004) Autophagy in health and disease: a double-edged sword. *Science*, 306: 990-995.
- Sidell, N, Feng, Y, Hao, L, Wu, J, Yu, J, Kane, MA, Napoli, JL & Taylor, RN. (2010). Retinoic acid is a cofactor for translational regulation of vascular endothelial growth factor in human endometrial stromal cells. *Mol Endocrinol*, 24:148-160.
- Sivaprasadarao, A, Sundaram, M, & Findlay, JB. (1998) Interactions of retinol binding protein with transthyretin and its rceptors. *Methods Mol Biol*, 89:155-163.
- Smith, TJ, Davis, FB & Davis, PJ. (1989). Retinoic acid is a modulator of thyroid hormone activation of Ca2+-ATPase in the human erythrocyte membrane. *J Biol Chem*, 264:687-689.

- Soprano, DR & Soprano, K.J. (2003) Role of RARs and RXRs in mediating the molecular mechanism of action of Vitamin A. In "Molecular Nutrition" (J.Zempleni and H. Daniels, Eds), pp. 135-149. CABI, Cambridge, MA.
- Staels, B. (2005) Fluid retention mediated by renal PPARgamma. *Cell Metab*, 2:77–78.
- Stocco, DM. (2001). Tracking the role of a star in the sky of the new millennium. *Mol Endocrinol*, 15:1245-1254.
- Suh, N, Wang, Y, Williams, CR, Risingsong, R, Gilmer, T, Willson, TM & Sporn, M.B. (1999) A new ligand for the peroxisome proliferator-activated receptor-gamma (PPAR-gamma), GW7845, inhibits rat mammary carcinogenesis. *Cancer Res*, 59:5671-5673.
- Sun SY, Yue P, Dawson MI, Shroot B, Michel S, Lamph WW, Heyman RA, Teng M, Chandraratna RAS, Shudo K, Hong WK. & Lotan R. (1997) Differential effects of synthetic nuclear retinoid receptor selective retinoids on the growth of human non-small cell lung carcinoma cells. *Cancer Res,* 57:4931-493.
- Stahn, C & Buttgereit, F. (2008). Genomic and nongenomic effects of glucocorticoids. *Nat Clin Pract Rheumatol*, 4:525-533.
- Susin, SA, Lorenzo, HK, Zamzami, N, Marzo, I, Snow, BE, Brothers, GM, Mangion, J, Jacotot, E, Costantini, P, Loeffler, M, Larochette, N, Goodlett, DR, Aebersold, R, Siderovski, DP, Penninger, JM & Kroemer, G. (1999). Molecular characterization of mitochondrial apoptosis-inducing factor. *Nature*, 397, 441-446.
- Takahashi, N & Breitman, TR. (1989) Retinoic acid (retinoylation) of a nuclear protein in the human acute myeloid leukemia cell line HL60. *J Biol Chem*, 264:5159–5163.
- Takahashi, N & Breitman, TR. (1990) Retinoic acid acylation: retinoylation. *Methods Enzymol*, 189:233–239.
- Takahashi, N & Breitman, TR. (1990). Retinoylation of HL-60 proteins. Comparison to labeling by palmitic and myristic acids. *J Biol Chem*, 265:19158-19162.
- Takahashi, N & Breitman, TR. (1994) Retinoylation of proteins in mammalian cells, in: R. Blomhoff (Ed.), Vitamin A in Health and Disease. Marcel Dekker, New York, pp. 257–273.
- Tang, GW & Russell, RM. (1990) 13-cis-retinoic acid is an endogenous compound in human serum. *J Lipid Res*, 31:175–182.
- Thompson, CB. (1995). Apoptosis in the pathogenesis and treatment of disease. *Science*, 267, 1456-1462.
- Thorens, B, Deriaz, N, Bosco, D, DeVos, A, Pipeleers, D, Schuit, F, Meda, P & Porret, A. (1996). Protein kinase A-dependent phosphorylation of GLUT2 in pancreatic beta cells. *J Biol Chem*, 271:8075-8081.
- Thornberry, NA & Lazebnik, Y. (1998). Caspases: enemies within. *Science*, 281, 1312-1316.
- Tontonoz, P, Hu E, Spiegelman BM. (1994) Stimulation of adipogenesis in fibroblasts by PPAR gamma 2, a lipid-activated transcription factor. *Cell*, 79:1147–1156.
- Tournier, S, Raynaud, F, Gerbaud, P, Lohmann, SM,. Anderson, WB & Evain-Brion, D. (1996) Retinoylation of the type II cAMP-binding regulatory subunit of cAMP-dependent protein kinase is increased in psoriatic human fibroblasts. *J Cell Physiol*, 167: 196–203.
- Tsubouchi, Y, Sano, H, Kawahito, Y, Mukai, S, Yamada, R, Kohno, M, Inoue, K, Hla, T & Kondo, M. (2000). Inhibition of human lung cancer cell growth by the peroxisome proliferator-activated receptor-gamma agonists through induction of apoptosis. *Biochem Biophys Res Commun*, 270:400-405.
- Tucci, P, Cione, E & Genchi, G. (2008). Retinoic acid-induced testosterone production and retinoylation reaction are concomitant and exhibit a positive correlation in Leydig (TM-3) cells. *J Bioenerg Biomembr*, 40:111-115.

- Tucci, P, Cione, E, Perri, M & Genchi, G. (2008). All-trans-retinoic acid induces apoptosis in Leydig cells via activation of the mitochondrial death pathway and antioxidant enzyme regulation. *J Bioenerg Biomembr*, 40, 315-323.
- Varani, J, Burmeister, W, Bleavins, MR & Johnson, K. (1996). All-trans retinoic acid reduces membrane fluidity of human dermal fibroblasts. Assessment by fluorescence redistribution after photobleaching. *Am J Pathol*, 148:1307-1312.
- Vaux, DL & Korsmeyer, SJ. (1999). Cell death in development. *Cell*, 96, 245-254.
- Veronesi, U, De, PG, Marubini, E, Costa, A, Formelli, F, Mariani, L, Decensi, A, Camerini, T, Del Turco, MR, Di Mauro, MG, Muraca, MG, Del, VM, Pinto, C, D'Aiuto, G, Boni, C, Campa, T, Magni, A, Miceli, R, Perloff, M, Malone, WF & Sporn, MB. (1999). Randomized trial of fenretinide to prevent second breast malignancy in women with early breast cancer. *J Natl Cancer Inst*, 91, 1847-1856.
- Vieira, HL, Haouzi, D, El, HC, Jacotot, E, Belzacq, AS, Brenner, C & Kroemer, G. (2000). Permeabilization of the mitochondrial inner membrane during apoptosis: impact of the adenine nucleotide translocator. *Cell Death Differ*, 7, 1146-1154.
- Von Haefen, C, Wieder, T, Gillissen, B, Starck, L, Graupner, V, Dorken, B & Daniel, PT. (2002). Ceramide induces mitochondrial activation and apoptosis via a Bax-dependent pathway in human carcinoma cells. *Oncogene*, 21:4009-4019.
- Wang, H, Maechler, P, Antinozzi, PA, Hagenfeldt, KA & Wollheim, CB. (2000) Hepatocyte nuclear factor 4alpha regulates the expression of pancreatic beta-cell genes implicated in glucose metabolism and nutrient-induced insulin secretion. *J Biol Chem*, 275:35953-35959.
- Wang, XD, Tang, GW, Fox, JX, Krinsky, NI & Russel RM. (1991) Enzymatic conversion of beta-carotene into beta-apocarotenals and retinoids by human, monkey, ferret, and rat tissues. *Arch Biochem Biophys*, 285:8–16.
- Wei, LN. (2004) Retinoids and receptor interacting protein 140 (RIP140) in gene regulation. *Curr Med Chem*, 11:1527-1532.
- Westin, S, Rosenfeld, MG & Glass, CK. (2000) Nuclear receptor coactivators. *Adv Pharmacol*.,47:89-112.
- Weston, AD, Blumberg, B & Underhill, TM. (2003). Active repression by unliganded retinoid receptors in development: less is something more. *J Cell Biol*, 161:223-228.
- Wickremasinghe, RG & Hoffbrand, AV. (1999). Biochemical and genetic control of apoptosis: relevance to normal hematopoiesis and hematological malignancies. *Blood*, 93, 3587-3600.
- Wolbach, SB & Howe, PR. (1978). Nutrition Classics. The Journal of Experimental Medicine 42: 753-77, 1925. Tissue changes following deprivation of fat-soluble A vitamin. S. Burt Wolbach and Percy R. Howe. *Nutr Rev*, 36:16-19.
- Wolf, G. (2000). Cellular retinoic acid-binding protein II: a coactivator of the transactivation by the retinoic acid receptor complex RAR.RXR. *Nutr Rev*, 58:151-153.
- Wudarczyk, J, Debska, G & Lenartowicz, E. (1996). Relation between the activities reducing disulfides and the protection against membrane permeability transition in rat liver mitochondria. *Arch Biochem Biophys*, 327, 215-221.
- Wu, Q, Dawson, MI, Zheng, Y, Hobbs, PD, Agadir, A, Jong, L, Li, Y, Liu, R, Lin, BZ & Zhang, XK.. (1997) Inhibition of trans retinoic acid resistant human breast cancer cell growth by retinoid X receptor selective retinoids. *Mol Cell Biol*, 17:6598-6608.

- Wyllie, AH, Kerr, JF & Currie, AR. (1980). Cell death: the significance of apoptosis. *Int Rev Cytol*, 68, 251-306.
- Xu, L, Glass, CK. & Rosenfeld, MG. (1999) Coactivator and corepressor complexes in nuclear receptor function. *Curr Opin Genet Dev*, 9:140-147.
- Yang, JC & Cortopassi, GA. (1998). Induction of the mitochondrial permeability transition causes release of the apoptogenic factor cytochrome c. *Free Radic Biol Med*, 24, 624-631.
- Yang, Q, Sakurai, Y & Kakudo, K. (2002) Retinoid, retinoic acid receptor beta and breast cancer. *Breast Cancer Res Treat*, 76: 167-173.
- Yee, LD, Williams, N, Wen, P, Young, DC, Lester, J, Johnson, MV, Farrar, WB, Walker, MJ, Povoski, SP, Suster, S & Eng, C. (2007). Pilot study of rosiglitazone therapy in women with breast cancer: effects of short-term therapy on tumor tissue and serum markers. *Clin Cancer Res*, 13:246-252.
- Yoshimori, T. (2004) Autophagy: a regulated bulk degradation process inside cells. *Biochem Biophys Res Commun*, 313: 453–8.
- Yoshioka, M, Kayo, T, Ikeda, T & Koizumi A. (1997) A novel locus, Mody4, distal to D7Mit189 on chromosome 7 determines early-onset NIDDM in non obese C57BL/6 (Akita) mutant mice. *Diabetes*, 46:887-894.
- Yuan, CX, Ito, M, Fondell, JD, Fu, ZY & Roeder, RG. (1998) The TRAP220 component of a thyroid hormone receptor associated protein (TRAP) coactivator complex interacts directly with nuclear receptors in a ligand-dependent fashion. *Proc Natl Acad Sci*, U. S. A 95:7939-7944.
- Zamzami, N & Kroemer, G. (2001). The mitochondrion in apoptosis: how Pandora's box opens. *Nat Rev Mol Cell Biol*, 2, 67-71.
- Zhang, J, Li, C, Chen, K, Zhu, W, Shen, X & Jiang, H. (2006). Conformational transition pathway in the allosteric process of human glucokinase. *Proc Natl Acad Sci U S A*, 103:13368-13373.

J Bioenerg Biomembr
DOI 10.1007/s10863-007-9097-7

ORIGINAL PAPER

Synthesized esters of ferulic acid induce release of cytochrome *c* from rat testes mitochondria

E. Cione · P. Tucci · V. Senatore · M. Perri · S. Trombino · F. Iemma · N. Picci · G. Genchi

Received: 20 July 2007 / Accepted: 17 August 2007

Abstract Ferulic acid plays a chemopreventive role in cancer by inducing tumor cells apoptosis. As mitochondria play a key role in the induction of apoptosis in many cells types, here we investigate the mitochondrial permeability transition (MPT) and the release of cytochrome *c* induced by ferulic acid and its esters in rat testes mitochondria, in TM-3 and MLTC-1 cells. While ferulic acid, but not its esters, induced MPT and cytochrome *c* release in rat testes isolated mitochondria, in TM-3 cells we found that both ferulic acid and its esters induced cytochrome *c* release from mitochondria in a dose-dependent manner, suggesting a potential target of these compounds in the induction of cell apoptosis. The apoptosis induced by ferulic acid is therefore associated with the mitochondrial pathway involving cytochrome *c* release and caspase-3 activation.

Keywords Ferulic acid · Cytochrome *c* · Apoptosis · Mitochondria · TM-3 cells · MLTC-1 cells

Introduction

Apoptosis, an active and programmed form of cell death, is a multistep process (Hengartner 2000) that plays an important role in the regulation of development morphogenesis (Vaux and Korsmeyer 1999), cell homeostasis, and diseases such as cancer, stroke, and ischemic heart disease (Thompson 1995). Two apoptotic pathways by which cells can initiate and execute the cell death process, the extrinsic and the intrinsic, have been identified (Green 2000; Johnstone et al. 2002). The extrinsic pathway is initiated by ligation of transmembrane death receptors (CD95, TNF receptor, and TRAIL receptor) to activate membrane proximal caspases (caspase-8 and -10). The mammalian caspase family comprises at least 13 known members, most of which have been definitively implicated in apoptosis. *In vitro* experiments suggest that several caspases could activate by themselves, while others require activation by other caspases, acting as a proteolytic cascade (Nicholson and Thornberry 1997). Caspase-3, -6, and -7 are terminal members of caspase cascade and recognize critical cellular substrates, whose cleavage contributes to the morphological and functional changes associated with apoptosis (Thornberry and Lazebnik 1998). Caspase-3 activation also results in DNA cleavage via inactivation of an inhibitor of the DNA fragmentation factor, the endonuclease responsible for internucleosomal cleavage of chromatin (Wickremasinghe and Hoffbrand 1999). Recent findings showed that caspase-3 has a mitochondrial and cytosolic distribution in non-apoptotic cells (Mancini et al. 1998). The mitochondrial caspase-3, which is located in the intermembrane space, was shown to be activated by numerous pro-apoptotic stimuli and this activation could be blocked by bcl-2 (Mancini et al. 1998). Once the caspases are activated, the cell is irreversibly committed to cell death (Reed et al. 1997).

The intrinsic pathway is initiated in the cells by the loss of integrity of the outer mitochondrial membrane and the release of cytochrome *c* into the cytosol (Hirsch et al. 1997; Green and Reed 1998; Joza et al. 2001; Zamzami and

Cione and Tucci have equally contributed to this article.

E. Cione · P. Tucci · V. Senatore · M. Perri · G. Genchi (✉)
Dipartimento Farmaco-Biologico, Laboratorio di Biochimica, Edificio Polifunzionale, Università della Calabria, 87036 Rende, CS, Italy
e-mail: genchi@unical.it

S. Trombino · F. Iemma · N. Picci
Dipartimento di Scienze Farmaceutiche, Laboratorio di Chimica Organica, Edificio Polifunzionale, Università della Calabria, 87036 Rende, CS, Italy

Kroemer 2001). Then cytochrome *c*, an essential constituent of the respiratory chain, is released from mitochondria into the cytosol and induces a conformational change in Apaf-1 (apoptotic protease activating factor-1) that results in the activation of a cascade of caspase proteases with consequent cell death (Yang and Cortopassi 1998; Susin et al. 1999). The release of cytochrome *c* is associated with the mitochondrial permeability transition (MPT). Indeed, it is associated with depolarization of the mitochondrial inner membrane potential, loss of the H^+ gradient, uncoupling of oxidative phosphorylation, ATP depletion, mitochondrial swelling and disruption of the outer mitochondrial membrane (Wudarczyk et al. 1996; Bindoli et al. 1997; Kowaltowski et al. 1997; Bossy-Wetzel et al. 1998; Vicira et al. 2000). Among the non proteic effectors, calcium ion is the most important inducer of MPT (Petronilli et al. 1993; Schild et al. 2001).

Ferulic acid is one of the most ubiquitous compounds in nature, especially rich as an ester form in rice bran pitch, which is obtained when rice oil is produced (Yagi and Ohishi 1979). This antioxidant compound is currently expected not only to prevent lipid oxidation in food but also to prevent free-radical-induced diseases such as cancer and atherosclerosis or aging caused by oxidative tissue degeneration (Niki 1997). In general, the inhibitory effect of ferulic acid as antioxidant on lipid oxidation is due to its phenolic nucleus and its conjugated side chain forming a resonance-stabilized phenoxy radical (Frankel 2001). Although ferulic acid and its esters have been recognized as antioxidants, there are few reports on systematic evaluation of the antioxidant properties of ferulic acid and its derivatives under different conditions.

In this paper we describe the apoptotic activities of substances obtained by chemical synthesis. Our results indicate that ferulic acid, but not its synthetic esters, can induce MPT and promote cytochrome *c* release from rat testes mitochondria. In addition, a testes cell-free model of apoptosis is described consisting of a cytosolic extract from mouse Leydig cells (TM-3) and tumoral cells (MLTC-1).

Materials and methods

Chemicals

Ferulic acid was obtained from Polichimica (Bologna, Italia). Butyl alcohol, pentyl alcohol, octyl alcohol, EDTA, EGTA, SDS, acrylamide and methylenbisacrylamide were purchased from Sigma-Aldrich (Milano, Italia). DMEM/F12, horse serum, foetal calf serum, penicillin and streptomycin was from Gibco (Invitrogen Life Technologies, Italia). All other chemicals used were of the highest purity commercially available.

Synthesis of ferulate esters

The ferulate esters were synthesized according to the procedure described in the literature (EP 0681 825 B1). A solution of ferulic acid (1.0 g, 5.15 mmol) and *p*-toluensulfonic acid (0.07 g, 0.34 mmol), in 10 ml dry toluene was added to aliphatic alcohols (butyl alcohol 0.40 g, pentyl alcohol 0.48 g, and octyl alcohol 0.7 g, 5.4 mmol) under stirring and N_2 at room temperature. After addition was complete, the solution was stirred under N_2 for 12 h at 110°C. After cooling at room temperature, the solvent was evaporated under reduced pressure, and the residue was treated with 15 ml of water and the aqueous phase was extracted with chloroform (4×15 ml). The combined organic phases were collected, dried (Na_2SO_4) and the solvent was removed by rotary evaporation to give compounds 2, 3, 4 (Scheme 1) as yellow oils, and purified by Merck silica gel (60–230 mesh) column chromatography using chloroform/hexane, 60/40 (v/v), as eluent. The solvent of eluted esters was evaporated under reduced pressure. The ferulate esters were obtained with a yield of 80–90%. IR, m/z and ^{1}H-NMR data were assigned according to the literature.

Isolation of mitochondria and monitoring of the MPT

Rats were killed by decapitation, according to good practice procedures approved by the ethics committee, and testes were immediately removed. Rat testes mitochondria were isolated by differential centrifugation as described by Genchi and Olson (Genchi and Olson 2001). Mitochondria were suspended in a medium containing 250 mM sucrose, 10 mM Tris/HCl, pH 7.4, 1 mM EDTA at a concentration of 15–18 mg protein/ml. Protein concentration was determined by the Lowry procedure (Lowry et al. 1951) with BSA as the reference standard. This mitochondrial suspension either was used immediately or was frozen at −70°C. For swelling studies, mitochondria (1 mg/ml) were suspended in a solution of 250 mM sucrose, 10 mM Tris/HCl, pH 7.4,

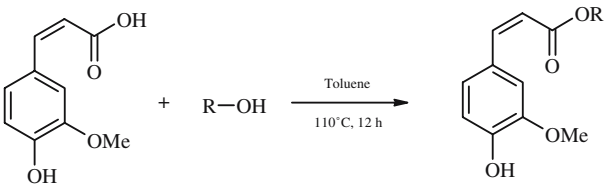

1

2 R= $CH_3(CH_2)_3$-
3 R= $CH_3(CH_2)_4$-
4 R= $CH_3(CH_2)_7$-

Scheme 1 Reaction conditions to synthesize the compounds 2, 3 and 4

2 μM rotenone and were preincubated with 5 mM succinate. After 5 minutes, different concentrations of ferulic acid and ferulate esters or $CaCl_2$ were added and mitochondrial swelling was followed spectrophotometrically by the decrease in absorbance at 540 nm (Rigobello et al. 1999).

Release of cytochrome *c* from isolated rat testes mitochondria

1 mg of rat testes mitochondria was incubated in the presence and in the absence of ferulic acid and its esters for 1 h at 25°C in a final volume of 1 ml of buffer consisting of 250 mM sucrose, 10 mM Tris/HCl, pH 7.4. The mitochondria were separated from the supernatant by centrifugation at 13,000×g for 10 min at 4°C. The supernatant (20–30 μg of cytosolic proteins) was subjected to SDS-PAGE on 15% gel, and the proteins were transferred to a nitrocellulose membrane. This membrane was incubated at room temperature for 1 h with 5% non-fat milk in TBST (25 mM Tris–HCl pH 7.8, 150 mM NaCl, 0.1% Tween 20) and then for 2 h with a mouse monoclonal antibody to cytochrome *c* (1:1,000 dilution in TBST). After three washes with TBST the membrane was incubated for 1 h with horseradish peroxidase-conjugate antibodies to mouse immunoglobulin G (1:2,000 dilution). The membrane was washed three times more with TBST, after which immune complexes were detected with chemiluminescence reagents (ECL Amersham).

Cell cultures

The Leydig (TM-3) cell line, derived from testes of immature BALB/c mice was obtained from Dr. V. Pezzi (University of Calabria) and cultured in DMEM/F12 medium supplemented with 5% horse serum (HS) and 5% foetal calf serum (FCS), 2 mM glutamine and 1% of a stock solution containing 10,000 IU/ml penicillin and 10,000 μg/ml streptomycin. The MLTC-1 cell line, derived from testes of C57BL/6 mice, was obtained from Dr. S. Andò (University of Calabria) and cultured in DMEM/F12 medium supplemented with 10% FCS, 2 mM glutamine and 1% of a stock solution containing 10,000 IU/ml penicillin and 10,000 μg/ml streptomycin.

Cellular cultures were grown on 90 mm plastic tissue culture dishes in a humidified atmosphere of 5% CO_2 in air at 37°C. Cells from exponentially growing stock cultures were removed from the plate with trypsin (0.05% w/v) and EDTA (0.02% w/v). The trypsin/EDTA action was inhibited with an equal volume of DMEM/F12 medium. Cell number was estimated with a Burker camera and cell viability by trypan blue dye exclusion. For both cellular lines, the medium was changed twice weekly. TM-3 were subcultivated when confluent, while MLTC-1 cells were subcultured when they formed island domes.

Cytosolic extracts of TM-3 and MLTC-1 cells and detection of cytochrome *c*

Cytochrome *c* was detected by western blotting in cytoplasmatic fractions. TM-3 cells were treated with 5, 25, 50 and 100 μM ferulic acid, while MLTC-1 cells were treated with a concentration range of ferulic acid between 0.5 and 100 μM; both cellular lines were incubated for 24 h at 37°C in a humidified atmosphere of 5% CO_2 in air. In other experiments, both cells lines were treated with ferulate esters at the same concentrations and conditions. After above treatments, TM-3 and MLTC-1 cells were collected by scraping and harvested by centrifugation at 1,200×g for 10 min at 4°C. The pellets were solubilized in 36 μl lysis buffer (250 mM sucrose, 1.5 mM EGTA, 1.5 mM EDTA, 1 mM $MgCl_2$, 25 mM Tris/HCl, pH 6.8, 1 mM DTT, 10 μg/ml aprotinin, 50 mM phenylmethylsulfonylfluoride and 50 mM sodium orthovanadate). After the addition of 4 μl of 0.1% digitonine, the cells were incubated for 15 min at 4°C and centrifuged at 13,000×*g* for 30 min at 4°C. Proteins of the cytosolic fractions were determined by the Lowry method (Lowry et al. 1951). Equal amounts of protein (15–20 μg) were resolved by 15% SDS-PAGE and electrotransferred to a nitrocellulose membrane. The membrane was incubated with 5% non-fat milk in TBST over night at 4°C, followed by incubation with 1:1,000 sheep polyclonal antihuman cytochrome *c* antibody (2 h, room temperature) and then with HRP-conjugated secondary antibody (1:2,000) for 2 h at 4°C. Peroxidase activity was visualized with the Amersham Pharmacia Biotech ECL system according to the manufacturer instructions. The loading control was detected by immunoblot of β-actin protein.

Western blot analysis of caspase-3

TM-3 cells were lysed with 200 μl ice-cold PBS (phosphate buffered saline, 1.5 mM KH_2PO_4, 8.1 mM Na_2HPO_4, 136,9 mM NaCl, pH 7.2) containing 1% Triton X-100, 0.5% sodium deoxycholate, 0.1% SDS and protease inhibitors (1 mM phenylmethylsulfonylfluoride, 10 mg/ml aprotinin and 10 mg/ml leupeptin). Lysates were centrifuged (13,000×g at 4°C for 30 min) and the supernatant protein content was determined by the Lowry method (Lowry et al. 1951). Equal amounts of protein (20 μg) were resolved by 15% SDS-PAGE and electrotransferred to a nitrocellulose membranes. After blocking, the membranes were incubated (2 h, room temperature) with 1:2,000 rabbit polyclonal antihuman caspase-3 antibody and then (1 h, room temperature) with 1:3,000 HRP-conjugated secondary antibody. Peroxidase activity was visualized with the Amersham Pharmacia Biotech ECL system according to the manufacturer instructions. The caspase-3 protein content was determined densitometri-

cally. The loading control was detected by immunoblot of β actin protein.

Statistical analyses

Statistical differences were determined by one-way analysis of variance (ANOVA) followed by Dunnet method, and the results were expressed as mean±SD from three independent experiments. Differences were considered statistically significant for $P<0.05$.

Results

Mitochondrial swelling attributable to the MPT was monitored by measuring the decrease in optical density at 540 nm of a mitochondrial suspension (Rigobello et al. 1999). Isolated rat testes mitochondria were energized with 5 mM succinate for 5 minutes in the presence of 2 μM rotenone, after which ferulic acid and its esters (10, 50, 100 μM) or 200 μM calcium ion, a well established inducer of MPT (Petronilli et al. 1993; Schild et al. 2001), were added. Incubation of testes mitochondria with ferulic acid caused swelling in a dose-dependent manner (Fig. 1a). The presence of 200 μM calcium ion in the incubation medium together with ferulic acid synergistically stimulated the extent of swelling (Fig. 1b). On the contrary, the incubation of mitochondria with ferulate esters did not cause any swelling effect (not shown).

Mitochondria are vulnerable targets to toxic injury by a variety of compounds because of their crucial role in maintaining cellular structure and function via oxidative phosphorylation and ATP production. Mitochondrial membrane damage induces apoptosis by releasing cytochrome *c* into the cytoplasm (Hirsch et al. 1997; Green and Reed 1998; Joza et al. 2001; Zamzami and Kroemer 2001). Under normal cellular conditions, cytochrome *c* is present in the mitochondrial intermembrane space loosely bound to the inner membrane. To investigate the role of ferulic acid and its esters in inducing cytochrome *c* release, a crude preparation of rat testes mitochondria was incubated for 1 h at 25°C with increasing concentrations (5, 25, 50 and 100 μM) of ferulic acid, butyl ferulate, pentyl ferulate and octyl ferulate. After centrifugation of mitochondria, the resulting supernatants were subjected to western-blot analysis with a monoclonal antibody to cytochrome *c*. As shown in Fig. 2a, incubation of intact mitochondria with increasing concentrations of ferulic acid resulted in a increase of cytochrome *c* in the supernatants at 25, 50 and 100 μM. On the other hand, in the supernatants from mitochondria incubated in the presence of butyl ferulate, pentyl ferulate and octyl ferulate the release of cytochrome *c* was very low or not detectable (data not shown).

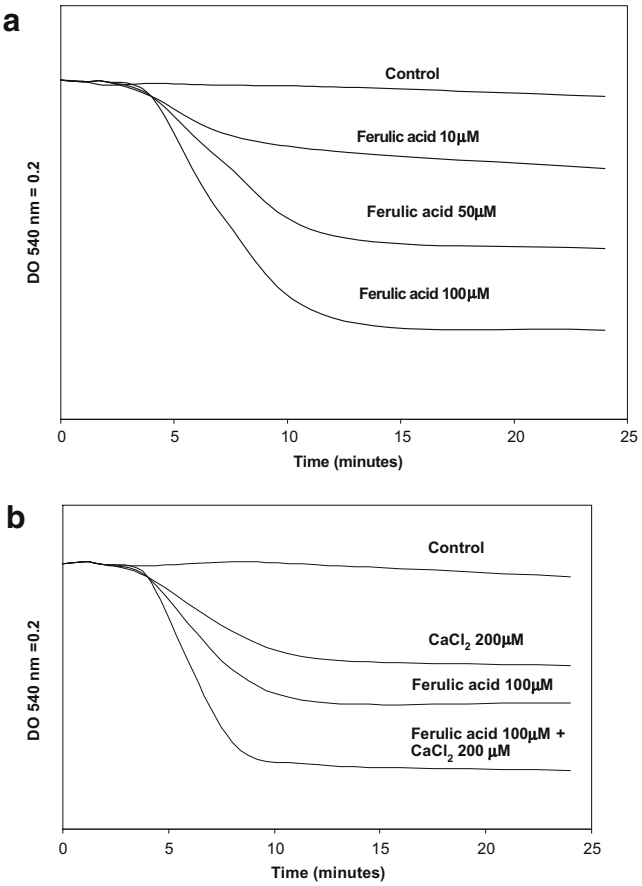

Fig. 1 Induction of MPT in rat testes mitochondria by ferulic acid and $CaCl_2$. Mitochondria were suspended in a solution of 250 mM sucrose, 10 mM TRIS/HCl, pH 7.4, in the presence of 2 μM rotenone and preincubated with 5 mM succinate for 5 min, after which (**a**) ferulic acid (10, 50 and 100 μM) and (**b**) $CaCl_2$ (200 μM), ferulic acid (100 μM) and ferulic acid (100 μM) plus $CaCl_2$ (200 μM) were added. The mitochondrial swelling was monitored by measuring the decrease in optical density at 540 nm

To establish a testes cell-free model of apoptosis, we obtained cytosolic extracts from TM-3 and MLTC-1 cells. Apoptosis is an orderly cascade of cellular events that ultimately results in the demise of the cell. Cytochrome c release from mitochondria has also been shown to be a central event in the regulation of apoptosis. To examine whether ferulic acid and its esters induce release of cytochrome *c* in TM-3, the cells were treated without (only vehicle) and with 5, 25, 50 and 100 μM ferulic acid. After 24 h exposure, TM-3 cells were collected, lysed and the cytosolic protein fractions were assayed for cytochrome *c* to determine its presence into the cytoplasm. As shown in Fig. 2b, the amount of cytochrome *c* released from the cells treated with 50 μM ferulic acid was higher than control ($P<0.05$). The release of cytochrome *c* was evident only after 24 h incubation (data not shown).

During the process of apoptosis, the cytochrome *c*, released into the cytosol from the mitochondria, activates the caspases, a family of killer proteases. In particular, the

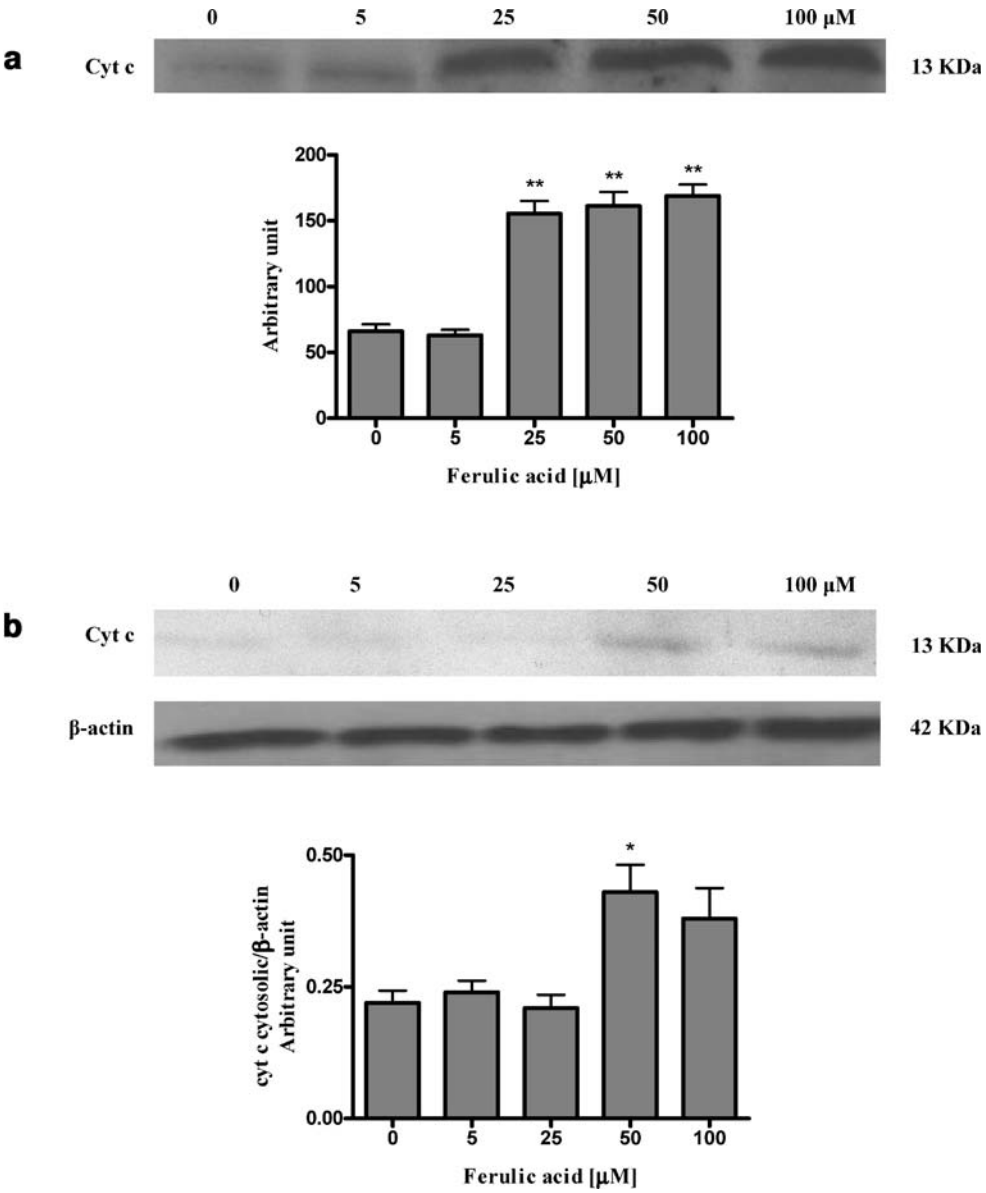

Fig. 2 Effect of ferulic acid on cytochrome *c* release from rat testes isolated mitochondria and TM-3 cells. Mitochondria were incubated with ferulic acid at 0, 5, 25, 50 and 100 μM for 1 h (**a**), TM-3 cells were incubated with ferulic acid at 0, 5, 25, 50 and 100 μM for 24 h (**b**) and cytochrome *c* release was measured by immunoblotting (representative of three experiments) The cytochrome *c* protein content was determined densitometrically. β-Actin, used as internal control, was detected at the position corresponding to a molecular weight of 42 KDa. Results are presented as the mean±SD. **P*<0.05 compared to the control; ***P*<0.01 compared to the control

activated caspase-3 has many cellular targets, and produces the morphological features of apoptosis. Western blot analyses, using a caspase-3 antibody that recognizes the caspase-3 holoenzyme as well as the p17 cleavage product of caspase-3, were performed to investigate whether enzymatic processing occurred following ferulic acid exposure. At 24 h post-exposure, 25, 50 and 100 μM ferulic acid treated cells showed a decrease of the 32 kDa caspase-3 protein, as well as an increase of the 17 kDa cleavage product (Fig. 3).

Release of cytochrome *c* by ferulic acid esters

To compare the efficacy of ferulic acid with pharmaceutically active compounds, we have evaluated the release of cytochrome *c* by esters of ferulic acid obtained by chemical synthesis. This could be of relevance, offering not only a different therapeutical efficacy but a distinct tissue distribution and pharmacokinetics, thus offering different side effects.

Therefore we have treated TM-3 cells with 5, 25, 50 and 100 μM of butyl ferulate, pentyl ferulate and octyl ferulate. Greater cytochrome *c* release has been found when treating TM-3 cells with 50 μM of each ester. Octyl ferulate, among the esters used, is the most effective in inducing cytochrome *c* release (Fig. 4).

To verify that ferulic acid and its esters act as apoptotic inducers, we have treated tumoral Leydig cells at concentrations lower in a range among 0.5–100 μM than those used in TM-3 cells. After 24 h exposure, MLTC-1 cells were collected, lysed and the cytosolic protein fractions

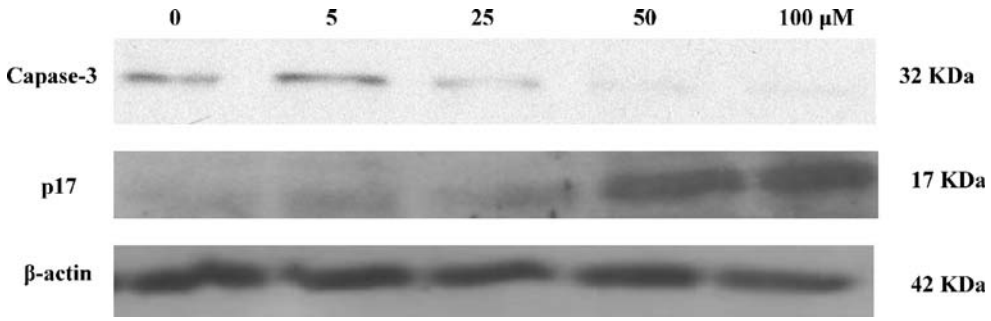

Fig. 3 Effect of ferulic acid on caspase-3 and p17 fragment activation in TM-3 cells. Cells were incubated with ferulic acid at 0, 5, 25, 50 and 100 μM. At 24 h post-exposure, cells were washed with PBS. Equal amounts of cytosolic proteins were separated by SDS-PAGE, transferred to a nitrocellulose membrane, and probed as described in Materials and methods. Caspase-3 and p17 fragment were detected by chemiluminescence. β-Actin, used as internal control, was detected at the position corresponding to a molecular weight of 42 KDa

were assayed for cytochrome *c* to determine its presence into the cytoplasm. As shown in Fig. 5a, the amount of cytochrome *c* released from the cells treated with ferulic acid was highly significant ($P<0.01$) already at 0.5 μM. However, as regards ferulate esters, the release of cytochrome *c* into the cytoplasm was significant ($P<0.05$) at 25 μM for both butyl and octyl ferulate and highly significant ($P<0.01$) for pentyl ferulate at the same concentration (Fig. 5b–d).

Discussion

Current approaches to cancer treatment are mostly based on cytotoxic and cytostatic mechanisms to eliminate malignant cells. These pharmacological strategies, although efficacious toward the malignant cells, show a number of toxic side effects which frequently hamper or drastically reduce their use. A newer dimension in cancer management is the increasing awareness that chemoprevention, namely the

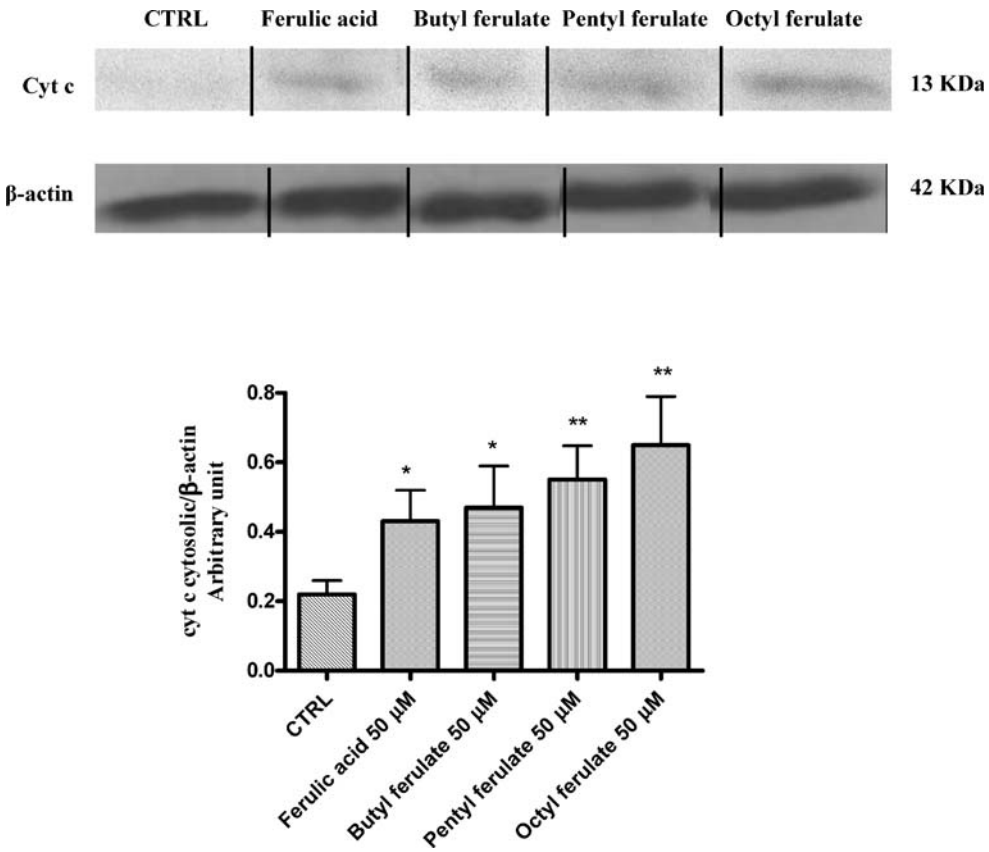

Fig. 4 Effect of ferulic acid and its esters on cytochrome *c* release from TM-3 cells. TM-3 cells were incubated in the presence of free-medium, ferulic acid, butyl ferulate, pentyl ferulate and octyl ferulate at 50 μM. At 24 h post-exposure, cells were washed with PBS; equal amounts of cytosolic proteins were separated by SDS-PAGE, transferred to a nitrocellulose membrane, and probed as described in Materials and methods. Cytochrome *c* was detected by chemiluminescence. The cytochrome *c* protein content was determined densitometrically. β-Actin, used as internal control, was detected at the position corresponding to a molecular weight of 42 KDa. Results are presented as the mean±SD. *$P<0.05$ compared to the control; **$P<0.01$ compared to the control

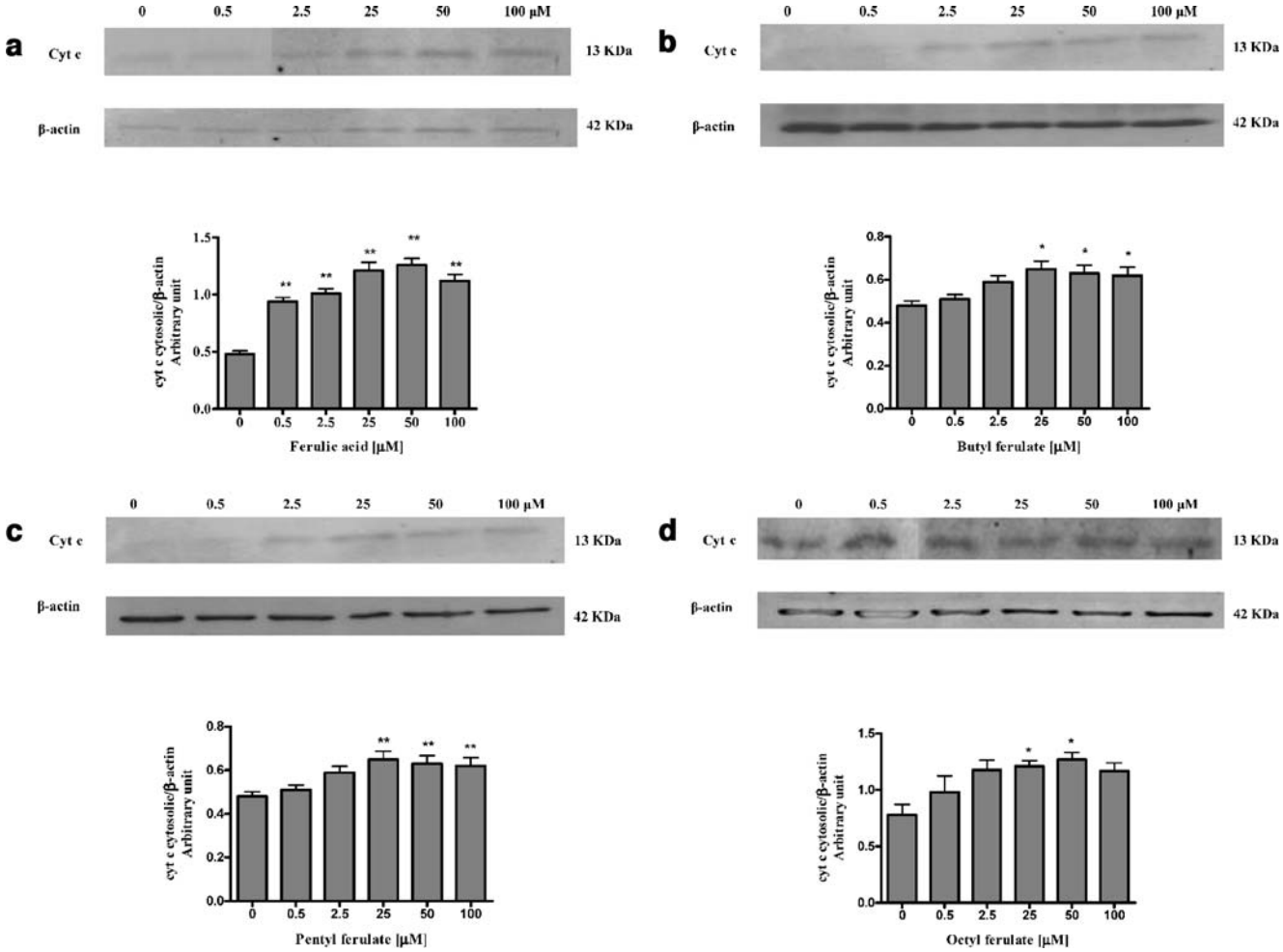

Fig. 5 Effect of ferulic acid and its esters on cytochrome *c* release from MLT-1 cells. Cells were incubated with ferulic acid (**a**), butyl ferulate (**b**), pentyl ferulate (**c**) and octyl ferulate (**d**) at 0, 0.5, 2.5, 25, 50 and 100 μM for 24 h and cytochrome *c* release was measured by immunoblotting (representative of three experiments). The cytochrome *c* protein content was determined densitometrically. β-Actin, used as internal control, was detected at the position corresponding to a molecular weight of 42 KDa. Results are presented as the mean±SD. **P*<0.05 compared to the control; ***P*<0.01 compared to the control

administration of chemical agents (both natural and synthetic) to prevent the early events of carcinogenesis, could be the most direct way to counteract malignancy development and progression (Della Ragione et al. 2000). In the search for new cancer chemopreventive compounds, hundreds of naturally occurring molecules have been evaluated over the past few years. Among the agents able to lower the rate of malignant transformation, antioxidants appear to be very promising. Indeed, diets rich in antioxidant molecules are clearly associated with a diminished risk of cancer at various anatomical sites (Della Ragione et al. 2000). However, some intervention studies have questioned the effectiveness of specific antioxidants in tumor prevention. This suggests that the use of these compounds as chemopreventive agents must await more detailed knowledge of their mechanism of action and their interactions with genetic phenotypes and environment (Della Ragione et al. 2000).

Numerous studies have suggested that ferulic acid and its related compounds exert antioxidants activities (Yagi and Ohishi 1979) and they are currently expected not only to prevent lipid oxidation in food but also to prevent free-radical-induced diseases such as cancer and atherosclerosis or aging caused by oxidative tissue degeneration (Niki 1997). Apoptosis is an active mode of programmed cell death that is induced by a variety of physiological and pathological stimuli. However, apoptosis can also be induced by a variety of toxicants, including many toxic organic compounds, resulting in loss of cell viability. The translocation of cytochrome *c* into the cytosol represents a central point in many forms of apoptosis, since cytochrome *c* is a fundamental component of the apoptosome, responsible for caspase activation. In the current report we have described a novel and unexpected effect of ferulic acid: the induction of cytochrome *c* release from rat testes mitochondria.

We have shown that ferulic acid but not its esters induce MPT opening in isolated rat testes mitochondria and that calcium added in the incubation buffer increases this swelling, resulting in release of cytochrome *c* into the

cytoplasm. On the other hand, in TM-3 cells we have found that ferulic acid and its esters induce apoptosis, associated primarily with the mitochondrial pathway involving release of cytochrome *c*. Ferulic acid, in fact, induces release of cytochrome *c* after 24 h of incubation. The release of cytochrome *c* may result in the activation of members of a family of serine-proteases such as the caspase, another hallmark of apoptosis. Caspases play a central role in terminal biochemical events that ultimately lead to apoptotic cell death. Western blot analysis also indicates marginal appearance of the 32 kDa and 17 kDa caspase-related proteins in TM-3 cells treated with ferulic acid.

As regards ferulate esters, butyl ferulate and pentyl ferulate were less effective than octyl ferulate and the release of cytochrome *c* was clearly evident when their concentrations were 50 μM. The same experimental procedures were done with tumoral Leydig MLTC-1 cells at concentrations lower than those used in TM-3 cells. After 24 h exposure with ferulic acid cytochrome *c* was found into the cytoplasm already at 0.5 μM ferulic acid. The same result is not obtained with ferulate esters; the release began to be evident at 25 μM.

Taken together these observations suggest that ferulic acid activates the mitochondrial pathway of the apoptotic process inducing cytochrome *c* release in isolated mitochondria and in Leydig cells both normal and tumoral, while its esters are able to produce this results only in TM-3 and in MLTC-1 cells, but not in isolated mitochondria. Probably the MPT and the release of cytochrome *c* induced by ferulic acid in isolated mitochondria is due to its phenolic nucleus and its conjugated side chain. In case of complex biological system both ferulic acid and its esters provoked release of cytochrome *c* from mitochondria but there was no significant difference among the release induced by ferulic acid and its esters both in TM-3 and in MLTC-1 cells. So the active compound should be ferulic acid and not the long chain of the esters; in biological systems in fact there are enzymes (esterases) that can hydrolize ester bonds.

Aknowledgments This research was supported by grants from Ministero dell'Istruzione, dell'Università e della Ricerca (MIUR; Italia) and OASI (Maria Santissima, IRCS).

References

Bindoli A, Callegaro MT, Barzon E, Benetti M, Rigobello MP (1997) Arch Biochem Biophys 342:22–28
Bossy-Wetzel E, Newmeyer DD, Green DR (1998) EMBO J 17:37–49
Della Ragione F, Cucciola V, Borriello A, Della Pietra V, Pontoni G, Racioppi L, Manna C, Galletti P, Zappia V (2000) Biochem Biophys Res Commun 278:733–739
Frankel EN (2001) J Oleo Sci 50:387–391
Genchi G, Olson JA (2001) Biochim Biophys Acta 1530:146–154
Green DR (2000) Cell 102:1–4
Green DR, Reed JC (1998) Science 281:1309–1312
Hengartner MO (2000) Nature 407:770–776
Hirsch T, Marzo I, Kroemer G (1997) Biosci Rep 17:67–76
Johnstone RW, Ruefli AA, Lowe SW (2002) Cell 108:153–164
Joza N, Susin SA, Daugas E, Stanford WL, Cho SK, Li CY, Sasaki T, Elia AJ, Cheng HY, Ravagnan L, Ferri KF, Zamzami N, Wakeham A, Hakem R, Yoshida H, Kong YY, Mak TW, Zuniga-Pflucker JC, Kroemer G, Penninger JM (2001) Nature 410:549–554
Kowaltowski AJ, Vercesi AE, Castilho RF (1997) Biochim Biophys Acta 1318:395–402
Lowry OH, Rosebrough NJ, Randall RJ (1951) J Biol Chem 193:265–275
Mancini M, Nicholson DW, Roy S, Thornberry NA, Peterson EP, Casciola-Rosen LA, Rosen A (1998) J Cell Biol 140:1485–1495
Nicholson DW, Thornberry NA (1997) Trends Biochem Sci 22:299–306
Niki E (1997) In: Ohigashi H, Osawa T, Terao J, Watanabe S, Yoshikawa T (eds) Food factors for cancer prevention: free radicals, antioxidant and cancer. Springer, Tokyo, Japan, pp 55–57
Petronilli V, Lola C, Bernardi P (1993) J Biol Chem 268:1011–1016
Reed JC, Zha H, Aime-Sempe C, Takayama S, Wang HG (1997) Adv Exp Med Biol 406:99–112
Rigobello MP, Scutari G, Friso A, Barzon E, Artusi S, Bindoli A (1999) Biochem Pharmacol 58:665–670
Schild L, Keilhoff G, Augustin W, Reiser G, Striggow F (2001) FASEB J 15:565–567
Susin SA, Lorenzo HK, Zamzami N, Marzo I, Snow BE, Brothers GM, Mangion J, Jacotot E, Costantini P, Loeffler M, Larochette N, Goodlett DR, Aebersold R, Siderovski DP, Penninger JM, Kroemer G (1999) Nature 397:441–446
Thompson CB (1995) Science 267:1456–1462
Thornberry NA, Lazebnik Y (1998) Science 281:1312–1316
Vaux DL, Korsmeyer SJ (1999) Cell 96:245–254
Vicira HLA, Haouzi D, El Hanel CH, Jacocot E, Belzacq AS, Brenner C, Kroemer G (2000) Cell Death 7:1146–1154
Wickremasinghe RG, Hoffbrand AV (1999) Blood 93:3587–3600
Wudarczyk J, Debska G, Lenartowicz E (1996) Arch Biochem Biophys 327:215–221
Yagi K, Ohishi N (1979) J Nutr Sci Vitaminol 25:127–130
Yang JC, Cortopassi GA (1998) Free Radic Biol Med 24:624–663
Zamzami N, Kroemer G (2001) Nat Rev Mol Cell Biol 2:67–71

J Bioenerg Biomembr (2008) 40:315–323
DOI 10.1007/s10863-008-9156-8

All-*trans*-retinoic acid induces apoptosis in Leydig cells via activation of the mitochondrial death pathway and antioxidant enzyme regulation

Paola Tucci · Erika Cione · Mariarita Perri · Giuseppe Genchi

Received: 15 May 2008 / Accepted: 3 June 2008 / Published online: 31 July 2008

Abstract In addition to playing a fundamental role in diverse processes, such as vision, growth and differentiation, vitamin A and its main biologically active derivative, retinoic acid (RA), are clearly involved in the regulation of testicular functions. The present study was undertaken to examine the direct effect of RA treatment on Leydig (TM-3) cells. TM-3 cells were cultured and treated with varying concentrations of RA for 24h. High doses of RA (1–20μM) induced a decrease in cell vitality and an increase in lipid peroxidation. RA treatment also induced a corresponding increase in apoptosis in the same cells in a dose-dependent manner. Apoptosis proceeded via the mitochondrial dependent pathway, as demonstrated by the release of cytochrome c, caspase-3 enzymatic activation and DNA fragmentation. Conversely, at physiological doses (0.1–500nM) RA did not increase lipid peroxidation or cell death and resulted in an increase of antioxidant enzyme activity.

Keywords Retinoic acid · Apoptosis · Leydig cells · Mitochondria · Antioxidant enzymes

Abbreviations

RA	All-*trans*-retinoic acid
CAT	Catalase
GST	Glutathione *S*-transferase
SOD	Superoxide dismutase
MTT	3-(4,5-dimethylthiazol-2-yl)-2,5-diphenyltetrazolium bromide
MPMS	1-methoxyphenazine methosulfate
HS	Horse serum
FCS	Foetal calf serum
PBS	Phosphate buffered saline
TBARS	Thiobarbituric acid reactive species
TBA	Thiobarbituric acid
TCA	Trichloroacetic acid

P. Tucci · E. Cione · M. Perri · G. Genchi (✉)
Dipartimento Farmaco-Biologico, Laboratorio di Biochimica, Edificio Polifunzionale, Università della Calabria, 87036 Rende, Cosenza, Italy
e-mail: genchi@unical.it

Introduction

Retinoids are natural and synthetic substances structurally related to vitamin A (retinol). They exert antiproliferative and differentiation-inducing effects on cancer cells and are used in the prevention and treatment of certain types of human cancer and precancerous lesions (Gudas et al. 1994; Lotan 1996). Their action is mediated by two types of receptors, the retinoic acid receptors (RARs) and retinoid X receptors (RXRs) (Chambon 1996) belonging to the steroid/thyroid hormone receptors superfamily. There is substantial evidence *in vitro* that retinoids exert their effect through the induction of apoptosis in tumor cells including hepatoma, leukemia, breast cancer and embryonal carcinoma cell lines (Nagy et al. 1995; Nakamura et al. 1995; Horn et al. 1996; Kim et al. 1996; Li et al. 1999). The action of retinoids in promoting apoptosis may explain the anti-carcinogenic properties of these compounds.

Apoptosis, a specific form of programmed cell death, is a biological process that plays a crucial role in normal development and tissue homeostasis (Woodle and Kulkarni 1998). Apoptosis is characterized by morphological changes including progressive cell shrinkage with condensation, fragmentation of nuclear chromatin and membrane blebbing (Kerr et al. 1997). The ability of the cell to undergo or resist apoptosis is modulated by several factors

including the expression of mitochondrial-associated pro- and anti-apoptotic Bcl-2 family member proteins. Interestingly the expression of Bcl-2 has been observed to be decreased in cells treated with retinoids (Delia et al. 1992; Agarwal and Mehta 1997; Lu et al. 1997; Toma et al. 1997).

Recent observations indicate that mitochondria play an important role in the induction of apoptosis (Liu et al. 1996; Li et al. 1997); indeed Bcl-2 is localized in the outer mitochondrial membrane (Nakai et al. 1993) and, among other actions, prevents the release of apoptogenic factors such as cytochrome c (Liu et al. 1996). Cytochrome c, after its displacement to cytosol, stimulates the formation of a complex with Apaf-1 and caspase-9 in the presence of dATP (Liu et al. 1996). This association leads to the activation of caspase-9 which, in turn, cleaves and activates caspase-3 and hence triggering DNA fragmentation (Li et al. 1997). Caspases are known to mediate a crucial stage of the apoptotic process and are expressed in many mammalian cells (Garcia-Calvo et al. 1999). Of particular interest is caspase-3, the most widely studied member of the caspases family and one of the key executors of apoptosis, which is responsible for several proteolytic cleavage of many proteins (Cohen 1997; Nagata 1997).

In this work we investigated the effect of RA on Leydig cells, using the TM-3 cell line. We found that high doses of RA induce apoptosis in TM-3 cells and that this effect is primarily associated with the mitochondrial pathway involving cytochrome c release and caspase-3 activation. As higher RA doses induced lipid peroxidation whilst decreasing cell viability we also investigated the effects of physiological RA treatment (at nM concentration) in TM-3 cells. In order to detect changes in the antioxidant defences we measured the glutathione *S*-transferase (GST), the superoxide dismutase (SOD) and the catalase (CAT) activities in RA treated and non-treated TM-3 cells. RA increased the activity of antioxidant enzymes under physiological doses, thereby preventing oxidative cell damage as shown by the malondialdehyde (MDA) content and cell viability.

Materials and methods

Chemicals

All-*trans*-retinoic acid, EGTA, EDTA, 3-(4,5-dimethylthiazol-2-yl)-2,5-diphenyltetrazolium bromide (MTT) and 1-methoxyphenazine methosulfate (MPMS) were obtained from Sigma-Aldrich (Milano, Italia). DMEM/F12, foetal calf serum (FCS), horse serum (HS), penicillin and streptomycin were obtained from Gibco (Invitrogen Life Technologies, Italia). GST, SOD and CAT enzymatic activities were assayed using kit obtained from Sigma-Aldrich (Milan, Italia). All other chemicals used were of analytical reagent grade. RA was prepared prior to use by dilution in 100% ethanol, evaporated under nitrogen, suspended in the same volume of DMSO and diluted into medium at the indicated concentrations. All experiments involving RA were performed under yellow light, and the tubes and culture plates containing RA were covered with aluminium foils.

Cell cultures

The TM-3 cell line, derived from testes of immature BALB/c mice, was originally characterized, based on its morphology, hormone responsiveness and metabolism of steroids. This cell line was kindly provided by Dr. S. Andò (University of Calabria) and cultured in DMEM/F12 medium supplemented with 2mM glutamine, serum (5% HS and 5% FCS) and 1% of a stock solution containing 10,000IU/ml penicillin and 10,000μg/ml streptomycin. Cell cultures were grown on Petri plastic tissue culture dishes at 37°C in a humidified atmosphere of 5% CO_2 in air. Cells from exponentially growing stock cultures were removed from the plate with trypsin (0.05% *w*/*v*) and EDTA (0.02% *w*/*v*). The trypsin/EDTA was inhibited adding to the plates an equal volume of DMEM/F12 medium supplemented with serum. The medium was changed twice weekly, and the cells were subcultivated when confluent. Cell number was estimated using a Burker camera.

MTT cytotoxicity assay

Cell viability was determined by MTT assay (Mosmann 1983). In order to determine the cytotoxicity of RA cells (2×10^5cells/ml) were treated with RA at different concentrations for 3 and 24h. Control cells were treated with vehicle alone. One hundred microlitres of MTT (5mg/ml) was added to each well and the plates incubated for 4h at 37°C. Subsequently 1ml 0.04N HCl in isopropanol was added to solubilize the cells. The absorbance was measured with the Ultrospec 2100 pro spectrophotometer (Amersham-Biosciences) at a test wavelength of 570nm with a reference wavelength of 690nm. The optical density (O.D.) was calculated as the difference between the absorbance at the reference wavelength and that at the test wavelength. Percent viability was calculated as (O.D. of drug-treated sample/control O.D.) ×100.

Oxidative stress parameters

Following sonication of TM-3 cells in PBS (phosphate-buffered saline, 1.5mM KH_2PO_4, 8.1mM Na_2HPO_4, 136.9mM NaCl, pH7.2) buffer the crude homogenate was divided into two equal parts. One part was processed for assay of lipid peroxidation, while the second part was centrifuged at 10,000rpm for 5min and the supernatant

utilized in assays for glutathione *S*-transferase, superoxide dismutase and catalase activities.

Lipid peroxidation and antioxidant enzymes activity

The level of lipid peroxidation was assayed through the formation of thiobarbituric acid reactive species (TBARS) during an acid-heating reaction as previously described (Esterbauer and Cheeseman 1990). Briefly, the samples were mixed with 1ml of 10% trichloroacetic acid (TCA) and 1ml of 0.67% thiobarbituric acid (TBA), then heated in a boiling water bath for 15min. TBARS were determined by the absorbance at 535nm and were expressed as malondialdehyde equivalents (nmol/mg protein).

The enzymatic activities in the cell samples of SOD, CAT and GST were determined by the methods of Das et al. (2000), Aebi (1974) and Habig et al. (1973) respectively. Protein concentration in samples was estimated by the Lowry method (Lowry et al. 1951).

Immunoblot analysis of cytochrome c release

Cytochrome c was detected by western blotting in mitochondrial and cytoplasmatic fractions. The cells were harvested by centrifugation at 1,200 × g for 10min at 4°C. The pellets were suspended in 36μl lysis buffer (250mM sucrose, 1.5mM EGTA, 1.5mM EDTA, 1mM $MgCl_2$, 25mM Tris-HCl, pH6.8, 1mM DTT, 10μg/ml aprotinin, 50mM phenylmethylsulfonylfluoride and 50mM sodium orthovanadate) and then 4μl of 0.1% digitonine was added. The cells were incubated for 15min at 4°C and centrifuged at 12,000rpm for 30min at 4°C. The resulting mitochondrial pellet was resuspended in 3% Triton X-100, 20mM Na_2SO_4, 10mM PIPES and 1mM EDTA, pH7.2, and centrifuged at 12,000rpm for 10min at 4°C. Equal amounts of protein (2–5μg) were resolved by 15% SDS-PAGE and electrotransferred to nitrocellulose membranes. The membranes were incubated in blocking buffer over night at 4°C, followed by incubation with 1:1,000 sheep polyclonal antihuman cytochrome c antibody (2h, room temperature) and then with HRP-conjugated (horse radish peroxidase-conjugated) secondary antibody (1:2,000) for 2h at 4°C. Peroxidase activity was visualized with the Amersham Pharmacia Biotech ECL system according to manufacturer's instructions. The cytochrome c protein content was determined densitometrically. Immunoblotting for β-actin was carried out to confirm equal loading.

Western blot determination of caspase-3

Leydig cells were lysed with ice-cold PBS (pH7.4) containing 1% Triton X-100, 0.5% sodium deoxycholate, 0.1% SDS and protease inhibitors (1mM phenylmethylsulfonylfluoride, 10mg/ml aprotinin and 10mg/ml leupeptin). Lysates were centrifuged (13,000rpm at 4°C for 30min) and supernatant protein content determined. Equal amounts of protein (20μg) were resolved by 15% SDS-PAGE, electrotransferred to nitrocellulose membranes and immunoblotted for caspase-3 as previously described.

DNA extraction and agarose gel electrophoresis

Agarose gel electrophoresis of extracted DNA was performed to detect damage to nuclear chromatin, a characteristic biochemical feature of apoptosis, indicated by laddering of oligonucleosomal fragments (180–200bp) as described by Mu et al. (2001).

Briefly, 1×10^6 cells, treated without and with 5, 10 and 20μM of RA for 24h, were trypsinized and washed with PBS. Then the cells were spun down and resuspended in 0.5ml of lysis buffer (50mM Tris-HCl, pH 7.8, 10mM EDTA, and 0.5% SDS). RNase A was added to a concentration of 0.5mg/ml and incubated at 37°C for 60min. The protein content was degraded with proteinase K (0.5mg/ml) at 50°C for 60min. DNA was obtained with two extractions. The first extraction was carried out with an equal volume of phenol–chloroform–isoamylic alcohol (25:24:1) and the second with chloroform–isoamylic alcohol (24:1). DNA was precipitated from the upper aqueous phase with 0.1vol. of 3M sodium acetate, 2.5vol. of ice-cold ethanol and left at −20°C over night. After centrifugation the DNA pellet was solubilized in 25μl sterile water. DNA fragments were separated by electrophoresis in 1.2% agarose gel and visualized by staining with ethidium bromide.

Lactate dehydrogenase assay

The amount of lactate dehydrogenase (LDH) released by the cells was determined as described by Abe and Matsuki (2000) with little modifications. The culture supernatant (250μl) was mixed with 250μl of the LDH substrate mixture (2.5mg/ml L-lactate lithium salt, 2.5mg/ml NAD^+, 100μM MPMS, 600μM MTT, and 0.1% Triton X-100 in 0.2M Tris-HCl buffer, pH 8.2). The reaction was carried out for 5min at 37°C and stopped by adding 0.5ml of 0.04N HCl in isopropanol. The absorbance was measured with the spectrophotometer at a test wavelength of 570nm, and a reference wavelength of 655nm. In these assay conditions, MTT was converted into MTT formazan in proportion to LDH activity. LDH release was calculated as (sample LDH-blank)/(total LDH-blank) ×100.

Statistical analyses

Statistical differences were determined by one-way analysis of variance (ANOVA) followed by Dunnet's method, and

the results were expressed as mean ± SD from n independent experiments. Differences were considered statistically significant for $P < 0.05$.

Results

Effect of RA on vitality of TM-3 cells

In order to examine the cytotoxic effect of RA on TM-3 cells, they were cultured with RA in a concentration range from 0.1 to 20μM for 24h and MTT assay was carried out with cells cultured in RA-free media as control. No significant change in viability was observed in TM-3 treated in 0–0.5μM RA concentration range (Fig. 1A). Upon incubation with RA concentration of 1–20μM a significant reduction of vitality, however, observed. As shown in Fig. 1A, the cell viability was less than 20% after exposure to 20μM RA for 24h. The effect of RA at μM doses on cell viability was also time-dependent, since the cell survival declined drastically following an increase in the treatment time from 3 to 24h in cells incubated with 10 and 20μM RA (Fig. 1B). The present results show that RA exerts a cytotoxic effect on TM-3 cells in a concentration and time dependent manner (Fig. 1A,B).

Biochemical markers of apoptosis

In order to examine whether apoptosis was the cause of the loss of cell viability, the cells were treated with μM doses of RA and subjected to various biochemical analyses to detect biomarkers of apoptosis. Mitochondria are vulnerable targets for toxic injury and act as crucial executors of apoptosis by releasing cytochrome c into the cytoplasm (Cai et al. 1998). 24h post-exposure TM-3 cells were collected and the cytosolic protein fraction was assayed for cytochrome c release. As shown in Fig. 2A,B, cytochrome c was detectable in cytoplasm following exposure to 0.5μM RA and the protein increased significantly at higher RA exposure (10–20μM) when compared to time matched

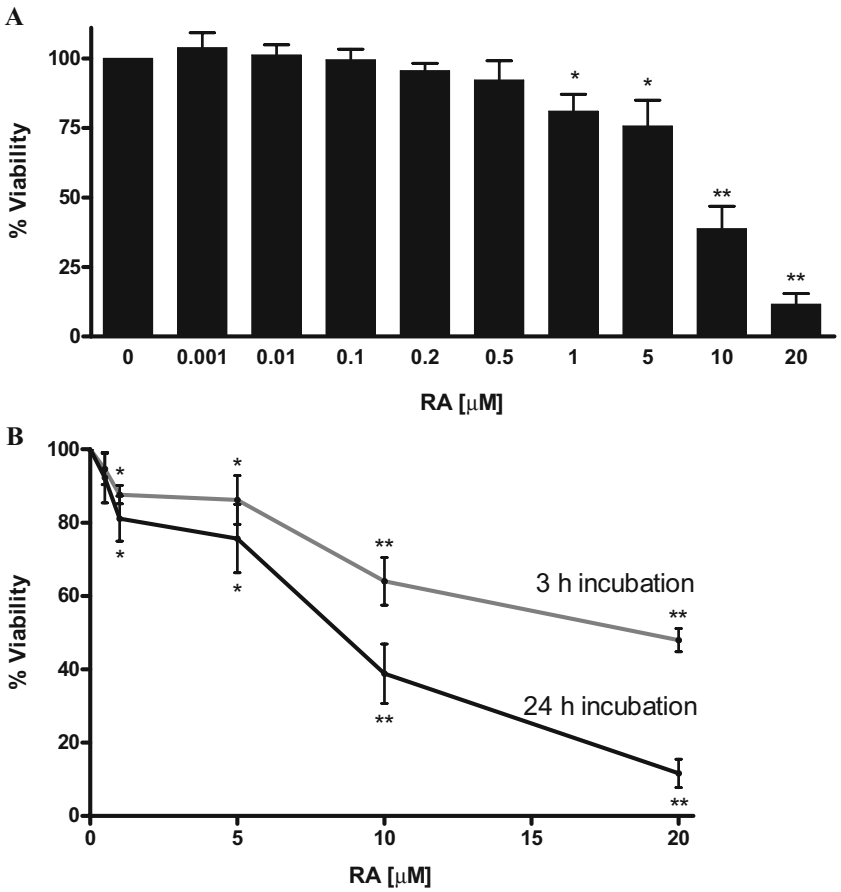

Fig. 1 The effect of RA on TM-3 cell survival. **A** Cells were incubated with indicated concentrations of RA and then the cell viability was determined by MTT assay as described in "Materials and methods". **B** The cell viability was evaluated at 3 and 24 h post-exposure with RA (at μM doses). The data represent means±SD of four independent experiments with triplicate well and are presented as the percentage of the control cell number. *P<0.05 compared to the control. **P<0.01 compared to the control

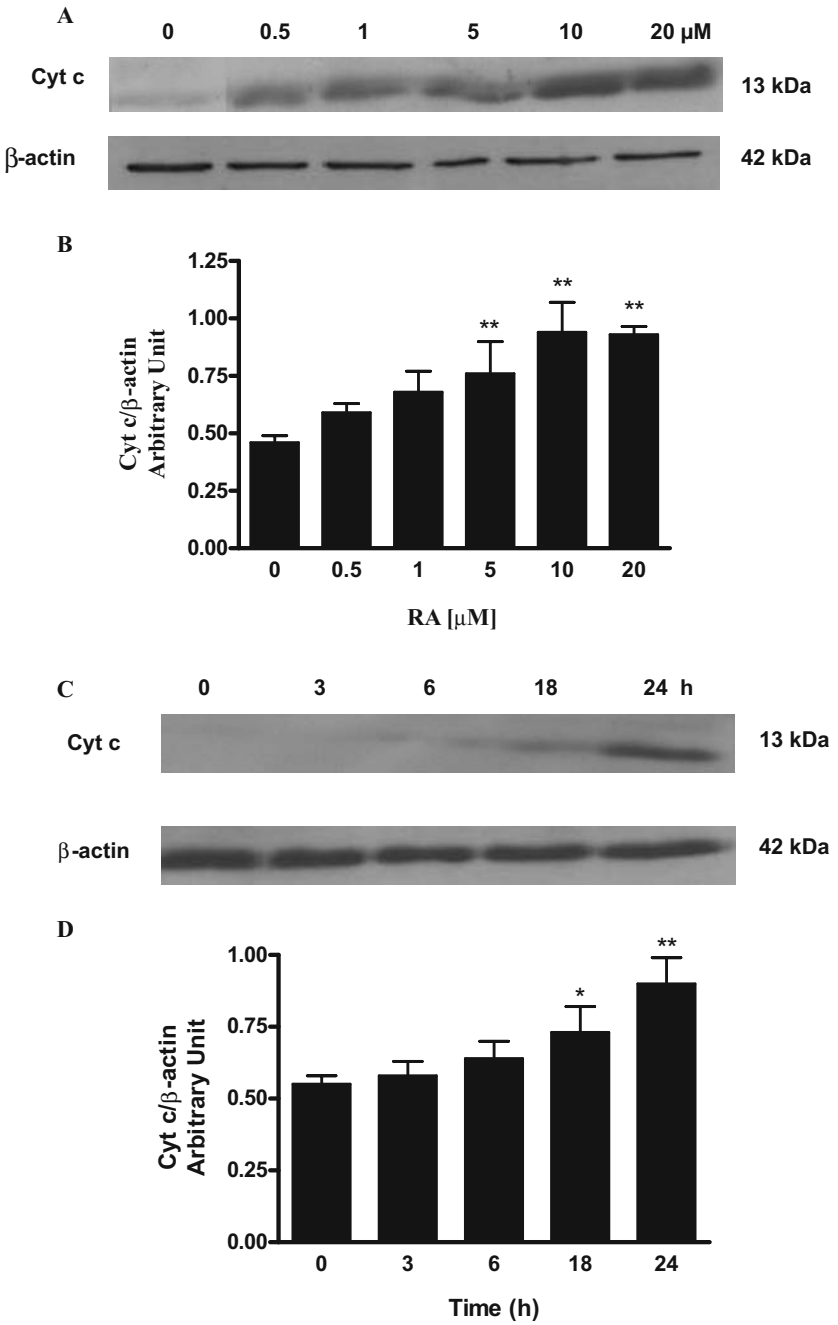

Fig. 2 Biochemical markers of apoptosis. **A** TM-3 cells were incubated both in the absence and in the presence of 0.5, 1, 5, 10 and 20 μM RA for 24 h. After incubation, cells were washed with PBS; equal amounts of cytosolic proteins (2–5 μg) were separated by 15% SDS-PAGE, transferred to a nitrocellulose membrane, and probed as described in "Materials and methods". Cytochrome c was detected by chemiluminescence. β-actin, used as internal control, was detected at the position corresponding to a molecular weight of 42 kDa. **B** The cytochrome c protein content was determined densitometrically. Results are presented as the mean±SD of three independent experiments. *$P<0.05$ compared to the control; **$P<0.01$ compared to the control. **C** TM-3 cells were incubated with 20 μM RA and release of cytochrome was evaluated at 0, 3, 6, 18 and 24 h post-exposure. **D** The cytochrome c protein content was determined densitometrically. Results are presented as the mean±SD of three independent experiments. *$P<0.05$ compared to the control; **$P<0.01$ compared to the control. **E** Cells were incubated with 0, 0.5, 1, 5, 10 and 20 μM RA. At 24 h post-exposure, cells were washed with PBS. Equal amounts of cytosolic proteins (20 μg) were separated by 15% SDS-PAGE, transferred to a nitrocellulose membrane, and probed as described in "Materials and methods". Procaspase-3 and p17 fragment were detected by chemiluminescence. β-actin, used as internal control, was detected at the position corresponding to a molecular weight of 42 kDa. **F** The cells were treated with various concentrations of RA for 24 h; then the DNA was extracted, separated by electrophoresis on 1.2% agarose gel and visualized by staining with ethidium bromide. *Lane 1*, control; *lane 2*, 5 μM RA; *lane 3*, 10 μM RA; *lane 4*, 20 μM RA

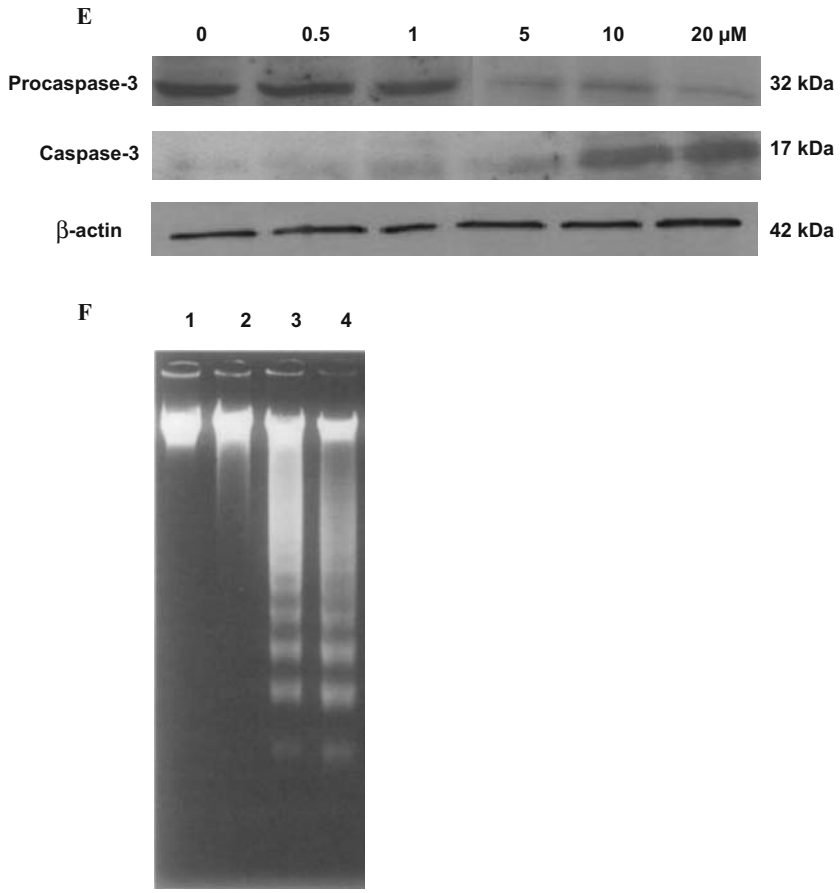

Fig. 2 (continued)

controls. The time-course of cytochrome c release from the mitochondria into the cytosol was also determined after 3, 6, 18 and 24h of incubation in the presence of 20μM RA. As shown in Fig. 2C,D, detectable release of cytochrome c was, only apparent, after 18h of treatment.

The activation of the caspase family members is a hallmark of apoptosis. After treatment for 24h with RA, western blot analysis, using a caspase-3 antibody that recognizes the caspase-3 holoenzyme as well as the p17 cleavage product of caspase-3, was performed to investigate whether enzymatic processes had been activated. Procaspase-3 is synthesized as a precursor of 32kDa which is then proteolitically cleaved. Immunoblotting analysis revealed that procaspase-3 levels decreased in cells treated with 5, 10 and 20μM RA for 24h in a dose-dependent manner; while a band, corresponding to the activated form of caspase-3 (17kDa), was increased over the same dose-response curve (Fig. 2E).

In order to evaluate the induction of apoptosis by RA we measured DNA fragmentation using DNA electrophoresis and fluorescent staining. The genomic DNA extracted from cells, treated with 5, 10 and 20μM RA for 24h, was subjected to 1.2% agarose gel electrophoresis. DNA ladders, which are typical of apoptosis, were detected only in the cells treated with 10 and 20μM RA (Fig. 2F).

LDH activity in the culture media was measured spectrophotometrically as an index of plasma membrane damage and loss of membrane integrity and therefore a parameter of cytotoxicity. RA treatment for 24h resulted in a dose-dependent induction of LDH release (Fig. 3A). To summarise, we have demonstrated that RA-induced cell death occurred by classical apoptosis, whilst at higher concentrations there is also evidence of necrotic death.

RA-induced apoptosis is not mediated by an increase of ceramide generation

Ceramide, as a second messenger, is generated by the hydrolysis of the cell membrane sphingomyelin or is derived from *de novo synthesis* in response to inducers of apoptosis (Bose et al. 1995). Previous studies have shown that ceramide induces cell apoptosis by the mechanisms of activation of a ceramide-activated protein phosphatase (CAPP); moreover, ceramide up-regulates the apoptosis effector, Bax, or down-regulates the apoptosis inhibitor, Bcl-2, leading to caspase activation (Pinton et al. 2001;

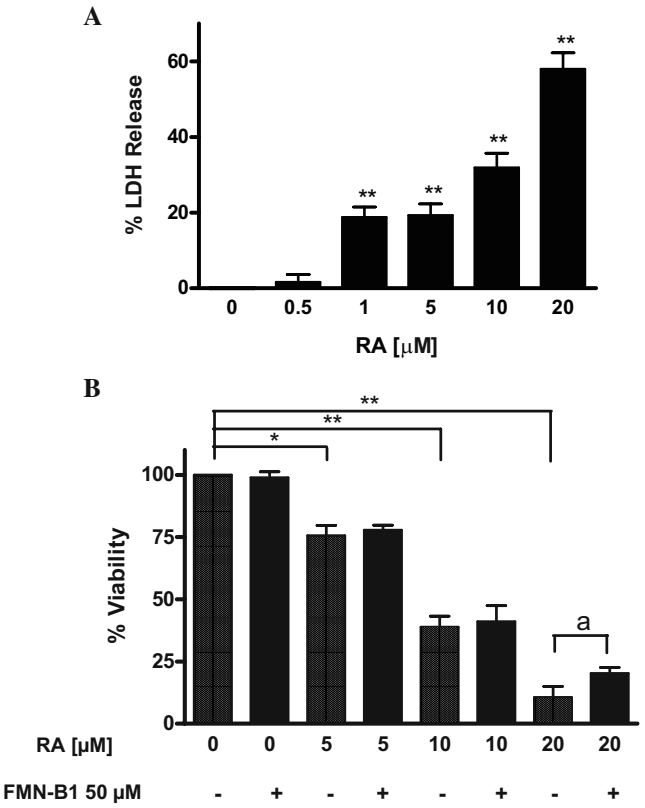

Fig. 3 The effect of RA on LDH release and the effect of ceramide synthase inhibitor on TM-3 cell survival. **A** The TM-3 cells were treated with various concentrations of RA as indicated for 24 h, and the amount of LDH released was determined as described in "Materials and methods". **B** The cells were treated with various concentrations of RA (0, 5, 10 and 20 μM) with and without 50 μM fumonisin B1 (FMN-B1), a ceramide synthase inhibitor, for 24 h, and the cell viability was determined by MTT assay as described in "Materials and methods". The data represent means±SD of four independent experiments with triplicate well and are presented as a percentage of viable cells in the control sample. *$P<0.05$ compared to the control. **$P<0.01$ compared to the control. *a* $P<0.05$ compared to identical RA group

Kolesnick 2002; Von Haefen et al. 2002). To identify the possible mechanisms mediating RA-induced Leydig cell apoptosis we measured the cytotoxicity of RA in cell cultures in the presence or absence of the ceramide synthase inhibitor, fumonisin B1. As shown in Fig. 3B, fumonisin B1 treatment alone had no effect on cell survival. The apoptotic effect of RA was not mediated by ceramide because 50μM of this compound could not prevent the apoptotic effect of various concentrations of RA (5–10μM range). At 20μM RA there was an increase in ceramide generation providing evidence of necrotic death.

Oxidative stress

TM-3 cells were treated with RA and the lipid peroxidation was estimated by TBARS formation as described in "Materials and methods". RA treatment (0–1μM concentration range, for 24h treatment) did not considerably increase TBARS content in cultured TM-3 cells, while RA doses higher than 1μM increased lipid peroxidation levels (Fig. 4A). In agreement with this, RA at higher doses (at μM doses) induced a decrease in cell viability (Fig. 1A). As higher RA doses induced lipid peroxidation and apoptosis, we decided to investigate only the effects of RA treatment at nM physiological concentrations in TM-3 cells. In order to investigate changes in antioxidant defences we measured the GST, SOD and CAT activities in RA treated and non treated TM-3 cells. GST activity increased with 10, 100 and 200nM RA (Fig. 4B), while SOD and CAT activities increased only with 100 and 200nM RA (Fig. 4C,D).

Discussion

Over the last decade retinoids have been the object of intense investigation. Vitamin A and carotenoids have been considered as physiologically important antioxidants. Despite our understanding on important physiological functions of retinoids (Livrea and Packer 1993), the effects of retinoid supplementation at supra-physiological doses, in addition to their known physiological actions, are not well defined. Retinoid action is mediated by specific nuclear retinoic acid receptors (RARs) and retinoid X receptors (RXRs) belonging to the steroid/thyroid super-family of transcription factors (Giguere 1994). The wide spectrum of physiological and pharmacological retinoids effects is, however, attributed to both receptor-dependent and receptor-independent mechanisms (Radominska-Pandya et al. 2000).

In this context, the mechanism of the antioxidant effect of RA remains unclear. We report here that supplementation with RA caused lipid peroxidation. This damage seems to be induced only by supra-physiological doses, since physiological doses did not induce TBARS. In response, a decrease in cell viability was observed at the same doses where TBARS was found to be enhanced.

Our data strongly suggest that RA induces apoptosis as determined by cytochrome c release from the mitochondria to bind to Apaf-1, which in turn initiates a caspase cascade, the executionary machinery of apoptotic cell death. Our results showed there was a measurable release of cytochrome c into the cytoplasm following exposure to RA. This release of cytochrome c may result in the activation of members of the caspase family of proteases, another hallmark of apoptosis. Caspases, and in particular caspase-3, play a central role in the terminal biochemical events that ultimately lead to apoptotic cell death. We observed a dose-dependent increase in caspase-3 activity after incubation for

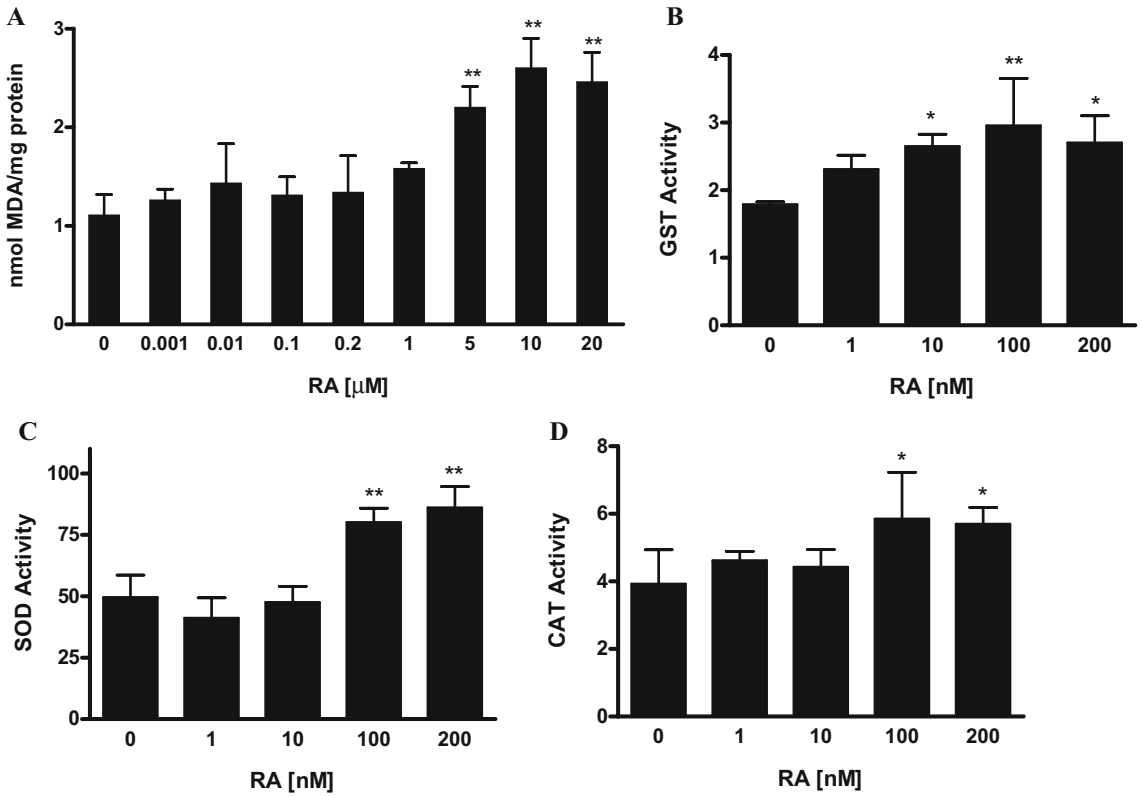

Fig. 4 Determination of TBARS and antioxidant enzymes activities in TM-3 treated with RA for 24 h. **A** Cells were incubated with increasing concentrations of RA as indicated and lipid peroxidation was evaluated by TBARS assay as described in "Materials and methods". Cells were treated with the indicated concentrations of RA for 24 h and GST (**B**), SOD (**C**) e CAT (**D**) activities were measured as described in "Materials and methods". Enzymes activities are expressed as μmol substrate/min/mg protein. Results are presented as the mean±SD of three individual experiments. *$P<0.05$ compared to the control. **$P<0.01$ compared to the control

24h with RA. As a consequence, DNA was cleaved by endonucleases, as observed by condensation and fragmentation of chromatin. Taken together, these observations suggest that RA activates the classic mitochondrial dependent apoptotic process.

Since higher doses of RA (μM) induced lipid peroxidation and cell death, we decided to investigate only the effects of RA treatment at physiological doses in TM-3 cells. In order to investigate changes in antioxidant defences we measured the SOD, CAT and GST activities in TM-3 cells treated with RA. The SOD, CAT and GST activities increased with 100 and 200nM RA treatment. Interestingly, at these same doses RA did not increase lipid peroxidation and no effect on cell viability was observed. These findings suggest that RA increased the activity of antioxidant enzymes at physiological doses, thereby preventing oxidative cell damage which is manifest at higher doses of RA as may be evidenced by TBARS content and cell viability. In accordance with earlier studies (Livera et al. 2000) we observed no significant effect of 1μM RA on DNA fragmentation (date not shown). This concentration of RA was able, however, to decrease cell viability by 15–18% and trigger a low level of cytochrome c release indicating that 1μM RA could represent a threshold limit for non apoptosis inducing RA treatments.

Hurnanen et al. (1997) have shown that low RA concentrations stimulated cell growth and proliferation but that high concentrations inhibited cell proliferation. Moreover, higher RA concentrations increased lipid peroxidation. There was a significant negative correlation between lipid peroxidation and cell proliferation, which suggests that RA may generate free radicals. The mechanism of RA-mediated lipid peroxidation is not fully understood. There are, however, at least two possible mechanisms: (i) RA can stimulate the activity of Δ-6-desaturase resulting in an increase of polyunsaturated fatty acids (PUFA), which are then easily oxidized (Alam et al. 1984). Δ-6-desaturase is the enzyme responsible for inserting double bonds during PUFA synthesis. A loss or decreased activity of this enzyme has been found in some malignant tumors. (ii) RA can also directly increase free radical generations which could result in increased lipid peroxidation (Davis et al. 1990). Moreover, 13-*cis*-RA was shown to directly increase levels of superoxide anion, hydrogen peroxide and hydroxyl anions in isolated chick neural crest cells (Davis et al. 1990). It is noteworthy that every antioxidant is in fact a

redox agent, protecting against free radicals in some circumstances and promoting free radicals generation in others (Herbert 1996).

Our results suggest the importance of keeping vitamin status within the normal range, as a deficit or administration of greater than the upper physiological limits could explain in part the adverse effects found in the literature. The concentrations of RA used in this study range from physiological to pharmacological plasma concentrations. RA is present constitutively in the plasma at a concentration of 4–14nM (De Leen Heer et al. 1982; Kane et al. 2005). Pharmacological RA doses result in transient plasma concentration in the same μM range at which we observed TBARS formation and decreased cell viability.

In conclusion, the above findings indicate that retinoic acid at μM doses raises oxidative stress and induces apoptosis in Leydig cells through cytochrome c release and caspase-3 activation. Conversely, at physiological doses (0.1–500nM) RA modulates antioxidant enzymes through an increase of GST, SOD and CAT activities. An understanding of the RA behavior will, therefore, be necessary to define how it may be used both alone as a chemopreventive agent and also in combination with chemotherapeutic agents for cancer treatment.

Acknowledgements This research was supported by grants from Ministero dell'Università e della Ricerca (MUR, Italia) and IRCCS Associazione Oasi Maria SS.

References

Abe K, Matsuki N (2000) Neurosci Res 38:325–329
Aebi H (1974) Catalase. In: Bergmeyer HU (ed) Methods in enzymatic analysis. Academic Press, New York, pp 631–684
Agarwal N, Mehta K (1997) Biochem Biophys Res Commun 230:251–253
Alam SQ, Alam BS, Chen TW (1984) Biochim Biophys Acta 792:110–117
Bose R, Verheij M, Haimovitz-Friedman A, Scotto K, Fuks Z, Kolesnick R (1995) Cell 82:405–414
Cai J, Yang J, Jones DP (1998) Biochim Biophys Acta 1366:139–149
Chambon P (1996) FASEB J 10:940–954
Cohen GM (1997) Biochem J 326:1–16
Das K, Samanta L, Chainy GBN (2000) IJBB 37:201–204
Davis WL, Crawford LA, Cooper OJ, Farmer GR, Thomas D, Freeman BL (1990) J Craniofac Genet Dev Biol 10:295–310
De Leen Heer AP, Lambert WE, Claeys I (1982) J Lipid Res 23:1362–1367
Delia D, Aiello A, Soligo D, Fontanella E, Melani C, Pezzella F, Pienotti MA, Della-Porta G (1992) Blood 79:1291–1298
Esterbauer H, Cheeseman KH (1990) Methods Enzymol 186:407–421
Garcia-Calvo M, Peterson EP, Rasper DM, Vaillancourt JP, Zamboni R, Nicholson DW, Thoberry NA (1999) Cell Death Differ 6:362–369
Giguere V (1994) Endocr Rev 15:61–79
Gudas LJ, Sporn MB, Roberts AB (1994) Cellular biology and biochemistry of the retinoids. In: Sporn MB, Roberts AB, Goodman DS (eds) The retinoids: biology, chemistry, and medicine. Raven Press, New York, pp 443–520
Habig WH, Pabst MJ, Jakoby WB (1973) J Biol Chem 249:7130–7139
Herbert V (1996) J Nutr 126:1197–1200
Horn R, Minucci C, Ogryzko VV, Adamson ED, Howard BH, Levin AA, Ozato K (1996) FASEB J 10:1071–1077
Hurnanen D, Chan M, Kubow S (1997) J Pharmacol Exp Ther 283:1520–1528
Kane MA, Chen N, Sparks S, Napoli JL (2005) Biochem J 388:363–369
Kerr JF, Wyllie AH, Currie AR (1997) Br J Cancer 26:239–257
Kim DG, Jo BH, You KR, Ahn DS (1996) Cancer Lett 107:149–159
Kolesnick R (2002) J Clin Invest 110:3–8
Li P, Nijhawan D, Budihardjo I, Srinivasula SM, Ahmad M, Alnemri ES, Wang X (1997) Cell 91:479–489
Li Y, Hashimoto Y, Agadir A, Kagechika H, Zhang X (1999) J Biol Chem 274:15360–15366
Liu X, Kim CN, Yang J, Jemmerson R, Wang X (1996) Cell 86:147–157
Livera G, Rouiller-Fabre V, Durand P, Habert R (2000) Biol Reprod 62:1303–1314
Livrea MA, Packer L (1993) Retinoids—progress in research and clinical applications. Dekker, New York
Lotan R (1996) FASEB J 10:1031–1039
Lowry OH, Rosebrough NJ, Randall RJ (1951) J Biol Chem 193:265–275
Lu XP, Fanjul A, Picard N, Pfahl M, Rungta D, Nared-Hood K, Carter B, Piedrafita J, Tang S, Fabbrizio E, Pfahl M (1997) Nat Med 3:686–690
Mosmann T (1983) J Immunol Methods 65:55–63
Mu YM, Yanase T, Nish Y, Tanaka A, Saito M, Jin C, Mukasa C, Okabe T, Nomura M, Goto K, Navata H (2001) Endocrinology 142:3590–3597
Nagata S (1997) Cell 88:355–365
Nagy LV, Thomazy GL, Shipley L, Fesus W, Lamph RA, Heyman RA, Chandraratna PJ (1995) Mol Cell Biol 15:3540–3551
Nakai M, Takeda A, Cleary ML, Endo T (1993) Biochem Biophys Res Commun 196:233–239
Nakamura N, Shidoji Y, Yamada Y, Hatakeyama H, Moriwaki H, Muto Y (1995) Biochem Biophys Res Commun 207:382–388
Pinton P, Ferrari D, Rapizzi E, Virgilio FD, Pozzan T, Rizzuto R (2001) EMBO J 20:2690–2701
Radominska-Pandya A, Chen G, Czernik PJ, Little JM, Samokyszyn VM, Carter CA, Nowak G (2000) J Biol Chem 275:22324–22330
Toma S, Isnardi L, Raffo P, Dastoli G, De Francisci E, Riccardi L, Palombo R, Bollag W (1997) Int J Cancer 70:619–627
Von Haefen C, Wieder T, Gillissen B, Starck L, Graupner V, Dorken B, Daniel PT (2002) Oncogene 21:4009–4019
Woodle ES, Kulkarni S (1998) Transplantation 66:681–691

Biochimica et Biophysica Acta xxx (2010) xxx–xxx

Contents lists available at ScienceDirect

Biochimica et Biophysica Acta

journal homepage: www.elsevier.com/locate/bbagen

Proliferative and anti-proliferative effects of retinoic acid at doses similar to endogenous levels in Leydig MLTC-1/R2C/TM-3 cells

Mariarita Perri [1], Attilio Pingitore [1], Erika Cione, Emma Vilardi, Valentina Perrone, Giuseppe Genchi *

Dipartimento Farmaco-Biologico, Laboratorio di Biochimica, Edificio Polifunzionale, Università della Calabria, 87036 Rende (CS), Italy

ARTICLE INFO

Article history:
Received 25 February 2010
Received in revised form 8 June 2010
Accepted 11 June 2010
Available online xxxx

Keywords:
Retinoic acid
Leydig cell
Proliferation
Apoptosis
Autophagy

ABSTRACT

Background: Vitamin A is suggested to be protective against oxidative stress. However, different authors observed pro-oxidant effects of retinoids both in experimental works and clinical trials. These discordances are the bases for the investigation of the proliferative and anti-proliferative properties of retinoic acid (RA) in biological systems.

Methods: Cell viability is determined with the MTT assay. Oxidative stress parameters are detected measuring catalase (CAT) and glutathione *S*-transferase (GST) enzymatic activities. FABP5 mRNA levels are measured by RT-PCR. Autophagy and apoptosis are analyzed by Monodansylcadaverine (MDC) staining and TUNEL assay, respectively.

Results and conclusions: RA, at nutraceutic/endogenous doses (10–200 nM), increases cell viability of testes tumor Leydig cell lines (MLTC-1 and R2C) and modulates antioxidant enzyme activities, as CAT and GST. RA is able to induce proliferation through non-classical and redox-dependent mechanisms accompanied by increased levels of FABP5 mRNA. The redox environment of the cell is currently thought to be extremely important for controlling either apoptosis or autophagy. Apoptosis occurs at pharmacological doses, while autophagy, which plays a critical role in removing damaged or surplus organelles in order to maintain cellular homeostasis, is triggered at the critical concentration of 500 nM RA, both in normal and tumoral cells. Slight variations of RA concentrations are evaluated as a threshold value to distinguish between the proliferative or anti-proliferative effects.

General significance: Although retinoids have a promising role as antineoplastic agents, physiological levels of RA play a key role in Leydig cancer progression, fostering proliferation and growth of testicular tumoral mass.

1. Introduction

Oxidative stress is a major factor in the aetiology of male infertility, able to destroy the steroidogenic capability of the testes Leydig cells [1], as well as to reduce the capability of the germinal epithelium to differentiate normal spermatozoa [2]. The poor vascularization of the testes results in reduced oxygen demand compared with other tissues, stimulating intense competition for this vital element within the organ. Since both spermatogenesis [3] and Leydig cell steroidogenesis [4] are vulnerable to oxidative stress, the low oxygen demand that characterizes this tissue may be an important component of the mechanisms by which the testes protect themselves from free radical-mediated damage. In addition, testes contain an elaborate array of antioxidant enzymes and free radical scavengers to ensure that both spermatogenic and steroidogenic functions are not influenced by oxidative stress.

Retinoids, vitamin A derivatives, have redox-related properties and influence the redox status of the cell [5,6]. It has been suggested that retinoids act as antioxidants in biological systems, assuming a role in antioxidant therapies for treatment and prevention of malignant and neurodegenerative diseases [7]. However, clinical trials have shown that retinoids can also be deleterious and are associated with the activation of proto-oncogenes, leading to an increased incidence of neoplasias [8].

Retinoic acid (RA), whose endogenous concentration are now available to the scientific community [9], regulates multiple biological processes and plays key roles in embryonic development and in tissue remodeling of adults. It has been well established that many activities of RA are mediated by retinoic acid receptors (RARα, β, and γ), ligand-inducible transcription factors that are members of the superfamily of nuclear hormone receptors [10]. Transcriptional activation of the nuclear receptor RAR by RA often leads to inhibition of cell growth. However, in some tissues RA promotes cell survival and hyperplasia: these activities are unlikely to be mediated by RAR [11,12]. In addition

* Corresponding author. Dipartimento Farmaco-Biologico, Università della Calabria, 87036 Rende (CS), Italy. Tel.: +39 0984 493454; fax: +39 0984 493271.
E-mail address: genchi@unical.it (G. Genchi).
[1] Equally contributed.

0304-4165/$ – see front matter © 2010 Elsevier B.V. All rights reserved.
doi:10.1016/j.bbagen.2010.06.006

to activate RARs, RA can also stimulate the nuclear receptor PPARβ/δ (peroxisome proliferator-activated receptor β/δ), and therefore the list of genes and cellular responses controlled by this hormone include both RAR and PPARβ/δ-targets.

The partition of RA between its two receptors is regulated by cognate intracellular lipid binding proteins (iLBPs); moreover, cellular retinoic acid binding protein II (CRABP-II) delivers RA to RARs, while fatty acid binding protein 5 (FABP5) shuttles the RA to PPARβ/δ [13]. In cells with high CRABP-II/FABP5 ratio, RA functions through RAR acting as a pro-apoptotic agent, while signaling through PPARβ/δ promotes survival in those cells highly expressing FABP5. The opposing effects of RA on cell growth thus emanate from alternate activation of two different nuclear receptors [13].

Retinoids are also promising agents in chemoprevention [7,14,15] therefore the apparently conflicting data regarding the pro-oxidant/anti-oxidant and proliferative/anti-proliferative potential of different retinoids molecules, stimulated us to investigate the effect of RA on cell proliferation and its mechanisms in two different tumor Leydig cell lines (MLTC-1 and R2C) using as normal phenotype counterpart the Leydig TM-3 cell line. Previous studies from our group had already demonstrated how pharmacological doses of RA induce cell death via the apoptotic pathway in Leydic TM-3 cell line [16]. Here we report that dose–response treatment of TM-3, MLTC-1 and R2C with RA at nutraceutic/physiological doses, promotes cell proliferation accompanied by stimulaton of antioxidant enzymes activity (CAT, GST), decreases p21 levels and fosters cell cycle progression via activation of the IP_3K/Akt pathway in the cancer cell line while administration of pharmacological doses of RA results in apoptosis either in TM-3 in agreement with the literature [16] and R2C and MLTC-1 tumoral cell line. Interestingly treatment with 0.5 μM RA resulted in cytosolic vacuolization, hallmark of the autophagic process.

2. Materials and methods

2.1. Chemicals

Retinoic acid (RA), 3-(4,5-dimethylthiazol-2-yl)-2,5-diphenyltetrazolium bromide (MTT), monodansylcadaverine (MDC) RIPA buffer, DMEM/F12, F-12 Nutrient Mixture (Ham) and RPMI-1640, fetal bovine serum (FBS), horse serum (HS), fetal calf serum (FCS), glutamine, penicillin/streptomycin, GST and CAT assay kits were purchased from Sigma-Aldrich (Milano, Italia). ECL system was obtained by Amersham Pharmacia Biotech. All other chemicals used were of analytical reagent grade. RA solution was prepared just before use. All experiments involving RA were performed under safe yellow light, and the tubes and culture plates containing RA were covered with aluminium foils.

2.2. Cell cultures

The Leydig (TM-3) cell line was cultured in DMEM/F12 medium supplemented with 5% horse serum (HS) and 5% fetal calf serum (FCS). Tumoral MLTC-1 cell line was cultured in RPMI-1640 medium supplemented with 10% FCS. The R2C cell line was cultured in F-12 Nutrient Mixture (Ham) supplemented with 2.5% fetal bovin serum (FBS), 15% horse serum (HS). Culture media for all cell lines were supplemented with 2 mM glutamine and 1% of a stock solution containing 10,000 IU/ml penicillin and 10,000 μg/ml streptomycin. Cell cultures were grown on 90 mm plastic tissue culture dishes in a humidified atmosphere of 5% CO_2 in air at 37 °C. Cells from exponentially growing stock cultures were removed from the dishes with trypsin (0.05% w/v) and EDTA (0.02% w/v). The trypsin/EDTA action was inhibited with an equal volume of DMEM/F12, F-12 Nutrient Mixture (Ham) or RPMI-1640 medium. Cell number was estimated with a Burker camera and cell viability by trypan blue dye exclusion. For all cellular lines, the medium was changed twice per week. TM-3 and R2C cells were subcultivated when confluent, while MLTC-1 cells were subcultured when they formed island domes.

2.3. MTT proliferation assay

Cell viability was determined with the MTT assay [17]. In order to determine the proliferative effect of RA, cells (2×10^5 cells/ml) were treated with increasing RA concentrations for 48 to 72 h. Control cells were treated with vehicle alone. A 100 μl of MTT (5 mg/ml) was added to each well in 1 ml of medium without phenol red, and the plates were incubated for 4 h at 37 °C. Then, 1 ml 0.04 N HCl in isopropanol was added to solubilize the cells. The absorbance was measured with the *Ultrospec 2100-pro* spectrophotometer (Amersham-Biosciences) at a test wavelength of 570 nm with a reference wavelength of 690 nm. The optical density (OD) was calculated as the difference between the absorbance at the reference wavelength and that at the test wavelength. Percent viability was calculated as (OD of drug-treated sample/OD of control) × 100.

2.4. Isolation of mitochondrial fraction from MLTC-1 and R2C cells

After trypsinization and centrifugation of cells at 1,800 rpm for 5 min at 4 °C mitochondria were isolated solubilizing the pellet with 200 μl RIPA buffer, supplemented with 0.1% digitonin; the cells were incubated for 15 min at 4 °C and the mitochondria were isolated by differential centrifugations at 4 °C as described by Cione et al. [18].

2.5. Oxidative stress parameters

Following sonication of TM-3, R2C and MLTC-1 cells in PBS (phosphate-buffered saline, 1.5 mM KH_2PO_4, 8.1 mM Na_2HPO_4, 136.9 mM NaCl, pH 7.2), the suspension was centrifuged at 10,000 rpm for 5 min and the supernatant was utilized in assays for glutathione *S*-transferase (GST) and catalase (CAT). The enzymatic activities in the cell samples of CAT and GST were determined by Aebi [19] and Habig et al. [20], respectively. Protein amount was estimated by Lowry method [21].

2.6. Western blotting

Cultured cells were lysed with 200 μl ice-cold PBS containing 1% Triton X-100, 0.5% sodium deoxycholate, 0.1% SDS and protease inhibitors (1 mM phenylmethylsulfonylfluoride, 10 mg/ml aprotinin and 10 mg/ml leupeptin). Lysates were centrifuged (13,000 × *g* at 4 °C for 30 min) and the supernatant protein content was determined by the Lowry method [21]. Proteins (50 μg) were resolved by 15% SDS-PAGE, and transferred to a nitrocellulose membrane (Hybond-C; Amersham Biosciences, Piscataway, NJ). The membrane was blocked with 5% bovine serum albumin and probed with specific primary antibodies such as anti-phospho-Akt1/2/3 (Ser 473)-R (Santa Cruz Biotechnology Inc., Santa Cruz, CA), anti-Akt (Santa Cruz Biotechnology Inc.), anti-cyclin D1 (Santa Cruz Biotechnology Inc.), anti-p21 (Santa Cruz Biotechnology Inc.) and anti-cyt *c* (Santa Cruz Biotechnology Inc.), respectively. After washing, membranes were incubated with HRP-conjugated secondary antibody. Peroxidase activity was visualized with the Amersham Pharmacia Biotech ECL system according to the manufacturer's instructions. The protein content was determined densitometrically. The loading control was detected by immunoblot of β-actin protein.

2.7. JC-1 mitochondrial membrane potential detection assay

The loss of mitochondrial membrane potential (ΔΨm) was monitored with the 5,5′,6,6′tetra-chloro-1,1′,3,3′-tetraethylbenzimidazolyl-carbocyanine iodide dye (JC-1) (Biotium, Hayward, USA). The negative charge established by the intact ΔΨm, allows the lipophilic

Please cite this article as: M. Perri, et al., Proliferative and anti-proliferative effects of retinoic acid at doses similar to endogenous levels in Leydig MLTC-1/R2C/TM-3 cells, Biochim. Biophys. Acta (2010), doi:10.1016/j.bbagen.2010.06.006

dye JC-1 to selectively enter the mitochondrial matrix, where it aggregates and emits a red fluorescence. When the $\Delta\Psi m$ is lost the JC-1 cannot accumulate within these organelles and remains in the cytoplasm in the monomeric form emitting green fluorescence [22]. MLTC-1 and R2C cell lines were grown in 10 cm dishes and treated with 1 μM RA for 24 h, then the cells were trypsinized, washed in ice-cold PBS, and incubated with 10 mM JC-1 at 37 °C in a 5% CO_2 incubator for 20 min. Subsequently, cells were washed twice with PBS and analyzed by fluorescence microscopy according to manufacturer's instructions.

2.8. Mitochondrial ATP determination

The amount of endogenous ATP in isolated mitochondria and in cytosolic extract from MLTC-1 and R2C cell lines was determined using the bioluminescence method described by Drew and Leeuwenburgh [23]. With a Molecular Probes kit, ATP was assayed in cells lysed with RIPA buffer containing a proteases inhibitors mixture (Sigma) and cleared of cellular debris by centrifugation (10 min, 4 °C). An aliquot of each sample was mixed with 100 μl of reaction cocktail (25 mM Tricine buffer, pH 7.8, 5 mM $MgSO_4$, 100 μM EDTA, 1 mM DTT) containing firefly luciferase and 0.5 mM luciferin. Emitted light was measured in a luminometer (Berthold).

2.9. Monodansylcadaverine staining

MDC was used to evaluate autophagic vacuoles in cells as previously reported [24]. A 10 mM stock solution of MDC was prepared in PBS. Following treatment with 0.5 μM RA for 24 h, cells were stained with MDC at a final concentration of 10 μM for 10 min at 37 °C, and fixed using 3% paraformaldehyde solution in PBS for 30 min. Cells were washed and then examined by fluorescence microscopy (Leica AF2006).

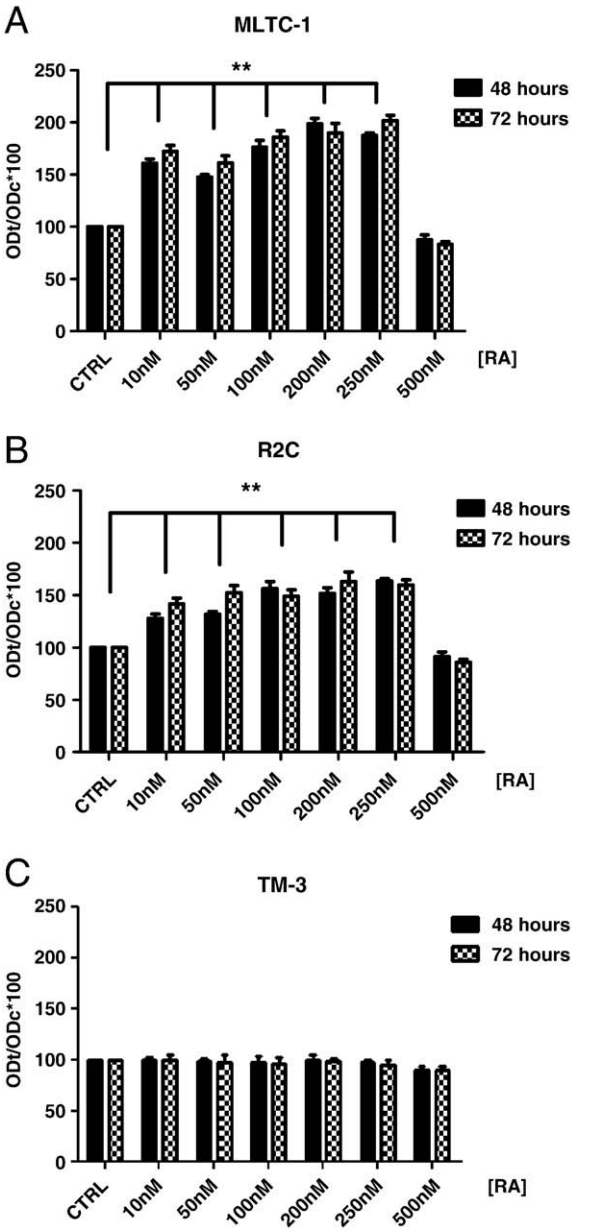

Fig. 1. Cell viability by MTT assay MLTC-1 (A), R2C (B) and TM-3 (C) cells were incubated at the indicated concentrations of RA. Cell viability was determined by MTT assay as described in Materials and methods at 48 and 72 h post-exposure. The data represent the mean ± SD of four independent experiments in triplicate and are presented as the percentage of the control cell number. $^{**}P<0.01$ compared to the control.

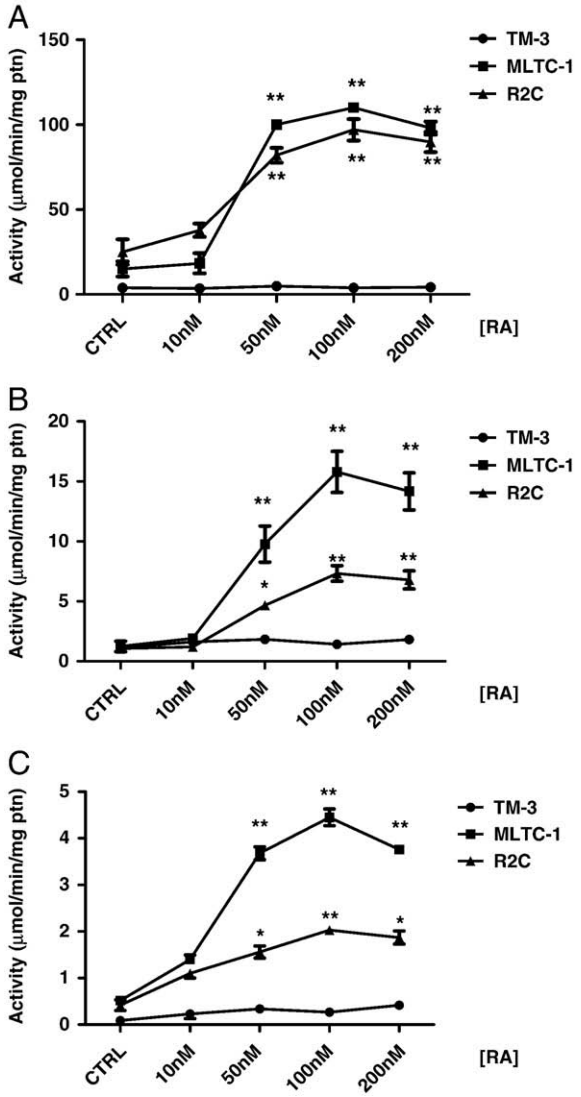

Fig. 2. Antioxidant enzyme activity Cells were treated at the indicated concentrations of RA for 6 h and CAT (A), GST (B) and mitochondrial GST (C) activities were measured as described in Materials and methods. Enzyme activity is expressed as μmol substrate/min/mg protein. Results are presented as the mean ± SD of three individual experiments. $^{*}P<0.05$, $^{**}P<0.01$ compared to the control.

Please cite this article as: M. Perri, et al., Proliferative and anti-proliferative effects of retinoic acid at doses similar to endogenous levels in Leydig MLTC-1/R2C/TM-3 cells, Biochim. Biophys. Acta (2010), doi:10.1016/j.bbagen.2010.06.006

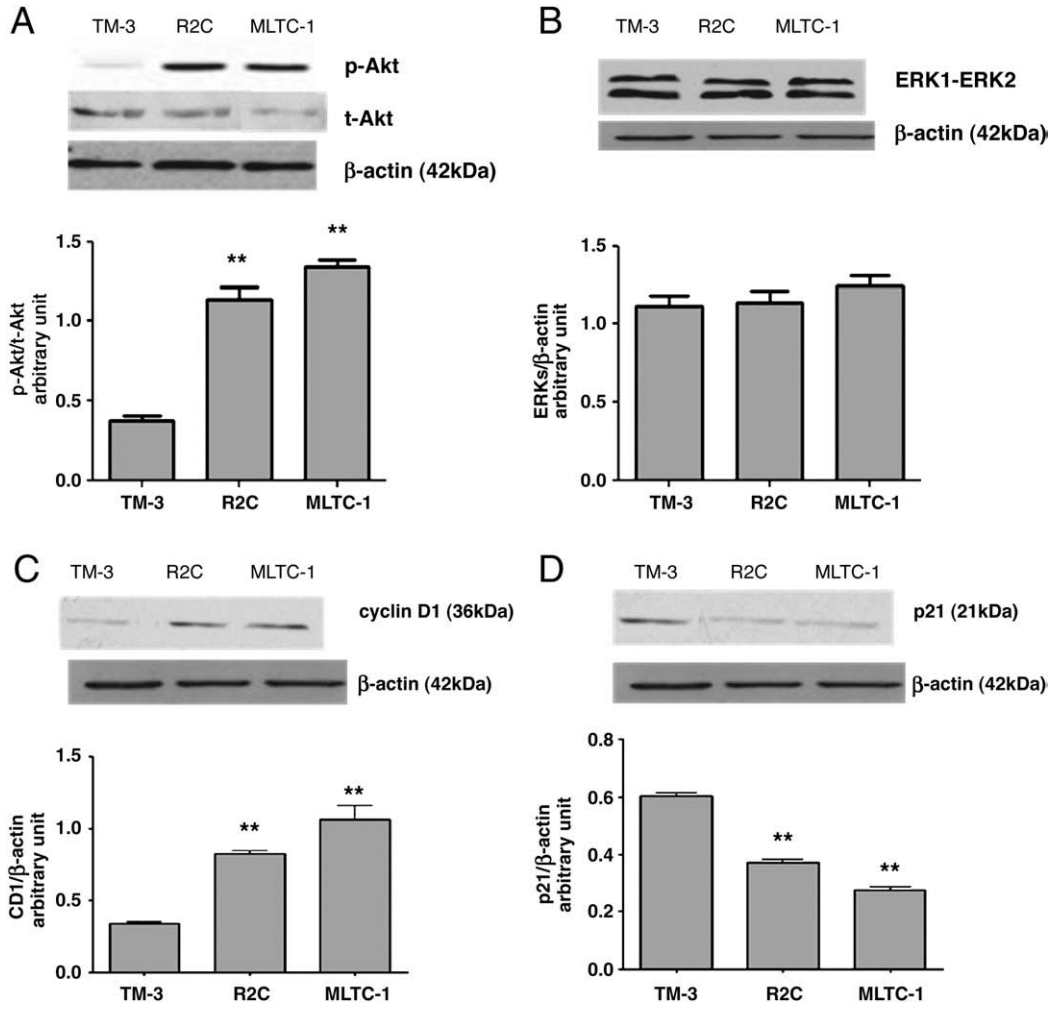

Fig. 3. Effect of RA on IP_3K/Akt signaling pathways and cell cycle progression TM-3, R2C, MLTC-1 cells were incubated in the presence of 10 nM RA for 48 h. After incubation, cells were washed with PBS; 50 μg of protein was separated by 15% SDS-PAGE, transferred to a nitrocellulose membrane, and blotted as described in Materials and methods. β-Actin was used as internal control. Activation of p-Akt after 15 min (A). No activation of ERK1/2 pathway (B). Up-regulation of cyclin D1 (C). Down-regulation of p21 (D). Protein content was determined densitometrically. Results are presented as the mean ± SD of three independent experiments. $^{**}P<0.01$ compared to the normal TM-3 cell line (as control).

2.10. Flow cytometry assay

Cells (1×10^6 cells/well) were grown in 6 well plates and shifted to serum free medium for 24 h before treating for further 48 h. Thereafter, cells were trypsinized, centrifuged at 3,000 rpm for 3 min and washed with PBS. A 0.5 μl of fluorescein isothiocyanate-conjugated antibodies anti-caspase-9 (Calbiochem, Milan, Italy) was added in all samples and then incubated for 45 min at 37 °C according to manufacturer's instruction. Samples were analyzed with the FACScan (Becton Dickinson and Co., Franklin Lakes, NJ).

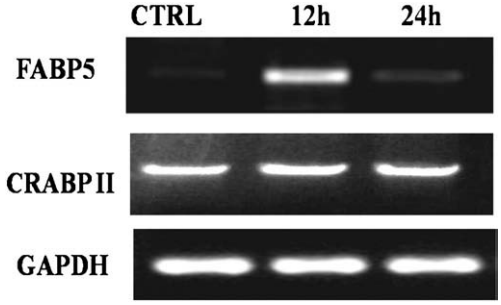

Fig. 4. Influence of RA on FABP5 and CRABP II mRNA expressions FABP5 and CRABP II mRNA expression in MLTC-1 cells treated with 10 nM RA for 12/24 h.

2.11. TUNEL assay

Apoptosis was determined by enzymatic labeling of DNA strand breaks using terminal deoxynucleotidyl transferase-mediated deoxyuridine triphosphate nick end-labeling (TUNEL). TUNEL labeling was conducted using APO-BrdU™. TUNEL Assay Kit (Molecular Probes) and performed according to the manufacturer's instructions. Cells were incubated for 30 min at room temperature protected from light and photographed by using a fluorescent microscope (Leica AF2006).

2.12. Reverse transcription-PCR assay

MLTC-1 cells were grown in 10 cm dishes from 70/80% confluence and exposed to RA treatments as indicated in Fig. 4 caption. Total cellular RNA was extracted using Trizol reagent (Invitrogen) as suggested by the manufacturer. The purity and the integrity of total RNA were checked spectroscopically before carrying out the analytical procedures. RNA was then reverse transcribed with High Capacity cDNA Reverse Transcription Kit (Applied Biosystems). The cDNA obtained was amplified by PCR using the following primers: FABP5 (NM 010634) 5′-ACGGCTTTGAGGAGTACATGA-3′ (forward) and 5′-TCCTACCCTTC-TACTAGCAC-3′ (reverse), CRABP II (NM 007759) 5′-CGATCG-GAAAACTTTGAGGA-3′ (forward) and 5′-CAACACACGTGGTCCCAGAT-3′ (reverse). The resulting PCR products were separated by

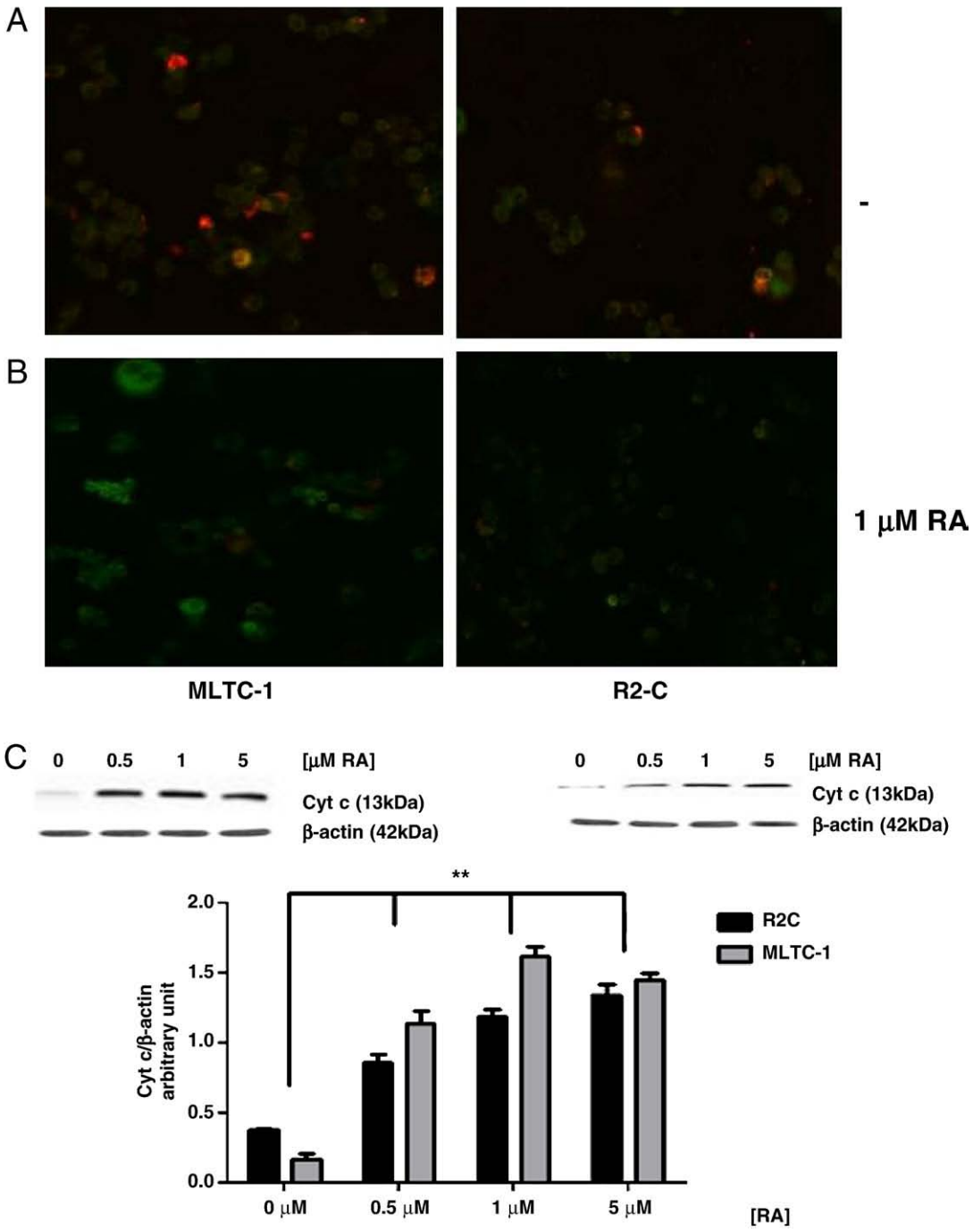

Fig. 5. Mitochondria involvement MLTC-1 and R2C cells were treated with 1 μM RA for 24 h and, after washing in ice-cold PBS, incubated with 10 mM JC-1 at 37 °C for 20 min in a 5% CO_2 incubator. The cells were washed twice with PBS and analyzed by fluorescent microscopy. In control non-apoptotic cells, the dye stains the mitochondria in red (A). In treated apoptotic cells, JC-1 remains in the cytoplasm fluorescing green (B). MLTC-1 and R2C were treated for 24 h with 0.5–1–5 μM RA and cytochrome *c* was detected (C). β-Actin was used as loading control. Figure is representative of three independent experiments.

electrophoresis in a 2% agarose gel in TBE (Tris-Borate-EDTA) and stained with ethidium bromide.

2.13. Statistical analysis

Statistical differences were determined by one-way analysis of variance (ANOVA) followed by Dunnet's method, and the results were expressed as mean ± SD from n independent experiments. Differences were considered statistically significant for $P<0.05$ (*), $P<0.01$ (**).

3. Results

As shown in Fig. 1, treatment of MLTC-1 (A) and R2C (B) with RA resulted in a significant cell proliferation in a concentration range of 10–250 nM with a slight but not significant decrement at 500 nM RA (≈10%) compared to the control. Although the data show dose dependence, no time dependence could be addresses as there is no difference in proliferation between 72 and 48 h. No change in cell viability was observed in RA treated TM-3 (C).

Please cite this article as: M. Perri, et al., Proliferative and anti-proliferative effects of retinoic acid at doses similar to endogenous levels in Leydig MLTC-1/R2C/TM-3 cells, Biochim. Biophys. Acta (2010), doi:10.1016/j.bbagen.2010.06.006

In order to investigate a potential modulation of the antioxidant defenses, cell lines were treated with RA (0–200 nM) for 6 h and the activities of CAT and GST were assayed comparing RA treated TM-3, MLTC-1 and R2C versus untreated ones (control). No modulation of these activities was reported in TM-3 at any RA concentration while CAT and cytosolic GST activities increased significantly both in MLTC-1 and R2C in a dose dependent manner (Fig. 2A and B). The mitochondrial GST (mGST) activity increased in both MLTC-1 and R2C, in particular at 100 nM (Fig. 2C).

Moreover, activation of the anti-apoptotic factor Akt was assayed by WB using an antibody raised against its phosphorylated form (p-Akt). As shown in Fig. 3A, 10 nM RA induced a rapid activation of p-Akt after 15 min of incubation. A strong signal of p-Akt was reported in MLTC-1 and R2C with no activation of ERK (Fig. 3B). Furthermore, RA supplementation increased cyclin D1 protein levels both in MLTC-1 and R2C cell lines (Fig. 3C) with a concomitant decrement of p21 expression already at 10 nM RA and in both MLTC-1 and R2C after 48 h treatment (Fig. 3D). Neither Akt was activated nor p21 levels modified in the TM-3.

On these bases the ability of nanomolar doses of RA to modulate FABP5 and CRABPII were investigated in MLTC-1. A 10 nM RA induced a significant up-regulation of FABP-5 mRNA levels after 12 h while the same treatment does no elicit any effect after 24 h. No changes in the CRABPII mRNA were observed in presence of 10 nM RA after 12 and 24 h (Fig. 4).

As to pharmacological treatment with RA of MLTC-1/R2C, 1 μM RA for 24 h resulted in disruption of mitochondrial membrane potential evidenced with a change in the emission of the lipophilic dye JC-1 (Fig. 5A and B) turning more towards green than red. At the same time, cytochrome *c* release occurred already at 0.5 μM RA (Fig. 5C) followed by no activation of caspases 3 and 9 (data not shown) while the amount of mitochondrial ATP decreased after 24 h treatment with RA 0.5 and 1 μM in dose-dependent manner.

To identify the potential direct induction of autophagy at 0.5 μM RA, after 24 h treatment, TM-3 cells were labeled with MDC, the selective stain for autophagosomes (Fig. 6A and B).

As shown in Fig. 7A, tumoral cell lines suffered cell death induction after treatment with 1 and 5 μM RA for 24 h; treatment with 10 μM RA for 24 h resulted in almost 80% reduction of cell viability with a massive decrement of cell growth both in MLTC-1 and R2C, supported by activation of caspase 9 already at RA 1 μM (Table 1). To further verify the activation of the programmed cell death, apoptosis in MLTC-1 and R2C was determined by enzymatic labeling of DNA strand breaks via TUNEL assay (Fig. 7B) supporting the already known RA mediated apoptosis induction [16].

4. Discussion

The influence of retinoids on cell growth and differentiation has been investigated during the recent years. There are a growing number of *in vitro* experiments demonstrating that active retinoids, as well as RA, antagonize cell growth in a variety of non-tumoral and tumoral cells, characterizing them as potential chemotherapeutic agents [7,14,15]. In addition, some authors suggest that retinoids act as anti-oxidants and could be potential agents in anti-oxidant supplementation protocols for treatment and prevention of malignant and neurodegenerative diseases [7,15]. On the other hand, there is also evidence that retinoids present pro-oxidant properties in biological systems, which might induce cell damage, proto-oncogene activation, proliferation and neoplastic transformation [6,8,26–31]. The pro-oxidant retinoid molecules, the mechanisms underlying—their pro-oxidant effects, and their consequences on cell proliferation or death remain to be better elucidated. Indeed, despite the important physiological functions of retinoids, the effects of supra-physiological doses of retinoids as well as their physiological action are not well defined. In an interesting work, Hurnanen et al. [32] showed that low RA concentrations stimulated growth proliferation, but high concentrations inhibited proliferation in human breast cancer cells.

In the present work we show that RA, at endogenous concentrations (0–250 nM), increases cell viability in tumor Leydig cell lines but not in the normal TM-3 counterpart. This suggests that slight variations in the concentrations of RA may trigger changes in the cellular redox state. The ability to survive the threat posed by endogenous levels of retinoids represents a biological adaptation, in many cases, to survival [33]. Strategies such as sequestration, scavenging and binding, and catalytic biotransformation have evolved as important biochemical protection mechanisms against toxic chemical species. Cells possess an impressive array of enzymes capable of bio-transforming a wide range of different chemical structures and functionalities. Since higher doses of RA induced apoptosis, we decided to investigate only the effects of low doses of RA treatment in TM-3, MLTC-1 and R2C cells showing that physiological levels of RA trigger proliferation and growth of the testicular tumoral mass.

In order to investigate changes in anti-oxidant defences, we measured the CAT and GST activities in RA-treated and non-treated TM-3, R2C and MLTC-1 cells. Of these enzymes, involved in the detoxification of the cells from reactive oxygen species, CAT metabolizes hydrogen peroxide and alterations in its activity can lead to unbalanced free radicals production, while GST is essential to maintain the homeostasis of reactive species production and clearance. In addition, cytosolic and mitochondrial GST isoforms can

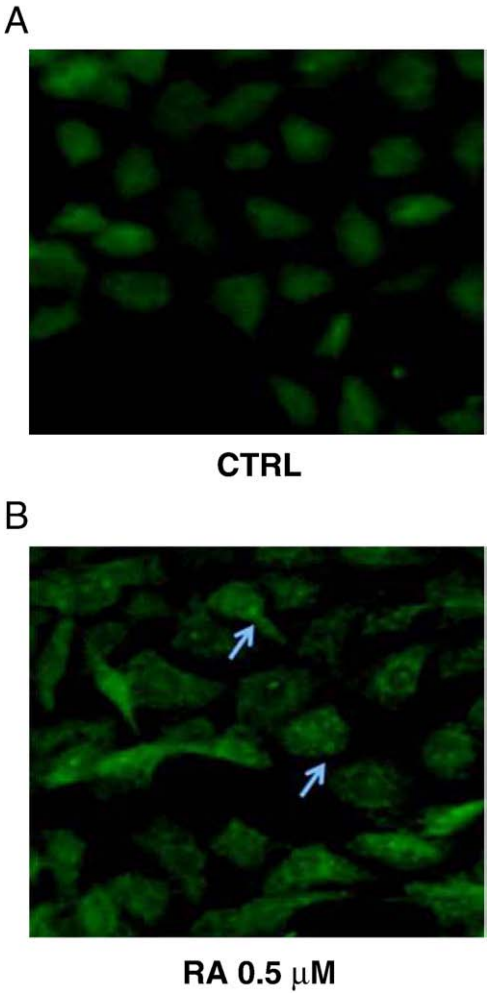

Fig. 6. Autophagy in TM-3 Leydig cells by MDC labeling TM-3 cells were treated with 0.5 μM RA and were incubated for 24 h. Cells were stained with MDC as detailed under Materials and methods. Figure is representative of three independent experiments.

Please cite this article as: M. Perri, et al., Proliferative and anti-proliferative effects of retinoic acid at doses similar to endogenous levels in Leydig MLTC-1/R2C/TM-3 cells, Biochim. Biophys. Acta (2010), doi:10.1016/j.bbagen.2010.06.006

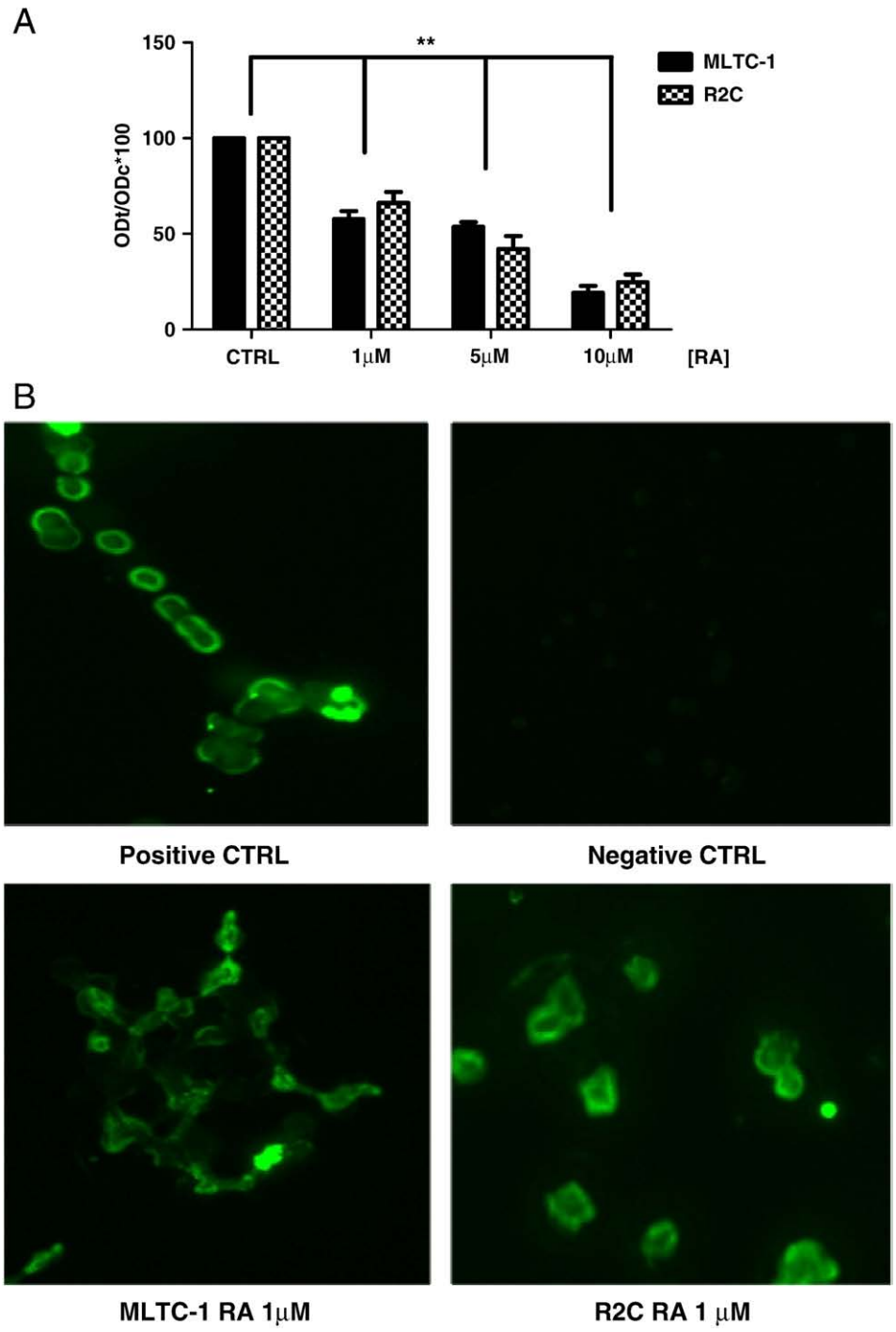

Fig. 7. Apoptosis in MLTC-1/R2C cell lines induced with 1–10 μM RA after 24 h incubation MLTC-1 and R2C cells were stimulated for 24 h by the presence of 1, 5 or 10 μM RA. Viability was analyzed by MTT assay (A). Data are presented as mean ± SD of triplicate experiments. $^{**}P<0.01$ compared to the control. Apoptosis in MLTC-1 and R2C cells was determined by TUNEL assay after treatment with 1 μM RA (B). Figure is representative of three independent experiments.

discriminate between stressed and non-stressed cells [34]. The increase of cell viability of tumor Leydig cell lines (Fig. 1) was accompanied by a strong activation of both anti-oxidant enzymes after 6 h of incubation at physiological RA concentrations (Fig. 2). This enhanced RA-induced proliferation influences cell cycle progression, associated with the increment of cyclin D1 expression (Fig. 3C). In agreement with cell proliferation, immuno-detection of the cyclin-dependent kinase (CDK) inhibitor, p21, showed that 10 nM RA already decreases its levels. Our data suggest that the proliferative effect of RA was mediated also by IP_3K/Akt pathway (Fig. 3D). In agreement with this, 10 nM RA induced a rapid activation of phosphorylated Akt after 15 min of incubation, which was not followed by ERK pathway activation. Activation/inhibition of Akt is directly linked to the regulation of cell proliferation/death. Data suggest that Akt, an anti-apoptotic factor, is involved in retinoid-induced MLTC-1 and R2C proliferation.

Moreover it is worthy to note that a specific concentration range of RA (10–200 nM) induces cell proliferation and that a clear threshold value discriminating the proliferative from the anti-proliferative effect of RA does exist in our experimental system. In fact, at 0.5 μM RA we observed the activation of the autophagy process (Fig. 6) which in turns plays a critical role in removing damaged or surplus

Please cite this article as: M. Perri, et al., Proliferative and anti-proliferative effects of retinoic acid at doses similar to endogenous levels in Leydig MLTC-1/R2C/TM-3 cells, Biochim. Biophys. Acta (2010), doi:10.1016/j.bbagen.2010.06.006

Table 1
Caspase 9 activation. MLTC-1 and R2C cells were stimulated for 24 h by the presence of 1–5–10 μM RA. The activation of caspase-9 was analyzed by flow cytometry. Data are presented as mean ± SD of triplicate experiments.

Treatment	Cell line	% of Caspase-9 activation	SD
CTRL	MLTC-1	12.34	±2.76
RA 1 μM	MLTC-1	25.87	±0.56
RA 5 μM	MLTC-1	28.75	±1.86
RA 10 μM	MLTC-1	37.13	±2.12
CTRL	R2C	15.45	±1.85
RA 1 μM	R2C	27.82	±1.12
RA 5 μM	R2C	24.65	±0.92
RA 10 μM	R2C	32.64	±3.17

Table 2
Mitochondrial ATP determination. Cells were treated with 0.5–1 μM RA for 24 h and mitochondrial ATP amount was determined as described in Materials and methods. Data are presented as mean ± SD of triplicate experiments.

	ATP concentration (nM)
MLTC-1 DMSO	10.20 ± 0.32
MLTC-1 0.5 μM RA	4.12 ± 0.11
MLTC-1 1 μM RA	2.23 ± 0.13
R2C DMSO	10.84 ± 0.42
R2C 0.5 μM RA	5.41 ± 0.26
R2C 1 μM RA	3.78 ± 0.19

organelles in order to maintain cellular homeostasis. Autophagy sometimes occurs with apoptosis: the relationship between autophagy and cell death is complex, since autophagy can be involved either in cell death or in survival depending on the cellular context [34,35]. The survival function of autophagy has been demonstrated under different physiological situations, such as interruption of maternal nutrient supply in newborn mice [36] or in cells deprived of growth factors and nutrients [25,37,38]. Both apoptosis and autophagy can occur concomitantly in the same cells, suggesting the involvement of common regulatory mechanisms [39]. Moreover the redox environment of the cell is currently thought to be extremely important to control either apoptosis or autophagy [40,41].

Mitochondria are acknowledged as the central coordinators of apoptotic events that determine the intrinsic pathway of apoptosis [42]. Several intracellular signals converge on mitochondria to induce mitochondrial membrane permeability (MMP), which causes the dissipation of mitochondrial transmembrane potential ($\Delta\Psi m$) and the release of pro-apoptotic factors, in particular the release of cytochrome *c* that leads to the activation of caspases and subsequent cell death [34,35]. It is documented that when the change in mitochondrial membranes permeability entails less than 66% of the mitochondria, the autophagic pathway is activated, while the apoptotic death is triggered when the percentage raises toward higher values involving most of the mitochondrial population [34]. Besides that, in both cases, a change of permeability causes swelling and depolarization of the mitochondrial membranes, impairing the oxidative phosphorylation capability. The latter leads to reduced ATP production and a consequent depletion of ATP levels. It is hypothesized that amino-acidic and insulin regulation [43] can act in a synergistic manner in the control of autophagy. It seems that the signal, mediated from both insulin and amino acids, can converge at the level of the enzyme mammalian Target of Rapamycin (mTOR), a kinase that activates protein synthesis and, at the same time, inhibits autophagy [44]. As amino acids are able to activate mTOR, RA is able to exert the same effect in the hippocampal neurons at a concentration of 10 nM [45,46]. The enzyme is inhibited due to lack of energy indicated by a decrease in the ATP/AMP ratio. In our experimental system, treatment for 24 h with 0.5 μM RA triggers disruption of mitochondrial membrane potential (Fig. 5A and B) with release of cytochrome *c* followed by no activation of caspase 3 and 9 (data not shown) with a notable decrease in endogenous mitochondrial ATP, as shown in Table 2, and cytosolic vacuolization, hallmark of autophagy.

Upon treatment with 1 μM RA, we observed a significant induction of cell death by apoptosis. Changes in mitochondrial membrane permeability are concomitant with collapse of the electrochemical gradient across the mitochondrial membrane through the formation of pores leading to the release of cytochrome *c*, followed by cleavage of procaspase-9 and DNA fragmentation highlighted by TUNEL assay. This cascade of events was caused by pharmacological doses of RA in both MLTC-1/R2C cells, as already documented in TM-3 [16].

A model outlining the dual proliferative/anti-proliferative effects of RA is described by Schug et al. [13]. CRABP-II and FABP5 target RA to RAR and PPARβ/δ, respectively. In cells that express a high CRABP-II/FABP5 ratio, RA is 'channeled' to RAR, often resulting in growth inhibition. Conversely, in the presence of a low CRABP-II/FABP5 expression ratio, RA is targeted to PPARβ/δ, thereby up-regulating survival pathways. As shown in Fig. 4, the highest increase in the FABP5 mRNA expression was observed after 12 h in MLTC-1 cells during the proliferation process simultaneously with no changes in CRABP II mRNA expression. These results provide further strength to the hypothesis of altered retinoid homeostasis/metabolism in neoplastic diseases.

Acknowledgements

We thank Prof. Andò for the gift of all the used cell lines. This research was supported by grants from Ministero dell'Istruzione, dell'Università e della Ricerca (MIUR, Italia).

References

[1] D.B. Hales, J.A. Allen, T. Shankara, P. Janus, S. Buck, T. Diemer, K. Held Hales, Mitochondrial function in Leydig cell steroidogenesis, Ann. N. Y. Acad. Sci. 1061 (2005) 120–134.
[2] C.K. Naughton, A.K. Nangia, A. Agarwal, Pathophysiology of varicoceles in male infertility, Hum. Reprod. Update 7 (2001) 473–481.
[3] V. Peltola, E. Mantyla, I. Huhtaniemi, M. Ahotupa, Lipid peroxidation and antioxidant enzyme activities in the rat testis after cigarette smoke inhalation or administration of polychlorinated biphenyls or polychlorinated naphthalenes, J. Androl. 15 (1994) 353–361.
[4] H. Chen, J. Liu, L. Luo, M.U. Baig, J.M. Kim, B.R. Zirkin, Vitamin E, aging and Leydig cell steroidogenesis, Exp. Gerontol. 40 (2005) 728–736.
[5] M. Murata, S. Kawanishi, Oxidative DNA damage by vitamin A and its derivative via superoxide generation, J. Biol. Chem. 275 (2000) 2003–2008.
[6] F. Klamt, F. Dal-Pizzol, R. Rohers, R.B. Oliveira, R.J. Dalmolin, J.A. Henriques, H.H. Andrades, A.L. Paula Ramos, J. Saffi, J.C. Moreira, Genotoxicity, recombinogenicity and cellular preneoplasic transformation induced by vitamin A supplementation, Mutat. Res. 539 (2003) 117–125.
[7] M. Okuno, S. Kojima, R. Matsushima-Nishiwaki, H. Tsurumi, Y. Muto, S.L. Friedman, H. Moriwaki, Retinoids in cancer chemoprevention, Curr. Cancer Drug Targets 4 (2004) 285–298.
[8] G.S. Omenn, Chemoprevention of lung cancers: lessons from CARET, the beta-carotene and retinol efficiency trial, and prospects for the future, Eur. J. Cancer Prev. 16 (2007) 184–191.
[9] M.A. Kane, A.E. Folias, C. Wang, J.L. Napoli, Quantitative profiling of endogenous retinoic acid in vivo and in vitro by tandem mass spectrometry, Anal. Chem. 80 (5) (Mar 1 2008) 1702–1708.
[10] V. Laudet, H. Gronemeyer, The Nuclear Receptor, FactsBook, Academic Press, London and San Diego, 2002.
[11] P.D. Henion, J.A. Weston, Retinoic acid selectively promotes the survival and proliferation of neurogenic precursors in cultured neural crest cell populations, Dev. Biol. 161 (1994) 243–250.
[12] A. Rodriguez-Tebar, H. Rohrer, Retinoic acid induces NGF-dependent survival response and high-affinity NGF receptors in immature chick sympathetic neurons, Development 112 (1991) 813–820.
[13] T.T. Schug, D.C. Berry, N.S. Shaw, S.N. Travis, N. Noy, Dual transcriptional activities underlie opposing effects of retinoic acid on cell survival, Cell 129 (2007) 723–733.
[14] Y. Kuratomi, Y. Kumamoto, H. Yamashita, T. Yamamoto, A. Inokuchi, K. Tomita, Comparison of survival rates of patients with nasopharyngeal carcinoma treated with radiotherapy, 5-fluorouracil and vitamin A ('FAR' therapy) vs FAR therapy plus adjunctive cisplatin and peplomycin chemotherapy, Eur. Arch. Otorhinolaryngol. 256 (1999) S60–S63.
[15] K.H. Dragnev, W.J. Petty, E. Dmitrovsky, Retinoid targets in cancer therapy and chemoprevention, Cancer Biol. Ther. 2 (2003) S150–S156.

Please cite this article as: M. Perri, et al., Proliferative and anti-proliferative effects of retinoic acid at doses similar to endogenous levels in Leydig MLTC-1/R2C/TM-3 cells, Biochim. Biophys. Acta (2010), doi:10.1016/j.bbagen.2010.06.006

[16] P. Tucci, E. Cione, M. Perri, G. Genchi, All-trans-retinoic acid induces apoptosis in Leydig cells via activation of the mitochondrial death pathway and antioxidant enzyme regulation, J. Bioenerg. Biomembr. 40 (2008) 315–323.
[17] T. Mosmann, Rapid colorimetric assay for cellular growth and survival: application to proliferation and cytotoxicity assays, J. Immunol. Methods 65 (1983) 55–63.
[18] E. Cione, A. Pingitore, M. Perri, G. Genchi, Influence of all-trans-retinoic acid on oxoglutarate carrier via retinoylation reaction, Biochim. Biophys. Acta 1791 (2009) 3–7.
[19] H. Aebi, Catalase, in: H.U. Bergmeyer (Ed.), Methods in Enzymatic Analysis, Academic Press, New York, 1974, pp. 673–678.
[20] W.H. Habig, M.J. Pabst, W.B. Jakoby, Glutathione S-transferase, the first enzymatic step in mercapturic acid formation, J. Biol. Chem. 249 (1973) 7130–7139.
[21] O.H. Lowry, N.J. Rosebrough, R.J. Randall, Protein measurement with the Folin phenol reagent, J. Biol. Chem. 193 (1951) 265–275.
[22] A. Cossarizza, M. Baccarani-Contri, G. Kalashnicova, C. Franceschi, A new method for the cytofluorimetric analysis of mitochondrial membrane potential using the J-aggregate forming lipophilic cation 5, 5′, 6, 6′-tetrachloro-1, 1′, 3, 3′ tetraethylbenzimidazolylcarbo-cyanine iodide (JC-1), Biochem. Biophys. Res. Commun. 197 (1993) 40–45.
[23] B. Drew, C. Leeuwenburgh, Method for measuring ATP production in isolated mitochondria: ATP production in brain and liver mitochondria of Fischer-344 rats with age and caloric restriction, Am. J. Physiol. Regul. Integr. Comp. Physiol. 285 (2003) R1259–R1267.
[24] A. Biederbick, H.F. Kern, H.P. Elsasser, Monodansylcadaverine (MDC) is a specific in vivo marker for autophagic vacuoles, Eur. J. Cell. Biol. 66 (1995) 3–14.
[25] P.J. Plomp, E.J. Wolvetang, A.K. Groen, A.J. Meijer, P.B. Gordon, P.O. Seglen, Energy dependence of autophagic protein degradation in isolated rat hepatocytes, Eur. J. Biochem. 164 (1987) 197–203.
[26] K.L. Penniston, S.A. Tanumihardjo, The acute and chronic toxic effects of vitamin A, Am. J. Clin. Nutr. 83 (2006) 191–201.
[27] D.P. Gelain, J.C.F. Moreira, Evidence of increased reactive species formation by retinol, but not retinoic acid, in PC12 cells, Toxicol. In Vitro 22 (2008) 553–558.
[28] A. Gimeno, R. Zaragoza, I. Vivo-Sese, J.R. Viña, V.J. Miralles, Retinol, at concentrations greater than the physiological limit, induces oxidative stress and apoptosis in human dermal fibroblasts, Exp. Dermatol. 13 (2004) 45–54.
[29] F. Dal-Pizzol, F. Klamt, R.J. Dalmolin, E.A. Bernard, J.C. Moreira, Mitogenic signaling mediated by oxidants in retinol treated Sertoli cells, Free Radic. Res. 35 (2001) 749–755.
[30] D.P. Gelain, M. Cammarota, A. Zanotto-Filho, R.B. de Oliveira, F. Dal-Pizzol, I. Izquierdo, L.R. Bevilaqua, J.C. Moreira, Retinol induces the ERK1/2-dependent phosphorylation of CREB through a pathway involving the generation of reactive oxygen species in cultured Sertoli cells, Cell Signal 18 (2006) 1685–1694.
[31] F. Klamt, R.M. de Oliveira, J.C. Moreira, Retinol induces permeability transition and cytochrome c release from rat liver mitochondria, Biochim. Biophys. Acta 1726 (2005) 14–20.
[32] D. Hurnanen, M. Chan, S. Kubow, The protective effect of metallothionein against lipid peroxidation caused by retinoic acid in human breast cancer cells, J. Pharmacol. Exp. Ther. 283 (1997) 1520–1528.
[33] J.D. Hayes, L.I. McLellan, Glutathione and glutathione-dependent enzymes represent a co-ordinately regulated defence against oxidative stress, Free Radic. Res. 31 (1999) 273–300.
[34] A.S. Alva, S.H. Gultekin, E.H. Baehrecke, Autophagy in human tumors: cell survival or death? Cell Death Differ. 11 (2004) 1046–1048.
[35] Y. Chen, S.B. Gibson, Is mitochondrial generation of reactive oxygen species a trigger for autophagy? Autophagy 4 (2008) 246–248.
[36] E.H. Baehrecke, Autophagy: dual roles in life and death? Nat. Rev. Mol. Cell. Biol. 6 (2005) 505–510.
[37] A. Kuma, M. Hatano, M. Matsui, A. Yamamoto, H. Nakaya, T. Yoshimori, Y. Ohsumi, T. Tokuhisa, N. Mizushima, Nature 432 (2004) 1032–1036.
[38] J. Lum, D. Bauer, M. Kong, M. Harris, C. Li, T. Lindsten, C. Thompson, Growth factor regulation of autophagy and cell survival in the absence of apoptosis, Cell 120 (2005) 237–248.
[39] Y. Kondo, T. Kanzawa, R. Sawaya, S. Kondo, The role of autophagy in cancer development and response to therapy, Nat. Rev. Cancer 5 (2005) 726–734.
[40] M. Jaattela, Multiple cell death pathways as regulators of tumour initiation and progression, Oncogene 23 (2004) 2746–2756;
FASEB J. 22 (2008) 236–245.
[41] N. Gurusamy, D.K. Das, Autophagy, redox signaling, and ventricular remodeling, Antioxid. Redox Signal. 11 (2009) 1975–1988.
[42] M.B. Azad, Y. Chen, S.B. Gibson, Regulation of autophagy by reactive oxygen species (ROS): implications for cancer progression and treatment, Antioxid. Redox Signal. 11 (2009) 777–790.
[43] L. Scorrano, Opening the doors to cytochrome c: changes in mitochondrial shape and apoptosis, Int. J. Biochem. Cell Biol. 41 (2009) 1875–1883.
[44] T. Kanazawa, I. Taneike, R. Akaishi, F. Yoshizawa, N. Furuya, S. Fujimura, M. Kadowaki, Amino acids and insulin control autophagic proteolysis through different signaling pathways in relation to mTOR in isolated rat hepatocytes, J. Biol. Chem. 279 (2003) 8452–8459.
[45] T. Schmelzle, M.N. Hall, TOR, a central controller of cell growth, Cell 103 (2000) 253–262.
[46] N. Chen, J.L. Napoli, All-trans-retinoic acid stimulates translation and induces spine formation in hippocampal neurons through a membrane-associated RARalpha, FASEB J. 22 (1) (Jan 2008) 236–245.

Please cite this article as: M. Perri, et al., Proliferative and anti-proliferative effects of retinoic acid at doses similar to endogenous levels in Leydig MLTC-1/R2C/TM-3 cells, Biochim. Biophys. Acta (2010), doi:10.1016/j.bbagen.2010.06.006

Biochimica et Biophysica Acta 1791 (2009) 3–7

Contents lists available at ScienceDirect

Biochimica et Biophysica Acta

journal homepage: www.elsevier.com/locate/bbalip

Influence of all-*trans*-retinoic acid on oxoglutarate carrier via retinoylation reaction

E. Cione, A. Pingitore, M. Perri, G. Genchi *

Department of Pharmaco-Biology, University of Calabria, Edificio Polifunzionale, 87036 Rende (CS), Italy

ARTICLE INFO

Article history:
Received 1 May 2008
Received in revised form 17 September 2008
Accepted 24 September 2008
Available online 14 October 2008

Keywords:
Retinoic acid
2-Oxoglutarate carrier
Retinoylation reaction

ABSTRACT

All-*trans*-retinoic acid (atRA), an activated metabolite of vitamin A, is incorporated covalently into proteins both *in vivo* and *in vitro*. AtRA reduced the transport activity of the oxoglutarate carrier (OGC) isolated from testes mitochondria to 58% of control via retinoylation reaction. Labeling of testes mitochondrial proteins with ^{3}HatRA demonstrated the binding of atRA to a 31.5 KDa protein. This protein was identified as OGC due to the competition for the labeling reaction with 2-oxoglutarate, the specific OGC substrate. The role of retinoylated proteins is currently being explored and here we have the first evidence that retinoic acids bind directly to OGC and inhibit its activity in rat testes mitochondria via retinoylation reaction. This study indicates the evidence of a specific interaction between atRA and OGC and establishes a novel mechanism for atRA action, which could influence the physiological biosynthesis of testosterone in situations such as retinoic acid treatment.

1. Introduction

Oxoglutarate carrier (OGC), also known as the oxoglutarate/malate carrier, catalyzes the transport of 2-oxoglutarate in electroneutral exchange for some other dicarboxylates to which malate is bound with the highest affinity. In proteoliposomes OGC has been shown to exist as a homodimer and to function according to a sequential antiport mechanism. These results have been interpreted by assuming two separate and coordinated substrate translocation pathways, one in each monomer. OGC plays an important role in the malate–aspartate shuttle and is also involved in the oxoglutarate–isocitrate shuttle, nitrogen metabolism and gluconeogenesis from lactate when the carbon skeleton for gluconeogenesis is provided by 2-oxoglutarate exported from the mitochondria by the OGC [1].

Vitamin A and its metabolites play important roles in vision, reproduction, cell proliferation and differentiation, embryogenesis, immune response, and growth. The all-*trans*- and 9-*cis*-isomers of retinoic acid interact with the nuclear retinoid receptors, RAR and RXR, inducing differentiation and apoptosis of many types of cells [2–4]. Some biological effects of vitamin A, however, are not dependent on retinoic acid receptors; 11-*cis*-retinal in vision [5], all-*trans*-retinol in embryologic development [6], and 14-hydroxy-4,14-retroretinol in the growth of B lymphoblastoid cells and in the maintenance of T-cell activation [7] in particular. Moreover, in enucleated 3T3 fibroblasts, atRA inhibits phorbol ester-induced fibronectin release [8] and binds to and inhibits the adenine nucleotide translocator in bovine heart and mouse liver mitochondria [9]. AtRA is incorporated into proteins of cells in culture [10–13] and of rat tissues both *in vivo* [14] and *in vitro* [15–18]. The covalent linkage between RA and proteins is probably a thioester or labile O-ester bond in most cases [10]. Retinoylated proteins that have been identified so far include cAMP-binding proteins, vimentin, the cytokeratins, and some nuclear proteins [10–16]. In our current investigation, we have studied OGC carrier activity both from mitochondria extracted from whole rat testes and TM-3 cells. Previously we have demonstrated that mitochondria from rat testes [17,18] and TM-3 cells [19] were extremely active in incorporating retinoic acid. Moreover, it was highlighted how the retinoylation reaction and testosterone biosynthesis are positively correlated when Leydig cell cultures are incubated with atRA at 100 nM [20].

It is well known that many biosynthetic pathways of testosterone are NAPDH or NADH dependent; therefore OGC was chosen as the experimental target for its involvement in the malate–aspartate shuttle and oxoglutarate–isocitrate shuttle to provide the necessary reducing equivalents between cytosol and mitochondria and vice versa. In this study we demonstrate how the activity of OGC is influenced by retinoic acid. The efforts were focused on the OGC from rat testes as the retinoylation process is more efficient in this tissue.

2. Materials and methods

2.1. Chemicals

[11-12 ^{3}H] all-*trans*-retinoic acid (^{3}HatRA) (50 Ci/mmol), [1-^{14}C] 2-oxoglutarate and ECL were purchased from PerkinElmer (Boston USA). All-*trans*-retinoic acid (atRA) was obtained from Sigma-Aldrich (Milano, Italia); egg yolk phospholipids from Fluka; DMEM/F12, fetal calf serum (FCS), penicillin and streptomycin from Gibco (Invitrogen Life Technologies, Italia). All other chemicals used were of analytical reagent grade.

* Corresponding author. Dipartimento Farmaco-Biologico, Università della Calabria, 87036 Rende (CS), Italy. Tel.: +39 0984 493454; fax: +39 0984 493271.
E-mail address: genchi@unical.it (G. Genchi).

1388-1981/$ – see front matter © 2008 Elsevier B.V. All rights reserved.
doi:10.1016/j.bbalip.2008.09.004

Table 1
Effect of mitochondrial carrier inhibitors on retinoylation reaction

Carrier inhibitors on retinoylation reaction	pmol/mg ptn×90 min	SEM	*n*	% Inhibition
Control	21,47	2,44	23	
Mersalyl 1 mM	1,84	0,09	5	91,43
NEM 5 mM	2,47	0,28	5	88,49
2-Cyano-4-hydroxycinnamate 5 mM	11,90	1,23	3	44,58
1,2,3-Benzenetricarboxylate 5 mM	18,93	1,99	3	11,83

Mitochondria from testes were incubated 90 min in a buffer as described in materials and methods with ^{3}HatRA, 100 nM final concentration, at 37 °C. Then the reaction was stopped with TCA and the radioactivity detected in a liquid scintillation counter. Results are presented as Mean ± SEM of three independent experiments. $^{**}P<0.01$ compared to the control. 1,2,3-Benzenetricarboxylate $P>0.05$.

2.2. Isolation of mitochondria

Rats were killed by decapitation, according to practice procedures approved by the ethical committee, and testes were immediately removed. Mitochondria were isolated by differential centrifugation as described by Cione and Genchi [18] and suspended in a medium containing 250 mM sucrose, 10 mM Tris/HCl, pH 7.4, 1 mM EDTA at a concentration of 15–18 mg protein/ml. Protein concentration was determined by the Lowry procedure [21] with BSA as the reference standard. This mitochondrial suspension was either used immediately or frozen at −80 °C. The purity of the mitochondrial preparation for both whole testes and TM-3 cells was checked by assaying marker enzymes for lysosomes, peroxisomes and plasma membranes.

2.3. Incubation and extraction

AtRA or ^{3}HatRA were dissolved in ethanol and 3 μL of the solution was added to the tissue preparation (0.5 mg protein), and incubated in the presence of 10 mM ATP, 150 μM CoA, 27 mM $MgCl_2$, 50 mM sucrose, and 100 mM Tris, pH 7.4, in a total volume of 0.5 ml at 37 °C for 90 min. The inhibitors were added together with ^{3}HatRA. The mitochondrial suspensions were centrifuged and protein extracted in 3% Triton X-114, 20 mM Na_2SO_4, 1 mM EDTA, 10 mM Pipes, pH 7.0, and after 10 min on ice, the mixture was centrifuged at 13000 rpm for 5 min.

2.4. Reconstitution and determination of OGC activity

20 μg of protein from the Triton X-114 extract of mitochondria were added to 100 μL of sonicated phospholipids (10% w/v), 100 μL of 10% Triton X-114 in Pipes 10 mM, 40 μL of malate 200 mM, 230 μL Pipes 10 mM pH 7.0 in a final volume of 700 μL and were applied to an Amberlite XAD-2 column in agreement with Palmieri and Klingenberg [22]. All the operations were carried out at room temperature.

In order to determine the OGC transport activity, the external malate was removed by passing 650 μL of the proteoliposomal suspension through a Sephadex G-75 column pre-equilibrated with 50 mM NaCl and 10 mM Pipes, pH 7.0. The first 600 μL of the slightly turbid eluate, containing the proteoliposomes, were collected, transferred to 1.5 mL microcentrifuge tubes (150 μL each), and used for transport measurements by the inhibitor stop method [22]. Transport was carried out at 25 °C by adding 0.1 mM [^{14}C] 2-oxoglutarate and stopped after 10 min by the addition of 20 mM pyridoxal 5′-phosphate. In control samples, the pyridoxal 5′-phosphate was added together with the labeled substrate at time zero. To remove the external radioactivity, each sample was passed through a Sephadex G-75 column (0.5×8 cm). The liposomes, eluted with 50 mM NaCl, were collected in 4 mL of scintillation cocktail and counted using a Tricarb 2100 TR scintillation counter with a counting efficiency of about 70–73%. The exchange activity was evaluated as the difference between the experimental and the control values as previously published by Bisaccia et al. [23].

2.5. Labeling with ^{3}HatRA and western blot analysis

Direct labeling with ^{3}HatRA was performed according to a method described previously [24]. Under yellow safe-light, 5 μCi/5 μL of ^{3}HatRA (40–60 Ci/mmol) in ethanol (1 μCi/μL) were added to 1.5 mL glass microcentrifuge tubes for each sample tested. After the ethanol was removed under nitrogen, 20 μg of Triton extract of testes mitochondrial protein were added to each tube, and the final volume was adjusted to 10 μL with incubation buffer, pH 7.4, for a final concentration of 10 μM ^{3}HatRA, while 2-oxo-glutarate was added at a final concentration of 10 mM. The samples were incubated at 37 °C [11] and shaken for 90 min under yellow light, after which 10 μL of SDS-polyacrylamide gel electrophoresis sample buffer was added, the samples were boiled and then loaded to run with standard SDS-polyacrylamide gel electrophoresis techniques. The gel was stained with Coomassie Brilliant Blue, soaked in Amplify (Amersham Biosciences) and then used for fluorography at −80 °C for 30 days.

In order to verify the presence of the OGC protein, western blot analysis was performed using overnight rabbit monoclonal antibody to OGC at 4 °C (1:500 dilution in TBST). On the next day the membrane was incubated for 1 h at room temperature with horseradish peroxidase-conjugate antibodies to rabbit immunoglobulin G (1:2000 dilution) and the immune complex was detected with chemiluminescence reagents (ECL).

2.6. Cell cultures

Leydig (TM-3) cell line, derived from testes of immature BALB/c mice, was generously donated by Dr. S. Andò (University of Calabria), and cultured in DMEM/F12 medium supplemented with 10% FCS, 2 mM glutamine, 1% of a stock solution containing 10,000 IU/mL penicillin and 10,000 μg/mL streptomycin and was grown on 90 mm plastic tissue culture dishes in a humidified atmosphere of 5% CO_2 in air at 37 °C. Cells from exponentially growing stock cultures were removed from the plate with trypsin (0.05% w/v) and EDTA (0.02% w/v). Cell number was estimated with a Burker camera and cell viability by trypan blue dye exclusion. The medium was changed twice weekly. TM-3 cells were subcultured when confluent.

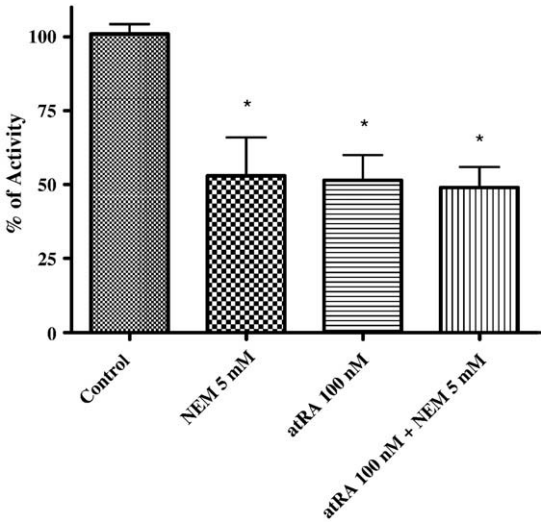

Fig. 1. Effects of N-ethylmaleimide on OGC activity after retinoylation reaction. Mitochondria from testes were incubated for 90 min in buffer with atRA, 100 nM final concentration, at 37 °C. OGC was extracted as described in materials and methods. After extraction and reconstitution into liposomes the exchange activity was assayed by adding ^{14}C 2-oxo-glutarate 0.1 mM. Results are presented as Mean ± SEM of three independent experiments. $^*P<0.05$ compared to the control.

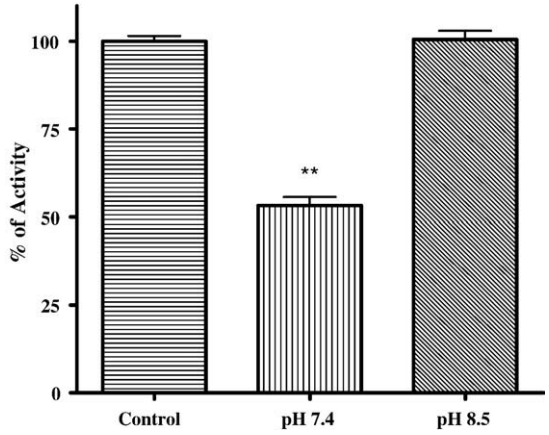

Fig. 2. Effects of pH on OGC activity after retinoylation reaction. Mitochondria from testes were incubated for 90 min at different pH with atRA, 100 nM final concentration, at 37 °C. OGC was extracted as described in materials and methods. After extraction and reconstitution in liposomes the exchange activity was assayed. The optimum pH for OGC activity was found at 7.5 while no effects were highlighted at a pH higher than 7.5. Results are presented as Mean±SEM of five independent experiments. $^{**}P<0.01$ compared to the control.

2.7. TM-3 cells treated with atRA and mitochondrial isolation

TM-3 cells growing exponentially were removed by trypsin/EDTA, harvested by centrifugation and resuspended at 1×10^6 cells/mL in DMEM/F12 medium supplemented with serum. The next day the medium was removed and replaced with serum-free DMEM/F12. The cells were incubated at 37 °C in a humidified atmosphere of 5% CO_2 in air for 24 h in the presence of 10 or 100 nM atRA dissolved in DMSO and diluted into the growth medium such that the final DMSO concentration was no higher than 0.01%. After the above mentioned treatments, TM-3 cells were collected by trypsinization and isolated by centrifugation at 1200 ×g for 5 min at 4 °C. The pellet was solubilized in 180 μL RIPA buffer. After the addition of 20 μL of 0.1% digitonin, the cells were incubated for 15 min at 4 °C and mitochondria were isolated by differential centrifugation at 4 °C.

2.8. Statistical analysis

Statistical analysis was performed by ANOVA followed by Dunnett's multiple comparison test. Values are shown as mean± SEM of (n) independent experiments. Differences were considered significant at values of $P<0.05$.

3. Results

3.1. Carrier inhibitors on retinoylation reaction

As shown in Table 1, both mercurial and maleimide compounds strongly inhibit the retinoylation processes by about 90%. In addition, 2-cyano-4-hydroxycinnamate, an inhibitor of OGC [25], shows 45% inhibition when used at a concentration of 5 mM; conversely at the same concentration 1,2,3-benzentricarboxylate, an inhibitor of citrate carrier, has a very weak effect (12% inhibition).

3.2. Effects of N-ethylmaleimide, atRA and pH on OGC activity

The sulphydryl group reagent, NEM, at 5 mM, markedly reduced the OGC activity by 47%. A similar inhibition of 51% was highlighted for 100 nM atRA, and when the two compounds are co-incubated the activity was reduced to 49%, equal to RA alone as shown in Fig. 1. Fig. 2 shows the pH effect on OGC activity. The optimum pH for atRA inhibition was found at 7.4 while no effects were highlighted at pH 8.5.

3.3. AtRA binds to OGC

To study a direct interaction between atRA and OGC, we labeled testes mitochondrial proteins with ^{3}HatRA in the incubation buffer. As shown in Fig. 3, few mitochondrial proteins bind to ^{3}HatRA and specifically a 31.5-kDa protein was detected. We observed that the labeling of the 31.5-kDa protein was prevented when 2-oxo-glutarate, the specific OGC substrate, was added. This demonstrates that OGC was labeled by ^{3}HatRA. It is presumed that the binding is covalent on the basis of the work of Takahashi and Breitman [10]. In Fig. 4 (A–B) the effects of different concentrations of atRA on isolated mitochondria from the TM-3 cell line are shown. OGC activity decreased to 54% of control values with 10 nM atRA and 38% of control values when

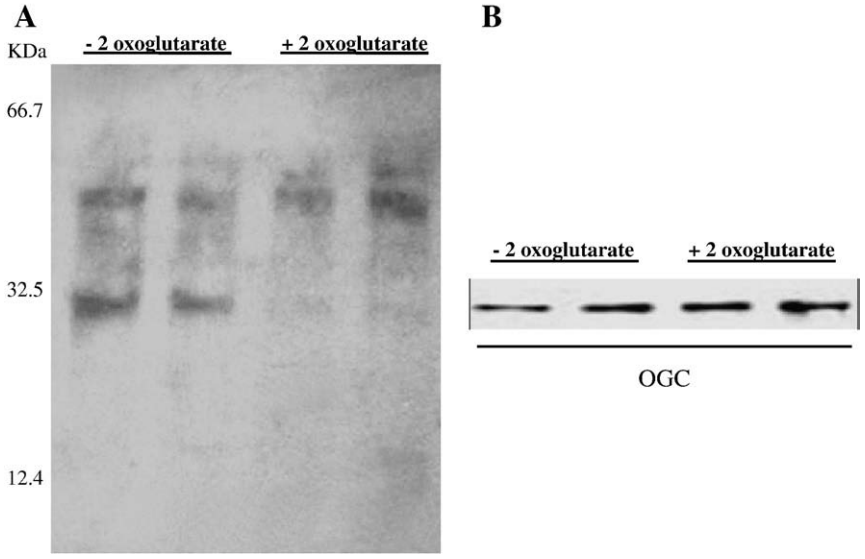

Fig. 3. Labeling of OGC by ^{3}HatRA. (A) Testes mitochondrial protein was labeled with ^{3}HatRA by retinoylation process as described in materials and methods. In fluorography, lanes 1 and 2 correspond to 20 μg of mitochondrial testes protein labeled with ^{3}HatRA. In lanes 3 and 4 10 mM of α-ketoglutarate was added to 20 μg of mitochondrial testes protein together with ^{3}HatRA. (B) OGC presence was verified by immunoblotting.

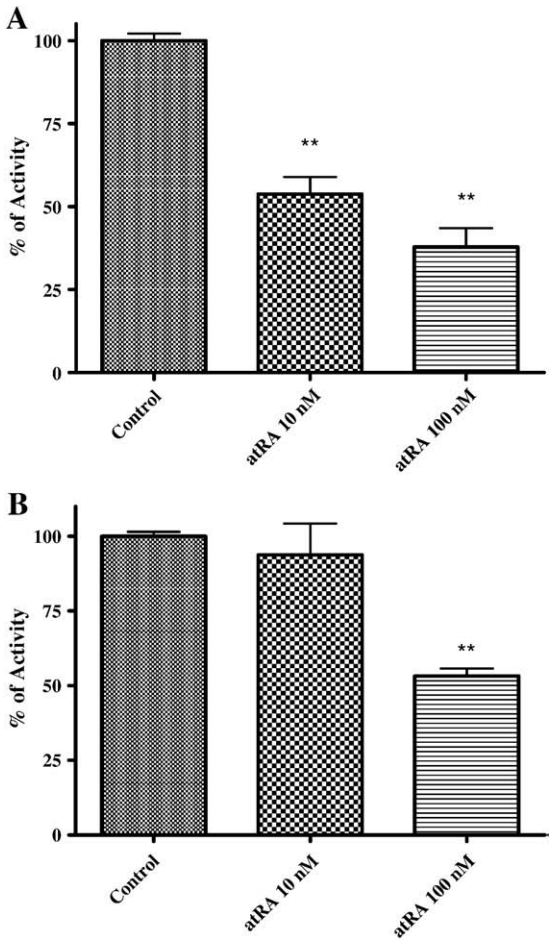

Fig. 4. Effect of atRA on OGC from TM-3 cells. (A) 1×10^6/mL cells were treated with various concentrations of atRA for 24 h; then the mitochondria were isolated, the OGC extracted and the activity assayed as described in materials and methods. (B) Mitochondria from testes were incubated for 90 min as described in materials and methods with different concentrations of atRA at 37 °C. The proteins were then extracted and the OCG exchange activity assayed as described in materials and methods. Results are presented as Mean±SEM of three individual experiments. $^{**}P<0.01$ compared to the control.

atRA was used at a concentration of 100 nM as shown in Fig. 4A. Conversely no effect was highlighted at 10 nM of atRA on OGC extracted from whole tissue, as shown in Fig. 4B. Similar effects were highlighted when 13-*cis*-RA was used at the same concentrations of atRA in TM-3 with the exception that 10 nM 13-*cis*-RA was more active in inhibiting OGC activity (Fig. 5A–B).

4. Discussion

Retinoylation is one of several covalent modifications of proteins. Biochemical similarities exist among retinoylation, palmitoylation and myristoylation: in all of these processes the substrate binds covalently to pre-existing protein via a thioester bond after the formation of a CoA-protein intermediate [26,27]. As the biosynthetic steps that lead to testosterone production are mainly NADH/NADPH dependent, the oxoglutarate carrier (OGC) was chosen as the experimental target for its involvement in the oxoglutarate–isocitrate shuttle that provides for the necessary exchange of reducing equivalents between the mitochondria and the cytosol. In addition, the strong inhibitory effect of 2-cyano-4-hydroxycinnamate (an inhibitor of OGC) but not 1,2,3-benzentricarboxylate (an inhibitor of citrate carrier) on the retinoylation processes (as highlighted in Table 1) was the start point for our further investigation in this paper. Our results showed that transport activity of OGC from rat testes mitochondria was strongly influenced by NEM and atRA (Fig. 1). In humans, cows and rats there is only one gene encoding OCG: according to the amino acid sequence the bovine OGC protein contains three cysteines: Cys184 located in TMS IV and Cys221 and Cys224 in TMS V. Mercurials and maleimides interact only with Cys184 of the purified and reconstituted OGC, as Cys221 and Cys224 are linked by a disulphide bridge [1]. Therefore we propose that atRA, via retinoylation reaction, could bind the OGC on the same residue (Cys184), as the inhibitory effect of atRA is still the same when NEM is present concomitantly as shown in Fig. 1, leading us to hypothesize the existence of a putative amino acid sequence related to the atRA binding site in OGC. For what concerns OCG and its involvement in testosterone biosynthesis, the first enzymatic step is to convert cholesterol in pregnenolone: the reaction occurs in the mitochondrial matrix and requires reducing equivalents mainly as NADPH; conversely the role of the OGC is to carry out reducing equivalents from the mitochondria to the cytoplasm.

Previously we have demonstrated that there is a positive correlation between retinoylation reaction and testosterone biosynthesis [20]: the action of RA to slow down the OGC transport activity is in agreement with the testosterone synthetic process as reducing equivalents are more necessary to convert cholesterol in the matrix rather than in the cytoplasm [28]. At the same time the retinoylation

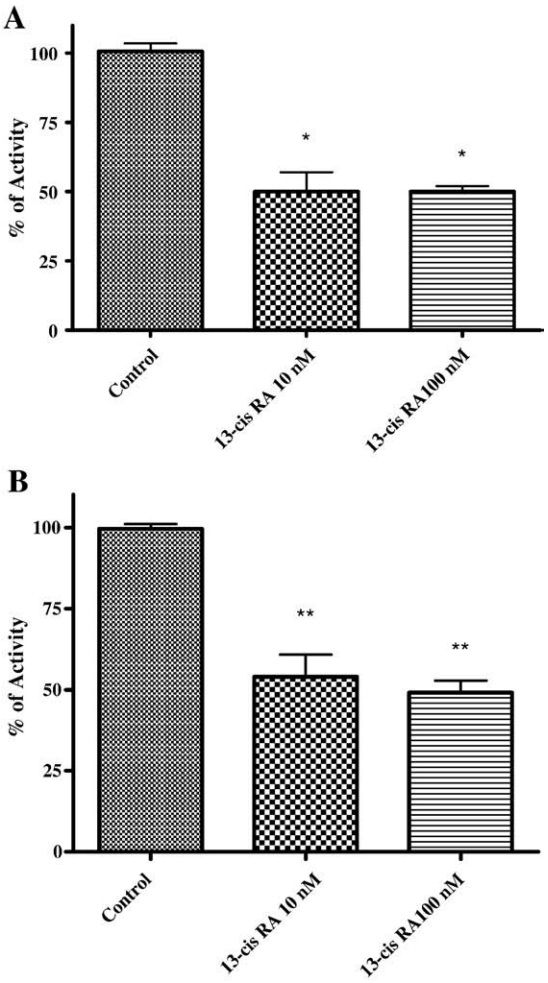

Fig. 5. Effect of 13-*cis*-RA on OGC. (A) 1×10^6/mL TM-3 cells were treated with various concentrations of 13-*cis*-RA for 24 h and then the mitochondria were isolated, proteins extracted and the activity assayed as described in materials and methods. (B) Mitochondria from testes were incubated for 90 min with different concentrations of 13-*cis*-RA at 37 °C. Then the OGC was extracted and the activity tested as described in materials and methods. Results are presented as Mean±SEM of three individual experiments. $^{**}P<0.01$ compared to the control.

reaction is tightly dependent on the pH: in fact the inhibitory effect of atRA on OGC is lost when the pH is higher than 7.5 (Fig. 2). To gain insight into the interaction of atRA and OGC two separate assays could be performed: the first through photolabeled testes mitochondrial protein with ^{3}HatRA, because atRA binds covalently to proteins under UV light exposure [35], and the second via retinoylation reaction with ^{3}HatRA [24]. Performing the latter we observed how the atRA binding to a 31.5 KDa protein was prevented by 2-oxoglutarate, the specific OGC substrate (Fig. 3). Fluorography of the electrophoresed proteins revealed the labeling of very few mitochondrial proteins. Under normal conditions, atRA is present in the testes at nanomolar concentrations [29]. Our results show that, only in mitochondria derived from the Leydig TM-3 cell line, does atRA have effects on OGC at concentration of 10 nM and in a stronger manner inhibit the OGC activity at a concentration of 100 nM (Fig. 4A). Interestingly, the concentrations of atRA required for producing this effect in steroidogenic cells are lower than those required with mitochondria isolated from the whole organ, supporting the above-mentioned view that steroidogenic cells can be more sensitive to atRA than isolated mitochondria (Fig. 4B). In addition 13-*cis*-RA has been shown as a competitive inhibitor of atRA in the retinoylation process [18]. In this case 13-*cis*-RA exerts its effects of reducing OGC transport activity on mitochondria from whole tissue at a lower concentration than atRA (Fig. 5A), most likely thanks to the altered conformation of this isomer that may allow it to better interact with OGC both in mitochondria from cultured cells or whole tissue (Fig. 5B). Our study, along with others [9,30,31], suggests that specific interactions occur among retinoids and non-nuclear receptor proteins, such as PKC, ANT and OGC, which are different from nuclear receptors, take place. Thus, the extra-nuclear action of retinoids seems to be a more general and important phenomena leading to both physiological and also pharmacological relevance.

It is known that retinoids play an essential role in spermatogenesis in rodents. In fact, a vitamin A-deficient diet causes the cessation of spermatogenesis, loss of mature germ cells and a reduction in testosterone level in mice and rat testes [32,33].

There is argument in favour of biological action of atRA through OGC binding and inhibition. AtRA does not exist in the cell in free form but is bound to proteins such as cellular retinoic acid binding protein (CRABP). The existence of a CRABP associated with mitochondria that binds and keeps retinoic acid in the organelle has been described by Ruff and Ong [34]. This mitochondrial CRABP could explain how retinoic acids could concentrate and regulate OGC in the mitochondrial compartment *in vivo*. In conclusion, in the present study we demonstrate that atRA via retinoylation reaction is able to influence OGC and that this effect is another level of control in steroidogenesis.

Acknowledgements

We thank Dr. James Chithalen for the helpful comments and English revision. This research was supported by grants from Ministero dell'Istruzione, dell'Università e della Ricerca (MIUR, Italia) and IRCCS Associazione Oasi Maria SS. We also thank Dr. F. Palmieri (University of Bari) for the generous gift of oxo-glutarate carrier antibody.

References

[1] F. Palmieri, The mitochondrial transporter family (SLC25): physiological and pathological implications, Eur. J. Physiol. 447 (2004) 689–709.
[2] D.J. Mangelsdorf, K. Umesono, R.M. Evans, The retinoid receptors, in: M.B. Sporn, A.B. Roberts, D.S. Goodman (Eds.), The Retinoids: Biology, Chemistry, and Medicine, Raven Press, New York, 1994, pp. 319–349.
[3] P. Chambon, A decade of molecular biology of retinoid receptors, FASEB J. 10 (1996) 940–954.
[4] M.B. Rogers, Life and death decisions influenced by retinoids, Curr. Top. Dev. Biol. 35 (1997) 1–46.
[5] J.C. Saari, Retinoids in photosensitive system, in: M.b. Sporn, A.B. Roberts, D.S. Goodman (Eds.), The Retinoids: Biology, Chemistry, and Medicine, Raven Press, New York, 1994, pp. 351–385.
[6] D.M. Wellik, D.H. Norback, H.F. DeLuca, Retinol is specifically required during mid gestation for neonatal survival, Am. J. Physiol. 272 (1997) E25–E29.
[7] J. Buck, F. Derguini, E. Levi, K. Nakanishi, U. Hammerling, Intracellular signaling by 14-hydroxy-4,14-retroretinol, Science 254 (1991) 1654–1656.
[8] S.D. Bolmer, G. Wolf, Retinoids and phorbol esters alter release of fibronectin from enucleated cells, Proc. Natl. Acad. Sci. U. S. A. 79 (1982) 6541–6545.
[9] B. Notario, M. Zamora, O. Vinas, T. Mampel, All-*trans*-retinoic acid binds to and inhibits adenine nucleotide translocase and induces mitochondrial permeability transition, Mol. Pharmacol. 63 (2003) 224–231.
[10] N. Takahashi, T.R. Breitman, Retinoic acid (retinoylation) of a nuclear protein in the human acute myeloid leukemia cell line HL60, J. Biol. Chem. 264 (1989) 5159–5163.
[11] N. Takahashi, T.R. Breitman, Retinoic acid acylation: retinoylation, Methods Enzymol. 189 (1990) 233–239.
[12] N. Takahashi, T.R. Breitman, Retinoylation of proteins in mammalian cells, in: R. Blomhoff (Ed.), Vitamin A in Health and Disease, Marcel Dekker, New York, 1994, pp. 257–273.
[13] S. Tournier, F. Raynaud, P. Gerbaud, S.M. Lohmann, W.B. Anderson, D. Evain-Brion, Retinoylation of the type II cAMP-binding regulatory subunit of cAMP-dependent protein kinase is increased in psoriatic human fibroblasts, J. Cell Physiol. 167 (1996) 196–203.
[14] A.M. Myhre, N. Takahashi, R. Blomhof, T.R. Breitman, K.R. Norum, Retinoylation of proteins in rat liver, kidney, and lung in vivo, J. Lipid Res. 37 (1996) 1971–1977.
[15] B. Renstrom, H.F. DeLuca, Incorporation of retinoic acid into proteins via retinoyl-CoA, Biochim. Biophys. Acta 998 (1996) 69–74.
[16] A.M. Myhre, E. Hagen, R. Blomhoff, K.R. Norum, Retinoylation of proteins in a macrophage tumor cell line J774, following uptake of chylomicron remnant retinyl ester, J. Nutr. Biochem. 9 (1998) 705–711.
[17] G. Genchi, J.A. Olson, Retinoylation of proteins in cell-free fractions of rat tissues in vitro, Biochim. Biophys. Acta 1530 (2001) 146–154.
[18] E. Cione, G. Genchi, Characterization of rat testes mitochondrial retinoylating system and its partial purification, J. Bioenerg. Biomembr. 36 (2004) 211–217.
[19] E. Cione, P. Tucci, A. Chimento, V. Pezzi, G. Genchi, Retinoylation reaction of proteins in Leydig (TM-3) cells, J. Bioenerg. Biomembr. 37 (2005) 43–48.
[20] P. Tucci, E. Cione, G. Genchi, Retinoic acid-induced testosterone production and retinoylation reaction are concomitant and exhibit a positive correlation in Leydig (TM-3) cells, J. Bioenerg. Biomembr (in press), doi:10.1007/s10863-008-9156.
[21] O.H. Lowry, N.J. Rosebrough, R.J. Randall, Protein measurement with the Folin phenol reagent, J. Biol. Chem. 193 (1951) 265–275.
[22] F. Palmieri, M. Klingenberg, Direct methods for measuring metabolite transport and distribution in mitochondria, Methods Enzymol. 56 (1979) 279–301.
[23] F. Bisaccia, C. Indiveri, F. Palmieri, Purification and reconstitution of two anion carriers from rat liver mitochondria: the dicarboxylate and the 2-oxoglutarate carrier, Biochim. Biophys. Acta 993 (1998) 229–240.
[24] N. Takahashi, T.R. Breitman, Retinoylation of HL-60 Proteins, J. Biol. Chem. 266 (1990) 19158–19162.
[25] R. Bolli, K.A. Nalecz, A. Azzi, Monocarboxylate and α-ketoglutarate carriers from bovine heart mitochondria. Purification by affinity chromatography on immobilized 2-cyano-4-hydroxycinnamate, J. Biol. Chem. 263 (1989) 18024–18030.
[26] A.M. Schultz, L.E. Henderson, S. Oroszlan, Fatty acylation of proteins, Annu. Rev. Cell Biol. 4 (1988) 611–647.
[27] M. Wada, T. Fukui, Y. Kubo, N. Takahashi, Formation of retinoyl-CoA in rat tissues, J. Biochem. 130 (2001) 457–463.
[28] D.M. Stocco, Tracking the role of a star in the sky of the new millennium, Mol. Endocrinol. 15 (2001) 1245–1254.
[29] M.A. Kane, A.E. Folias, C. Wang, J.L. Napoli, Quantitative profiling of endogenous retinoic acid in vivo and in vitro by tandem mass spectrometry, Anal. Chem. 80 (2008) 1702–1708.
[30] E. Rial, M. González-Barroso, C. Fleury, S. Iturrizaga, D. Sanchis, J. Jiménez-Jiménez, D. Ricquier, M. Goubern, F. Bouillaud, Retinoids activate proton transport by the uncoupling proteins UCP1 and UCP2, EMBO J. 18 (1999) 5827–5833.
[31] A. Radominska-Pandya, G. Chen, P.J. Czernik, J.M. Little, V.M. Samokyszyn, C.A. Carter, G. Nowak, Direct interaction of all-trans-retinoic acid with protein kinase C (PKC). Implications for PKC signaling and cancer therapy, J. Biol. Chem. 275 (2000) 22324–22330.
[32] S.B. Wolbach, P.R. Howe, Nutrition classics: tissue changes following deprivation of fat soluble A vitamin, J. Exp. Med. 42 (1925) 753–777.
[33] D.R. Appling, F. Chytil, Evidence of a role for retinoic acid (vitamin A-acid) in the maintenance of testosterone production in male rats, Endocrinology 108 (1981) 2120–2124.
[34] S.J. Ruff, D.E. Ong, Cellular retinoic acid binding protein is associated with mitochondria, FEBS Lett. 487 (2000) 282–286.
[35] P.S. Bernstein, S-Y. Choi, Y-C. Ho, R.R. Rando, Photoaffinity labeling of retinoic acid-binding proteins, Proc. Natl. Acad. Sci. U. S. A. 92 (1995) 654–658.

The American Journal of Pathology, Vol. 175, No. 3, September 2009

DOI: 10.2353/ajpath.2009.081078

Tumorigenesis and Neoplastic Progression

Combined Low Doses of PPARγ and RXR Ligands Trigger an Intrinsic Apoptotic Pathway in Human Breast Cancer Cells

Daniela Bonofiglio,* Erika Cione,* Hongyan Qi,* Attilio Pingitore,* Mariarita Perri,* Stefania Catalano,* Donatella Vizza,* Maria Luisa Panno,† Giuseppe Genchi,* Suzanne A.W. Fuqua,‡ and Sebastiano Andò†§¶

From the Departments of Pharmaco-Biology, and Cellular Biology,† the Centro Sanitario,§ and the Faculty of Pharmacy Nutritional and Health Sciences,¶ University of Calabria, Arcavacata di Rende (Cosenza), Italy; and the Lester and Sue Smith Breast Center,‡ Department of Medicine, Baylor College of Medicine, Houston, Texas*

Ligand activation of peroxisome proliferator-activated receptor (PPAR)γ and retinoid X receptor (RXR) induces antitumor effects in cancer. We evaluated the ability of combined treatment with nanomolar levels of the PPARγ ligand rosiglitazone (BRL) and the RXR ligand 9-*cis*-retinoic acid (9RA) to promote antiproliferative effects in breast cancer cells. BRL and 9RA in combination strongly inhibit of cell viability in MCF-7, MCF-7TR1, SKBR-3, and T-47D breast cancer cells, whereas MCF-10 normal breast epithelial cells are unaffected. In MCF-7 cells, combined treatment with BRL and 9RA up-regulated mRNA and protein levels of both the tumor suppressor p53 and its effector $p21^{WAF1/Cip1}$. Functional experiments indicate that the nuclear factor-κB site in the p53 promoter is required for the transcriptional response to BRL plus 9RA. We observed that the intrinsic apoptotic pathway in MCF-7 cells displays an ordinated sequence of events, including disruption of mitochondrial membrane potential, release of cytochrome *c*, strong caspase 9 activation, and, finally, DNA fragmentation. An expression vector for p53 antisense abrogated the biological effect of both ligands, which implicates involvement of p53 in PPARγ/RXR-dependent activity in all of the human breast malignant cell lines tested. Taken together, our results suggest that multidrug regimens including a combination of PPARγ and RXR ligands may provide a therapeutic advantage in breast cancer treatment. ***(Am J Pathol 2009, 175:1270–1280; DOI: 10.2353/ajpath.2009.081078)***

Breast cancer is the leading cause of death among women in the world. The principal effective endocrine therapy for advanced treatment on this type of cancer is anti-estrogens, but therapeutic choices are limited for estrogen receptor (ER)α-negative tumors, which are often aggressive. The development of cancer cells that are resistant to chemotherapeutic agents is a major clinical obstacle to the successful treatment of breast cancer, providing a strong stimulus for exploring new approaches *in vitro*. Using ligands of nuclear hormone receptors to inhibit tumor growth and progression is a novel strategy for cancer therapy. An example of this is the treatment of acute promyelocytic leukemia using all-*trans* retinoic acid, the specific ligand for retinoic acid receptors.[1–3] A further paradigm for the use of retinoids in cancer therapy is for early lesions of head and neck cancer[4] and squamous cell carcinoma of the cervix.[5]

The retinoic acid receptor, retinoid X receptor (RXR), and peroxisome proliferator receptor (PPAR)γ, ligand-activated transcription factors belonging to the nuclear hormone receptor superfamily, are able to modulate gene networks involved in controlling growth and cellular differentiation.[6] Particularly, heterodimerization of PPARγ with RXR by their own ligands greatly enhances DNA binding to the direct-repeated consensus sequence AGGTCA, which leads to transcriptional activation.[7] Previous data show that PPARγ, poorly expressed in normal breast epithelial cells,[8] is present at higher levels in

Supported by AIRC, MURST, and Ex 60%.

Portions of this work were presented as an Abstract at Società Italiana di Patologia XXIX National Congress in Rende, Italy, on September 10–13, 2008.

Accepted for publication June 5, 2009.

Supplemental material for this article can be found on *http://ajp.amjpathol.org*.

Address reprint requests to Prof. Sebastiano Andò, Faculty of Pharmacy Nutritional and Health Sciences, University of Calabria, 87036 Arcavacata - Rende (Cosenza), Italy. E-mail: sebastiano.ando@unical.it.

breast cancer cells,[9] and its synthetic ligands, such as thiazolidinediones, induce growth arrest and differentiation in breast carcinoma cells *in vitro* and in animal models.[10–11] Recently, studies in human cultured breast cancer cells show the thiazolidinedione rosiglitazone (BRL), promotes antiproliferative effects and activates different molecular pathways leading to distinct apoptotic processes.[12–14]

Apoptosis, genetically controlled and programmed death leading to cellular self-elimination, can be initiated by two major routes: the intrinsic and extrinsic pathways. The intrinsic pathway is triggered in response to a variety of apoptotic stimuli that produce damage within the cell, including anticancer agents, oxidative damage, and UV irradiation, and is mediated through the mitochondria. The extrinsic pathway is activated by extracellular ligands able to induce oligomerization of death receptors, such as Fas, followed by the formation of the death-inducing signaling complex, after which the caspases cascade can be activated.

Previous data show that the combination of PPARγ ligand with either all-*trans* retinoic acid or 9-*cis*-retinoic acid (9RA) can induce apoptosis in some breast cancer cells.[15] Furthermore, Elstner et al demonstrated that the combination of these drugs at micromolar concentrations reduced tumor mass without any toxic effects in mice.[8] However, in humans PPARγ agonists at high doses exert many side effects including weight gain due to increased adiposity, edema, hemodilution, and plasma-volume expansion, which preclude their clinical application in patients with heart failure.[16–18] The undesirable effects of RXR-specific ligands on hypertriglyceridemia and suppression of the thyroid hormone axis have been also reported.[19] Thus, in the present study we have elucidated the molecular mechanism by which combined treatment with BRL and 9RA at nanomolar doses triggers apoptotic events in breast cancer cells, suggesting potential therapeutic uses for these compounds.

Materials and Methods

Reagents

BRL49653 (BRL) was from Alexis (San Diego, CA), the irreversible PPARγ-antagonist GW9662 (GW), and 9RA were purchased from Sigma (Milan, Italy).

Plasmids

The p53 promoter-luciferase plasmids, kindly provided by Dr. Stephen H. Safe (Texas A&M University, College Station, TX), were generated from the human p53 gene promoter as follows: p53-1 (containing the −1800 to + 12 region), p53-6 (containing the −106 to + 12 region), p53-13 (containing the −106 to −40 region), and p53-14 (containing the −106 to −49 region).[20] As an internal transfection control, we cotransfected the plasmid pRL-CMV (Promega Corp., Milan, Italy) that expresses Renilla luciferase enzymatically distinguishable from firefly luciferase by the strong cytomegalovirus enhancer promoter. The pGL3 vector containing three copies of a peroxisome proliferator response element sequence upstream of the minimal thymidine kinase promoter ligated to a luciferase reporter gene (3XPPRE-TK-pGL3) was a gift from Dr. R. Evans (The Salk Institute, San Diego, CA). The p53 antisense plasmid (AS/p53) was kindly provided from Dr. Moshe Oren (Weizmann Institute of Science, Rehovot, Israel).

Cell Cultures

Wild-type human breast cancer MCF-7 cells were grown in Dulbecco's modified Eagle's medium-F12 plus glutamax containing 5% newborn calf serum (Invitrogen, Milan, Italy) and 1 mg/ml penicillin-streptomycin. MCF-7 tamoxifen resistant (MCF-7TR1) breast cancer cells were generated in Dr. Fuqua's laboratory similar to that described by Herman[21] maintaining cells in modified Eagle's medium with 10% fetal bovine serum (Invitrogen), 6 ng/ml insulin, penicillin (100 units/ml), streptomycin (100 μg/ml), and adding 4-hydroxytamoxifen in tenfold increasing concentrations every weeks (from 10^{-9} to 10^{-6} final). Cells were thereafter routinely maintained with 1 μmol/L 4-hydroxytamoxifen. SKBR-3 breast cancer cells were grown in Dulbecco's modified Eagle's medium without red phenol, plus glutamax containing 10% fetal bovine serum and 1 mg/ml penicillin-streptomycin. T-47D breast cancer cells were grown in RPMI 1640 medium with glutamax containing 10% fetal bovine serum, 1 mmol/L sodium pyruvate, 10 mmol/L HEPES, 2.5g/L glucose, 0.2 U/ml insulin, and 1 mg/ml penicillin-streptomycin. MCF-10 normal breast epithelial cells were grown in Dulbecco's modified Eagle's medium-F12 plus glutamax containing 5% horse serum (Sigma), 1 mg/ml penicillin-streptomycin, 0.5 μg/ml hydrocortisone, and 10 μg/ml insulin.

Cell Viability Assay

Cell viability was determined with the 3-(4,5-dimethylthiazol-2-yl)-2,5-diphenyltetrazolium (MTT) assay.[22] Cells (2×10^5 cells/ml) were grown in 6 well plates and exposed to 100 nmol/L BRL, 50 nmol/L 9RA alone or in combination in serum free medium (SFM) and in 5% charcoal treated (CT)-fetal bovine serum; 100 μl of MTT (5 mg/ml) were added to each well, and the plates were incubated for 4 hours at 37°C. Then, 1 ml 0.04 N HCl in isopropanol was added to solubilize the cells. The absorbance was measured with the Ultrospec 2100 Pro-spectrophotometer (Amersham-Biosciences, Milan, Italy) at a test wavelength of 570 nm.

Immunoblotting

Cells were grown in 10-cm dishes to 70% to 80% confluence and exposed to treatments in SFM as indicated. Cells were then harvested in cold PBS and resuspended in lysis buffer containing 20 mmol/L HEPES (pH 8), 0.1 mmol/L EGTA, 5 mmol/L $MgCl_2$, 0.5 M/L NaCl, 20% glycerol, 1% Triton, and inhibitors (0.1 mmol/L sodium orthovanadate, 1% phenylmethylsulfonylfluoride, and 20

mg/ml aprotinin). Protein concentration was determined by Bio-Rad Protein Assay (Bio-Rad Laboratories, Hercules, CA). A 40 μg portion of protein lysates was used for Western blotting, resolved on a 10% SDS-polyacrylamide gel, transferred to a nitrocellulose membrane, and probed with an antibody directed against the p53, $p21^{WAF1/Cip1}$ (Santa Cruz Biotechnology, CA). As internal control, all membranes were subsequently stripped (0.2 M/L glycine, pH 2.6, for 30 minutes at room temperature) of the first antibody and reprobed with anti-glyceraldehyde-3-phosphate dehydrogenase antibody (Santa Cruz Biotechnology). The antigen–antibody complex was detected by incubation of the membranes for 1 hour at room temperature with peroxidase-coupled goat anti-mouse or anti-rabbit IgG and revealed using the enhanced chemiluminescence system (Amersham Pharmacia, Buckinghamshire UK). Blots were then exposed to film (Kodak film, Sigma). The intensity of bands representing relevant proteins was measured by Scion Image laser densitometry scanning program.

Reverse Transcription-PCR Assay

MCF-7 cells were grown in 10 cm dishes to 70% to 80% confluence and exposed to treatments in SFM as indicated. Total cellular RNA was extracted using TRIZOL reagent (Invitrogen) as suggested by the manufacturer. The purity and integrity were checked spectroscopically and by gel electrophoresis before carrying out the analytical procedures. Two micrograms of total RNA were reverse transcribed in a final volume of 20 μl using a RETROscript kit as suggested by the manufacturer (Promega). The cDNAs obtained were amplified by PCR using the following primers: 5′-GTGGAAGGAAATTTGCGTGT-3′ (p53 forward) and 5′-CCAGTGTGATGATGGTGAGG-3′ (p53 reverse), 5′-GCTTCATGCCAGCTACTTCC-3′ (p21 forward) and 5′-CTGTGCTCACTTCAGGGTCA-3′ (p21 reverse), 5′-CTCAACATCTCCCCCTTCTC-3′ (36B4 forward) and 5′-CAAATCCCATATCCTCGTCC-3′ (36B4 reverse) to yield, respectively, products of 190 bp with 18 cycles, 270 bp with 18 cycles, and 408 bp with 12 cycles. To check for the presence of DNA contamination, reverse transcription (RT)-PCR was performed on 2 μg of total RNA without Monoley murine leukemia virus reverse transcriptase (the negative control). The results obtained as optical density arbitrary values were transformed to percentage of the control taking the samples from untreated cells as 100%.

Transfection Assay

MCF-7 cells were transferred into 24-well plates with 500 μl of regular growth medium/well the day before transfection. The medium was replaced with SFM on the day of transfection, which was performed using Fugene 6 reagent as recommended by the manufacturer (Roche Diagnostics, Mannheim, Germany) with a mixture containing 0.5 μg of promoter-luc or reporter-luc plasmid and 5 ng of pRL-CMV. After transfection for 24 hours, treatments were added in SFM as indicated, and cells were incubated for an additional 24 hours. Firefly and Renilla luciferase activities were measured using the Dual Luciferase Kit (Promega). The firefly luciferase values of each sample were normalized by Renilla luciferase activity, and data were reported as relative light units.

MCF-7 cells plated into 10 cm dishes were transfected with 5 μg of AS/p53 using Fugene 6 reagent as recommended by the manufacturer (Roche Diagnostics). The activity of AS/p53 was verified using Western blot to detect changes in p53 protein levels. Empty vector was used to ensure that DNA concentrations were constant in each transfection.

Electrophoretic Mobility Shift Assay

Nuclear extracts from MCF-7 cells were prepared as previously described.[23] Briefly, MCF-7 cells plated into 10-cm dishes were grown to 70% to 80% confluence, shifted to SFM for 24 hours, and then treated with 100 nmol/L BRL, 50 nmol/L 9RA alone and in combination for 6 hours. Thereafter, cells were scraped into 1.5 ml of cold PBS, pelleted for 10 seconds, and resuspended in 400 μl cold buffer A (10 mmol/L HEPES-KOH [pH 7.9] at 4°C, 1.5 mmol/L $MgCl_2$, 10 mmol/L KCl, 0.5 mmol/L dithiothreitol, 0.2 mmol/L phenylmethylsulfonyl fluoride, and 1 mmol/L leupeptin) by flicking the tube. Cells were allowed to swell on ice for 10 minutes and were then vortexed for 10 seconds. Samples were then centrifuged for 10 seconds and the supernatant fraction was discarded. The pellet was resuspended in 50 μl of cold Buffer B (20 mmol/L HEPES-KOH [pH 7.9], 25% glycerol, 1.5 mmol/L $MgCl_2$, 420 mmol/L NaCl, 0.2 mmol/L EDTA, 0.5 mmol/L dithiothreitol, 0.2 mmol/L phenylmethylsulfonyl fluoride, and 1 mmol/L leupeptin) and incubated in ice for 20 minutes for high-salt extraction. Cellular debris was removed by centrifugation for 2 minutes at 4°C, and the supernatant fraction (containing DNA-binding proteins) was stored at −70°C. The probe was generated by annealing single-stranded oligonucleotides and labeled with [^{32}P]ATP (Amersham Pharmacia) and T4 polynucleotide kinase (Promega) and then purified using Sephadex G50 spin columns (Amersham Pharmacia). The DNA sequence of the nuclear factor (NF)κB located within p53 promoter as probe is 5′-AGTTGAGGGGACTTTCCCAGGC-3′ (Sigma Genosys, Cambridge, UK). The protein-binding reactions were performed in 20 μl of buffer [20 mmol/L HEPES (pH 8), 1 mmol/L EDTA, 50 mmol/L KCl, 10 mmol/L dithiothreitol, 10% glycerol, 1 mg/ml bovine serum albumin, 50 μg/ml polydeoxyinosinic deoxycytidylic acid] with 50,000 cpm of labeled probe, 20 μg of MCF7 nuclear protein, and 5 μg of polydeoxyinosinic deoxycytidylic acid. The mixtures were incubated at room temperature for 20 minutes in the presence or absence of unlabeled competitor oligonucleotides. For the experiments involving anti-PPARγ and anti-RXRα antibodies (Santa Cruz Biotechnology), the reaction mixture was incubated with these antibodies at 4°C for 30 minutes before addition of labeled probe. The entire reaction mixture was electrophoresed through a 6% polyacrylamide gel in 0.25× Tris borate-EDTA for 3 hours at 150 V. Gel was dried and subjected to autoradiography at −70°C.

Chromatin Immunoprecipitation Assay

MCF-7 cells were grown in 10 cm dishes to 50% to 60% confluence, shifted to SFM for 24 hours, and then treated for 1 hour as indicated. Thereafter, cells were washed twice with PBS and cross-linked with 1% formaldehyde at 37°C for 10 minutes. Next, cells were washed twice with PBS at 4°C, collected and resuspended in 200 μl of lysis buffer (1% SDS, 10 mmol/L EDTA, 50 mmol/L Tris-HCl, pH 8.1), and left on ice for 10 minutes. Then, cells were sonicated four times for 10 seconds at 30% of maximal power (Vibra Cell 500 W; Sonics and Materials, Inc., Newtown, CT) and collected by centrifugation at 4°C for 10 minutes at 14,000 rpm. The supernatants were diluted in 1.3 ml of immunoprecipitation buffer (0.01% SDS, 1.1% Triton X-100, 1.2 mmol/L EDTA, 16.7 mmol/L Tris-HCl [pH 8.1], 16.7 mmol/L NaCl) followed by immunoclearing with 60 μl of sonicated salmon sperm DNA/protein A agarose (DBA Srl, Milan, Italy) for 1 hour at 4°C. The precleared chromatin was immunoprecipitated with anti-PPARγ, anti-RXRα, or anti-RNA Pol II antibodies (Santa Cruz Biotechnology). At this point, 60 μl salmon sperm DNA/protein A agarose was added, and precipitation was further continued for 2 hours at 4°C. After pelleting, precipitates were washed sequentially for 5 minutes with the following buffers: Wash A [0.1% SDS, 1% Triton X-100, 2 mmol/L EDTA, 20 mmol/L Tris-HCl (pH 8.1), 150 mmol/L NaCl]; Wash B [0.1% SDS, 1% Triton X-100, 2 mmol/L EDTA, 20 mmol/L Tris-HCl (pH 8.1), 500 mmol/L NaCl]; and Wash C [0.25 M/L LiCl, 1% NP-40, 1% sodium deoxycholate, 1 mmol/L EDTA, 10 mmol/L Tris-HCl (pH 8.1)], and then twice with 10 mmol/L Tris, 1 mmol/L EDTA. The immunocomplexes were eluted with elution buffer (1% SDS, 0.1 M/L NaHCO3). The eluates were reverse cross-linked by heating at 65°C and digested with proteinase K (0.5 mg/ml) at 45°C for 1 hour. DNA was obtained by phenol-chloroform-isoamyl alcohol extraction. Two microliters of 10 mg/ml yeast tRNA (Sigma) were added to each sample, and DNA was precipitated with 95% ethanol for 24 hours at −20°C and then washed with 70% ethanol and resuspended in 20 μl of 10 mmol/L Tris, 1 mmol/L EDTA buffer. A 5 μl volume of each sample was used for PCR with primers flanking a sequence present in the p53 promoter: 5′-CTGAGAGCAAACGCAAAAG-3′ (forward) and 5′-CAGCCCGAACGCAAAGTGTC- 3′ (reverse) containing the κB site from −254 to −42 region. The PCR conditions for the p53 promoter fragments were 45 seconds at 94°C, 40 seconds at 57°C, and 90 seconds at 72°C. The amplification products obtained in 30 cycles were analyzed in a 2% agarose gel and visualized by ethidium bromide staining. The negative control was provided by PCR amplification without a DNA sample. The specificity of reactions was ensured using normal mouse and rabbit IgG (Santa Cruz Biotechnology).

JC-1 Mitochondrial Membrane Potential Detection Assay

The loss of mitochondrial membrane potential was monitored with the dye 5,5′,6,6′tetra-chloro-1,1′,3,3′-tetraethylbenzimidazolyl-carbocyanine iodide (JC-1) (Biotium, Hayward). In healthy cells, the dye stains the mitochondria bright red. The negative charge established by the intact mitochondrial membrane potential allows the lipophilic dye, bearing a delocalized positive charge, to enter the mitochondrial matrix where it aggregates and gives red fluorescence. In apoptotic cells, the mitochondrial membrane potential collapses, and the JC-1 cannot accumulate within the mitochondria, it remains in the cytoplasm in a green fluorescent monomeric form.[24] MCF-7 cells were grown in 10 cm dishes and treated with 100 nmol/L BRL and/or 50 nmol/L 9RA for 48 hours, then cells were washed in ice-cold PBS, and incubated with 10 mmol/L JC-1 at 37°C in a 5% CO_2 incubator for 20 minutes in darkness. Subsequently, cells were washed twice with PBS and analyzed by fluorescence microscopy. The red form has absorption/emission maxima of 585/590 nm. The green monomeric form has absorption/emission maxima of 510/527 nm. Both healthy and apoptotic cells can be visualized by fluorescence microscopy using a wide band-pass filter suitable for detection of fluorescein and rhodamine emission spectra.

Cytochrome C Detection

Cytochrome *C* was detected by western blotting in mitochondrial and cytoplasmatic fractions. Cells were harvested by centrifugation at 2500 rpm for 10 minutes at 4°C. The pellets were suspended in 36 μl RIPA buffer plus 10 μg/ml aprotinin, 50 mmol/L PMSF and 50 mmol/L sodium orthovanadate and then 4 μl of 0.1% digitonine were added. Cells were incubated for 15 minutes at 4°C and centrifuged at 12,000 rpm for 30 minutes at 4°C. The resulting mitochondrial pellet was resuspended in 3% Triton X-100, 20 mmol/L Na_2SO_4, 10 mmol/L PIPES, and 1 mmol/L EDTA (pH 7.2) and centrifuged at 12,000 rpm for 10 minutes at 4°C. Proteins of the mitochondrial and cytosolic fractions were determined by Bio-Rad Protein Assay (Bio-Rad Laboratories). Equal amounts of protein (40 μg) were resolved by 15% SDS-polyacrylamide gel electrophoresis, electrotransferred to nitrocellulose membranes, and probed with an antibody directed against the cytochrome *C* (Santa Cruz Biotechnology). Then, membranes were subjected to the same procedures described for immunoblotting.

Flow Cytometry Assay

MCF-7 cells (1×10^6 cells/well) were grown in 6 well plates and shifted to SFM for 24 hours before adding treatments for 48 hours. Thereafter, cells were trypsinized, centrifuged at 3000 rpm for 3 minutes, washed with PBS. Addition of 0.5 μl of fluorescein isothiocyanate-conjugated antibodies, anti-caspase 9 and anti-caspase 8 (Calbiochem, Milan, Italy), in all samples was performed and then incubated for 45 minutes in at 37°C. Cells were centrifuged at 3000 rpm for 5 minutes, the pellets were washed with 300 μl of wash buffer and centrifuged. The last passage was repeated twice, the supernatant removed, and cells dissolved in 300 μl of wash buffer.

Finally, cells were analyzed with the FACScan (Becton Dickinson and Co., Franklin Lakes, NJ).

DNA Fragmentation

DNA fragmentation was determined by gel electrophoresis. MCF-7 cells were grown in 10 cm dishes to 70% confluence and exposed to treatments. After 56 hours cells were collected and washed with PBS and pelleted at 1800 rpm for 5 minutes. The samples were resuspended in 0.5 ml of extraction buffer (50 mmol/L Tris-HCl, pH 8; 10 mmol/L EDTA, 0.5% SDS) for 20 minutes in rotation at 4°C. DNA was extracted three times with phenol-chloroform and one time with chloroform. The aqueous phase was used to precipitate nucleic acids with 0.1 volumes of 3M sodium acetate and 2.5 volumes cold ethanol overnight at −20°C. The DNA pellet was resuspended in 15 μl of H_2O treated with RNase A for 30 minutes at 37°C. The absorbance of the DNA solution at 260 and 280 nm was determined by spectrophotometry. The extracted DNA (40 μg/lane) was subjected to electrophoresis on 1.5% agarose gels. The gels were stained with ethidium bromide and then photographed.

Statistical Analysis

Statistical analysis was performed using analysis of variance followed by Newman-Keuls testing to determine differences in means. $P < 0.05$ was considered as statistically significant.

Results

Nanomolar Concentrations of the Combined BRL and 9RA Treatment Affect Cell Viability in Breast Cancer Cells

Previous studies demonstrated that micromolar doses of PPARγ ligand BRL and RXR ligand 9RA exert antiproliferative effects on breast cancer cells.[13,15,25–26] First, we tested the effects of increasing concentrations of both ligands on breast cancer cell proliferation at different times in the presence or absence of serum media (see Supplemental Figure 1 at *http://ajp.amjpathol.org*). Thus, to investigate whether low doses of combined agents are able to inhibit cell growth, we assessed the capability of 100 nmol/L BRL and 50 nmol/L 9RA to affect normal and malignant breast cell lines. We observed that treatment with BRL alone does not elicit any significant effect on cell viability in all breast cell lines tested, while 9RA alone reduces cell vitality only in T47-D cells (Figure 1A). In the presence of both ligands, cell viability is strongly reduced in all breast cancer cells: MCF-7, its variant MCF-7TR1, SKBR-3, and T-47D; while MCF-10 normal breast epithelial cells are completely unaffected (Figure 1A). In MCF-7 cells the effectiveness of both ligands in reducing tumor cell viability still persists in SFM, as well as in 5% CT-FBS (Figure 1B).

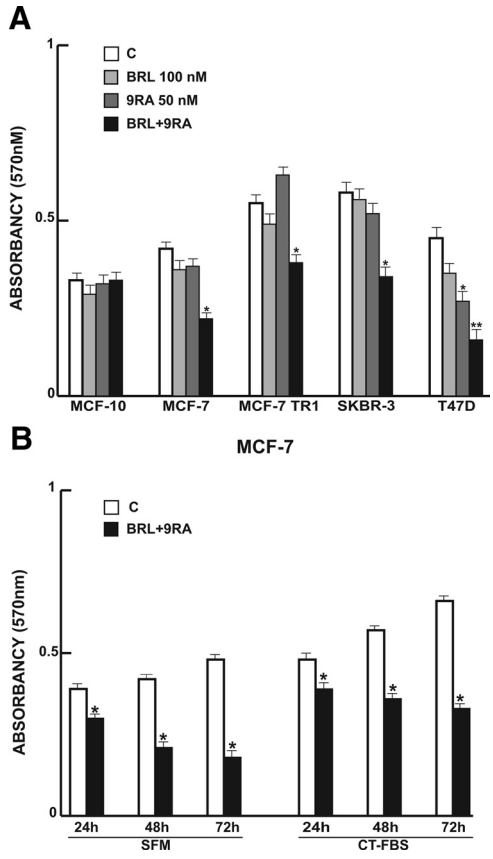

Figure 1. Cell vitality in breast cell lines. **A:** Breast cells were treated for 48 hours in SFM in the presence of 100 nmol/L BRL or/and 50 nmol/L. 9RA Cell vitality was measured by MTT assay. Data are presented as mean ± SD of three independent experiments done in triplicate. **B:** MCF-7 cells were treated for 24, 48, and 72 hours with 100 nmol/L BRL and 50 nmol/L 9RA in the presence of SFM and 5% CT-FBS. *$P < 0.05$ and **$P < 0.01$ treated versus untreated cells.

BRL and 9RA Up-Regulate p53 and p21$^{WAF1/Cip1}$ Expression in MCF-7 Cells

Our recent work demonstrated that micromolar doses of BRL activate PPARγ, which in turn triggers apoptotic events through an up-regulation of p53 expression.[12] On the basis of these results, we evaluated the ability of nanomolar doses of BRL and 9RA alone or in combination to modulate p53 expression along with its natural target gene p21$^{WAF1/Cip1}$ in MCF-7 cells. A significant increase in p53 and p21$^{WAF1/Cip1}$ content was observed by Western blot only on combined treatment after 24 and 36 hours (Figure 2A). Furthermore, we showed an up-regulation of p53 and p21$^{WAF1/Cip1}$ mRNA levels induced by BRL plus 9RA after 12 and 24 hours (Figure 2B).

Low Doses of PPARγ and RXR Ligands Transactivate p53 Gene Promoter

To investigate whether low doses of BRL and 9RA are able to transactivate the p53 promoter gene, we transiently transfected MCF-7 cells with a luciferase reporter construct (named p53-1) containing the upstream region of the p53 gene spanning from −1800 to + 12 (Figure

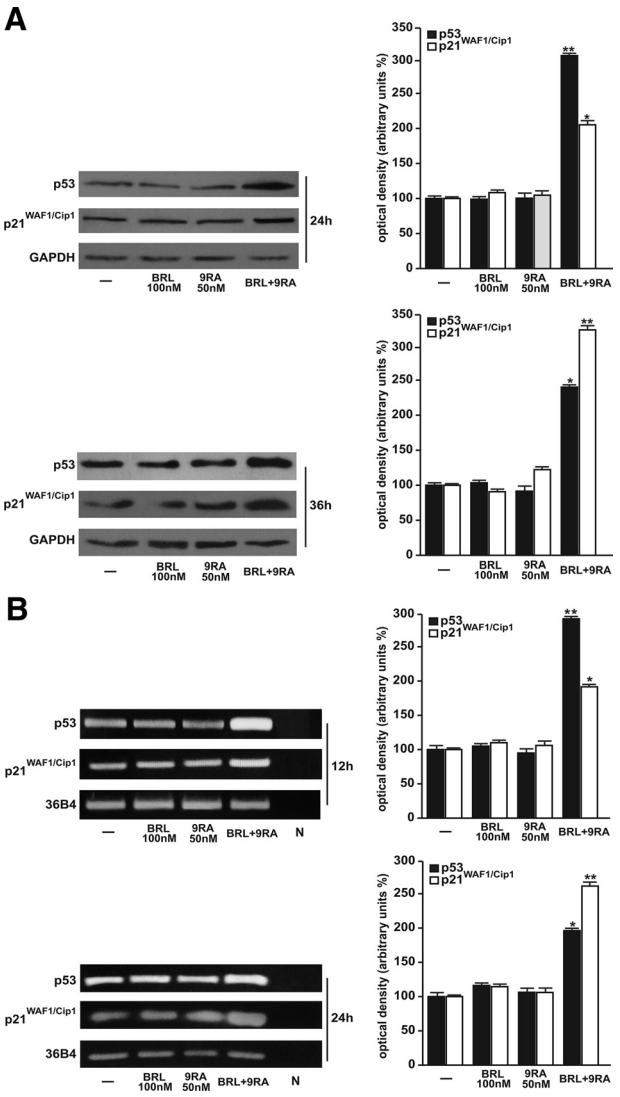

Figure 2. Upregulation of p53 and p21$^{WAF1/Cip1}$ expression induced by BRL plus 9RA in MCF-7 cells. **A:** Immunoblots of p53 and p21$^{WAF1/Cip1}$ from extracts of MCF-7 cell treated with 100 nmol/L BRL and 50 nmol/L 9RA alone or in combination for 24 and 36 hours. GAPDH was used as loading control. The side panels show the quantitative representation of data (mean ± SD) of three independent experiments after densitometry. **B:** p53 and p21$^{WAF1/Cip1}$ mRNA expression in MCF-7 cells treated as in A for 12 and 24 hours. The side panels show the quantitative representation of data (mean ± SD) of three independent experiments after densitometry and correction for 36B4 expression. $^{*}P < 0.05$ and $^{**}P < 0.01$ combined-treated versus untreated cells. N: RNA sample without the addition of reverse transcriptase (negative control).

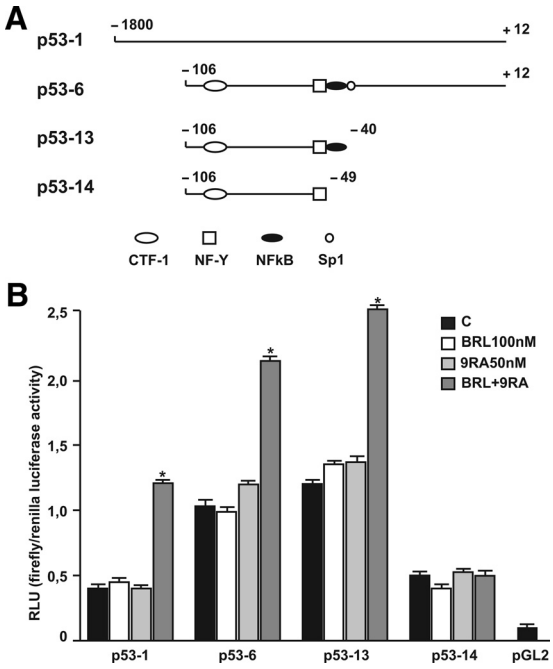

Figure 3. BRL and 9RA transactivate p53 promoter gene in MCF-7 cells. **A:** Schematic map of the p53 promoter fragments used in this study. **B:** MCF-7 cells were transiently transfected with p53 gene promoter-luc reporter constructs (p53-1, p53-6, p53-13, p53-14) and treated for 24 hours with 100 nmol/L BRL and 50 nmol/L 9RA alone or in combination. The luciferase activities were normalized to the Renilla luciferase as internal transfection control and data were reported as RLU values. Columns are mean ± SD of three independent experiments performed in triplicate. $^{*}P < 0.05$ combined-treated versus untreated cells. pGL2: basal activity measured in cells transfected with pGL2 basal vector; RLU, relative light units; CTF-1, CCAAT-binding transcription factor-1; NF-Y, nuclear factor-Y; NFκB, nuclear factor κB.

3A). Treatment for 24 hours with 100 nmol/L BRL or 50 nmol/L 9RA did not induce luciferase expression, whereas the presence of both ligands increased in the transactivation of p53-1 promoter (Figure 3B). To identify the region within the p53 promoter responsible for its transactivation, we used constructs with deletions to different binding sites such as CTF-1, nuclear factor-Y, NFκB, and GC sites (Figure 3A). In transfection experiments performed using the mutants p53-6 and p53-13 encoding the regions from −106 to + 12 and from −106 to −40, respectively, the responsiveness to BRL plus 9RA was still observed (Figure 3B). In contrast, a construct with a deletion in the NFκB domain (p53-14) encoding the sequence from −106 to −49, the transactivation of p53 by both ligands was absent (Figure 3B), suggesting that NFκB site is required for p53 transcriptional activity.

Heterodimer PPARγ/RXRα binds to NFκB Sequence in Electrophoretic Mobility Shift Assay and in Chromatin Immunoprecipitation Assay

To gain further insight into the involvement of NFκB site in the p53 transcriptional response to BRL plus 9RA, we performed electrophoretic mobility shift assay experiments using synthetic oligodeoxyribonucleotides corresponding to the NFκB sequence within p53 promoter. We observed the formation of a specific DNA binding complex in nuclear extracts from MCF-7 cells (Figure 4A, lane 1), where specificity is supported by the abrogation of the complex by 100-fold molar excess of unlabeled probe (Figure 4A, lane 2). BRL treatment induced a slight increase in the specific band (Figure 4A, lane 3), while no changes were observed on 9RA exposure (Figure 4A, lane 4). The combined treatment increased the DNA binding complex (Figure 4A, lane 5), which was immunodepleted and supershifted using anti-PPARγ (Figure 4A, lane 6) or anti-RXRα (Figure 4A, lane 7) antibodies. These data indicate that heterodimer PPARγ/RXRα binds to NFκB site located in the promoter of p53 *in vitro*.

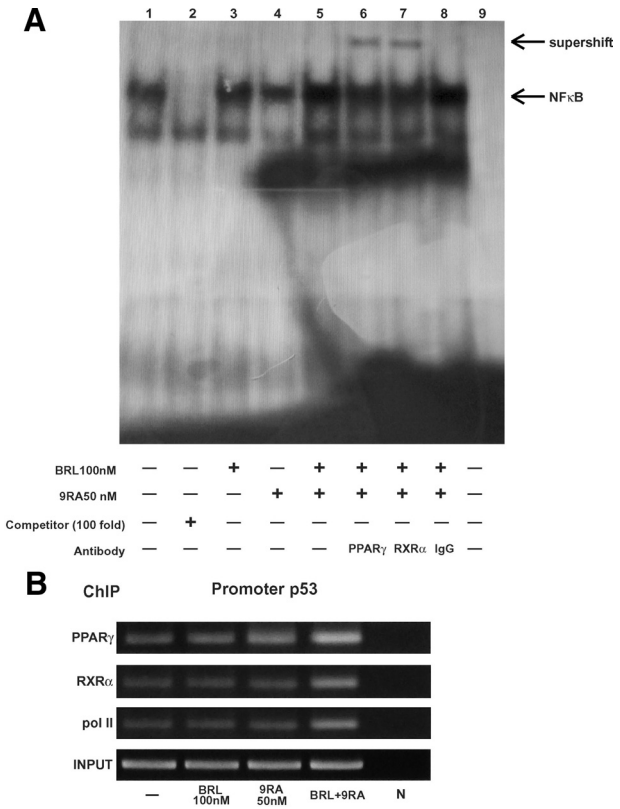

Figure 4. PPARγ/RXRα binds to NFκB sequence in electrophoretic mobility shift assay and in chromatin immunoprecipitation assay. **A:** Nuclear extracts from MCF-7 cells (lane 1) were incubated with a double-stranded NFκB consensus sequence probe labeled with [^{32}P] and subjected to electrophoresis in a 6% polyacrylamide gel. Competition experiments were done, adding as competitor a 100-fold molar excess of unlabeled probe (lane 2). Nuclear extracts from MCF-7 were treated with 100 nmol/L BRL (lane 3), 50 nmol/L 9RA (lane 4), and in combination (lane5). Anti-PPARγ (lane 6), anti-RXRα (lane 7), and IgG (lane 8) antibodies were incubated. Lane 9 contains probe alone. **B:** MCF-7 cells were treated for 1 hour with 100 nmol/L BRL and/or 50 nmol/L 9RA as indicated, and then cross-linked with formaldehyde and lysed. The soluble chromatin was immunoprecipitated with anti-PPARγ, anti-RXRα, and anti-RNA Pol II antibodies. The immunocomplexes were reverse cross-linked, and DNA was recovered by phenol/chloroform extraction and ethanol precipitation. The p53 promoter sequence containing NFκB was detected by PCR with specific primers. To control input DNA, p53 promoter was amplified from 30 μl of initial preparations of soluble chromatin (before immunoprecipitation). N: negative control provided by PCR amplification without DNA sample.

The interaction of both nuclear receptors with the p53 promoter was further elucidated by chromatin immunoprecipitation assays. Using anti-PPARγ and anti-RXRα antibodies, protein-chromatin complexes were immunoprecipitated from MCF-7 cells treated with 100 nmol/L BRL and 50 nmol/L 9RA. PCR was used to determine the recruitment of PPARγ and RXRα to the p53 region containing the NFκB site. The results indicated that either PPARγ or RXRα was constitutively bound to the p53 promoter in untreated cells and this recruitment was increased on BRL plus 9RA exposure (Figure 4B). Similarly, an augmented RNA-Pol II recruitment was obtained by immunoprecipitating cells with an anti-RNA-Pol II antibody, indicating that a positive regulation of p53 transcription activity was induced by combined treatment (Figure 4B).

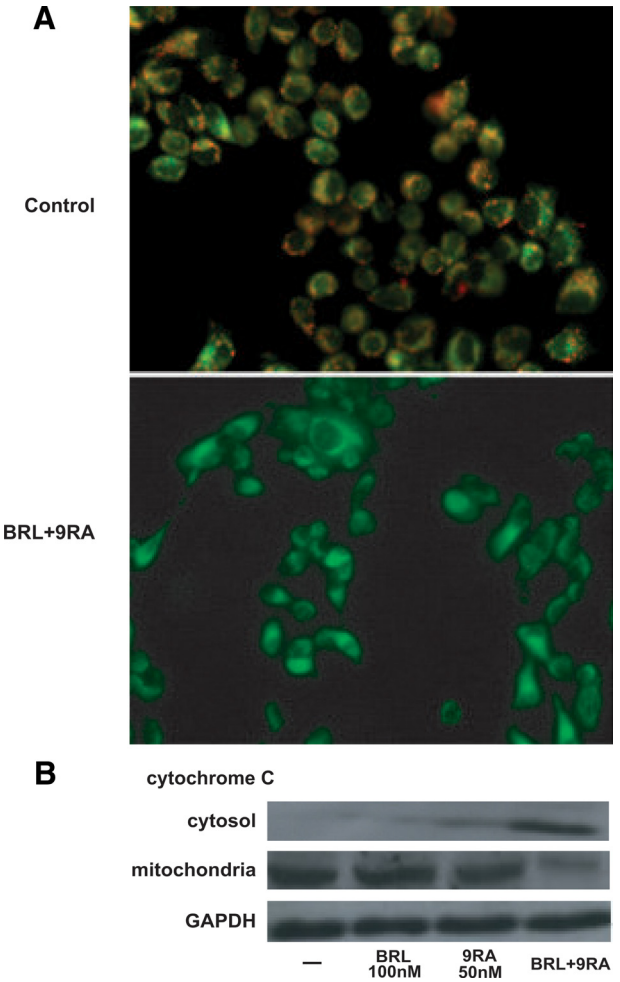

Figure 5. Mitochondrial membrane potential disruption and release of cytochrome *C* induced by BRL and 9RA in MCF-7 cells. **A:** MCF-7 cells were treated with 100 nmol/L BRL plus 50 nmol/L 9RA for 48 hours and then used fluorescent microscopy to analyze the results of JC-1 (5,5′,6,6′-tetrachloro-1,1′,3,3′- tetraethylbenzimidazolylcarbocyanine iodide) kit. In control non-apoptotic cells, the dye stains the mitochondria red. In treated apoptotic cells, JC-1 remains in the cytoplasm in a green fluorescent form. **B:** MCF-7 cells were treated for 48 hours with 100 nmol/L BRL and/or 50 nmol/L 9RA. GAPDH was used as loading control.

BRL and 9RA Induce Mitochondrial Membrane Potential Disruption and Release of Cytochrome C from Mitochondria into the Cytosol in MCF-7 Cells

The role of p53 signaling in the intrinsic apoptotic cascades involves a mitochondria-dependent process, which results in cytochrome *C* release and activation of caspase-9. Because disruption of mitochondrial integrity is one of the early events leading to apoptosis, we assessed whether BRL plus 9RA could affect the function of mitochondria by analyzing membrane potential with a mitochondria fluorescent dye JC-1.[24,27] In non-apoptotic cells (control) the intact mitochondrial membrane potential allows the accumulation of lipophilic dye in aggregated form in mitochondria, which display red fluorescence (Figure 5A). MCF-7 cells treated with 100 nmol/L BRL or 50 nmol/L 9RA exhibit red fluorescence indicating

Table 1. Activation of caspases in MCF-7 cells

	% of Activation	SD
Caspase 9		
Control	14.16	± 2.565
BRL 100 nmol/L	17.23	± 1.678
9RA 50 nmol/L	18.14	± 0.986
BRL + 9RA	33.88*	± 5.216
Caspase 8		
Control	9.20	± 1.430
BRL 100 nmol/L	8.12	± 1.583
9RA 50 nmol/L	7.90	± 0.886
BRL + 9RA	10.56	± 2.160

Cells were stimulated for 48 hours in presence of 100 nmol/L BRL and 50 nmol/L 9RA, alone or in combination. The activation of caspase 9 and caspase 8 was analyzed by flow cytometry. Data are presented as mean ± SD of triplicate experiments. *$P < 0.05$ combined-treated versus untreated cells.

intact mitochondrial membrane potential (data not shown). Cells treated with both ligands exhibit green fluorescence, indicating disrupted mitochondrial membrane potential, where JC-1 cannot accumulate within the mitochondria, but instead remains as a monomer in the cytoplasm (Figure 5A). Concomitantly, cytochrome *C* release from mitochondria into the cytosol, a critical step in the apoptotic cascade, was demonstrated after combined treatment (Figure 5B).

Caspase-9 Cleavage and DNA Fragmentation Induced by BRL Plus 9RA in MCF-7 Cells

BRL and 9RA at nanomolar concentration did not induce any effects on caspase-9 separately, but activation was observed in the presence of both compounds (Table 1). No effects were elicited by either the combined or the separate treatment on caspase-8 activation, a marker of extrinsic apoptotic pathway (Table 1). Since internucleosomal DNA degradation is considered a diagnostic hallmark of cells undergoing apoptosis, we studied DNA fragmentation under BRL plus 9RA treatment in MCF-7 cells, observing that the induced apoptosis was prevented by either the PPARγ-specific antagonist GW or by AS/p53, which is able to abolish p53 expression (Figure 6A).

To test the ability of low doses of both BRL and 9RA to induce transcriptional activity of PPARγ, we transiently transfected a peroxisome proliferator response element reporter gene in MCF-7 cells and observed an enhanced luciferase activity, which was reversed by GW treatment (see Supplemental Figure 2 at *http://ajp.amjpathol.org*). These data are in agreement with previous observations demonstrating that PPARγ/RXR heterodimerization enhances DNA binding and transcriptional activation.[28–29]

Finally, we examined in three additional human breast malignant cell lines: MCF-7 TR1, SKBR-3, and T-47D the capability of low doses of a PPARγ and an RXR ligand to trigger apoptosis. DNA fragmentation assay showed that only in the presence of combined treatment did cells undergo apoptosis in a p53-mediated manner (Figure 6B), implicating a general mechanism in breast carcinoma.

Discussion

The key finding of this study is that the combined treatment with low doses of a PPARγ and an RXR ligand can selectively affect breast cancer cells through cell growth inhibition and apoptosis.

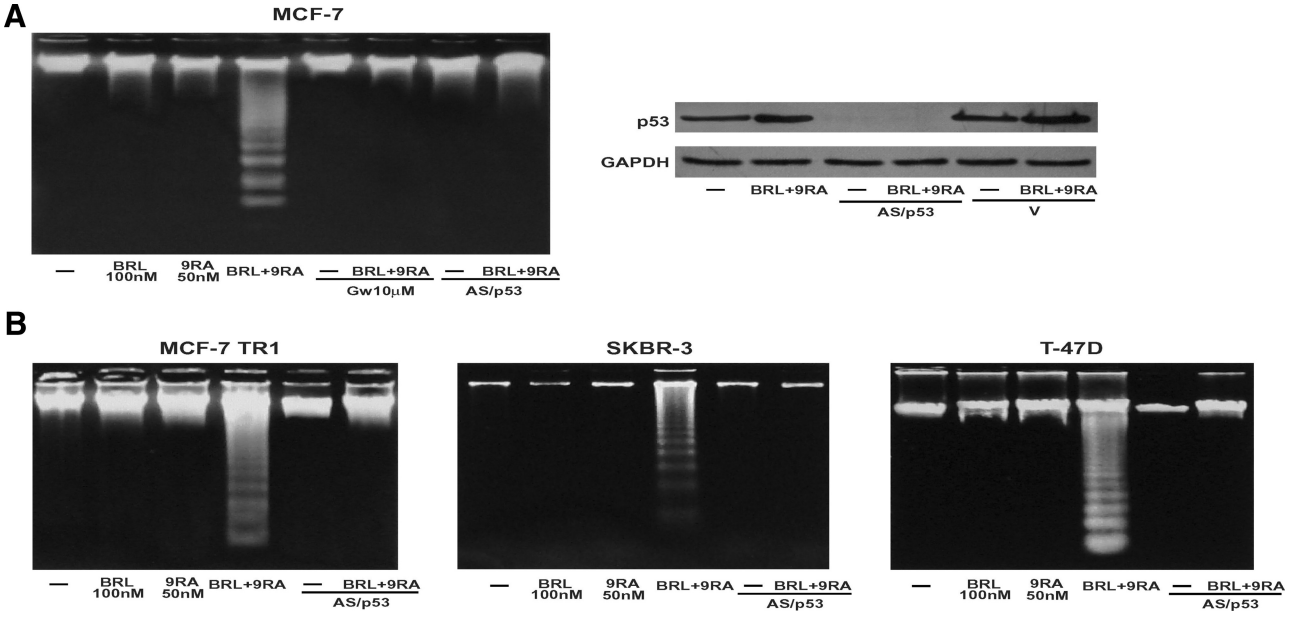

Figure 6. Combined treatment of BRL and 9RA trigger apoptosis in breast cancer cells. **A:** DNA laddering was performed in MCF-7 cells transfected and treated as indicated for 56 hours. One of three similar experiments is presented. The side panel shows the immunoblot of p53 from MCF-7 cells transfected with an expression plasmid encoding for p53 antisense (AS/p53) or empty vector (v) and treated with 100 nmol/L BRL plus 50 nmol/L 9RA for 56 hours. GAPDH was used as loading control. **B:** DNA laddering was performed in MCF-7 TR1, SKBR-3, and T47-D cells transfected with AS/p53 or empty vector (v) and treated as indicated. One of three similar experiments is presented.

The ability of PPARγ ligands to induce differentiation and apoptosis in a variety of cancer cell types, such as human lung,[30] colon,[31] and breast,[10] has been exploited in experimental cancer therapies.[32] PPARγ agonist administration in liposarcoma patients resulted in histological and biochemical differentiation markers *in vivo*.[33] However, a pilot study of short-term therapy with the PPARγ ligand rosiglitazone in early-stage breast cancer patients did not elicit significant effects on tumor cell proliferation, although the changes observed in PPARγ expression may be relevant to breast cancer progression.[34] On the other hand, the natural ligand for RXR, 9RA,[35] has been effective *in vitro* against many types of cancer, including breast tumor.[36–40] Recently, RXR-selective ligands were discovered to inhibit proliferation of all-*trans* retinoic acid–resistant breast cancer cells *in vitro* and caused regression of the disease in animal models.[41] The additive antitumoral effects of PPARγ and RXR agonists, both at elevated doses, have been shown in human breast cancer cells ([15,42] and references therein). However, high doses of both ligands have remarkable side effects in humans, such as weight gain and plasma volume expansion for PPARγ ligands,[16–18] and hypertriglyceridemia and suppression of the thyroid hormone axis for RXR ligands.[19]

In the present study, we demonstrated that nanomolar concentrations of BRL and 9RA in combination exert significant antiproliferative effects on breast cancer cells, whereas they do not induce noticeable influences on normal breast epithelial MCF10 cells. However, the induced overexpression of PPARγ in MCF10 cells makes these cells responsive to the low combined concentration of BRL and 9RA (data not shown). Although PPARγ is known to mediate differentiation in most tissues, its role in either tumor progression or suppression is not yet clearly elucidated. It has been demonstrated in animals studies that an overexpression of PPARγ increases the risk of breast cancer already in mice susceptible to the disease.[43] However, it remains still questionable if the enhanced PPARγ expression does correspond to an enhanced content of functional protein, which according to previous suggestion should be carefully controlled in a dose-response study.[44] For instance, the expression of PPARγ is under complex regulatory mechanisms, sustained by cell-specific distinct promoters mediating the changes in expression of PPARγ.[45]

Here we demonstrated for the first time the molecular mechanism underlying antitumoral effects induced by combined low doses of both ligands in MCF-7 cells, where an up-regulation of tumor suppressor gene p53 was concomitantly observed. Functional assays with deletion constructs of the p53 promoter showed that the NFκB site is required for the transcriptional response to BRL plus 9RA treatment. NFκB was shown to physically interact with PPARγ,[46] which in some circumstances binds to DNA cooperatively with NFκB.[47–49] It has been previously reported that micromolar doses of both PPARγ and RXR agonists synergize to generate an increased level of NFκB-DNA binding able to trigger apoptosis in Pre-B cells.[50] Our electrophoretic mobility shift assay and chromatin immunoprecipitation assay demonstrated that PPARγ/RXRα complex is present on p53 promoter in the absence of exogenous ligand. Only BRL and 9RA in combination increased the binding and the recruitment of either PPARγ or RXRα on the NFκB site located in the p53 promoter sequence. BRL plus 9RA at the doses tested also increased the recruitment of RNA-Pol II to p53 promoter gene illustrating a positive transcriptional regulation able to produce a consecutive series of events in the apoptotic pathway.

Changes in mitochondrial membrane permeability, an important step in the induction of cellular apoptosis, is concomitant with collapse of the electrochemical gradient across the mitochondrial membrane, through the formation of pores in the mitochondria leading to the release of cytochrome *C* into the cytoplasm, and subsequently with cleavage of procaspase-9. This cascade of events, featuring the mitochondria-mediated death pathway, was detected in BRL plus 9RA-treated MCF-7 cells. The activation of caspase 9, in the presence of no changes in the biological activity of caspase 8, support that in our experimental model only the intrinsic apoptotic pathway is the effector of the combined treatment with the two ligands.

The crucial role of p53 gene in mediating apoptosis is raised by the evidence that the effects on the apoptotic cascade were abrogated in the presence of AS/p53 in all breast cancer cell lines tested, including tamoxifen resistant breast cancer cells. In tamoxifen-resistant breast cancer cells, other authors have observed that epidermal growth factor receptor, insulin-like growth factor-1R, and c-Src signaling are constitutively activated and responsible for a more aggressive phenotype consistent with an increased motility and invasiveness.[51–53] Although more relevance of our findings should derive from *in vivo* studies, these results give emphasis to the potential use of the combined therapy with low doses of both BRL and 9RA as novel therapeutic tool particularly for breast cancer patients who develop resistance to anti-estrogen therapy.

References

1. Ryningen A, Stapnes C, Paulsen K, Lassalle P, Gjertsen BT, Bruserud O: In vivo biological effects of ATRA in the treatment of AML. Expert Opin Investig Drugs 2008, 17:1623–1633
2. Ravandi F, Estey E, Jones D, Faderl S, O'Brien S, Fiorentino J, Pierce S, Blamble D, Estrov Z, Wierda W, Ferrajoli A, Verstovsek S, Garcia-Manero G, Cortes J, Kantarjian H: Effective treatment of acute promyelocytic leukemia with all-trans-retinoic acid, arsenic trioxide, and gemtuzumab ozogamicin. J Clin Oncol 2009, 27:504–510
3. Montesinos P, Bergua JM, Vellenga E, Rayón C, Parody R, de la Serna J, León A, Esteve J, Milone G, Debén G, Rivas C, González M, Tormo M, Díaz-Mediavilla J, González JD, Negri S, Amutio E, Brunet S, Lowenberg B, Sanz MA: Differentiation syndrome in patients with acute promyelocytic leukemia treated with all-trans retinoic acid and anthracycline chemotherapy: characteristics, outcome, and prognostic factors. Blood 2009, 113:775–783
4. Sun SY, Yue P, Mao L, Dawson MI, Shroot B, Lamph WW, Heyman RA, Chandraratna RA, Shudo K, Hong WK, Lotan R: Identification of receptor-selective retinoids that are potent inhibitors of the growth of human head and neck squamous cell carcinoma cells. Clin Cancer Res 2000, 6:1563–1573
5. Abu J, Batuwangala M, Herbert K, Symonds P: Retinoic acid and retinoid receptors: potential chemopreventive and therapeutic role in cervical cancer. Lancet Oncol 2005, 6:712–720

6. Mangelsdorf DJ, Thummel C, Beato M, Herrlich P, Schütz G, Umesono K, Blumberg B, Kastner P, Mark M, Chambon P, Evans RM: The nuclear receptor superfamily: the second decade. Cell 1995, 83:835–839
7. Heyman RA, Mangelsdorf DJ, Dyck JA, Stein RB, Eichele G, Evans RM, Thaller C: 9-cis retinoic acid is a high affinity ligand for the retinoid X receptor. Cell 1992, 68:397–406
8. Elstner E, Müller C, Koshizuka K, Williamson EA, Park D, Asou H, Shintaku P, Said JW, Heber D, Koeffler HP: Ligands for peroxisome proliferator-activated receptor γ and retinoic acid receptor inhibit growth and induce apoptosis of human breast cancer cells *in vitro* and in BNX mice. Proc Natl Acad Sci USA 1998, 95:8806–8811
9. Tontonoz P, Hu E, Spiegelman BM: Stimulation of adipogenesis in fibroblasts by PPAR gamma 2, a lipid-activated transcription factor. Cell 1994, 79:1147–1156
10. Mueller E, Sarraf P, Tontonoz P, Evans RM, Martin KJ, Zhang M, Fletcher C, Singer S, Spiegelman BM: Terminal differentiation of human breast cancer through PPARγ. Mol Cell 1998, 1:465–470
11. Suh N, Wang Y, Williams CR, Risingsong R, Gilmer T, Willson TM, Sporn MB: A new ligand for the peroxisome proliferator-activated receptor-gamma (PPAR-gamma). GW7845, inhibits rat mammary carcinogenesis. Cancer Res 1999, 59:5671–5673
12. Bonofiglio D, Aquila S, Catalano S, Gabriele S, Belmonte M, Middea E, Qi H, Morelli C, Gentile M, Maggiolini M, Andò S: Peroxisome proliferator-activated receptor-gamma activates p53 gene promoter binding to the nuclear factor-kappaB sequence in human MCF7 breast cancer cells. Mol Endocrinol 2006, 20:3083–3092
13. Bonofiglio D, Gabriele S, Aquila S, Catalano S, Gentile M, Middea E, Giordano F, Andò S: Estrogen receptor alpha binds to peroxisome proliferator-activated receptor (PPAR) response element and negatively interferes with PPAR gamma signalling in breast cancer cells. Clin Cancer Res 2005, 11:6139–6147
14. Bonofiglio D, Gabriele S, Aquila S, Qi H, Belmonte M, Catalano S, Andò S: Peroxisome proliferator-activated receptor gamma activates fas ligand gene promoter inducing apoptosis in human breast cancer cells. Breast Cancer Res Treat 2009, 113:423–434
15. Elstner E, Williamson EA, Zang C, Fritz J, Heber D, Fenner M, Possinger K, Koeffler HP: Novel therapeutic approach: ligands for PPARγ and retinoid receptors induce apoptosis in bcl-2-positive human breast cancer cells. Breast Cancer Res Treat 2002, 74:155–165
16. Arakawa K, Ishihara T, Aoto M, Inamasu M, Kitamura K, and Saito A: An antidiabetic thiazolidinedione induces eccentric cardiac hypertrophy by cardiac volume overload in rats. Clin Exp Pharmacol Physiol 2004, 31:8–13
17. Rangwala SM and Lazar MA: Peroxisome proliferator-activated receptor gamma in diabetes and metabolism. Trends Pharmacol Sci 2004, 25:331–336
18. Staels B: Fluid retention mediated by renal PPARgamma. Cell Metab 2005, 2:77–78
19. Pinaire JA, Reifel-Miller A: Therapeutic potential of retinoid x receptor modulators for the treatment of the metabolic syndrome. PPAR Res 2007, 2007:94156
20. Qin C, Nguyen T, Stewart J, Samudio I, Burghardt R, Safe S: Estrogen up-regulation of p53 gene expression in MCF-7 breast cancer cells is mediated by calmodulin kinase IV-dependent activation of a nuclear factor κB/CCAAT-binding transcription factor-1 complex. Mol Endocrinol 2002, 16:1793–1809
21. Herman ME, Katzenellenbogen BS: Response-specific antiestrogen resistance in a newly characterized MCF-7 human breast cancer cell line resulting from long-term exposure to trans-hydroxytamoxifen. J Steroid Biochem Mol Biol 1996, 59:121–134
22. Mosmann T: Rapid colorimetric assay for cellular growth and survival: application to proliferation and cytotoxicity assays. J Immunol Methods 1983, 65:55–63
23. Andrews NC, Faller DV: A rapid micropreparation technique for extraction of DNA-binding proteins from limiting numbers of mammalian cells. Nucleic Acids Res 1991, 19:2499
24. Cossarizza A, Baccarani-Contri M, Kalashnikova G, Franceschi C: A new method for the cytofluorimetric analysis of mitochondrial membrane potential using the J-aggregate forming lipophilic cation 5,5′,6,6′-tetrachloro-1,1′,3,3′ tetraethylbenzimidazolylcarbo-cyanine iodide (JC-1). Biochem Biophys Res Commun 1993, 197:40–45
25. Mehta RG, Williamson E, Patel MK, Koeffler HP: A ligand of peroxisome proliferator-activated receptor gamma, retinoids, and prevention of preneoplastic mammary lesions. J Natl Cancer Inst 2000, 92:418–423
26. Crowe DL, Chandraratna RA: A retinoid X receptor (RXR)-selective retinoid reveals that RXR-alpha is potentially a therapeutic target in breast cancer cell lines, and that it potentiates antiproliferative and apoptotic responses to peroxisome proliferator-activated receptor ligands. Breast Cancer Res 2004, 6:R546–R555
27. Smiley ST, Reers M, Mottola-Hartshorn C, Lin M, Chen A, Smith TW, Steele GD, Chen LB: Intracellular heterogeneity in mitochondrial membrane potentials revealed by a J-aggregate forming lipophilic cation JC-1. Proc Natl Acad Sci USA 1991, 88:3671–3675
28. Kliewer SA, Umesono K, Mangelsdorf DJ, Evans RM: Retinoid X receptor interacts with nuclear receptors in retinoic acid, thyroid hormone, and vitamin D3 signaling. Nature 1992, 355:446–449
29. Zhang XK, Hoffmann B, Tran PBV, Graupner G, Pfahl M: Retinoid X receptor is an auxiliary protein for thyroid hormone and retinoic acid receptors. Nature 1992, 355:441–445
30. Tsubouchi Y, Sano H, Kawahito Y, Mukai S, Yamada R, Kohno M, Inoue K, Hla T, Kondo M: Inhibition of human lung cancer cell growth by the peroxisome proliferator activated receptor γ agonists through induction of apoptosis. Biochem Biophys Res Commun 2000, 270:400–405
31. Kitamura S, Miyazaki Y, Shinomura Y, Kondo S, Kanayama S, Matsuzawa Y: Peroxisome proliferator activated receptor γ induces growth arrest and differentiation markers of human colon cancer cells. Jpn J Cancer Res 1999, 90:75–80
32. Roberts-Thomson SJ: Peroxisome proliferator activated receptors in tumorigenesis: targets of tumor promotion and treatment. Immunol Cell Biol 2000, 78:436–441
33. Demetri GD, Fletcher CDM, Mueller E, Sarraf P, Naujoks R, Campbell N, Spiegelman BM, Singer S: Induction of solid tumor differentiation by the peroxisome proliferator activated receptor γ ligand troglitazone in patients with liposarcoma. Proc Natl Acad Sci USA 1999, 96:3951–3956
34. Yee LD, Williams N, Wen P, Young DC, Lester J, Johnson MV, Farrar WB, Walker MJ, Povoski SP, Suster S, Eng C: Pilot study of rosiglitazone therapy in women with breast cancer: effects of short-term therapy on tumor tissue and serum markers. Clin Cancer Res 2007, 13:246–252
35. Leblanc BP, Stunnenberg HG: 9-cis retinoic acid signaling: changing partners causes some excitement. Genes Dev 1995, 9:1811–1816
36. Gee MF, Tsuchida R, Eichler-Jonsson C, Das B, Baruchel S, Malkin D: Vascular endothelial growth factor acts in an autocrine manner in rhabdomyosarcoma cell lines and can be inhibited with all-trans-retinoic acid. Oncogene 2005, 24:8025–8037
37. Mizuguchi Y, Wada A, Nakagawa K, Ito M, Okano T: Antitumoral activity of 13-demethyl or 13-substituted analogues of all-trans retinoic acid and 9-cis retinoic acid in the human myeloid leukemia cell line HL-60. Biol Pharm Bull 2006, 29:1803–1809
38. Wan H, Hong WK, Lotan R: Increased retinoic acid responsiveness in lung carcinoma cells that are nonresponsive despite the presence of endogenous retinoic acid receptor (RAR) beta by expression of exogenous retinoid receptors retinoid X receptor alpha, RAR alpha, and RAR gamma. Cancer Res 2001, 61:556–564
39. Wu K, DuPré E, Kim H, Tin-U CK, Bissonnette RP, Lamph WW, Brown PH: Receptor-selective retinoids inhibit the growth of normal and malignant breast cells by inducing G1 cell cycle blockade. Breast Cancer Res Treat 2006, 96:147–157
40. Simeone AM, Tari AM: How retinoids regulate breast cancer cell proliferation and apoptosis. Cell Mol Life Sci 2004, 61:1475–1484
41. Bischoff ED, Gottardis MM, Moon TE, Heyman RA, Lamph WW: Beyond tamoxifen: the retinoid X receptor selective ligand LGD1069 (TARGRETIN) causes complete regression of mammary carcinoma. Cancer Res 1998, 58:479–484
42. Grommes C, Landreth GE, Heneka MT: Antineoplastic effects of peroxisome proliferator-activated receptor gamma agonists. Lancet Oncol 2004, 5:419–429
43. Saez E, Rosenfeld J, Livolsi A, Olson P, Lombardo E, Nelson M, Banayo E, Cardiff RD, Izpisua-Belmonte JC, Evans RM: PPARgamma signaling exacerbates mammary gland tumor development. Genes Dev 2004, 18:528–40
44. Sporn MB, Suh N, Mangelsdorf DJ: Prospects for prevention and treatment of cancer with selective PPARgamma modulators (SPARMs). Trends Mol Med 2001, 7:395–400
45. Wang X, Southard RC, Kilgore MW: The increased expression of

peroxisome proliferator-activated receptor-gamma1 in human breast cancer is mediated by selective promoter usage. Cancer Res 2004, 64:5592–5596
46. Chung SW, Kang BY, Kim SH, Pak YK, Cho D, Trinchieri G, Kim TS: Oxidized low density lipoprotein inhibits interleukin-12 production in lipopolysaccharide-activated mouse macrophages via direct interactions between peroxisome proliferator-activated receptor-γ and nuclear factor κB. J Biol Chem 2000, 275:32681–32687
47. Couturier C, Brouillet A, Couriaud C, Koumanov K, Bereziat G, Andreani M: Interleukin 1beta induces type II-secreted phospholipase A2 gene in vascular smooth muscle cells by a nuclear factor κB and peroxisome proliferator-activated receptor-mediated process. J Biol Chem 1999, 274:23085–23093
48. Sun YX, Wright HT, Janciasukiene S: Alpha1-antichymotrypsin/Alzheimer's peptide Abeta (1–42) complex perturbs lipid metabolism and activates transcription factors PPARγ and NFκB in human neuroblastoma (Kelly) cells. J Neurosci Res 2002, 67:511–522
49. Ikawa H, Kameda H, Kamitani H, Baek SJ, Nixon JB, His LC, Eling TE: Effect of PPAR activators on cytokine stimulated cyclooxygenase-2 expression in human colorectal carcinoma cells. Exp Cell Res 2001, 267:73–80
50. Schlezinger JJ, Jensen BA, Mann KK, Ryu HY, Sherr DH: Peroxisome proliferator-activated receptor γ-mediated NFkB activation and apoptosis in pre-B cells. J Immunol 2002, 169:6831–6841
51. Knowlden JM, Hutcheson IR, Jones HE, Madden T, Gee JMW, Harper ME, Barrow D, Wakeling AE, Nicholson RI: Elevated levels of EGFR/c-erbB2 heterodimers mediate an autocrine growth regulatory pathway in tamoxifen-resistant MCF-7 cells. Endocrinology 2003, 144:1032–1044
52. Jones HE, Goddard L, Gee JMW, Hiscox S, Rubini M, Barrow D, Knowlden JM, Williams S. Wakeling AE, Nicholson RI: Insulin-like growth factor-I receptor signaling and acquired resistance to gefitinib (ZD1839, Iressa) in human breast and prostate cancer cells. Endocr Relat Cancer 2004, 11:793–814
53. Hiscox S, Morgan L, Green TP, Barrow D, Gee J, Nicholson RI: Elevated Src activity promotes cellular invasion and motility in tamoxifen resistant breast cancer cells. Breast Cancer Res Treat 2005, 7:1–12

Identification of 9-*cis*-Retinoic acid as a pancreas-specific autacoid that attenuates glucose-stimulated insulin secretion

Maureen A. Kane[1], Alexandra E. Folias, Attilio Pingitore[1], Mariarita Perri[2], Kristin Obrochta, Charles R. Krois, Erika Cione[2], Joo Yeon Ryu & Joseph L. Napoli[*]

Nutritional Science and Toxicology, College of Natural Resources,

University of California, Berkeley, California 94720, USA

[1]Current address: Department of Pharmaceutical Sciences, School of Pharmacy, University of Maryland, Baltimore, MD 21201, USA

[2]Current address: Department of Pharmaco-Biology, University of Calabria, 87036 Rende (CS), Italy

[*]Address correspondence to: Joseph L. Napoli
119 Morgan Hall, MC#3104
University of California, Berkeley
Berkeley, CA 94720-3104
Email: jna@berkeley.edu
Phone: 510-642-5202
FAX: 510-642-0535

Classification: Biological Sciences, Physiology

Abstract

The all-*trans*-retinoic acid (atRA) isomer, 9-*cis*-retinoic acid (9cRA), activates retinoic acid receptors (RAR) and retinoid X receptors (RXR) *in vitro*. RAR control multiple genes, whereas RXR serve as partners for RAR and other nuclear receptors that regulate metabolism. Physiological function has not been determined for 9cRA, because it has not been detected in serum or multiple tissues with analytically validated assays. Here, we identify 9cRA in mouse pancreas by liquid-chromatography tandem mass spectrometry, and show that 9cRA decreases with feeding and after glucose dosing, and varies inversely with serum insulin. 9cRA reduces glucose-stimulated insulin secretion (GSIS) in mouse islets and in the rat β-cell line 832/13 within 15 min by reducing glucose transporter type 2 (Glut2) and glucokinase (GK) activities. 9cRA also reduces *Pdx-1* and *HNF4α* mRNA expression, ~8 and 80-fold, respectively: defects in *Pdx-1* or *HNF4α* cause maturity onset diabetes of the young (MODY4 and 1, respectively), as does a defective GK gene (MODY 2). Pancreas β-cells generate 9cRA, and mouse models of reduced β-cell number, heterozygous Akita mice and streptozotocin-treated mice, have reduced 9cRA. 9cRA is abnormally high in glucose intolerant mice, which have β-cell hypertropy, including mice with diet-induced obesity and *ob/ob* and *db/db* mice. These data establish 9cRA as a pancreas-specific autacoid with multiple mechanisms of action, and provide new insight into GSIS.

\body

Introduction

Impaired GSIS develops through multiple mechanisms, including actions of metabolic hormones and inflammatory cytokines, products of metabolic overload, and endoplasmic reticulum stress, yet mechanisms of GSIS and impaired glucose tolerance remain incompletely understood (1-4). Also uncertain is the contribution of impaired glucose tolerance to diminished pancreatic β-cell function and mass associated with type 2 diabetes (5). GSIS relies on the pancreas, and pancreas development, islet formation and function require normal vitamin A nutriture (6-8). Vitamin A-restriction during development impairs islet development and promotes glucose intolerance in adult rodents. On the other hand, restricting vitamin A in mature diabetes-prone rats reduces diabetes and insulitis, possibly though enhanced glucose sensing and metabolism. atRA, an activated metabolite of vitamin A, regulates pancreas development, and atRA does not enhance the incidence of diabetes in diabetes prone rats fed a vitamin A-deficient diet (7, 9, 10). Although the contribution of vitamin A to pancreas development through atRA seems clear, mechanisms whereby vitamin A affects mature pancreas function have not been determined in depth, nor have the specific vitamin A-metabolites been identified that contribute to GSIS control.

atRA induces differentiation and regulates cell processes by activating the nuclear receptors RAR α, β and γ, which regulate transcription and translation (11). atRA does not activate the nuclear receptors RXR α, β and γ, which serve as obligatory partners for RAR and numerous other nuclear receptors that regulate metabolism and

energy balance (12). 9cRA, an atRA isomer, binds both RAR and RXR with high affinity *in vitro*, and has diverse pharmacological actions distinct from atRA (13). For example, treating embryo day 11 pancreas organ cultures with 9cRA inhibits stellate cell activation more potently and quickly than atRA, and inhibits acini differentiation, but prompts ductal differentiation and endocrine maturation (9, 10). atRA, in contrast, induces acini rather than ductal differentiation. As a pan-agonist of six nuclear receptors, 9cRA has undergone extensive pharmacological assessment. As the drug alitretinoin, it is effective against chronic hand dermatitis and T-cell lymphoma (14). Used systemically, it alters energy metabolism (15). 9cRA also shows promise in reducing ischemic brain injury in a rat model, and in immunosuppressing human dendritic cells (16, 17). Regardless of the pharmacological utility of 9cRA, sensitive assays capable of quantifying individual RA isomers in biological matrices have not detected 9cRA in serum and in a variety of tissues (18, 19). This leaves uncertain whether 9cRA functions *in vivo* as an activated vitamin A metabolite with discrete physiological functions.

We applied an LC/MS/MS assay developed to distinguish and quantify RA isomers in biological matrices to identify retinoids in the pancreas, and detected not only atRA, but also 9cRA. Pancreas 9cRA, but not atRA, reacts within minutes to blood glucose fluctuations and attenuates the impact of glucose on GSIS through multiple mechanisms, including rapid action. These data validate 9cRA as a naturally occurring metabolite of vitamin A with a physiological function unique among retinoids, broaden insight into mechanisms of GSIS, and provide new perspective into vitamin A and islet function.

Results

9cRA as an endogenous pancreas retinoid. We applied a sensitive LC/MS/MS assay to compare pancreas RA isomers to those in serum and liver, because the endocrine pancreas expresses nuclear receptors that recognize RA isomers and responds to retinoid-induced signaling, and liver serves as the principal storage site of retinoids and contributes to retinoid homeostasis (20, 21). Consistent with previous work, prominent physiological RA isomers in serum and liver included atRA and 9,13-di-*cis*-RA (9,13dcRA), an RA isomer without known biological activity, but 9cRA was not detected (18, 19). In contrast, we identified 9cRA in pancreas, along with atRA and 9,13dcRA (Figure 1A). We confirmed that analysis did not generate 9cRA by adding retinoids to pancreata before homogenization, extraction, and assay (Figure 1B). Only 9cRA increased the 9cRA signal, excluding oxidation of the RA precursor retinal and/or isomerization of atRA during analyses as sources of 9cRA. Concentrations of 9cRA in pancreas occur within the range of concentrations of other RA isomers in tissues and serum (Figure 1C). These data provide an analytically rigorous identification of 9cRA as a naturally occurring retinoid. If 9cRA occurs in the tissues assayed other than pancreas, amounts would be <0.05 pmol/g, based on the LC/MS/MS assay's limit of detection in biomatrices.

9cRA varies with fasting, feeding, and glucose challenge. The fasted to fed transition resulted in a 36% decrease in 9cRA, which accompanied the increase in blood glucose and serum insulin, but caused no changes in pancreas atRA, 9,13-dcRA or retinol (Figure 2A and Figure S1). Consistent with this observation, challenging fasted

mice with a bolus of glucose decreased 9cRA >80% within 15 min, coinciding with the rapid rise in blood glucose (Figure 2B). 9cRA recovered markedly by 30 min and continued to rise thereafter. In contrast, glucose challenge had no impact on pancreas atRA or 9,13dcRA. During glucose challenge, 9cRA correlated inversely with serum insulin, further suggesting a contribution to pancreas function consistent with decreasing GSIS (Figure 2C). In addition, exogenous 9cRA reduced serum insulin during glucose challenge (Figure 2D).

9cRA promotes glucose intolerance. The inverse relationship between serum insulin and pancreas 9cRA during the GTT, and ability of 9cRA to reduce serum insulin, prompted testing whether 9cRA decreases glucose disposal. Mice were injected with 9-*cis*-retinol, a potential precursor of 9cRA, or 9cRA, prior to a GTT. Mice injected with 9-*cis*-retinol responded with a 2 to 2.7-fold increase in pancreas 9cRA, sustained at least 120 min (Figure 3A). Mice injected with 9cRA responded with a ~30-fold increase in pancreas 9cRA, which declined by 120 min to ~4-fold above control. Note that the decrease in endogenous 9cRA in the control (dosed only with glucose) at 30 min reflected the same degree of decrease (~40%) observed at 30 min in the GTT experiment of Figure 2B. Increases in pancreas 9cRA caused by both 9-*cis*-retinoids resulted in glucose intolerance, such that 120 min after the glucose challenge, blood glucose was at least 2-fold higher than in vehicle-dosed mice (Figure 3B). The lowest concentrations of 9cRA (40 nM) achieved after dosing either 9cRA or 9-*cis*-retinol arrested glucose disposal to the same extent as the higher concentrations achieved, indicating a dose-response relationship with a maximum effect near or below 40 nM 9cRA. These data suggest that the physiological decrease in pancreas 9cRA as

glucose increases permits optimum insulin secretion, and reveal that 9-*cis*-retinol can serve as a precursor to 9cRA.

9cRA rapidly attenuates glucose sensing and insulin secretion. Glucose uptake by the pancreas rapidly affects both Glut2 and GK activities through post-translational mechanisms (22, 23). Although GK activity limits the rate of glucose uptake by the β-cell, Glut2 contributes more than passive glucose transport by signaling glucose concentrations: phosphorylation decreases both the transport and signaling functions of Glut2 (22, 24). Forskolin, which stimulates cAMP synthesis and induces protein kinase A-dependent Glut2 phosphorylation in β-cells, decreases Glut2 activity. We repeated the experiment published with forskolin and compared its effect to that of 9cRA in the 832/13 β-cell line, established as a model of GSIS (25) (Figure 4A). We duplicated the published results with forskolin, and found that 9cRA decreased glucose-stimulated Glut2 activity ~40% within 15 min, similar to the impact of forskolin. Thirty nM 9cRA was as effective as 100 nM, consistent with the results of Figure 3, which indicated a marked effect of 40 nM 9cRA on glucose disposal.

In 15 min, 9cRA inhibited GK activity 70%, which persisted until 60 min in 832/13 β-cells treated with 23 mM glucose (Figure 4B). By 120 min, 9cRA inhibition of GK activity decreased to 34%. Despite the changes in Glut2 and GK activities, 9cRA did not affect Glut2 or GK mRNA by 15 min (Figure S2). 9cRA decreased ATP in 832/13 β-cells 30-40% from 15 through 60 min after introduction of 23 mM glucose and ATP recovered by 120 min (Figure 4C). After 60 min of 9cRA exposure in cells treated with 23 mM glucose, 9cRA reduced 832/13 β-cell intracellular Ca^{2+} 35%; Ca^{2+} returned to control levels by 2 hr (Figure 4D). Consistent with its impact on glucose sensing, 9cRA

reduced GSIS 40% in 832/13 β-cells after 60 min incubation with 23 mM glucose, but did not impair baseline insulin secretion in the presence of 3 mM glucose (Figure 4E). In pancreatic islets, 9cRA reduced GSIS 33-43% induced by 15 to 60 min incubation with 23 mM glucose, with islet sensitivity returning by 120 min (Figure 4F). A rise in ATP closes the β-cell K^+_{ATP} channel, which allows Ca^{2+} influx. This process serves as a "triggering signal" to initiate the first phase of GSIS (2). KCl induces insulin release in the absence of high glucose by circumventing the ATP effect on the K^+ channel. 9cRA had no impact on KCl-stimulated insulin secretion from islets (Figure 4G). To provide preliminary insight into the possible roles of RAR and RXR in short-term 9cRA action, the effects of the RAR panagonist TTNPB and the RXR panagonist bexarotene (BXR) were tested on GSIS in 832/13 cells (Figure S3) (26, 27). In contrast to 9cRA, neither decreased the fold increase in insulin secretion after 1 hr incubation with 23 mM glucose *vs.* 3 mM, but both decreased basal insulin secretion stimulated by 3 mM.

After 2 hr, 9cRA decreased expression of *Pdx-1* and *HNF4α* mRNA, 7 and 77-fold, respectively (Figure 4H). Pdx-1 induces glucokinase, Glut2 and insulin gene expression in the mature pancreas (28, 29). HNF4α regulates insulin release through controlling mitochondrial metabolism of glucose and HNF1α, Glut2 and insulin gene expression (30, 31).

Pancreas β-cells produce 9cRA. We analyzed pancreata from mice with decreased numbers of β-cells to identify sources of 9cRA. A point mutation in the insulin 2 gene of Ins2Akita mice induces β-cell apoptosis, which reduces the number of β-cells, indicated by a 46% reduction in pancreas insulin (32). Pancreata from fed heterozygous Akita mice had 40% lower 9cRA than wild type (WT), consistent with the decrease in β-

cells (Figures 5A and S3). In contrast, pancreas atRA increased and retinol did not differ from WT, demonstrating a unique relationship between 9cRA and β-cells. To confirm this insight, we injected mice with Stz, which causes β-cell necrosis (33). 9cRA in pancreas of Stz-treated mice decreased with time in direct proportion to the decrease in β-cells, assessed by insulin content (Figures 5B and C). Seventy-two hr after Stz dosing, β-cell numbers decreased 67%, accompanied by a 58% decrease in 9cRA, impaired glucose tolerance and elevated non-fasting blood glucose (Figure 5C and S4). By 96 hr, β-cells decreased 95% and 9cRA deceased 70%, consistent with β-cells serving as a major source of pancreas 9cRA. Based on the 9cRA remaining after β-cell destruction, other pancreas cells may contribute ~20-25% to the 9cRA pool.

The β-cell line 832/13 generated 9cRA and atRA from their respective 9-*cis*- or all-*trans*- retinol and retinal precursors at similar rates (Figure 5D). Pancreas microsomes contain both 9-*cis*- and all-*trans*-retinol (33 ± 1.4 and 76 ± 2 pmol/g protein, respectively; 3 replicate analyses of a 5 pancreata pool) (Figure 5E). Thus, β-cells have the capacity and a substrate to biosynthesize 9cRA.

Elevated 9cRA in models of glucose intolerance. To determine whether mouse models of glucose intolerance are accompanied by 9cRA increases, we assayed pancreata from *ob/ob* and *db/db* mice and mice with diet-induced obesity (DIO) (34). *Ob/ob* mice lack leptin, are obese and have high blood glucose and serum insulin (Figure S5A). *Ob/ob* mice had 2.2-fold higher 9cRA than WT controls (Figure 6A). Mice with DIO were glucose intolerant, weighed ~50% more than controls, and had ~2-fold higher 9cRA than controls (Figures 6B and S5C). *Db/db* mice, which lack the leptin receptor and have elevated blood glucose and serum insulin (Figure S5E), had 34%

higher 9cRA than lean controls (Figure 6C). Although atRA also increased in pancreas of *ob/ob* mice, the increase was modest, and atRA did not increase in pancreas of *db/db* mice. In DIO pancreata, the atRA increase exceeded the 9cRA increase. Neither the atRA nor the 9cRA changes in pancreas correlated with changes in retinol. Thus, 9cRA was the only endogenous retinoid assayed (9cRA, atRA and retinol) that changed consistently in pancreas with changes in glucose tolerance, regardless of the underlying cause of impaired glucose tolerance.

Discussion

With an analytically rigorous assay, we determined that 9cRA occurs as a naturally occurring retinoid in pancreas. This result addresses the long-standing questions whether or not 9cRA contributes to the biological activity of vitamin A *in vivo*, and if so, in what capacity? We found that 9cRA localizes to the pancreas, where it attenuates sensitivity to glucose through a rapid reduction of Glut2 and GK activities, without a concomitant rapid change in their mRNA. Reduction of glucose uptake and phosphorylation led to reduced ATP and insulin release. In the longer term, 9cRA reduces transcription of two genes required for insulin synthesis and secretion—*Pdx-1* and *HNF4α*. Notably, defects in either of these two genes and the gene that expresses GK cause the monogenic diseases known as maturity onset diabetes of the young (MODY): defects in HNF4α, GK, and Pdx-1 cause MODY1, 2 and 4, respectively (35, 36)**.** Therefore, at least three of six well-characterized MODY are caused by defects in genes regulated by 9cRA, or in a gene that encodes a protein regulated by 9cRA. These data clarify insight into the effects of vitamin A on pancreas function, *i.e.* atRA programs pancreas development and 9cRA attenuates GSIS in the developed

pancreas. This is consistent with need for vitamin A during pancreas development and with alleviation of glucose intolerance by restricting vitamin A in the mature pancreas. The observation of 9cRA in the pancreas justifies future work to determine when the pancreas begins producing 9cRA, to clarify its function during pancreas development.

β-cells, which are integral to GSIS, serve as a major source of 9cRA, and 9cRA effects on β-cell function were observed by 15 min. These data indicate that 9cRA acts as an autacoid in pancreas: it is generated *in situ* and executes rapid local actions of relatively brief duration. Rapid actions of retinoids are not unprecedented, although they have not been investigated as extensively as their transcriptional effects. 9cRA reportedly stimulates phosphorylation of p38 mitogen-activated protein kinase (37). Recent work has shown that atRA has rapid, non-genomic actions on neurite outgrowth and endothelial cell growth (38, 39)—indicating that retinoids, like several steroid hormones, do not solely regulate transcription (40-43).

The acute, non-genomic effects reported here for 9cRA differ from the effects of synthetic RXR analogs, known as rexinoids, in rodent diabetic models (44). Longer-term systemic treatment with rexinoids has been reported to promote insulin sensitization, presumably through cumulative effects on diverse receptors distributed throughout multiple tissues. In the case of the more RXR selective retinoids, insulin sensitization occurs by activating PPAR, presumably mainly in adipose (45).

By attenuating insulin secretion and biosynthesis, 9cRA functions physiologically to prevent hypoglycemia and to allow blood glucose levels raised (from glycogenolysis and gluconeogenesis) in response to decreasing blood glucose to increase to a greater extent than possible otherwise. Ultimately, reestablished higher blood glucose

decreases 9cRA, sensitizing the pancreas for optimum insulin secretion. Animal models of diabesity had both high pancreas 9cRA and high serum insulin—an abnormal occurrence. Either 9cRA target resistance or resistance of 9cRA concentration changes to glucose levels could contribute to the phenotypes manifested in these models, and to impaired glucose secretion. Alternatively, the β-cell hyperplasia that occurs in these models would contribute to, or underlie increased 9cRA (46).

Occurrence of 9cRA in pancreas, along with non-detectable concentrations in serum and a host other tissues, support the deduction based on genetic evidence that 9cRA does not serve as a universal retinoid X receptor-activating ligand *in vivo* (47). Validation of 9cRA as an autacoid in pancreas provides framework for evaluating whether it functions *via* RARs and/or RXRs, and for evaluating potential cross-signaling between atRA and 9cRA. The outcome of a potential 9cRA/atRA interaction with pancreas RAR cannot be predicted simply because both retinoids bind the same receptor. Nuclear receptor action depends on the ligand bound and the nucleotide sequence of the gene's response element—both influence receptor conformation, affinity for a particular response element, and function (48, 49).

Autacoid action in pancreas appears specific to 9cRA. Pancreas atRA did not change with an increase in blood glucose after the fasted to the fed transition, or after glucose injection, indicating that atRA does not regulate short-term modulation of GSIS. The increase in atRA in the pancreas during DIO and in *ob/ob* mice seems a compensating reaction to obesity, because disrupting atRA biogenesis by ablating *Rdh1* enhances adiposity, whereas chronic dosing of atRA to mice with DIO reduces weight by ~15% (15, 50).

In summary, this work demonstrates that 9cRA occurs as an endogenous pancreas retinoid, establishes a function for 9cRA in GSIS, and provides novel insight into retinoid function and glucose homeostasis. Of interest are the likely non-genomic effects of 9cRA. These studies provide insight into an essential element of pancreas-mediated glucose homeostasis, which should prove useful for understanding mechanisms of GSIS and diabesity.

Methods

Animals. Male C57BL/6 mice were used, unless noted otherwise, in accordance with institutional guidelines. Mice were fed either a stock diet with 30 IU/g vitamin A (Harlan Laboratories Teklad Global 18% protein rodent diet #2018S) or an AIN-93G purified rodent diet with 30 IU/g vitamin A (Dyets, Inc, #119139). The fatty acyl composition of the stock diet was (% of diet): 16:0, 0.7%; 18:0, 0.2%; 18:1,1.2%; 18:2, 3.1%; 18:3, 0.3%. The fatty acid content of the AIN-93G diet has been published (51). These diets are referred to as vitamin A-ample diets and produced similar results. Seven to 12-week-old WT, *ob/ob* mice, and mice heterozygous for the Akita spontaneous mutation (Ins2Akita) were purchased from the Jackson Lab. To establish DIO, 1-month-old mice were fed a high-fat diet for 5 months. The HFD was an AIN-93G purified rodent diet (Dyets Inc, diet# 180614) with 50% fat-derived calories. Lard served as the fat source. The fatty acyl composition of the lard was: 14:0, 1.5%; 16:0, 25.6%; 16:1, 3.4%; 18:0, 13.1%; 18:1, 44.1%; 18:2, 10.8%; 18:3, 1.5%. To deplete β-cells, Stz (170 mg/kg) was dosed i.p. once in 10 mM sodium citrate, pH 4.5. For glucose-tolerance tests (GTT), glucose (2 g/kg) was dosed i.p. in saline. The *db/db* mice were 5-months-old and fed

ad libitum. Insulin levels in this *db/db* colony at this age average 3-fold higher than controls, $P<0.01$ (52). Fasting was done for 12-16 hr. Mice were euthanized during the early light cycle.

Retinoids and retinoid quantification. Retinoids were purchased from Sigma, except for 9-cis-retinol, which was synthesized and characterized as described (18). Retinoids were used under yellow light as described (19, 53). Samples were harvested under yellow lights, frozen immediately in liquid nitrogen, and kept at -80 ^{o}C until extraction and retinoid quantification within one day by LC/MS/MS using selected reaction monitoring (RA isomers) or HPLC/UV (retinol isomers) as described in detail (19, 53).

β-cell line function assays. The pancreatic β-cell line 832/13 was cultured in growth medium (RPMI 1640 with 11 mM glucose and 10% fetal calf serum, 10 mM Hepes, 2 mM L-glutamine, 1 mM sodium pyruvate, and 50 mM β-mercaptoethanol, 100 units/ml penicillin and 100 mg/ml streptomycin at 37 °C) under 5% CO_2 in 100 mm Petri dishes as described (25). The medium was refreshed every 2-3 days. Cells were subcultured when they approached ≥70% confluence. Endogenous 9cRA in 832/13 cells at the time of experiments was $<0.04 \pm 0.0012$ pmol/10^6 cells (n = 9 plates).

To assay Glut2, GK and ATP, cells were transferred to 12-well plates until reaching 85% of confluence. Medium with 5 mM glucose was substituted for growth medium for 16 hr. Before assays, this medium was substituted with 2 mL HBSS containing 0.2% fatty-acid free BSA, pH 7.2 (sensing buffer) and 3 mM glucose for 2 hr (except for the glucose uptake assay). Experiments were then initiated by changing the sensing buffer to 0.8 ml/well of either fresh secretion buffer with 3 mM glucose or 23

mM glucose and/or 100 nM 9cRA, delivered in 5-10 μL DMSO, or vehicle alone. Incubations were done at 37 °C under yellow light.

9cRA biosynthesis. 832/13 cells were cultured in 12- or 6-well plates. At confluence, the growth medium was replaced with serum-free medium (11 mM glucose) and retinoids (1 μM) in DMSO (0.1% v/v) or vehicle alone were added and incubated 1 hr. Cells were lysed using Reporter lysis buffer (Promega) and combined with their medium for retinoid analyses.

*Insulin secretion studies***.** Islets were isolated by the UCSF Diabetes & Endocrinology Research Center (San Francisco, CA). Fifteen islets of similar size were incubated at 37 ^{o}C in 12-well plates with 5 mM D-glucose in RPMI1640 supplemented with 10% fetal bovine serum, 100 U/ml penicillin, 100 μg/ml streptomycin, 10 mM Hepes, 2 mM L-glutamine, 1 mM sodium pyruvate, 50 μM β-mercaptoethanol and 5% CO_2. After 16 hr, islets were washed and transferred to 1.5 ml tubes in secretion medium (HBSS with 20 mM Hepes and 1% bovine serum albumin, pH 7.2) containing 3 mM glucose. After 2 hr, secretion medium was replaced with fresh secretion medium containing 3 or 23 mM glucose with 100 nM 9cRA or vehicle alone (DMSO). Separate groups of islets were incubated in secretion medium containing 3 mM glucose with 35 mM KCl and 90 mM NaCl. Media were centrifuged for 2 min at 1000 x g to remove non-adherent cells and frozen at -80 ºC. Endogenous 9cRA in islets at the time of the experiment (after isolation and handling of islets) did not exceed 0.12 ± 0.008 pmol/plate (n = 5).

Statistics. Data are means ± SE. Statistical significance was assessed by two-tailed, unpaired Student's *t* tests for comparison of two groups, or by two-way ANOVA for comparison of two curves.

Acknowledgments

We thank Gregory Szot (UCSF Diabetes Center) for islet isolation, and Ron Tilton (University of Texas Medical Branch, Galveston, TX) for tissue samples from *db/db* mice. MK received support from a Ruth Kirschstein National Research Service Award postdoctoral fellowship (DK066924). AF, CK and KO received support from an NIH predoctoral training grant (DK061918). This work was funded in part by NIH grant to JN (DK47839). AP, MP, & EC were visiting scholars from the Department of Pharmaco-Biology, University of Calabria, 87036 Rende (CS), Italy. AP & MP were supported by Grants from Ministero Università e Ricerca Scientifica, Italy.

Figure Legends

Figure 1. 9cRA occurs in pancreas. (**A**) Representative LC/MS/MS chromatograms of RA isomers from analyses of mouse pancreas, liver and serum. (**B**) Representative LC/MS/MS chromatograms of pancreatic RA isomers before (solid lines) and after addition (dashed lines) of retinoids prior to homogenization, extraction and analysis. Each chromatogram shows one of triplicate analyses. (**C**) Quantification of RA isomers in mouse liver, serum, and pancreas: ND, not detected; 8 mice/group (s.e.m.)

Figure 2. 9cRA reflects fasting *vs*. feeding**.** (**A**) Blood glucose, serum insulin, and pancreas RA isomers in fed or 12-hr fasted mice. Data are means of 3 experiments with 6-10 mice/group/experiment: **P*≅0.03, ***P*<0.004, ****P*<0.003 *vs*. fed values. (**B**) 9cRA and atRA responses to a glucose challenge (2 g/kg glucose). Values are means of 2-5 experiments with 5-10 mice/point/experiment, except 9,13dcRA (1 experiment, 10 mice/time): **P*<0.05 from 0 time. The three glucose values after 0 min differ from control: **P*<0.05. (**C**) Inverse relationship between pancreas 9cRA and serum insulin after a glucose challenge: the slope differs significantly from 0, *P*=0.02; 10 mice/point. (**D**) 9cRA hinders insulin secretion: 9cRA (0.5 mg/kg in 60 µl DMSO) or vehicle alone were injected i.p. in mice 15 min before an i.p dose of glucose (0.5 g/kg). Data are means of 6-7 mice: **P*<0.05. All data s.e.m.

Figure 3. Exogenous 9cRA induces glucose intolerance**.** (**A**) Increases in total pancreas 9cRA after dosing with 9-*cis*-retinol or 9cRA (0.5 mg/kg in 100 µl DMSO). 9-*cis*-Retinol

and 9cRA were injected 60 and 15 min before glucose, respectively. Glucose (2 g/kg) was injected at 0 min: 5-8 mice/group; *$P \cong 0.01$ and **$P<0.003$ *vs*. vehicle control; $^{\&}P<0.005$ *vs*. 0 min. (**B**) GTT in mice dosed with 9-*cis*-retinol or 9cRA: 5-7 mice/group; *$P<0.04$, **$P<0.002$, ***$P<0.005$ *vs.* control. Mice were dosed with retinoids as described in A. All data s.e.m.

Figure 4. 9cRA attenuates pancreas glucose sensing. 832/13 β-cells and islets were pre-incubated 2 hr with 3 mM glucose. At 0 min, the medium was exchanged for medium containing 23 mM and agents indicated for the duration of experiments. (**A**) 9cRA reduces Glut2 activity in 832/13 cells after 15 min incubation: 4-8 replicates/group; *$P \leq 0.0003$ *vs*. no addition. (**B**) 9cRA reduces GK activity in 832/13 cells: 3-7 replicates/group, *$P<0.02$, **$P<0.002$ *vs.* control. (**C**) 9cRA reduces ATP content in 832/13 cells: 2-4 replicates/group, *$P<0.008$ *vs.* control. (**D**) 9cRA decreases Ca^{2+} influx into 832/13 cells: 2 replicates/group; *$P<0.02$. (**E**) 9cRA decreases GSIS by 832/13 cells: 3-11 replicates/group; *$P<0.01$ *vs*. control. (**F**) 9cRA decreases GSIS by pancreatic islets. The graph shows baseline insulin secretion during 3 mM glucose, and the effect of 9cRA on stimulation of insulin secretion by 23 mM glucose: 8-9 replicates/group; *$P<0.02$, **$P<0.002$ *vs.* control. (**G**) 9cRA does not affect KCl stimulated insulin secretion from islets: *$P<0.02$ *vs*. 0 time. (**H**) 9cRA reduces *Pdx-1* and *HNF4α* mRNA after 2 hr in 832/13 cells: 3 replicates/group. One hundred nM 9cRA was used in all experiments, unless noted otherwise. All data s.e.m.

Figure 5. Pancreas β-cells produce 9cRA. (**A**) Representative LC/MS/MS chromatograms and quantification of RA isomers in pancreas of WT and Akita mice: 8 mice/group; *P<0.05 *vs.* WT. (**B**) Immunohistochemistry showing loss of insulin in pancreas with time after a Stz dose: scale bars, 100 μm. (**C**) Effect of Stz on β-cell numbers (3-6 islets) and pancreas 9cRA (9-18 mice/group). (**D**) Biosynthesis of RA isomers from retinol and retinal isomers by the pancreas β-cell line 832/13: 3 replicates/substrate. (**E**) HPLC of retinol standards and representative analyses of pancreas microsomes. Arrows denote elution positions of 13-*cis*-, 9-*cis*- and all-*trans*-retinol, respectively. All data s.e.m.

Figure 6. Increased pancreas 9cRA accompanies glucose intolerance. (**A**) representative LC/MS/MS chromatograms and RA isomers in pancreas of fed WT and *ob/ob* mice: 8 mice/group; *P<0.008 *vs.* WT. (**B**) Increased 9cRA in pancreas of mice with DIO: 8-10 mice/group: *P<0.001 *vs*. lean. (**C**) RA isomers in pancreas of fed WT and *db/db* mice: 8 mice/group; **P=0.033. All data s.e.m.

References

1. Qatanani M & Lazar MA (2007) Mechanisms of obesity-associated insulin resistance: many choices on the menu. *Genes Dev* 21:1443-1455.
2. Jensen MV*, et al.* (2008) Metabolic cycling in control of glucose-stimulated insulin secretion. *Am J Physiol Endocrinol Metab* 295:E1287-1297.
3. Muoio DM & Newgard CB (2008) Mechanisms of disease: molecular and metabolic mechanisms of insulin resistance and beta-cell failure in type 2 diabetes. *Nat Rev Mol Cell Biol* 9:193-205.
4. Henquin JC, Ravier MA, Nenquin M, Jonas JC, & Gilon P (2003) Hierarchy of the beta-cell signals controlling insulin secretion. *Eur J Clin Invest* 33:742-750.
5. Lowell BB & Shulman GI (2005) Mitochondrial dysfunction and type 2 diabetes. *Science* 307:384-387.
6. Driscoll HK*, et al.* (1996) Vitamin A status affects the development of diabetes and insulitis in BB rats. *Metabolism* 45:248-253.
7. Matthews KA, Rhoten WB, Driscoll HK, & Chertow BS (2004) Vitamin A deficiency impairs fetal islet development and causes subsequent glucose intolerance in adult rats. *J Nutr* 134:1958-1963.
8. McCarroll JA*, et al.* (2006) Vitamin A inhibits pancreatic stellate cell activation: implications for treatment of pancreatic fibrosis. *Gut* 55:79-89.
9. Kadison A*, et al.* (2001) Retinoid signaling directs secondary lineage selection in pancreatic organogenesis. *J Pediatr Surg* 36:1150-1156.

10. Kobayashi H*, et al.* (2002) Retinoid signaling controls mouse pancreatic exocrine lineage selection through epithelial-mesenchymal interactions. *Gastroenterology* 123:1331-1340.

11. Noy N (2007) Ligand specificity of nuclear hormone receptors: sifting through promiscuity. *Biochemistry* 46:13461-13467.

12. Germain P*, et al.* (2006) International Union of Pharmacology. LXIII. Retinoid X receptors. *Pharmacol Rev* 58:760-772.

13. Ahuja HS, Szanto A, Nagy L, & Davies PJ (2003) The retinoid X receptor and its ligands: versatile regulators of metabolic function, cell differentiation and cell death. *J Biol Regul Homeost Agents* 17:29-45.

14. Cheng C, Michaels J, & Scheinfeld N (2008) Alitretinoin: a comprehensive review. *Expert Opin Investig Drugs* 17:437-443.

15. Berry DC & Noy N (2009) All-trans-retinoic acid represses obesity and insulin resistance by activating both peroxisome proliferation-activated receptor beta/delta and retinoic acid receptor. *Mol Cell Biol* 29:3286-3296.

16. Shen H*, et al.* (2009) 9-Cis-retinoic acid reduces ischemic brain injury in rodents via bone morphogenetic protein. *J Neurosci Res* 87:545-555.

17. Zapata-Gonzalez F*, et al.* (2007) 9-cis-Retinoic acid (9cRA), a retinoid X receptor (RXR) ligand, exerts immunosuppressive effects on dendritic cells by RXR-dependent activation: inhibition of peroxisome proliferator-activated receptor gamma blocks some of the 9cRA activities, and precludes them to mature phenotype development. *J Immunol* 178:6130-6139.

18. Kane MA, Chen N, Sparks S, & Napoli JL (2005) Quantification of endogenous retinoic acid in limited biological samples by LC/MS/MS. *Biochem J* 388:363-369.

19. Kane MA, Folias AE, Wang C, & Napoli JL (2008) Quantitative profiling of endogenous retinoic acid in vivo and in vitro by tandem mass spectrometry. *Anal Chem* 80:1702-1708.

20. Napoli JL (1999) Retinoic acid: its biosynthesis and metabolism. *Prog Nucleic Acid Res Mol Biol* 63:139-188.

21. Chuang JC, Cha JY, Garmey JC, Mirmira RG, & Repa JJ (2008) Research resource: nuclear hormone receptor expression in the endocrine pancreas. *Mol Endocrinol* 22:2353-2363.

22. Thorens B*, et al.* (1996) Protein kinase A-dependent phosphorylation of GLUT2 in pancreatic beta cells. *J Biol Chem* 271:8075-8081.

23. Zhang J*, et al.* (2006) Conformational transition pathway in the allosteric process of human glucokinase. *Proc Natl Acad Sci U S A* 103:13368-13373.

24. Ferber S*, et al.* (1994) GLUT-2 gene transfer into insulinoma cells confers both low and high affinity glucose-stimulated insulin release. Relationship to glucokinase activity. *J Biol Chem* 269:11523-11529.

25. Hohmeier HE*, et al.* (2000) Isolation of INS-1-derived cell lines with robust ATP-sensitive K+ channel-dependent and -independent glucose-stimulated insulin secretion. *Diabetes* 49:424-430.

26. Pignatello MA, Kauffman FC, & Levin AA (1997) Multiple factors contribute to the toxicity of the aromatic retinoid, TTNPB (Ro 13-7410): binding affinities and disposition. *Toxicol Appl Pharmacol* 142:319-327.

27. Boehm MF*, et al.* (1995) Design and synthesis of potent retinoid X receptor selective ligands that induce apoptosis in leukemia cells. *J Med Chem* 38:3146-3155.

28. Ashizawa S, Brunicardi FC, & Wang XP (2004) PDX-1 and the pancreas. *Pancreas* 28:109-120.

29. Babu DA, Deering TG, & Mirmira RG (2007) A feat of metabolic proportions: Pdx1 orchestrates islet development and function in the maintenance of glucose homeostasis. *Mol Genet Metab* 92:43-55.

30. Bartoov-Shifman R*, et al.* (2002) Activation of the insulin gene promoter through a direct effect of hepatocyte nuclear factor 4 alpha. *J Biol Chem* 277:25914-25919.

31. Wang H, Maechler P, Antinozzi PA, Hagenfeldt KA, & Wollheim CB (2000) Hepatocyte nuclear factor 4alpha regulates the expression of pancreatic beta -cell genes implicated in glucose metabolism and nutrient-induced insulin secretion. *J Biol Chem* 275:35953-35959.

32. Yoshioka M, Kayo T, Ikeda T, & Koizumi A (1997) A novel locus, Mody4, distal to D7Mit189 on chromosome 7 determines early-onset NIDDM in nonobese C57BL/6 (Akita) mutant mice. *Diabetes* 46:887-894.

33. Lenzen S (2008) The mechanisms of alloxan- and streptozotocin-induced diabetes. *Diabetologia* 51:216-226.

34. Leibel RL, Chung WK, & Chua SC, Jr. (1997) The molecular genetics of rodent single gene obesities. *J Biol Chem* 272:31937-31940.

35. Hattersley AT & Pearson ER (2006) Minireview: pharmacogenetics and beyond: the interaction of therapeutic response, beta-cell physiology, and genetics in diabetes. *Endocrinology* 147:2657-2663.

36. Bell GI & Polonsky KS (2001) Diabetes mellitus and genetically programmed defects in beta-cell function. *Nature* 414:788-791.

37. Teruel T, Hernandez R, Benito M, & Lorenzo M (2003) Rosiglitazone and retinoic acid induce uncoupling protein-1 (UCP-1) in a p38 mitogen-activated protein kinase-dependent manner in fetal primary brown adipocytes. *J Biol Chem* 278:263-269.

38. Chen N, Onisko B, & Napoli JL (2008) The nuclear transcription factor RARalpha associates with neuronal RNA granules and suppresses translation. *J Biol Chem* 283:20841-20847.

39. Sidell N*, et al.* (2010) Retinoic acid is a cofactor for translational regulation of vascular endothelial growth factor in human endometrial stromal cells. *Mol Endocrinol* 24:148-160.

40. Stahn C & Buttgereit F (2008) Genomic and nongenomic effects of glucocorticoids. *Nat Clin Pract Rheumatol* 4:525-533.

41. Raz L, Khan MM, Mahesh VB, Vadlamudi RK, & Brann DW (2008) Rapid estrogen signaling in the brain. *Neurosignals* 16:140-153.

42. Grossmann C & Gekle M (2009) New aspects of rapid aldosterone signaling. *Mol Cell Endocrinol* 308:53-62.

43. Maggiolini M & Picard D (2010) The unfolding stories of GPR30, a new membrane-bound estrogen receptor. *J Endocrinol* 204:105-114.

44. Mukherjee R*, et al.* (1997) Sensitization of diabetic and obese mice to insulin by retinoid X receptor agonists. *Nature* 386:407-410.

45. Leibowitz MD*, et al.* (2006) Biological characterization of a heterodimer-selective retinoid X receptor modulator: potential benefits for the treatment of type 2 diabetes. *Endocrinology* 147:1044-1053.

46. Lindstrom P (2007) The physiology of obese-hyperglycemic mice [ob/ob mice]. *ScientificWorldJournal* 7:666-685.

47. Calleja C*, et al.* (2006) Genetic and pharmacological evidence that a retinoic acid cannot be the RXR-activating ligand in mouse epidermis keratinocytes. *Genes Dev* 20:1525-1538.

48. Meijsing SH*, et al.* (2009) DNA binding site sequence directs glucocorticoid receptor structure and activity. *Science* 324:407-410.

49. Wang JC*, et al.* (2006) Novel arylpyrazole compounds selectively modulate glucocorticoid receptor regulatory activity. *Genes Dev* 20:689-699.

50. Zhang M, Hu P, Krois CR, Kane MA, & Napoli JL (2007) Altered vitamin A homeostasis and increased size and adiposity in the rdh1-null mouse. *FASEB J* 21:2886-2896.

51. Reeves PG (1997) Components of the AIN-93 diets as improvements in the AIN-76A diet. *J Nutr* 127:838S-841S.

52. Yin D*, et al.* (2006) Recovery of islet beta-cell function in streptozotocin- induced diabetic mice: an indirect role for the spleen. *Diabetes* 55:3256-3263.

53. Kane MA, Folias AE, & Napoli JL (2008) HPLC/UV quantitation of retinal, retinol, and retinyl esters in serum and tissues. *Anal Biochem* 378:71-79.

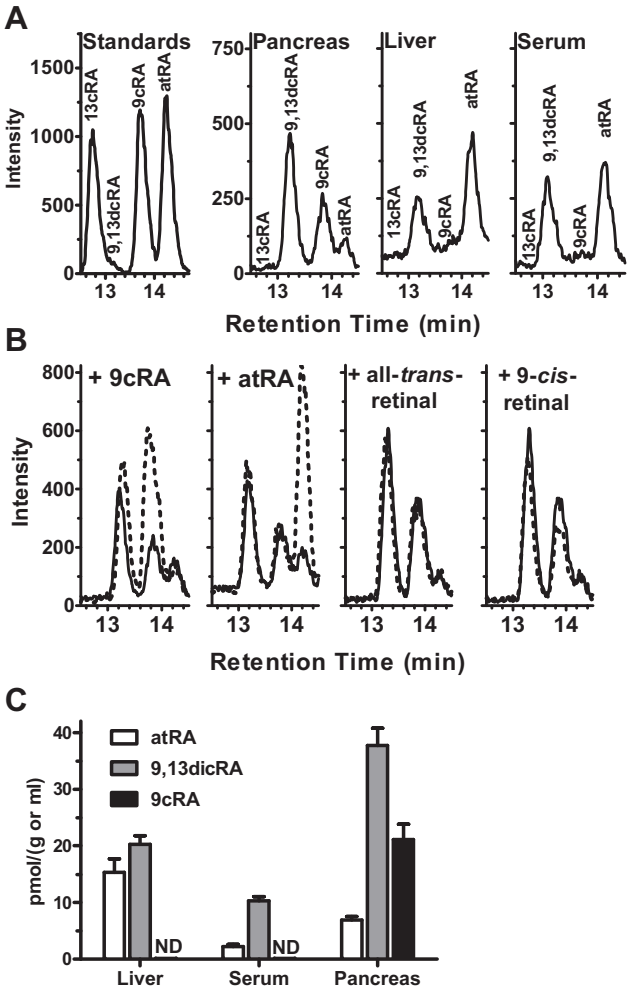
A
Standards
Pancreas
Liver
Serum
13cRA
9,13dcRA
9cRA
atRA
Intensity
Retention Time (min)
B
+ 9cRA
+ atRA
+ all-trans-retinal
+ 9-cis-retinal
Intensity
Retention Time (min)
C
atRA
9,13dicRA
9cRA
pmol/(g or ml)
ND
ND
Liver
Serum
Pancreas

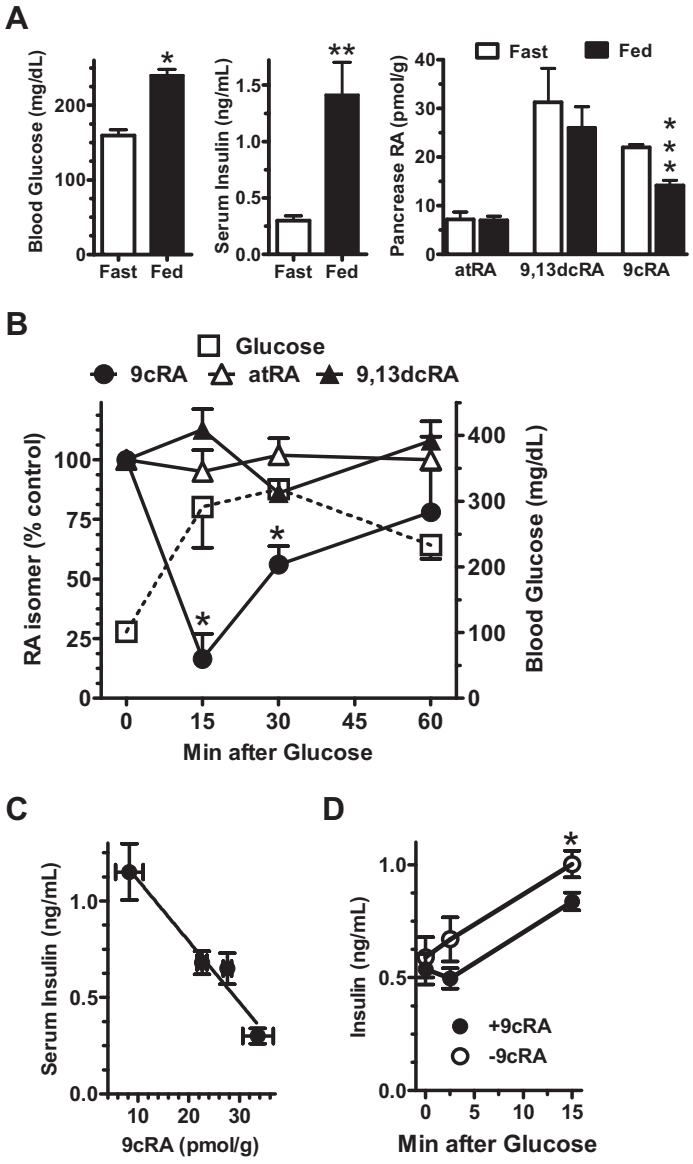
A
Blood Glucose (mg/dL)
Fast
Fed
Serum Insulin (ng/mL)
Pancrease RA (pmol/g)
atRA
9,13dcRA
9cRA
B
Glucose
9cRA
atRA
9,13dcRA
RA isomer (% control)
Blood Glucose (mg/dL)
Min after Glucose
C
Serum Insulin (ng/mL)
9cRA (pmol/g)
D
Insulin (ng/mL)
+9cRA
-9cRA
Min after Glucose

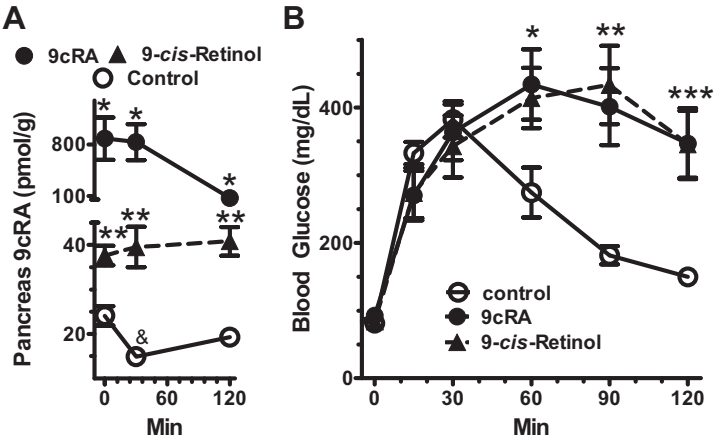
A
9cRA
9-cis-Retinol
Control
Pancreas 9cRA (pmol/g)
800
100
40
20
*
**
&
0
60
120
Min
B
Blood Glucose (mg/dL)
400
200
0
control
9cRA
9-cis-Retinol
*
**
***
0
30
60
90
120
Min

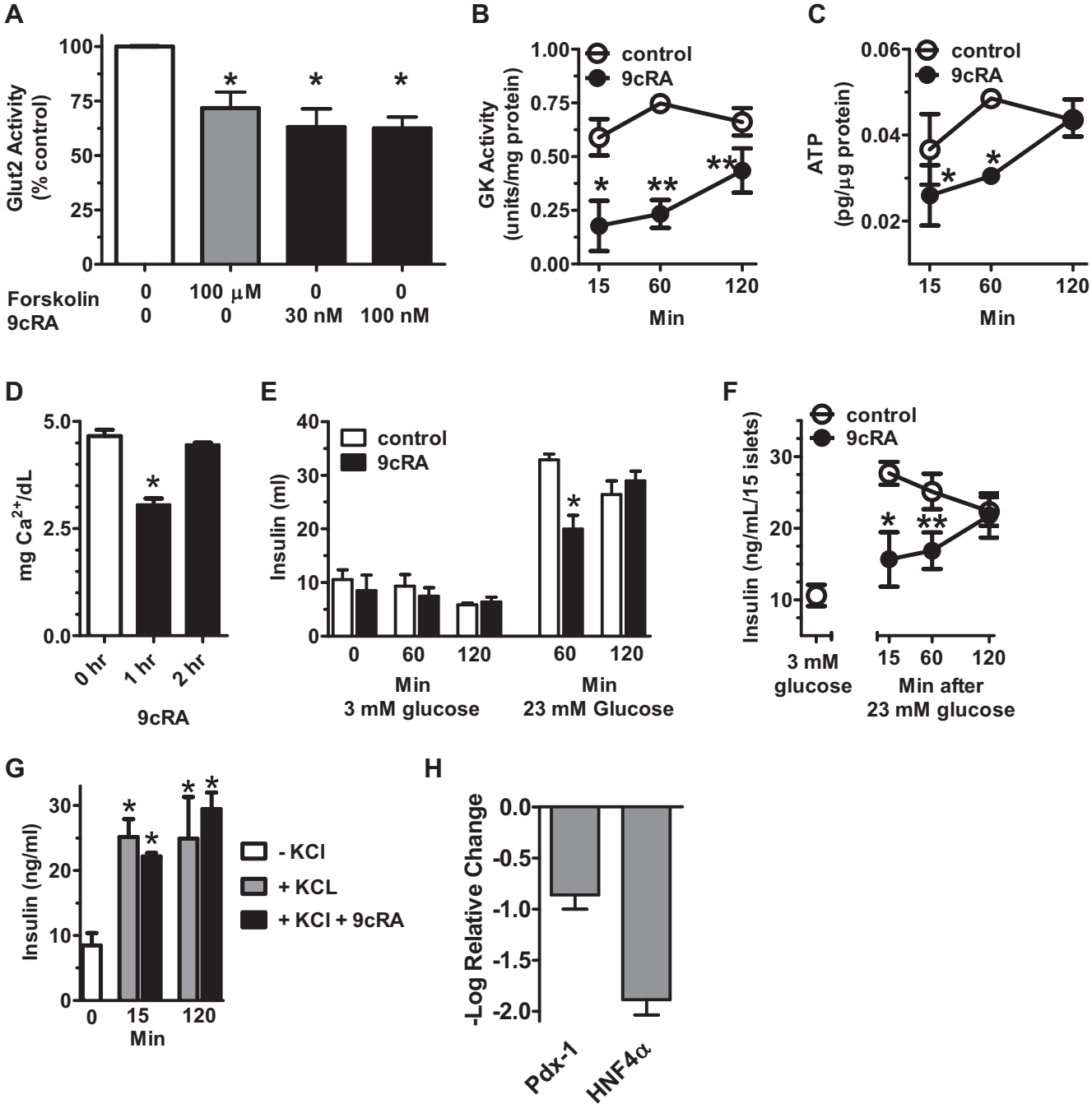
A
Glut2 Activity (% control)
100
75
50
25
0
Forskolin 0 100 µM 0 0
9cRA 0 0 30 nM 100 nM
B
GK Activity (units/mg protein)
1.00
0.75
0.50
0.25
0.00
control
9cRA
15 60 120
Min
C
ATP (pg/µg protein)
0.06
0.04
0.02
control
9cRA
15 60 120
Min
D
mg Ca2+/dL
5.0
2.5
0.0
0 hr 1 hr 2 hr
9cRA
E
Insulin (ml)
40
30
20
10
0
control
9cRA
0 60 120 60 120
Min Min
3 mM glucose 23 mM Glucose
F
Insulin (ng/mL/15 islets)
30
20
10
control
9cRA
3 mM glucose
15 60 120
Min after 23 mM glucose
G
Insulin (ng/ml)
30
20
10
0
- KCl
+ KCL
+ KCl + 9cRA
0 15 120
Min
H
-Log Relative Change
0.0
-0.5
-1.0
-1.5
-2.0
Pdx-1
HNF4α

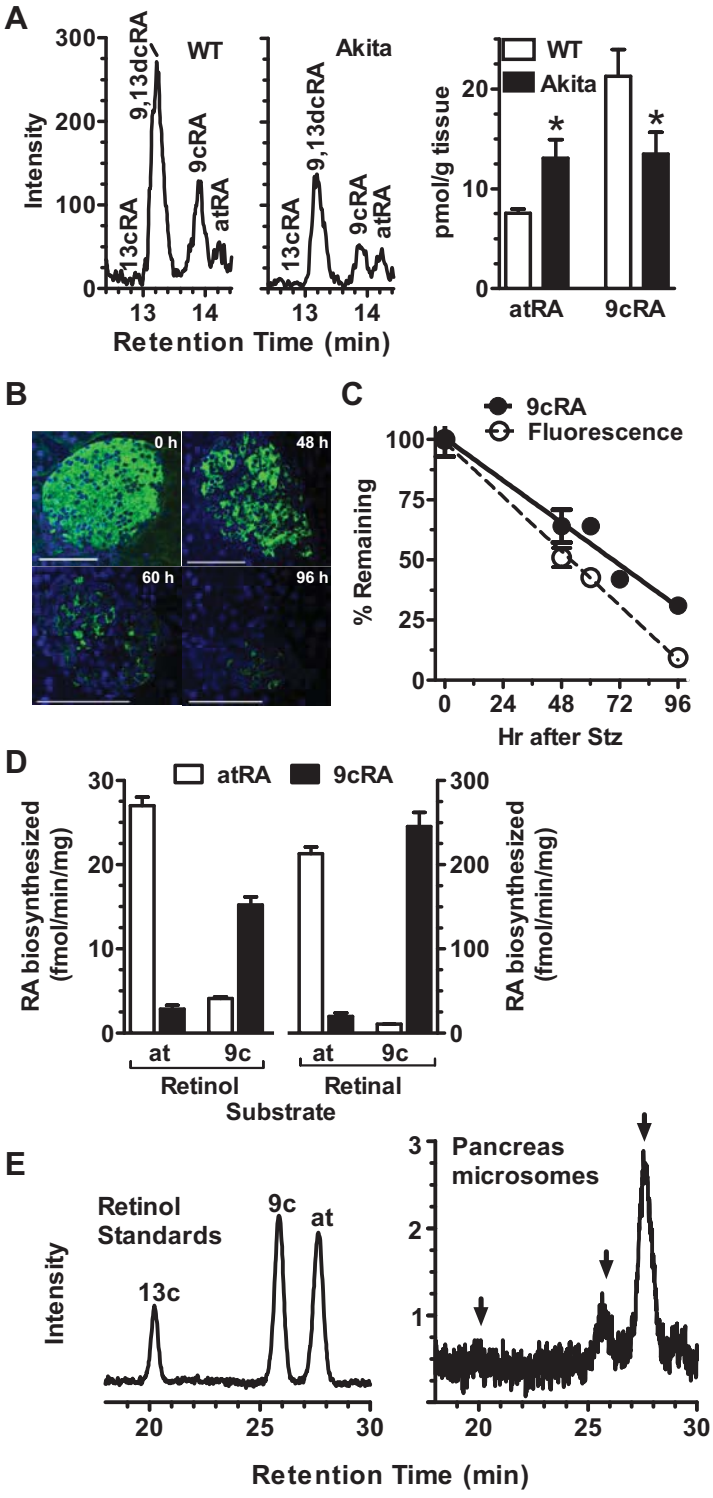
A
WT
Akita
9,13dcRA
9cRA
atRA
13cRA
Intensity
Retention Time (min)
pmol/g tissue
atRA
9cRA
B
0 h
48 h
60 h
96 h
C
9cRA
Fluorescence
% Remaining
Hr after Stz
D
atRA
9cRA
RA biosynthesized (fmol/min/mg)
at
9c
Retinol
Retinal
Substrate
E
Retinol Standards
13c
9c
at
Intensity
Pancreas microsomes
Retention Time (min)

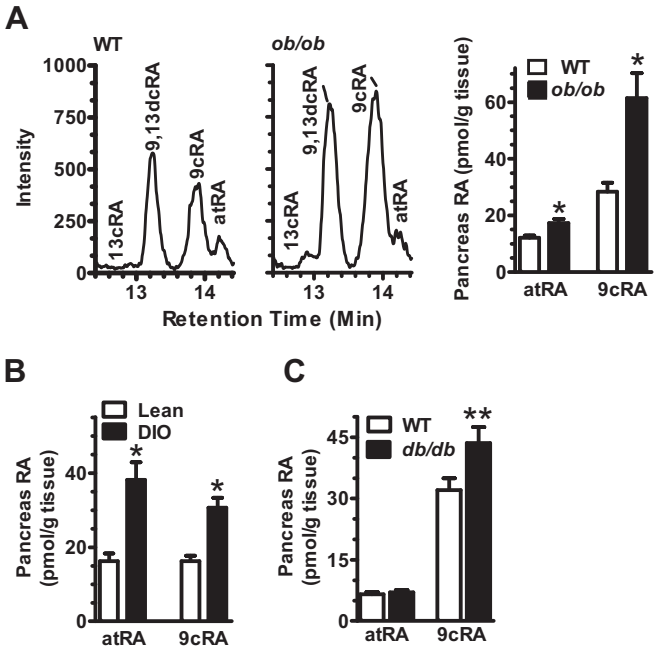
A
WT
ob/ob
1000
750
500
250
0
Intensity
13cRA
9,13dcRA
9cRA
atRA
13
14
Retention Time (Min)
Pancreas RA (pmol/g tissue)
WT
ob/ob
60
40
20
0
atRA
9cRA
B
Lean
DIO
Pancreas RA (pmol/g tissue)
40
20
0
atRA
9cRA
C
WT
db/db
45
30
15
0
atRA
9cRA